frontiers | Research Topics

Insights in neurotrauma: 2021

Edited by
Mårten Risling

Published in
Frontiers in Neurology

ISSN 1664-8714
ISBN 978-2-83251-616-4
DOI 10.3389/978-2-83251-616-4

About Frontiers

Frontiers is more than just an open access publisher of scholarly articles: it is a pioneering approach to the world of academia, radically improving the way scholarly research is managed. The grand vision of Frontiers is a world where all people have an equal opportunity to seek, share and generate knowledge. Frontiers provides immediate and permanent online open access to all its publications, but this alone is not enough to realize our grand goals.

Frontiers journal series

The Frontiers journal series is a multi-tier and interdisciplinary set of open-access, online journals, promising a paradigm shift from the current review, selection and dissemination processes in academic publishing. All Frontiers journals are driven by researchers for researchers; therefore, they constitute a service to the scholarly community. At the same time, the *Frontiers journal series* operates on a revolutionary invention, the tiered publishing system, initially addressing specific communities of scholars, and gradually climbing up to broader public understanding, thus serving the interests of the lay society, too.

Dedication to quality

Each Frontiers article is a landmark of the highest quality, thanks to genuinely collaborative interactions between authors and review editors, who include some of the world's best academicians. Research must be certified by peers before entering a stream of knowledge that may eventually reach the public - and shape society; therefore, Frontiers only applies the most rigorous and unbiased reviews. Frontiers revolutionizes research publishing by freely delivering the most outstanding research, evaluated with no bias from both the academic and social point of view. By applying the most advanced information technologies, Frontiers is catapulting scholarly publishing into a new generation.

What are Frontiers Research Topics?

Frontiers Research Topics are very popular trademarks of the *Frontiers journals series*: they are collections of at least ten articles, all centered on a particular subject. With their unique mix of varied contributions from Original Research to Review Articles, Frontiers Research Topics unify the most influential researchers, the latest key findings and historical advances in a hot research area.

Find out more on how to host your own Frontiers Research Topic or contribute to one as an author by contacting the Frontiers editorial office: frontiersin.org/about/contact

Insights in Neurotrauma: 2021

Topic editor
Mårten Risling — Karolinska Institutet (KI), Sweden

Citation
Risling, M., ed. (2023). *Insights in neurotrauma: 2021*. Lausanne: Frontiers Media SA.
doi: 10.3389/978-2-83251-616-4

Table of contents

frontiers | Frontiers in Neurology

TYPE Editorial
PUBLISHED 24 January 2023
DOI 10.3389/fneur.2023.1094723

OPEN ACCESS

EDITED AND REVIEWED BY
Jiyao Jiang,
Shanghai Jiao Tong University, China

*CORRESPONDENCE
Mårten Risling
✉ marten.risling@ki.se

SPECIALTY SECTION
This article was submitted to Neurotrauma, a section of the journal Frontiers in Neurology

RECEIVED 10 November 2022
ACCEPTED 12 January 2023
PUBLISHED 24 January 2023

CITATION
Risling M (2023) Editorial: Insights in neurotrauma: 2021. *Front. Neurol.* 14:1094723. doi: 10.3389/fneur.2023.1094723

Editorial: Insights in neurotrauma: 2021

Mårten Risling*

Department of Neuroscience, Karolinska Institutet, Solna, Sweden

KEYWORDS

traumatic brain injury (TBI), trauma, nervous system, clinical, experimental - animal models

Editorial on the Research Topic
Insights in neurotrauma: 2021

Insights collections is an initiative from Frontiers to highlight the recent advances in research within different fields of science. With this background, it was decided to invite authors to submit articles that could illustrate the advancements in understanding, diagnosis, or treatment of neurotrauma. The collection is titled "*Insights in Neurotrauma 2021*." The ten published articles cover several aspects of neurotrauma, in both experimental studies and clinical articles. The authors were encouraged to identify the greatest challenges in their sub-disciplines, and how to address such challenges.

The first published article in the collection is "*Age-At-Injury Influences the Glial Response to Traumatic Brain Injury in the Cortex of Male Juvenile Rats*" by Green et al.. This is an experimental study on juvenile rats. It was hypothesized that rats injured at post-natal day (PND) 17 would exhibit a greater glial response, that would persist into early adulthood, compared to rats injured at PND35. It is concluded that TBI at an early age may trigger a more prominent glial response. This article adds to the understanding of how age affects the response to neurotrauma and that the juvenile stage can show dynamic differences in a matter of days in terms of glial response.

The second article is "*Analgesia in the Neurosurgical Intensive Care Unit,*" by Kvolik et al.. This review article describes important considerations for pain control of neurosurgical intensive care patients. The preservation of adequate cerebral perfusion and oxygenation while managing intracranial pressure, mechanical ventilation, stability of circulation and fluid balance, temperature and glycemic control in neurosurgical patients is highly complex, and adequate pain control can improve outcomes. The article discusses pain control after a craniotomy. The review also describes the treatment of paroxysmal sympathetic hyperactivity, respiratory depression, gastroparesis, bowel paralysis, and hypotension. The treatment of addicted patients is another aspect covered in this review. Among unsolved questions, the article discusses whether the choice of analgesics may influence neurological recovery.

The article "*The Glial Cells Respond to Spinal Cord Injury*" by Wang et al. is a review of the response of astrocytes, oligodendrocytes, and microglia after spinal cord injury. The role of the different glial cells in the normal central nervous system (CNS) and the change after trauma is reviewed and discussed in this paper. The molecular pathways involved in the transition of the different glial cells function after injury are reviewed and discussed.

"*Decline in the Incidence of Chronic Subdural Hematoma During the Coronavirus Disease 2019 Pandemic: A Retrospective Single-Center Descriptive Study*" by Maeoka et al. is an article describing the change in the incidence of chronic subdural hematoma during the COVID-19 pandemic in Akashi city, Japan. The authors identify significant associations between the COVID-19 pandemic and a decline in the number of head traumas and chronic subdural hematomas.

The article "*Research Hotspots and Trends of Peripheral Nerve Injuries Based on Web of Science From 2017 to 2021: A Bibliometric Analysis*" by Zhang et al. is a systematic review of articles and reviews on peripheral nerve injury from 2017 to 2021, extracted from the Web of Science. The dorsal root ganglion and satellite glial cells are identified as hot topics in areas such as neuropathic pain relief. Tissue engineering techniques and the repair of Schwann cell phenotype were also discussed in the context of focus of future research.

"*Evaluation of decompressive craniectomy in mice after severe traumatic brain injury*" by Liu et al. is an article that describes the development of an experimental model for treatment of severe traumatic brain injury (TBI) in mice with decompressive craniectomy. The results show that the group that had been treated with decompressive craniectomy had significantly lower intracranial pressure and better neurological and motor function at 24 h after injury. However, at later stages, it is found that decompressive craniectomy had a negative effect on neurological function.

"*A Novel Therapeutic Approach With Sodium Pyruvate on Vital Signs, Acid–Base, and Metabolic Disturbances in Rats With a Combined Blast and Hemorrhagic Shock*" by Saha et al.. This study shows that sodium pyruvate resuscitation significantly improves the mean arterial pressure, heart rate, pulse pressure, hemodynamic stability, and autonomic response after hemorrhagic shock and/or blast injury.

"*Opinion: The Potential Role of Amyloid Beta Peptides as Biomarkers of Subconcussion and Concussion*" by Boutté et al.. In this article, the authors discuss the potential value of A-beta as a biomarker for subconcussion and concussion on the basis of findings in a limited cohort and previous data.

"*Immunoexpression of MMP-8 and MMP-9 in chronic subdural hematoma*" by Su et al.. In this study, the authors analyze matrix metallopeptidase (MMP)-8 and MMP-9 in 83 patients with chronic subdural hematoma and 50 normal individuals. The concentration of MMP-8 is significantly higher in peripheral blood from the normal group than that in the chronic subdural hematoma cases, whereas the level of MMP-9 is lower in the normal group.

The final paper published in this collection is "*Serum vitamin E level and functional prognosis after traumatic brain injury with intracranial injury: A multicenter prospective study*" by Park et al.. This study aims to evaluate the prognostic value of vitamin E on functional outcomes of traumatic brain injury (TBI) patients and is performed as a multi-center prospective cohort study. The data indicate that low serum vitamin E level is associated with poor prognosis at 1 and 6 months after TBI.

In summary, the Insights in Neurotrauma article collection represents an interesting mixture of ongoing research in neurotrauma, including experimental and clinical studies. Traumatic injuries to the nervous system represent an extensive field of various clinical problems. Many of the current problems are represented in this article collection. This is not a complete overview of the current research but can be regarded as a snapshot of different lines of research.

Author contributions

The author confirms being the sole contributor of this work and has approved it for publication.

Conflict of interest

The author declares that the research was conducted in the absence of any commercial or financial relationships that could be construed as a potential conflict of interest.

Publisher's note

frontiers in Neurology

ORIGINAL RESEARCH
published: 17 January 2022
doi: 10.3389/fneur.2021.804139

Age-At-Injury Influences the Glial Response to Traumatic Brain Injury in the Cortex of Male Juvenile Rats

Tabitha R. F. Green[1], *Sean M. Murphy*[1], *J. Bryce Ortiz*[1,2] *and Rachel K. Rowe*[1,3,4]*

[1] Department of Child Health, University of Arizona College of Medicine-Phoenix, Phoenix, AZ, United States, [2] Phoenix Veterans Affairs (VA) Health Care System, Phoenix, AZ, United States, [3] Department of Integrative Physiology, University of Colorado, Boulder, CO, United States, [4] BARROW Neurological Institute at Phoenix Children's Hospital, Phoenix, AZ, United States

Few translational studies have examined how age-at-injury affects the glial response to traumatic brain injury (TBI). We hypothesized that rats injured at post-natal day (PND) 17 would exhibit a greater glial response, that would persist into early adulthood, compared to rats injured at PND35. PND17 and PND35 rats ($n = 75$) received a mild to moderate midline fluid percussion injury or sham surgery. In three cortical regions [peri-injury, primary somatosensory barrel field (S1BF), perirhinal], we investigated the glial response relative to age-at-injury (PND17 or PND35), time post-injury (2 hours, 1 day, 7 days, 25 days, or 43 days), and post-natal age, such that rats injured at PND17 or PND35 were compared at the same post-natal-age (e.g., PND17 + 25D post-injury = PND42; PND35 + 7D post-injury = PND42). We measured Iba1 positive microglia cells (area, perimeter) and quantified their activation status using skeletal analysis (branch length/cell, mean processes/cell, cell abundance). GFAP expression was examined using immunohistochemistry and pixel analysis. Data were analyzed using Bayesian multivariate multi-level models. Independent of age-at-injury, TBI activated microglia (shorter branches, fewer processes) in the S1BF and perirhinal cortex with more microglia in all regions compared to uninjured shams. TBI-induced microglial activation (shorter branches) was sustained in the S1BF into early adulthood (PND60). Overall, PND17 injured rats had more microglial activation in the perirhinal cortex than PND35 injured rats. Activation was not confounded by age-dependent cell size changes, and microglial cell body sizes were similar between PND17 and PND35 rats. There were no differences in astrocyte GFAP expression. Increased microglial activation in PND17 brain-injured rats suggests that TBI upregulates the glial response at discrete stages of development. Age-at-injury and aging with an injury are translationally important because experiencing a TBI at an early age may trigger an exaggerated glial response.

Keywords: concussion, pediatric, juvenile, inflammation, microglia, astrocyte, aging

OPEN ACCESS

Edited by:
Mårten Risling,
Karolinska Institutet (KI), Sweden

Reviewed by:
Bridgette D. Semple,
Monash University, Australia
Rodney Ritzel,
University of Maryland School of Medicine, United States

***Correspondence:**
Rachel K. Rowe
rachel.rowe@colorado.edu

Specialty section:
This article was submitted to Neurotrauma, a section of the journal Frontiers in Neurology

Received: *28 October 2021*
Accepted: *14 December 2021*
Published: *17 January 2022*

Citation:
Green TRF, Murphy SM, Ortiz JB and Rowe RK (2022) Age-At-Injury Influences the Glial Response to Traumatic Brain Injury in the Cortex of Male Juvenile Rats. Front. Neurol. 12:804139. doi: 10.3389/fneur.2021.804139

INTRODUCTION

Toddlers (0–4 years) and adolescents (15–18 years) are vulnerable subgroups of the population in which the incidence of traumatic brain injury (TBI) peaks (1). Higher prevalence of TBIs in these age groups is primarily associated with participation in sports (2), car accidents, domestic violence (3, 4), and falls (5). Understanding the cellular response to injury in an age-specific manner is important to enable effective patient care and personalized medicine. Little is known about the specific glial response to TBI acquired as a toddler or an adolescent, which are two unique time periods for brain development. Support exists for these developmental periods being windows of both neuroprotection and increased vulnerability, phenomena that are likely mutually exclusive (6–8).

TBI results from mechanical forces applied to the brain, which can cause contusion, hemorrhage, diffuse axonal injury, and shearing (9). TBI triggers neuroinflammatory cascades that result in cellular damage and functional deficits. Neuroinflammation is mediated by microglia and astrocytes that change their morphology and transcriptional profile in response to injury (10). Acutely, microglia-mediated inflammation is beneficial and clears damaged cells and contents associated with TBI (11). Activation of microglia in juveniles following experimental TBI may also be important for the removal of dying neurons (12). However, long-term persistence of glial activation and cytokine release causes a self-perpetuating state of chronic inflammation, exacerbates the brain injury, and can lead to neuronal damage and neurodegeneration (11, 13). Microglia morphology is altered in response to injury (14). Activated microglia undergo a continuum of morphological transitions from a highly branched phenotype of surveying microglia to a rounded phagocytic morphology characterized by an enlarged cell body and retracted processes (14, 15). Microglial morphology can be assessed by immunohistochemistry using ionized calcium binding protein adapter molecule 1 (Iba1). Astrocytes also take on a hypertrophic phenotype when activated and increase their expression of glial fibrillary acidic protein (GFAP).

Herein, we used morphological changes in both microglia and astrocytes as physical indicators of distress, damage, and/or inflammation in the cortex of the brain, whereby reduced ramification was an indicator of microglial activation. Few pre-clinical models have examined TBI-associated pathology in juvenile rats (8). Therefore, we used a comprehensive time course after experimental TBI in rats to examine the acute and sub-acute cortical glial response (microglial activation and GFAP expression) to TBI. We used juvenile rats subjected to TBI at post-natal day (PND) 17, which models early childhood in humans, or PND35, which models adolescence in humans (13, 16).

We chose to investigate the glial response as a function of age-at-injury because of mounting evidence that indicates a differential immune response to injury throughout the lifespan (17, 18). During early life, the brain is undergoing vast circuit remodeling and is particularly vulnerable to injury and inflammation. As such, TBI incurred at a younger age may elicit a different inflammatory outcome compared to a brain injury at an older age. Previous studies have shown that different inflammatory signaling pathways are prevalent in the juvenile rodent brain when compared to adults (18, 19). Furthermore, younger animals experience a greater infiltration of leukocytes after TBI (20), which may contribute to the blood brain barrier breakdown observed in juvenile rats (17, 21). Infiltrating leukocytes can increase the number of inflammatory cells and subsequently elevate cytokine levels, free radical production, and protease release (22) . Together, these secondary injury processes contribute to tissue damage and microglial activation. Based on the age-dependent dimorphism in inflammatory signaling, we hypothesized that rats injured at PND17 would exhibit a greater cortical glial response, which would persist into early adulthood, compared to rats injured at PND35.

Abbreviations: ABC, Avidin-biotin complex; ARRIVE, Animal Research: Reporting *in vivo* Experiments; D, Day; DAB, 3,3′-diam-inobenzidine; FPI, Fluid percussion injury; GFAP, Glial fibrillary acidic protein; H, Hour; IACUC, Institutional Animal Care and Use Committee; Iba1, Ionized calcium binding adaptor molecule 1; mFPI, Midline fluid percussion; NHS, Normal horse serum; PBS, Phosphate buffered saline; PFA, Paraformaldehyde; pH, Potential hydrogen; PND, Post-natal day; S1BF, Primary somatosensory barrel field cortex; TBI, Traumatic brain injury.

METHODS

Study Design

We investigated the glial response relative to age-at-injury (PND17 or PND35), time post-injury (tissue collection: 2H, 1D, 7D, 25D, and 43D), and post-natal age, such that rats injured at PND17 or PND35 were compared at the same post-natal age (e.g., PND17 + 25D post-injury = PND42; PND35 + 7D post-injury = PND42; **Figure 1**).

Rigor

All experiments were performed according to the National Institutes of Health and Institutional Animal Care and Use Committee (IACUC) guidelines. The Animal Research: Reporting *in vivo* Experiments (ARRIVE) guidelines were followed. For data analyses, a total of 75 rats were used (sham $n = 31$, TBI $n = 44$). Exclusion criteria were predetermined such that rats that lost >20% of their body weight or had unmanageable pain were excluded; however, no rats in the study met these criteria and, therefore, none were excluded post-TBI. Pre-determined inclusion criteria included a righting reflex time >180 seconds and no breach of the dura during surgery. All samples and files were re-labeled with codenames by an investigator not associated with the current study to ensure that all experiments were conducted in blinded conditions. The group sizes for this study were: PND17 2H TBI $n = 4$, PND17 24H TBI $n = 5$, PND17 24H sham $n = 5$, PND17 7D TBI $n = 6$, PND17 7D sham $n = 4$, PND17 25D TBI $n = 5$, PND17 25D sham $n = 4$, PND17 43D TBI $n = 5$, PND17 43D sham $n = 5$, PND35 2H TBI $n = 4$, PND35 24H TBI $n = 5$, PND35 24H sham $n = 5$, PND35 7D TBI $n = 5$, PND35 7D sham $n = 4$, PND35 25D TBI $n = 5$, PND35 25D sham $n = 4$.

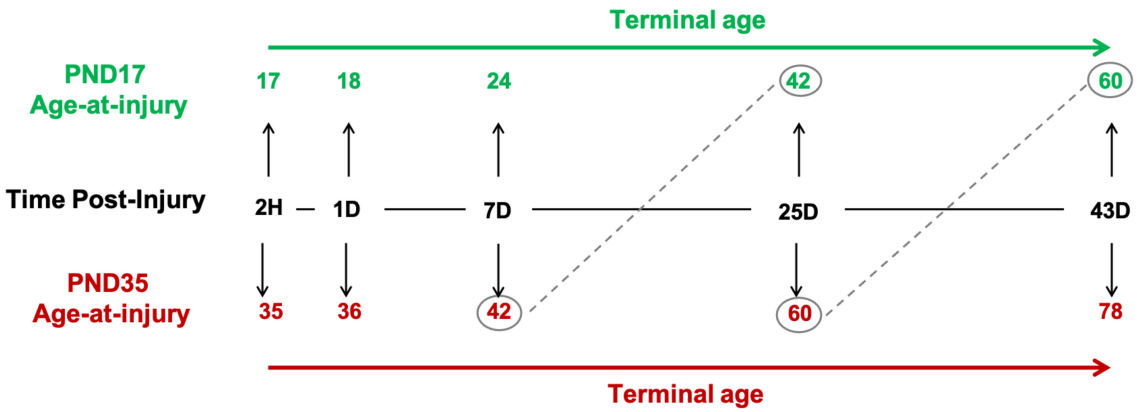

FIGURE 1 | Study design. Post-natal day (PND) 17 and PND35 rats ($n = 75$) received midline fluid percussion injury or sham surgery. In three cortical regions (peri-injury, S1BF, perirhinal), we investigated the glial response relative to age-at-injury (PND17/PND35), time post-injury (2H, 1D, 7D, 25D, and 43D), and post-natal-age, such that rats injured at PND17 or PND35 were compared at the same post-natal-age (e.g., PND17 + 25D post-injury = PND42; PND35 + 7D post-injury = PND42).

Animals

Male Sprague Dawley rats (Envigo, Indianapolis, IN) were used for all experiments. Rats were housed in a 12 h light: 12 h dark cycle at a constant temperature (23°C ± 2°C) with food and water available *ad libitum* according to the Association for Assessment and Accreditation of Laboratory Animal Care International guidelines. All rats were acclimated from shipping a minimum of one week prior to experiments. PND17 rats were shipped with the dam. After surgery, post-operative care via physical examination took place to monitor each animal's condition. PND17 rats were returned to their dam following surgery and midline fluid percussion injury (mFPI) until tissue collection (2H, 24H, 7D), or until they were weaned at PND24. Average PND17 pre-surgical weight was 28.2 ± 3.2 g. Average PND35 pre-surgical weight was 135.5 ± 14.3 g. Weights and health conditions were monitored and documented throughout the experiment. Animal care and experiments were approved by the Institutional Animal Care and Use Committee (IACUC) at the University of Arizona (protocol 13–460).

Midline Fluid Percussion Injury

For surgery, all rats were administered 5% isoflurane in 100% oxygen for 5 min and then secured in a stereotaxic frame. Anesthetization was maintained with continuous isoflurane delivery at 2.5% via nosecone. A midline incision was made and a craniectomy (outer diameter 3 mm in PND17 rats and 4 mm in PND35 rats) was trephined midway between bregma and lambda (23). The skull flap was then removed with care not to disrupt the dura or superior sagittal sinus underlying the craniectomy site. An injury hub (prepared from the female portion of a Luer-Loc needle hub) was fixed over the craniectomy using cyanoacrylate gel and methyl-methacrylate (Hygenic Corp., Akron, OH). Post-surgery, rats were placed on a heating pad and monitored until ambulatory.

Approximately 60–120 min after surgery, rats were subjected to mFPI with methods we have previously described for PND17 and PND35 rats (13, 23, 24). Rats were re-anesthetized with 5% isoflurane in 100% oxygen delivered for 3 min. The hub assembly on the skull was filled with saline and attached to the FPI device (custom design and fabrication, Virginia Commonwealth University, Richmond, VA). When a toe pinch withdrawal response was detected, the pendulum was released causing a fluid pulse directly onto the dura resulting in a mild to moderate brain injury in all rats [PND17 = 1.5 atmospheres pressure (atm), PND35 = 1.9 atm] (13, 23, 24). Sham rats were connected to the device, but the pendulum was not released. Hubs were removed immediately after injury or sham injury and rats were monitored for apnea, righting reflex time (time from the initial impact until the rat spontaneously righted itself from a supine position), and a fencing response (25). After rats spontaneously righted, brains were inspected for herniation, hematomas, and integrity of the dura. Brain-injured rats included in this study had an average righting reflex time of 318 s, indicative of a mild to moderate injury (23, 24), and had no disruption to the underlying dura. Sham rats spontaneously righted (∼20 s) when removed from the device. Rats were re-anesthetized and scalp incisions were cleaned with sterile saline and closed. Rats were placed in a heated recovery cage and monitored until ambulatory. Rat welfare was evaluated and documented daily during post-operative care via physical examination.

Cryoprotection and Tissue Sectioning

At pre-determined time points post-injury (2H, 1D, 7D, 25D, and 43D), a lethal dose of Euthasol® was administered. Rats underwent transcardial perfusion with 4% paraformaldehyde (PFA) after flushing vasculature with phosphate buffered saline (1× PBS). From the time of tissue harvest, tissue samples were treated identically throughout the experiment to reduce variation. Brains were harvested from the skull and drop fixed in 4% PFA for 24 h. Brains were cryoprotected by successive incubation in 15 and 30% sucrose, each for 24 h. Brains were then removed from sucrose and the left hemisphere

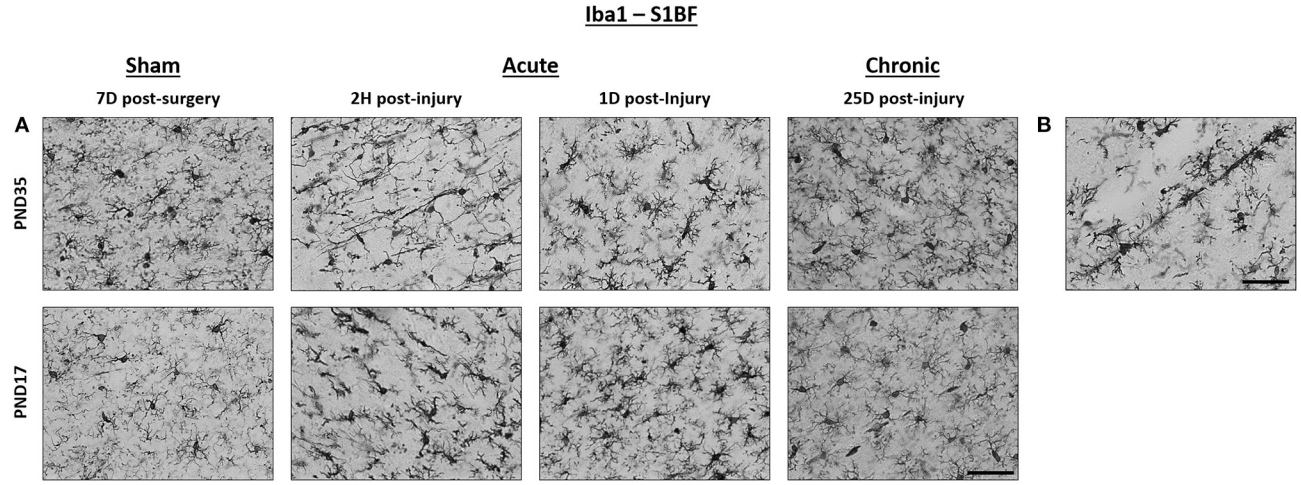

FIGURE 2 | TBI activated microglia in both PND17 and PND35 rats. Iba1 stained microglia in PND17 and PND35 rats. **(A)** At 2 h (H), 1 day (D), and 25D post-injury, microglial activation was observed in PND17 and PND35 rats subjected to TBI compared to uninjured shams. All representative images are from the S1BF. **(B)** Rod microglia were observed in PND17 rats but not PND35 rats. Scale bars = 50 μm. (sham $n = 39$, TBI $n = 35$).

from each animal was frozen in groups of 6–9 using the Megabrain technique as previously published (26). Megabrains were cryosectioned in the coronal plane at 40 μm and mounted on superfrost slides and stored at −80 °C. Sections were removed from the freezer and baked at 56°C for 3 h prior to undergoing immunohistochemistry.

Immunohistochemistry and Analysis

Each immunohistochemistry stain was performed on 4 randomly selected brain slices located between bregma and lambda from the left hemisphere of each animal (total area of 160 μm), and 3 regions of interest [peri-injury, primary somatosensory barrel field (S1BF), perirhinal] per slice were analyzed. Based on our findings of the biomechanical mechanism of mFPI (27), and our previously published work on TBI-induced neuropathology in juvenile rats (13), we chose three cortical regions of interest for the current study. We selected two cortical areas that, based on our previous research, exhibit extensive pathology after mFPI (peri-injury and S1BF), as well as a remote cortical region for comparison. Regions were selected using visual anatomical landmarks while the microscope was out of focus to allow accurate selection of brain region without sampling bias.

Iba1: To analyze microglia morphology, brains were stained for ionized calcium binding protein adapter molecule 1 (Iba1). To improve scientific rigor, Iba1 staining was performed in a single round of staining to minimize variance and allow comparisons. Slides were rehydrated in 1× PBS after baking (3 h). Antigen retrieval was performed using sodium citrate buffer (pH 6.0). Slides were then washed in 1× PBS. Hydrophobic barrier pen was applied to the perimeter of the slide and slides were placed in a humidity chamber. Blocking solution was immediately applied [4% normal horse serum (NHS), 0.1% Triton-100 in 1× PBS] with an incubation time of 60 min. Following blocking, primary antibody solution (rabbit anti-Iba1; WAKO cat #019919741; RRID: AB_839504; at 1:1000 concentration in 1% NHS, 0.1% triton-100 in 1× PBS) was applied and left to bind overnight at 4°C. Slides were then washed in 1× PBS + 0.1% tween-20. Secondary antibody solution [biotinylated horse anti-rabbit IgG (H + L); vector BA-1100; RRID: AB_2336201; at 1:250 concentration in 4% NHS and 0.4% triton-100 in 1× PBS] was applied and incubated for 60 min. Slides were washed in 1× PBS + 0.1% tween-20. Endogenous peroxidases were blocked in 200 ml 1× PBS + 8 ml H_2O_2 for 30 min. After washing in 1× PBS + 0.1% tween-20, Avidin-Biotin Complex (ABC) solution (Vectastain ABC kit PK-6100) was applied and incubated for 30 min. Slides were washed in PBS + 0.1% tween-20 and then 3,3′-diam-inobenzidine (DAB) solution (from Vector DAB peroxidase substrate kit SK-4100) was applied and incubated for 10 min and, following this, slides were immediately placed in water. Tissue was dehydrated in ethanol (70, 90, and 100%) and cleared with citrosolve. Coverslips, matching microscope specifications, were applied using dibutylphthalate polystyrene xylene mounting medium.

GFAP: To analyze astrocytes, brains were stained for glial fibrillary acidic protein (GFAP). An identical protocol was followed to that described for Iba1, using solutions; blocking = 5% NHS, 0.1% triton X-100 in 1× PBS; primary antibody solution = polyclonal rabbit anti-glial fibrillary acidic protein #Z0334; RRID: AB_10013382; at a 1:1000 concentration in 2% NHS and 1× PBS solution; secondary solution = biotinylated horse anti-rabbit IgG (H +L); vector BA-1100 at 1:250 concentration in 4% NHS and 0.4% triton-100 in 1× PBS. The DAB incubation time was 5 min.

Imaging and analysis: Z-stack images of stained tissue were taken at 400× (40× objective lens, 10× ocular lens) using Zeiss Imager A2 microscope via AxioCam MRc5 digital camera and Neurolucida 360 software, with consistent brightness, numerical aperture, and Z-stack height (**Figure 2**). Nyquist theorem was

followed to ensure the signal adequately represented our biological samples. Iba1 staining was analyzed using the skeletal analysis plugin following the protocol previously published (28, 29). Microglial cell somas were counted manually to obtain total microglial count. Branch length and processes were recorded and divided by the number of cells in each region of interest. Microglial cell bodies were measured using the multipoint area selection tool to calculate cell body area and perimeter. Although cell body area and perimeter are typically proportional, it is possible for a cell body to have a more complex shape but not larger total area. For this reason, both measurements were included in our analyses. To capture the hypertrophic morphological changes and increased GFAP expression seen in astrocytes after injury, GFAP images were analyzed for number of GFAP + cells and average number of pixels per cell using ImageJ software. Cell somas were counted manually. The average number of pixels per cell (referred to as cell coverage henceforth) was recorded to assess gross morphological changes in $GFAP^+$ astrocytes following mFPI. No alternations/settings changes were made to any images prior to analysis. All imaging analyses were performed on Z-stack images, which is the most appropriate sampling method to capture our sample.

Statistical Analyses

Outcomes in this study were counts, percentages, and distances or areas, which we analyzed using Poisson or negative-binomial regression, beta regression, and log-normal or Gaussian regression, respectively (30–32). Integer count outcomes were cell coverage (*n* pixels/cell), cells (*n*), and mean number of branches per microglial cell (*n*); pixel coverage was the only bounded percentage outcome; and microglial branch length (μm), cell body perimeter (μm), and cell body area (μm^2) were continuous outcomes with lower bounds truncated at zero but untruncated upper bounds. To determine whether Poisson or negative-binomial distributions were best suited for analyzing the count data, we tested for overdispersion (i.e., variance > mean) using the dispersiontest() function in the AER package (33, 34) of the R statistical computing environment (22).

For each outcome type, we fit three multivariate multi-level multiple regression models to test differences between treatment groups (sham vs. TBI) for each PND injury age (data collected from all time post-injury groups were pooled), PND terminal age, and time post-injury (35–38). In total, we fit 24 multivariate models, with each having three submodels, for a total of 72 models. The three submodels for each outcome type corresponded to the following population-level effects (*sensu* fixed effects): (1) an interaction between treatment group and time post-injury, (2) an interaction between treatment group and PND injury age, and (3) an interaction between treatment group and PND terminal age. In each model, we included group-level varying intercepts (*sensu* random effects) for surgery day to account for potential variation or dependency that may have been induced by groups of rats receiving surgery on the same day ($n = 9$ surgery days). For the cell body perimeter and area models, we also included group-level varying intercepts for animal ID, because each rat had multiple datapoints due to the multiple slides that were used to collect these data.

We fit all models in a Bayesian framework, primarily because Bayesian approaches (a) do not necessitate large sample sizes for accurate parameter estimation, (b) efficiently and effectively accommodate the hierarchical data generating processes and pseudoreplication that existed in some of our outcomes, and (c) provide intuitive interpretations that mirror the human reasoning process (39–41). For each model, we applied conservatively informative priors to model parameters and variance components, based on results of previous studies [e.g., (37, 38)], our knowledge of the study systems from preliminary studies conducted by our group, and recommendations from prior statistical research. Specifically, we applied ∼Normal (0, 1) priors to population-level parameters, ∼Cauchy (0, 5) priors to the variance scale parameters, and ∼Cauchy (0, 2) priors to the standard deviations of group-level effects, thereby appropriately restricting those variance components' parameter spaces to positive values (42). All models were fit using the Stan computational platform (43) via the R packages rstan and brms (44–46). Four Markov chains were run for each model, with each chain having a burn-in of 2,000 iterations of the No-U-Turn Sampler extension to Hamiltonian Monte-Carlo sampling, followed by 3,000 sampling iterations (37, 38). This approach produced 12,000 total posterior samples for each model. We assessed model convergence using trace plots and estimates of the potential scale reduction factor ($\hat{R}$) and effective sample sizes (n_{eff}). Optimal values for $\hat{R}$ and n_{eff} were strictly 1.00–1.01 and >1,000, respectively (47, 48). We assessed model fit using posterior predictive check plots created with the R package bayesplot, comparing 1,000 posterior predictive distribution samples to the observed data (49–51).

We based inferences on a combination of model parameter estimates (β; posterior means), their 95% credible intervals, corresponding conditional marginal effects under the posterior distributions, and posterior probabilities (*P*) and Bayes factors (*K*) (52) estimated from non-linear Bayesian hypothesis tests. Additionally, we calculated effect sizes (*d*) (53, 54) using the estimated group-specific posterior means and their pooled variances (55). The strength and magnitude of support for each effect was evaluated based on the following ranges of values for *P*, *K*, and *d*, as we have previously reported (37, 38) and which are detailed by (52, 56), among others. Posterior probability: Weak = 0.90–0.92; Moderate = 0.93–0.95; Strong = 0.96–0.98; Decisive/Substantial ≥0.99. Bayes factor: Weak < 3; Moderate = 3–10; Strong = 11–100; Decisive/Substantial >100. Effect size: Small = 0.10–0.49; Medium = 0.50–0.79; Large = 0.80–1.19; Very large ≥1.20. For introductions to Bayesian statistics, including the advantages of Bayesian modeling and explanations of the above metrics, we encourage readers to view the following articles (41, 57, 58).

RESULTS

Among count outcome variables, results of dispersion tests indicated that Poisson response distributions were appropriate for GFAP + cell coverage in all three cortical regions as well as Iba1 + mean number of branches per microglial

cell in all three cortical regions (dispersion range: 0.85–1.23; *z*-score range: −1.29 to 0.94). In contrast, overdispersion existed for GFAP+ cells and Iba1 + cells in all three cortical regions (dispersion range: 2.90–622.94; *z*-score range: 1.38–5.75). Therefore, negative-binomial response distributions were specified for all cell models.

Diffuse TBI Activated Microglia in the Peri-Injury Cortex of Rats Injured at Both PND17 and PND35

Overall, there were more microglia in the peri-injury cortex of PND17 rats than in PND35 rats, suggesting a greater inflammatory response in the PND17 rats. There were no differences in microglial branch lengths between sham and TBI rats across times post-injury, injury ages, or terminal ages (**Figures 2**, **3A–C**). However, PND35 shams had longer branch lengths than PND17 shams (95% CI: 0–10, $P = 0.97$, $K = 34.40$, $d = 0.11$; **Figure 3B**). There were no differences in number of cells between sham and TBI across times post-injury and terminal ages (**Figures 3D,F**). However, PND35 shams (95% CI: 0–10, $P = 0.98$, $K = 46.62$) and PND35 TBI rats (95% CI: −1 to 9, $P = 0.94$, $K = 17.04$) had fewer cells, respectively, compared to PND17 ($d = 0.06$–0.10; **Figure 3E**). Additionally, PND17 TBI rats had more cells than PND17 shams (95% CI: −3 to 7, $P = 0.90$, $K = 7.96$) and PND35 TBI rats had more cells than PND35 shams (95% CI: −2 to 7, $P = 0.97$, $K = 38.6$), respectively ($d = 0.02$–0.06; **Figure 3E**). Sham and TBI groups also had similar mean processes per microglial cell across times post-injury, injury ages, and terminal ages (**Figures 3G–I**). However, PND35 shams had more mean processes per microglial cell than PND17 shams (95% CI:−9–54, $P = 0.93$, $K = 12.42$, $d = 0.01$; **Figure 3H**).

Diffuse TBI Increased Microglial Cell Perimeter and Cell Area Size in the Peri-Injury Cortex of Rats Injured at Both PND17 and PND35

Overall, microglia in the peri-injury cortex of PND35 rats had a greater cell body perimeter than in the peri-injury cortex of PND17 rats, suggesting a greater phagocytic potential in PND35 rats. Our data support that TBI increased cell perimeter (**Figures 3J–L**) and cell area (**Figures 3M–O**). Across times post-injury, TBI rats had longer cell body perimeters than shams at 1D (95% CI: 2–23, $P > 0.99$, $K > 100$), 7D (95% CI: −1 to 15, $P = 0.98$, $K = 61.83$), and 43D post-injury (95% CI: −6 to 17, $P = 0.92$, $K = 11.75$), respectively ($d = 0.02$–0.03; **Figure 3J**). Additionally, TBI rats at 1D had longer cell body perimeters than TBI rats at 2H, 7D, and 25D post-injury (95% CI range: 2–22, $P > 0.99$, $K > 100$; **Figure 3J**). Similarly, TBI rats had larger cell body areas than shams at 1D (95% CI: −4 to 88, $P > 0.99$, $K > 100$), 7D (95% CI: −17 to 62, $P = 0.96$, $K = 22.53$), and 43D post-injury (95% CI: −34 to 83, $P = 0.91$, $K = 10.02$), respectively ($d < 0.01$; **Figure 3M**). Further, TBI rats at 1D had larger cell body areas than TBI rats at 2H, 7D, and 25D post-injury (95% CI range: −12 to 78, $P = 0.98$, $K = 52.10$; **Figure 3M**).

PND17 TBI rats had longer cell body perimeters than PND17 shams (95% CI: −3 to 11, $P = 0.93$, $K = 12.26$) and PND35 TBI rats had longer cell body perimeters than PND35 shams (95% CI: 2–18, $P > 0.99$, $K > 100$), respectively ($d = 0.01$–0.02; **Figure 3K**). Additionally, PND35 TBI rats had longer cell body perimeters than PND17 TBI rats (95% CI: −3 to 13, $P = 0.96$, $K = 24.53$, $d = 0.01$; **Figure 3K**). In contrast, there were no differences in cell body area between TBI and sham rats at PND17 ($P = 0.83$, $K = 2.56$) or between PND17 TBI rats PND35 TBI rats ($P = 0.88$, $K = 4.97$; **Figure 3N**). However, PND35 TBI rats had a larger cell body area than PND35 shams (95% CI: −13 to 68, $P = 0.98$, $K = 70.43$, $d = 0.003$; **Figure 3N**).

TBI rats had longer cell body perimeters than shams at terminal ages PND35 (95% CI: 1–23, $P > 0.99$, $K > 100$) and PND42 (95% CI: −3 to 16, $P = 0.95$, $K = 15.42$), respectively ($d = 0.02$–0.03; **Figure 3L**), and there were no other perimeter differences between TBI and sham rats. Additionally, TBI rats at terminal age PND24 had shorter cell body perimeters than TBI rats at all other terminal ages (95% CI range: 4–22, $P > 0.99$, $K > 100$, $d \leq 0.04$; **Figure 3L**). There were no differences in cell body area between TBI and shams across all terminal ages ($P < 0.90$, $K \leq 3.00$; **Figure 3O**); however, TBI rats at PND24 had smaller cell body areas than TBI rats at PND35, PND42, and PND60, but not PND17 (95% CI range: 7–95, $P > 0.99$, $K > 100$; **Figure 3O**).

Diffuse TBI Activated Microglia in the S1BF of Rats Injured at Both PND17 and PND35

Overall, there were more microglia in the S1BF of PND17 rats compared to the S1BF of PND35 rats, suggesting a greater inflammatory response in PND17 rats. TBI rats at 1D (95% CI: 1–13, $P > 0.99$, $K > 100$), 25D (95% CI: 0–13, $P = 0.99$, $K > 100$), and 43D post-injury (95% CI: 2–23, $P > 0.99$, $K > 100$) had shorter microglial branch lengths than shams, respectively ($d = 0.13$–0.18; **Figure 4A**). PND17 TBI rats had shorter microglia branch lengths in the S1BF than PND17 shams (95% CI: 0–10, $P > 0.99$, $K > 100$) and PND35 TBI rats had shorter branch lengths than PND35 shams (95% CI: 1–13, $P > 0.99$, $K > 100$), respectively ($d = 0.10$; **Figure 4B**). TBI rats at terminal ages PND35 (95% CI: 0–21, $P > 0.99$, $K > 100$) and PND60 (95% CI: 2–21, $P > 0.99$, $K > 100$) had shorter microglial branch lengths than shams, respectively ($d = 0.11$–0.14; **Figure 4C**).

There were no differences in cell number between sham and TBI across times post-injury, injury ages, or terminal ages (**Figures 4D–F**). However, both PND35 TBI and PND35 shams had fewer cells (95% CI: 0–8, $P = 0.97$, $K = 30.50$) than at PND17 (95% CI: 0–8, $P = 0.98$, $K = 41.18$), respectively ($d = 0.10$–0.13; **Figure 4E**).

TBI rats had fewer mean processes per microglial cell than shams at 1D (95% CI: −5 to 75, $P = 0.98$, $K = 49.5$) and 25D post-injury (95% CI: −11 to 75, $P = 0.97$, $K = 29.61$, $d = 0.02$; **Figure 4G**). PND17 TBI rats had fewer mean processes per microglia cell than PND17 shams (95% CI: −11 to 44, $P = 0.92$, $K = 11.40$), and PND35 TBI rats had fewer mean processes than PND35 shams (95% CI: 5–71, $P > 0.99$, $K > 100$), respectively ($d = 0.01$–0.02; **Figure 4H**). TBI rats at terminal age PND35 had fewer mean processes per microglial cell than shams (95% CI: 1–107, $P = 0.99$, $K > 100$, $d = 0.03$; **Figure 4I**). Rod microglia, a microglial phenotype associated with pathology

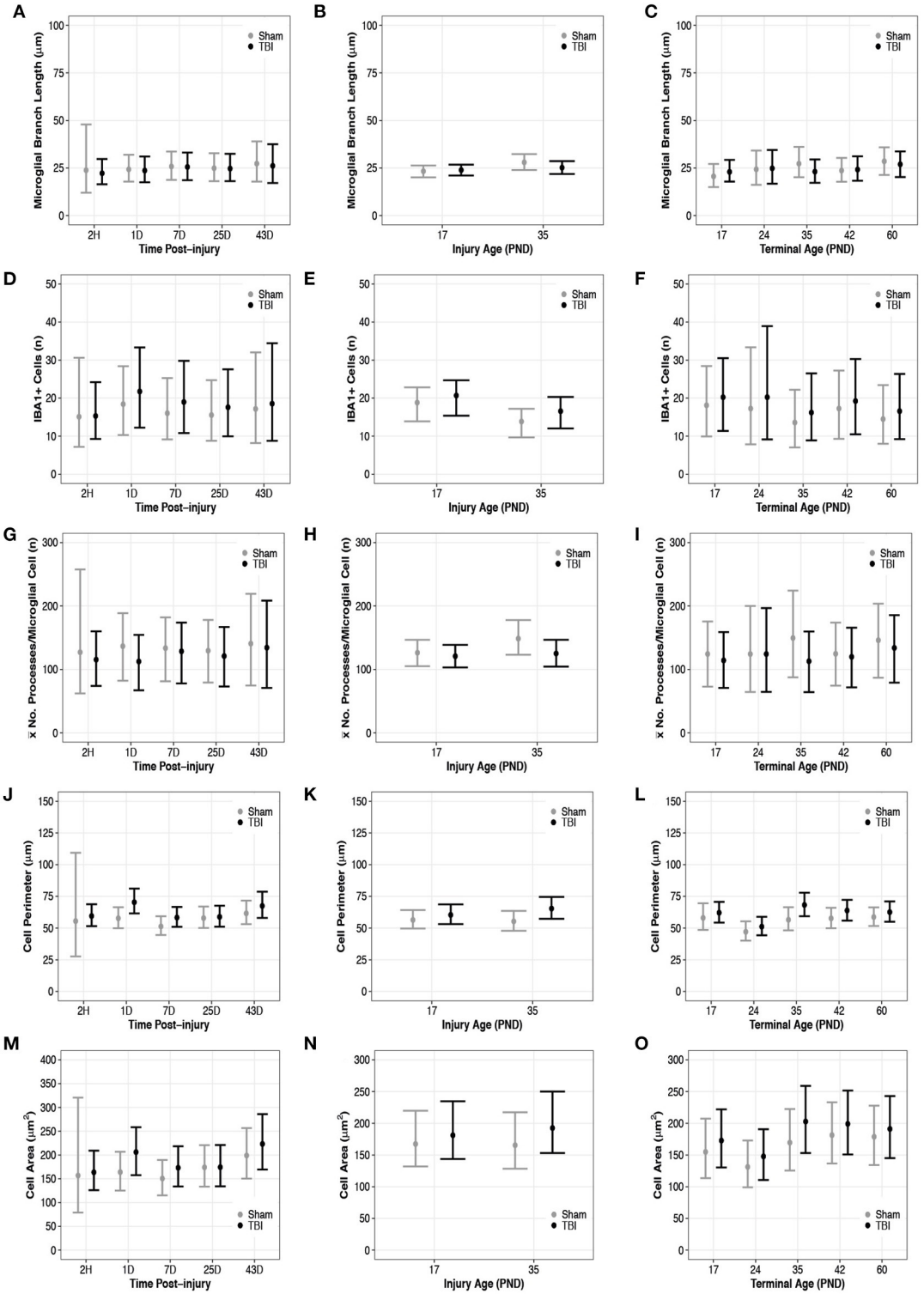

FIGURE 3 | Diffuse TBI activated microglia in the peri-injury cortex of rats injured at PND17 and PND35. Point estimates (posterior means) and corresponding 95% credible intervals (highest posterior density intervals) are presented. **(A–C)** There were no differences in microglial branch lengths between sham and TBI rats across

(Continued)

FIGURE 3 | times post-injury, injury ages, or terminal ages. **(B)** PND35 shams had longer branch lengths that PND17 shams. **(D,F)** There were no differences in number of cells between sham and TBI across times post-injury and terminal ages. **(E)** Sham and TBI rats at PND35 had fewer cells than sham and TBI rats at PND17. PND17 TBI rats had more cells than PND17 shams. PND35 TBI rats had more cells than PND35 shams. **(G–I)** Sham and TBI rats had similar mean processes per microglial cell across times post-injury, injury ages, and terminal ages, **(H)** and PND35 shams had more mean processes per microglial cell than PND17 shams. **(J)** TBI rats has a longer cell perimeter at 1D, 7D, and 43D post-injury compared to shams. TBI rats at 1D had a longer cell perimeter compared to TBI at 2H, 7D, and 25D post-injury. **(K)** TBI rats had a longer cell perimeter at PND17 and PND35 compared to their respective shams. **(L)** TBI rats had a longer cell perimeter at PND35 and PND42 compared to shams and PND24 had a shorter cell perimeter compared to all other ages. **(M)** TBI rats had a larger cell area at 1D, 7D, and 43D post-injury compared to shams. TBI rats at 1D had a larger cell area compared to 2H, 7D, and 25D post-injury. **(N)** PND35 TBI rats had a larger cell area compared to PND35 shams. **(O)** Cell area was shorter at PND24 compared to all other ages.

(59, 60), were observed in the S1BF of PND17 rats but not in PND35 rats (**Figure 2B**). Although rod microglia were not observed in cortical regions of interest in PND35 rats, this is not evidence for their absence in PND35 rats and therefore full brain analysis is warranted to reach that conclusion.

Diffuse TBI Increased Microglial Cell Area but Not Cell Perimeter Size in the S1BF of Rats Injured at Both PND17 and PND35

Overall, microglia in the S1BF of PND35 rats had an increased cell body area compared to the S1BF of PND17 rats, suggesting a greater phagocytic potential in PND35 rats. TBI did not affect cell perimeter in the S1BF (**Figures 4J–L)**, however, our data support TBI increased cell area in the S1BF (**Figures 4M–O**). There were no differences in cell body perimeter length between TBI and sham rats across times post-injury (**Figure 4J**); however, TBI rats at 1D post-injury had larger cell body areas than shams (95% CI: 28–145, $P > 0.99$, $K > 100$; $d = 0.01$; **Figure 4M**). There were no differences in cell body perimeter lengths between TBI and sham rats, or between TBI rats, at injury ages PND17 or PND35 ($P < 0.90$, $K \leq 3.00$; **Figure 4K**). However, PND35 TBI rats had larger cell body areas than both PND35 and PND17 shams (95% CI: 19–115, $P > 0.99$, $K > 100$), and PND17 TBI rats (95% CI: −3 to 92, $P > 0.99$, $K > 100$, $d < 0.01$; **Figure 4N**).

There were no differences in cell body perimeter length between TBI and sham rats across terminal ages (**Figure 4L)**, but TBI rats at terminal age PND35 had larger cell body areas than shams (95% CI: 42–156, $P > 0.99$, $K > 100$, $d = 0.01$; **Figure 4O**). Additionally, cell body area increased in TBI rats across time, given TBI rats at terminal age PND60 had larger cell body areas than TBI rats at terminal age PND17 (95% CI: −20 to 72, $P = 0.95$, $K = 16.97$, $d < 0.01$; **Figure 4O**).

Diffuse TBI Activated Microglia in the Perirhinal Cortex of Rats Injured at Both PND17 and PND35

Overall, there were more microglia in the perirhinal cortex of PND17 rats that had shorter branches and fewer processes compared to PND35, suggesting that TBI caused de-ramification and microglial activation in PND17 rats compared to PND35 rats in the perirhinal cortex. There were no differences in microglial branch lengths between sham and TBI across times post-injury (**Figure 5A).** PND17 TBI rats had shorter microglial branch lengths than PND17 shams (95% CI: −1 to 6, $P = 0.95$, $K = 20.43$) and PND35 TBI rats had shorter branch lengths than PND35 shams (95% CI: 0–9, $P = 0.98$, $K = 52.81$), respectively ($d = 0.10$–0.11; **Figure 5B)**. Additionally, PND35 TBI rats had longer microglial branch lengths than PND17 TBI rats (95% CI: 1–8, $P = 0.99$, $K > 100$, $d = 0.13$; **Figure 5B**). TBI rats had shorter microglial branch lengths than shams at terminal ages PND24 (95% CI: −4 to 13, $P = 0.91$, $K = 10.40$), PND42 (95% CI: 95% CI: −1 to 12, $P = 0.98$, $K = 60.86$) and PND60 (95% CI: −2 to 12, $P = 0.98$, $K = 49.85$), respectively ($d = 0.09$–0.10; **Figure 5C**).

There were no differences in number of microglia between sham and TBI rats across times post-injury, injury ages, and terminal ages (**Figures 5D–F**). However, PND35 shams (95% CI: 0–8, $P = 0.98$, $K = 47.39$) and PND35 TBI rats (95% CI: 1–8, $P = 0.99$, $K = 92.75$) had fewer microglia, respectively, compared to PND17 ($d = 0.14$; **Figure 5E**).

There were no differences in mean number of processes per microglial cell between sham and TBI rats across times post-injury (**Figure 5G**). TBI rats had fewer mean processes per microglial cell than shams at injury ages PND17 (95% CI: −4 to 38, $P = 0.98$, $K = 52.57$) and PND35 (95% CI: −10 to 46, $P = 0.95$, $K = 20.78$), respectively ($d = 0.01$–0.02; **Figure 5H**). Additionally, PND35 TBI rats had more mean processes per microglial cell than PND17 TBI rats (95% CI: 5–48, $P = 0.98$, $K = 61.50$, $d = 0.02$; **Figure 5H**). TBI rats had fewer mean processes per microglial cell than shams at terminal ages PND24 (95% CI: −22 to 75, $P = 0.96$, $K = 23.05$) and PND42 (95% CI: −11 to 73, $P = 0.99$, $K = 84.11$, $d = 0.02$; **Figure 5I**).

Diffuse TBI Did Not Affect Microglial Cell Perimeter or Cell Area Size in the Perirhinal Cortex of Rats Injured PND17 or PND35

There were no differences in cell body perimeter lengths among times post-injury, injury ages, or terminal ages in the perirhinal cortex (**Figures 5J–L**). Both TBI (95% CI: 3–91, $P > 0.99$, $K > 100$) and sham rats (95% CI: 9–98, $P > 0.99$, $K > 100$) at 43D post-injury had larger cell body areas than other times post-injury ($d = 0.01$; **Figure 5M**), which suggests increasing cell body size with time; however, there were no injury-induced differences in area between injury ages (**Figure 5N**).

There were no differences in cell body area between TBI and sham rats at each terminal age ($P \leq 0.91$, $K \leq 4.00$), but TBI rats at PND24 had a smaller cell body area than other time points (95% CI: 8–69, $P > 0.99$, $K > 100$), and both TBI and sham rats at PND60 had larger cell body areas than PND17, PND24, and PND35 (95% CI: −10 to 61, $P = 0.98$, $K = 45.33$, $d = 0.006$–0.01; **Figure 5O**). These findings further support increasing cell body size with time.

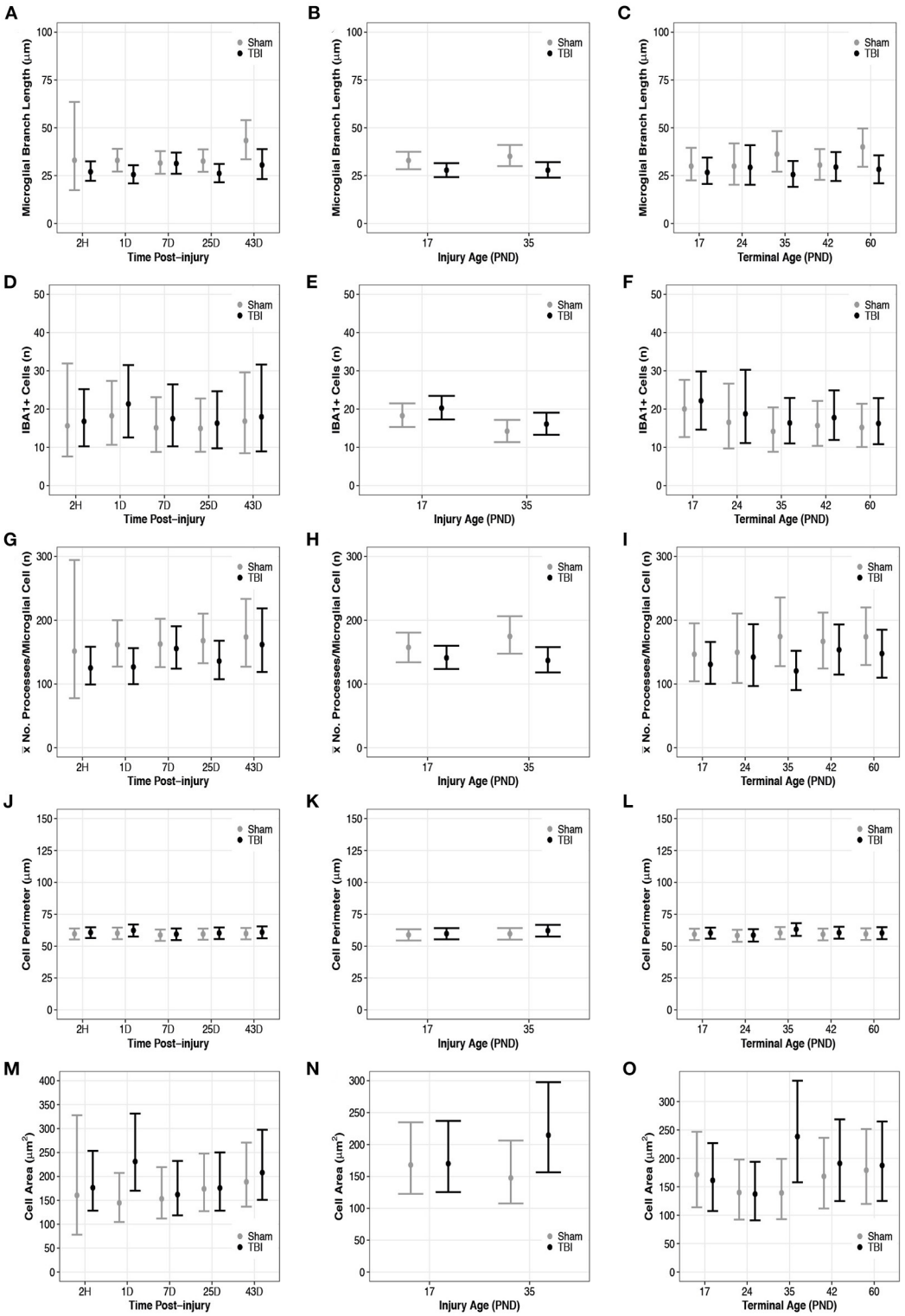

FIGURE 4 | Diffuse TBI activated microglia in the S1BF of rats injured at PND17 and PND35. Point estimates (posterior means) and corresponding 95% credible intervals (highest posterior density intervals) are presented. **(A)** TBI rats at 1D, 25D, and 43D post-injury had shorter microglial branch lengths than shams. **(B)** TBI rats

(Continued)

FIGURE 4 | had shorter microglial branch lengths than shams at both injury ages PND17 and PND35. **(C)** TBI rats at terminal ages PND35 and PND60 had shorter microglial branch lengths than shams. **(D–F)** There were no differences in cell number between sham and TBI across times post-injury, injury ages, or terminal ages. **(E)** Both sham and TBI rats had fewer cells at injury age PND35 compared to PND17. **(G)** TBI rats had fewer mean processes per microglial cell than shams at 1D and 25D post-injury. **(H)** TBI rats had fewer mean processes per microglia cell than shams at both injury age PND17 and PND35. **(I)** TBI rats at terminal age PND35 had fewer mean processes per cell than shams. **(J–L)** TBI did not affect cell perimeter. **(M)** TBI rats at 1D had a larger cell area than sham. **(N)** PND35 TBI rats had a larger cell area than PND35 shams and PND17 TBI. **(O)** TBI rats at terminal age PND35 had a larger cell area than shams, and TBI rats at PND60 had a larger area than TBI rats at PND17.

Diffuse TBI Did Not Affect GFAP Expression in the Peri-Injury Cortex of Rats Injured at PND17 or PND35

There were no differences in cell coverage between sham and TBI across time post-injury, injury ages, or terminal ages (**Figures 6, 7A–C**). There were also no differences in number of GFAP + cells between sham and TBI across times post-injury, injury ages, and terminal ages (**Figures 7D–F**). Sham and TBI also had similar pixel coverage values across time post-injury, injury ages, and terminal ages (**Figures 7G–I**).

Diffuse TBI Did Not Affect GFAP Expression in the S1BF of Rats Injured at PND17 or PND35

There were no differences in cell coverage between sham and TBI across times post-injury, injury ages, and terminal ages in the S1BF (**Figures 8A–C**). There were also no differences in number of GFAP + cells between sham and TBI across times post-injury, injury ages and terminal ages (**Figures 8D–F**). However, both sham (95% CI: −1 to 16, $P = 0.95$, $K = 18.45$) and TBI rats (95% CI: 0–15, $P = 0.97$, $K = 29.15$) had fewer GFAP + cells at terminal age PND42 ($d = 0.13$–0.16; **Figure 8F**). Sham and TBI also had similar pixel coverage values across terminal ages, injury ages, and times post-injury (**Figures 8G–I**).

Diffuse TBI Did Not Affect GFAP Expression in the Perirhinal Cortex of Rats Injured at PND17 or PND35

There were no differences in GFAP + cell coverage between sham and TBI rats across time post-injury, injury ages, and terminal ages in the perirhinal cortex (**Figures 9A–C**). There were also no differences in number of GFAP + cells between sham and TBI rats across time post-injury, injury ages, or terminal ages (**Figures 9D–F**). Sham and TBI rats also had similar pixel coverage values across time post-injury, injury ages, and terminal ages (**Figures 9G–I**).

DISCUSSION

Microglia play a key role in both the positive and negative effects of inflammation post-injury (61). It is important to understand microglial physiology under non-inflammatory and inflammatory conditions during early life. In this study, we found differences in the microglial response between PND17 and PND35 rats (both injured and sham) throughout the cortex using microglial branch length, microglial processes per cell, and microglial abundance as quantitative outcomes **(Figure 10)**. Our results show that TBI activated microglia in both PND17 and PND35 rats in comparison to uninjured shams. To our knowledge, this is the first study to comprehensively examine microglial morphology after mFPI in PND17 and PND35 rats at acute and sub-acute time points.

In agreement with previously published studies, we detected a change in microglial morphology and/or abundance after TBI regardless of age-at-injury (13, 28, 62). Similar to recent clinical observations (63), we found that microglial activation quickly ensued after TBI (1D post-injury) and was maintained into early adulthood (60D post-injury). This chronic maintenance of an activated morphology is supported by both pre-clinical and clinical data, as activated microglia have been observed in patients 17-years post-injury, and we have reported microglia activation at 9 months post-injury in rats (13, 64, 65). Such prolonged microglial activation is often associated with negative developmental outcomes, such as chronic behavioral deficits, progressive cortical thickness reduction, decreased corpus callosum area, neurodegeneration, and cognitive deficits (24, 66–69). In the clinic, behavioral and affective outcomes are exacerbated in patients injured at a younger age; therefore, our study introduces a plausible, microglia-centric reason for this (3, 66, 70).

In all regions tested, our results show that there were more microglial cell bodies in PND17 rats compared to PND35 rats, independent of injury. This suggests that, regardless of injury status, PND17 rats may have a greater density of microglia. The increased number of microglia may be the result of overshoot in microglia observed in early post-natal life (71). Alternatively, the number of microglia may decrease after they fulfill their role in neuronal circuit formation in the developing brain (postnatal weeks 1–3 in the rodent) (72, 73). We also found more microglial activation in the perirhinal cortex in PND17 rats compared to PND35 rats, which may be due to the increased circuit remodeling during this developmental period (74), as microglia have been shown to reach their full ramification level by PND14 (75). Furthermore, we observed the presence of rod microglia in the S1BF of PND17 rats but not PND35 rats. The rod microglial morphology is associated with inflammation and pathology; however, their exact role after TBI is unknown (59, 60, 76). The presence of rod microglia in PND17 brain-injured rats, but not PND35 rats, supports a differential immune response to diffuse TBI dependent on age-at-injury, where young rats may be more vulnerable to inflammatory pathology.

We examined the microglia cell body size (area and perimeter) because a larger cell body is a hallmark feature of microglia activation (77). Overall, TBI rats had a larger cell body (measured by area and perimeter) than sham rats, indicating that microglia

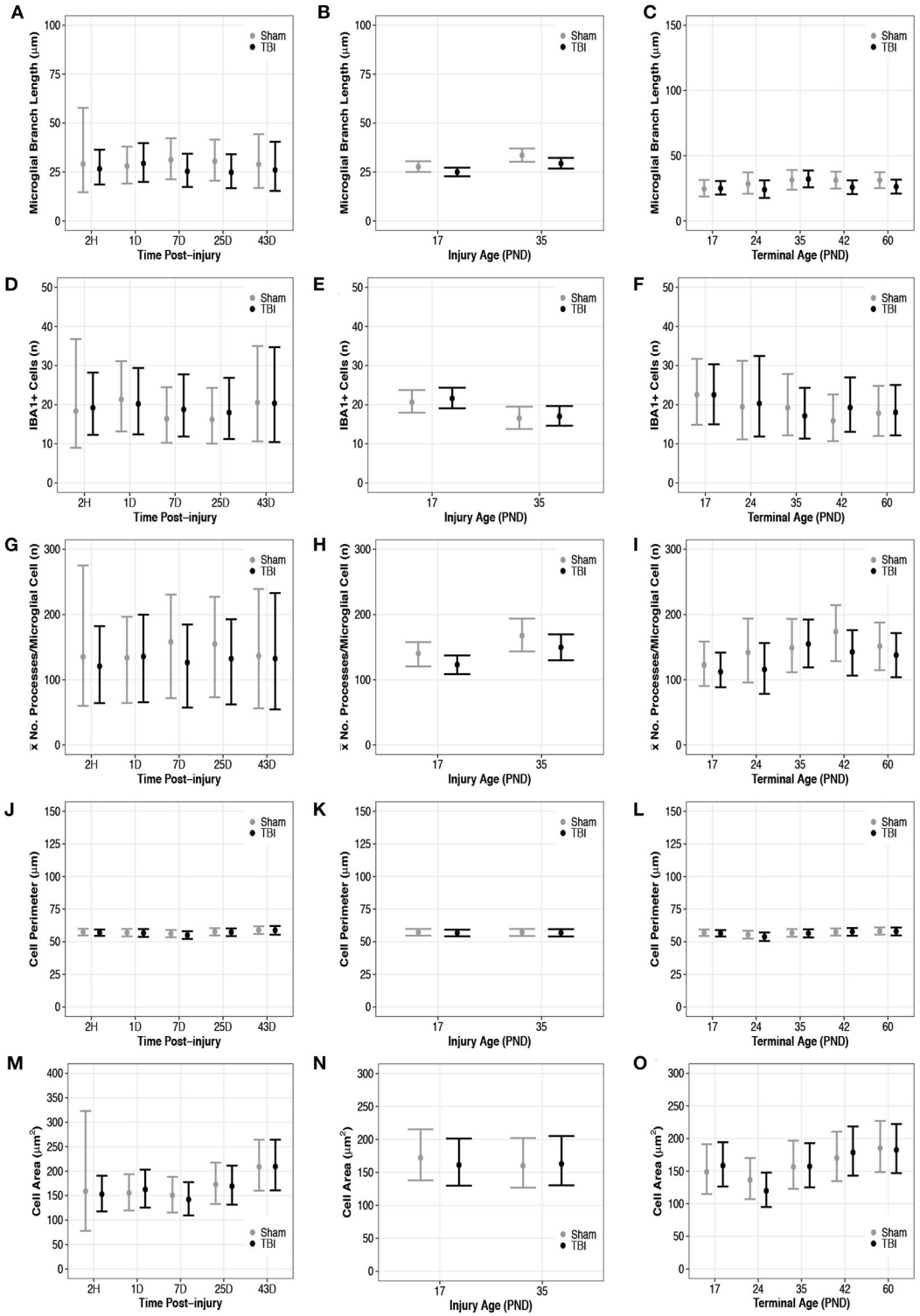

FIGURE 5 | Diffuse TBI activated microglia in the perirhinal cortex of rats injured at PND17 and PND35. Point estimates (posterior means) and corresponding 95% credible intervals (highest posterior density intervals) are presented. **(A)** There were no differences in microglial branch lengths between sham and TBI across times

(Continued)

FIGURE 5 | post-injury. **(B)** TBI rats had shorter microglial branch lengths compared to shams at injury ages PND17 and PND35. PND35 TBI rats had longer microglial branch lengths than PND17 TBI rats. **(C)** TBI rats had shorter microglial branch lengths than shams at terminal ages PND24, PND42, and PND60. **(D–F)** There were no differences in the number of microglia between sham and TBI rats across times post-injury, injury ages, and terminal ages. **(E)** Both sham and TBI rats at PND35 had fewer microglia than PND17 rats. **(G)** The mean number of processes per microglia in sham and TBI rats across times post-injury were similar. **(H)** TBI rats had fewer mean processes per microglia than shams at injury ages PND17 an PND35, and PND35 TBI rats had more mean processes per microglia than PND17 TBI rats. **(I)** TBI rats had fewer mean processes per microglia than shams at terminal ages PND24 and PND42. **(J–L)** There were no differences between TBI and sham rats in cell body perimeter lengths among times post-injury, injury ages, or terminal ages. **(M)** Both TBI and sham rats at 43D post-injury had larger cell body areas than other times post-injury. **(N)** There were no differences in cell body area between TBI and sham rats between injury ages. **(O)** TBI rats at PND24 had smaller cell body area than other time points, and both TBI and sham rats at PND60 had larger cell body areas than PND17, PND24, and PND35.

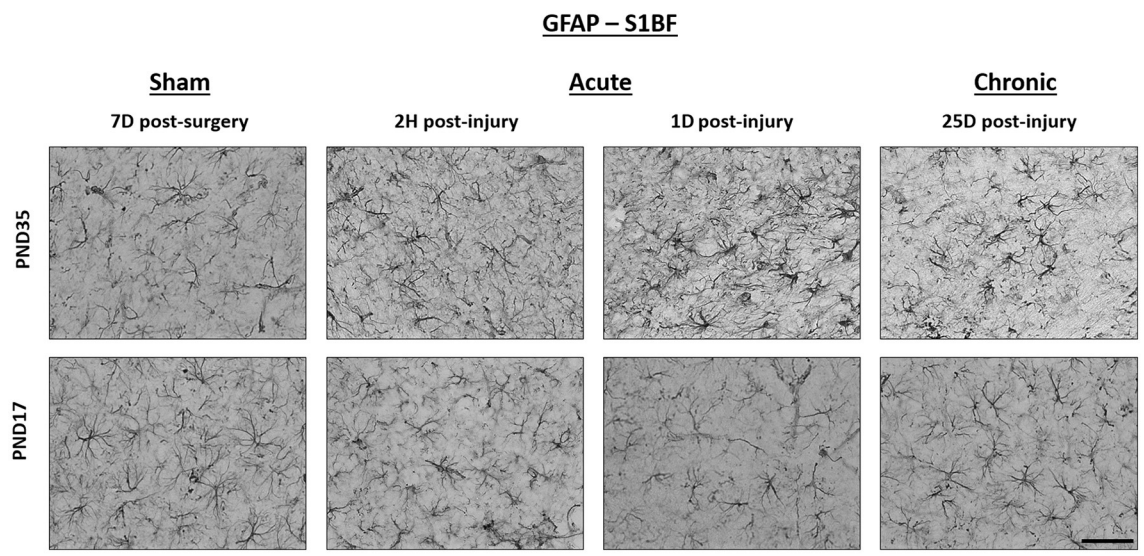

FIGURE 6 | TBI caused no detectable difference in GFAP expression in PND17 or PND35 rats. Immunohistochemistry was used to examine GFAP expression. Representative images shown are from both PND17 and PND35 injured rats at 7 days post-sham surgery and 2 hours (H), 1 day (D), and 25D post-injury. All representative images are from the S1BF. Scale bar = 50 μm. (sham $n = 39$, TBI $n = 35$).

adopt and sustain an activated phenotype after experimental TBI (sustained until PND60 in the peri-injury cortex). Post-injury enlargement of microglia cell soma size and ameboid morphology have been well-documented (78, 79). This is likely because of increased phagocytic activity of microglia in pathological conditions (15), though the size is rarely quantified. Rats subjected to TBI had larger cell bodies than shams in the peri-injury and S1BF cortices, and the cells were largest at 1D post-injury. This suggests that microglia may respond quickly to the excitotoxicity, cell death, and off-set homeostasis associated with TBI (80).

Although the primary objective of this study was to investigate the effects of age-at-injury on glial activation after diffuse TBI, we utilized a unique study design that also allowed evaluation of glial activation as a function of both time post-injury and animal age at the time of tissue collection (terminal age). In both the peri-injury cortex and the S1BF, there was extensive microglial activation at 1, 7, and 25 DPI that was, in part, resolved by 43 DPI. Minimal support existed for terminal age influencing microglial activation. Overall, we conclude that time post-injury had a greater impact on the microglial response to diffuse TBI compared to terminal age. Microglia were activated immediately after injury, with peak activation at 1 DPI. This result is congruous with our previous studies that showed microglial activation and number increase immediately after TBI and peak within the first 7 days post-injury (81, 82).

We also investigated whether age influenced microglia cell size, and if microglia grew as a rat aged. Our data did not support our hypothesis that microglia cell somas increase in size with brain growth. Some of our results weakly suggested that microglial cell bodies grew with time and were limited in the amount that their cell soma could grow during microglial activation at younger ages. For example, we found that in the peri-injury and S1BF cortices, microglial cell body perimeter and area were larger in PND35 rats than in PND17 rats. Overall, our evidence suggests that microglial cell bodies do not significantly grow between PND17 and PND60. These findings support the work of Dos Santos et al., who determined that microglial cell size is governed by a mechanism that evolved >200 million years ago and is not dependent on brain size (83). Microglial cell body size throughout post-natal development has not been well-documented and, to our knowledge, this is the first study to detail this in a TBI model. However, we caution that the effect sizes for our data

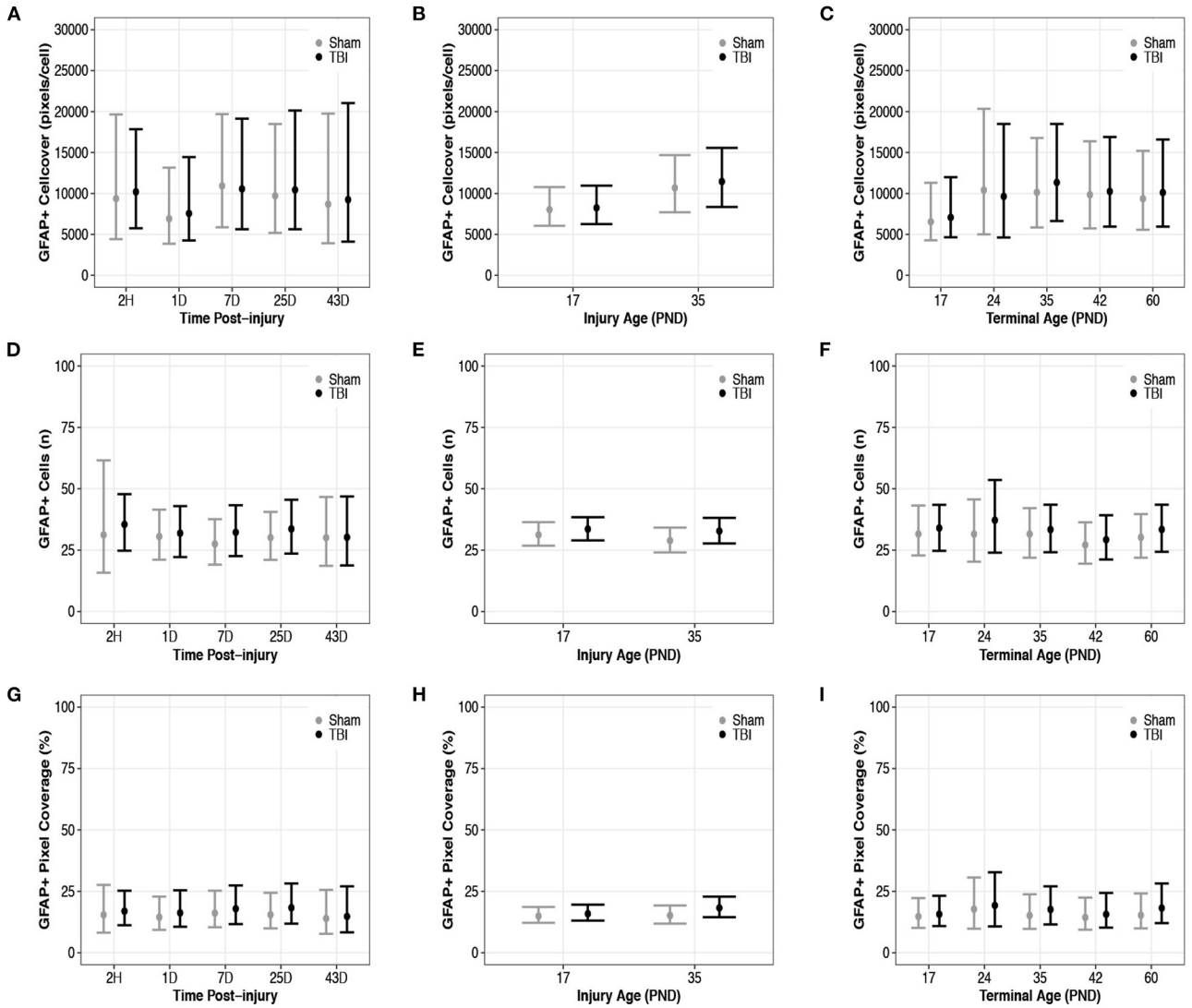

FIGURE 7 | Diffuse TBI did not affect GFAP expression in the peri-injury cortex. Point estimates (posterior means) and corresponding 95% credible intervals (highest posterior density intervals) are presented. There were no differences between sham and TBI rats across times post-injury, injury ages, or terminal ages **(A–C)** in cell coverage, **(D–F)** GFAP+ cell number, **(G–I)** or pixel coverage values.

were small, so any conclusions about cell soma size warrant further investigation.

Astrocytes become hypertrophic in response to injury (84). Astrocytes contain an intracellular network of the intermediate fiber GFAP, and upon mechanical stress, GFAP expression is upregulated (85–87); hence, GFAP has been heavily investigated as a blood biomarker of TBI (88, 89). We found no differences in GFAP expression between sham and TBI rats across time post-injury, terminal age, or injury age. These results are similar to our previously reported data where we observed no injury-induced changes in GFAP immunoreactivity at chronic time points compared to uninjured rats (13). Although GFAP upregulation is a common marker for distressed astrocytes (85, 86), it does not assess for astrocyte morphology. Considering there are up to eight distinct astrocyte morphologies (90), it is possible that the morphology changes in response to TBI without a detectable change in GFAP expression. Therefore, although our results suggest a negligible astrocytic response to TBI in these age groups, we cannot rule out morphological changes.

A primary limitation of this study was the use of only male rats, considering there is evidence of sex differences in cellular and systemic outcomes of TBI (37). Our ongoing

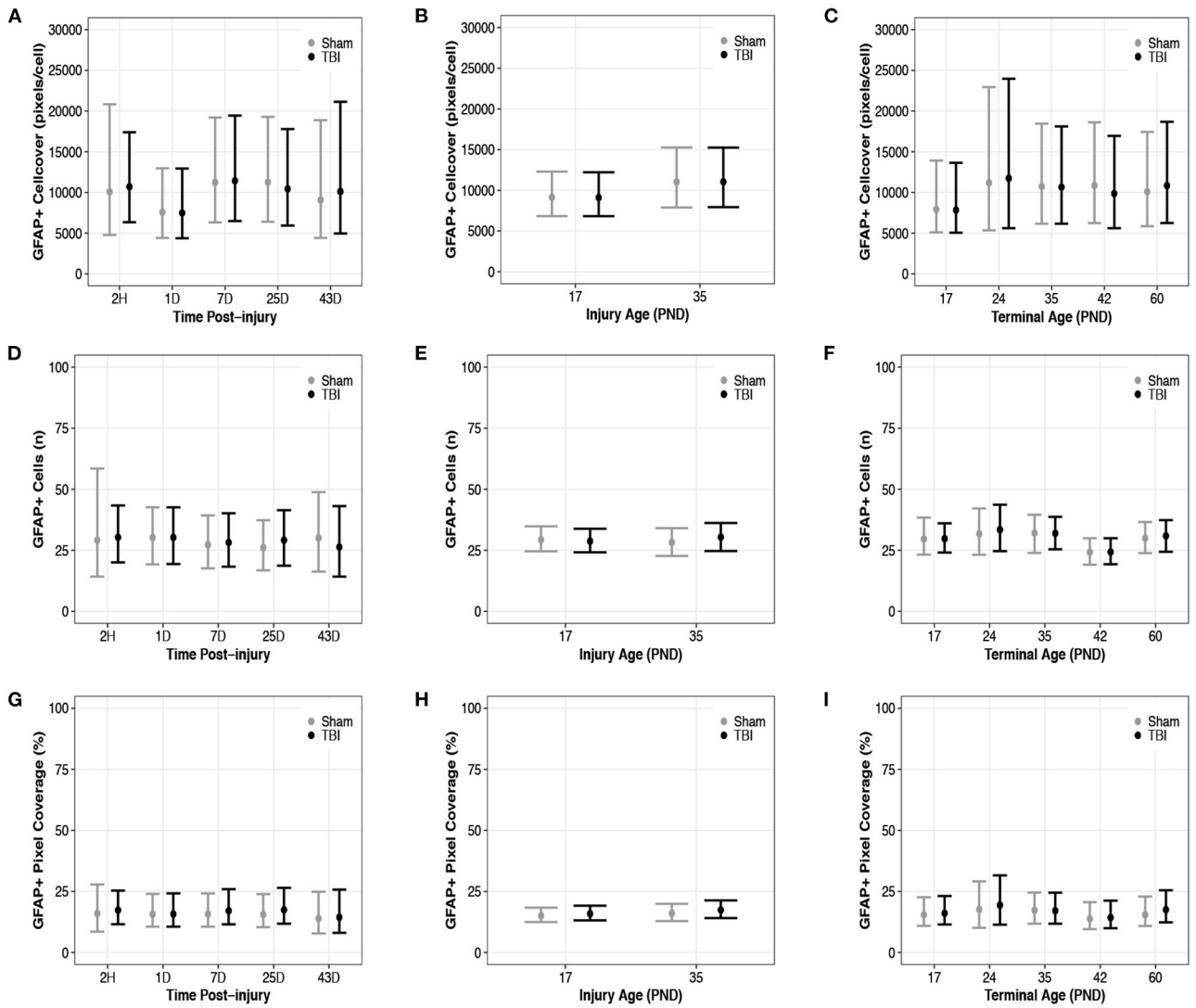

FIGURE 8 | Diffuse TBI did not affect GFAP expression in the S1BF. Point estimates (posterior means) and corresponding 95% credible intervals (highest posterior density intervals) are presented. **(A–C)** There were no differences in cell coverage between sham and TBI rats across times post-injury, injury ages, and terminal ages. **(D,E)** There were no differences in the number of GFAP + cells between sham and TBI rats across times post-injury or injury ages, **(F)** however, at terminal age PND42, both sham and TBI rats had fewer GFAP + cells than other terminal ages. **(G–I)** Sham and TBI rats had similar pixel coverage values across terminal ages, injury ages, and times post-injury.

studies in juvenile rats include sex as a biological variable that affects behavior and neuropathology. In the current study, we focused on cortical regions, but we have previously reported glial changes in white matter (13). Additional studies are needed to investigate the acute and sub-acute glial response in white matter tracts, as they likely differ substantially from those in gray matter in terms of both magnitude and phenotype. Another limitation of the current study is that the glial response to TBI was examined as an isolated event and future studies that investigate how glial activation influences neuropathology and functional outcome are warranted. We have previously shown that brain injury at PND17 or PND35 resulted in acute and sub-acute cognitive, motor, and affective deficits compared to adult-injured and naïve rats (24). We have also shown that regardless of age-at-injury, diffuse TBI resulted in neuropathology in juvenile rats (13). Based on those previous studies, glial activation likely contributes to TBI-induced behavioral deficits and neuropathology.

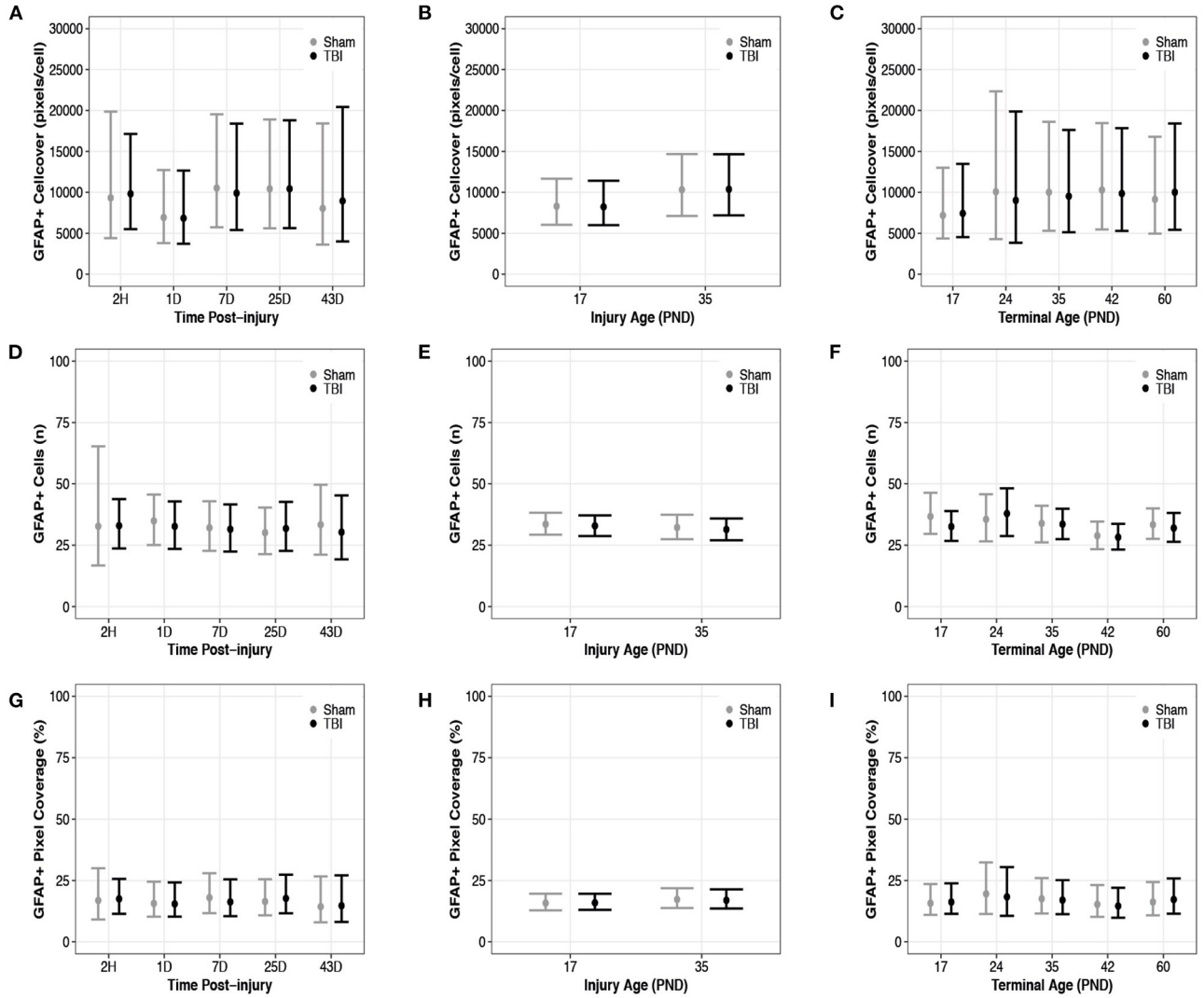

FIGURE 9 | Diffuse TBI did not affect GFAP expression in the perirhinal cortex. Point estimates (posterior means) and corresponding 95% credible intervals (highest posterior density intervals) are presented. There were no differences between sham and TBI rats across time post-injury, injury ages, or terminal ages **(A–C)** in cell coverage, **(D–F)** GFAP + cell number, **(G–I)** or pixel coverage values.

As with any histological study, there is the added limitation of working with 2-dimensional images in a 3-dimensional space. This means that cells could be sliced in different planes, rather than centrally, thereby increasing the probability of larger cells being caught in the slice. To combat this, and to ensure our images accurately represented the biological specimen, we used Z-stacked images that spanned the 40 μm tissue slice [microglial are around 15–30 μm in width/diameter (91), with the exception of rod microglia which have an elongated cell body (76)], and adhered to the rules of Nyquist sampling. Furthermore, despite the moderate to strong support for multiple differences between groups in this study, many effect sizes were small, which indicates that additional data need to be collected to further evaluate the magnitude and importance of identified effects.

CONCLUSIONS AND FUTURE DIRECTIONS

In conclusion, we found evidence that rats injured at PND17 had increased widespread microglial activation. A more activated phenotype was also seen in shams at

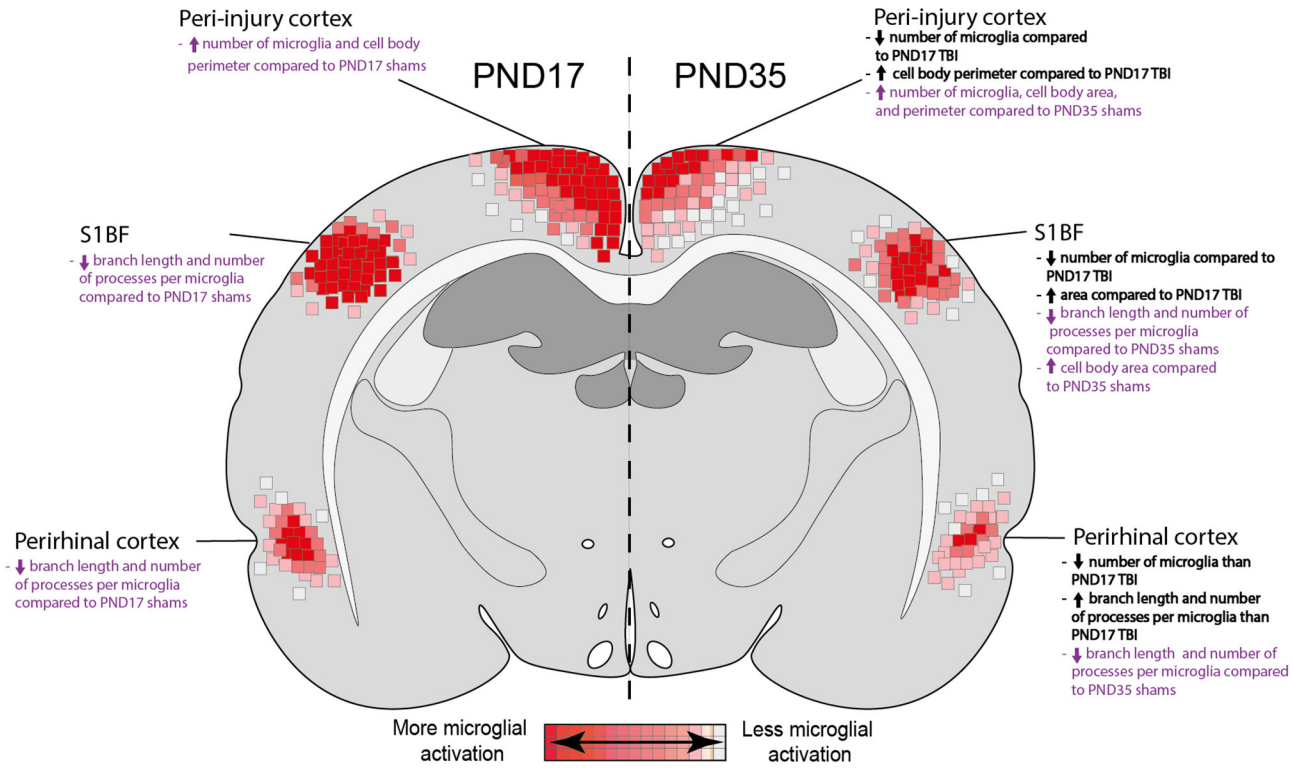

FIGURE 10 | Summary heat map of microglial activation in PND17 rats compared to PND35. Quantitative skeletal analysis was used to assess microglia morphology (number of microglia, number of microglia branches, branch processes per cell) and results are summarized in a heat map. Results in bold black text indicate differences between PND35 TBI and PND17 TBI. Results in purple text indicate differences between TBI groups and their respective shams. Overall, TBI activated microglia in both ages. Rats injured at PND35 had fewer microglia in all cortical regions of interest compared to rats injured at PND17. PND17 had more microglial activation (de-ramification) compared to rats injured at PND35, indicated by at least one measured outcome in each cortical region of interest.

PND17, but injury still further decreased the amount of ramification. This suggests some physiological differences between microglia in the PND17 rat compared to microglia in the PND35 rat, and that injury might cause more de-ramification in PND17 microglia. We therefore conclude that age-at-injury significantly influenced the microglial response to TBI. Such de-ramification of younger microglia and their smaller cell body size may render them less able to respond to injury and therefore make them more vulnerable to injury-induced physiological and affective deficits.

AUTHOR'S NOTE

RR was an employee of Phoenix Children's Hospital during the data collection for this study.

DATA AVAILABILITY STATEMENT

The datasets presented in this study can be found in online repositories. The name of the repository and accession number can be found below: Dryad, https://doi.org/10.5061/dryad.5tb2rbp4r.

ETHICS STATEMENT

The animal study was reviewed and approved by Institutional Animal Care and Use Committee (IACUC) at the University of Arizona (protocol 13–460). The Animal Research: Reporting *in vivo* Experiments (ARRIVE) guidelines were followed.

AUTHOR CONTRIBUTIONS

TG helped execute the experiments, led data collection, analyzed data, constructed figures, and led manuscript writing. SM analyzed data, helped construct figures, and assisted with writing and editing the manuscript. JO helped collect data and assisted with writing and editing the manuscript. RR conceived and designed the study, executed the experiments, analyzed data, constructed figures, and assisted with writing and editing the manuscript. All authors contributed to the article and approved the submitted version.

FUNDING

This study was supported by a grant from the National Institute of Neurological Disorders and Stroke (R21NS120022 to RR) and the University of Arizona College of Medicine—Phoenix and Phoenix Children's Hospital Mission Support (RR).

ACKNOWLEDGMENTS

The authors would like to thank Jonathan Lifshitz, Jordan Harrison, and Kelsey Newbold for their assistance on the project.

SUPPLEMENTARY MATERIAL

The Supplementary Material for this article can be found online at: https://www.frontiersin.org/articles/10.3389/fneur.2021.804139/full#supplementary-material

Supplementary Figure 1 | Iba1 stained microglia in the peri-injury cortex at 2 h (H), 1 day (D), and 25D post-injury compared to uninjured shams at 7D. All representative images were taken in the peri-injury cortex. Scale bars = 50 μm (sham $n = 39$, TBI $n = 35$).

Supplementary Figure 2 | Iba1 stained microglia in the perirhinal cortex at 2 h (H), 1 day (D), and 25D post-injury compared to uninjured shams at 7D. All representative images were taken in the perirhinal cortex. Scale bars = 50 μm (sham $n = 39$, TBI $n = 35$).

Supplementary Figure 3 | GFAP stained microglia in the peri-injury cortex at 2 h (H), 1 day (D), and 25D post-injury compared to uninjured shams at 7D. All representative images were taken in the peri-injury cortex. Scale bars = 50 μm (sham $n = 39$, TBI $n = 35$).

Supplementary Figure 4 | GFAP stained microglia perirhinal cortex at 2 h (H), 1 day (D), and 25D post-injury compared to uninjured shams at 7D. All representative images were taken in the perirhinal cortex. Scale bars = 50 μm (sham $n = 39$, TBI $n = 35$).

REFERENCES

1. Peterson AB, Zhou H, Thomas KE, Daughtery J. *Traumatic Brain Injury-related Hospitalizations and Deaths by Age Group, Sex, and Mechanism of Injury*. Atlanta, GA: National Center for Injury Prevention and Control (U.S.). (2017).
2. Prins ML, Hales A, Reger M, Giza CC, Hovda DA. Repeat traumatic brain injury in the juvenile rat is associated with increased axonal injury and cognitive impairments. *Dev Neurosci.* (2010) 32:510–8. doi: 10.1159/000316800
3. Sayrs LW, Ortiz JB, Notrica DM, Kirsch L, Kelly C, Stottlemyre R, et al. Intimate partner violence, clinical indications, and other family risk factors associated with pediatric abusive head trauma. *J Interpers Viol.* (2020). doi: 10.1177/0886260520967151
4. Rowe RK, Murphy SM, Handmaker H, Lifshitz J. Population-level epidemiology of concussion concurrent with domestic violence in Arizona, USA. *J Neurotrauma*. (2021). 38:2301–2310. doi: 10.1089/neu.2021.0022
5. Dewan MC, Mummareddy N, Wellons, 3rd JC, Bonfield CM. epidemiology of global pediatric traumatic brain injury: qualitative review. *World Neurosurg.* (2016) 91:97–509 e491. doi: 10.1016/j.wneu.2016.03.045
6. Anderson V, Catroppa C, Morse S, Haritou F, Rosenfeld J. Functional plasticity or vulnerability after early brain injury? *Pediatrics.* (2005) 116:1374–82. doi: 10.1542/peds.2004-1728
7. Ryan NP, Anderson V, Godfrey C, Beauchamp MH, Coleman L, Eren S, et al. Predictors of very-long-term sociocognitive function after pediatric traumatic brain injury: evidence for the vulnerability of the immature "social brain". *J Neurotrauma.* (2014) 31:649–57. doi: 10.1089/neu.2013.3153
8. Serpa RO, Ferguson L, Larson C, Bailard J, Cooke S, Greco T, et al. Pathophysiology of pediatric traumatic brain injury. *Front Neurol.* (2021) 12:696510. doi: 10.3389/fneur.2021.696510
9. Greig NH, Tweedie D, Rachmany L, Li Y, Rubovitch V, Schreiber S, et al. Incretin mimetics as pharmacologic tools to elucidate and as a new drug strategy to treat traumatic brain injury. *Alzheimers Dement.* (2014) 10:S62–75. doi: 10.1016/j.jalz.2013.12.011
10. Shinozaki Y, Shibata K, Yoshida K, Shigetomi E, Gachet C, Ikenaka K, et al. Transformation of astrocytes to a neuroprotective phenotype by microglia via P2Y. *Cell Rep.* (2017) 19:1151–64. doi: 10.1016/j.celrep.2017.04.047
11. Donat CK, Scott G, Gentleman SM, Sastre M. Microglial activation in traumatic brain injury. *Front Aging Neurosci.* (2017) 9:208. doi: 10.3389/fnagi.2017.00208
12. Hanlon LA, Raghupathi R, Huh JW. Depletion of microglia immediately following traumatic brain injury in the pediatric rat: implications for cellular and behavioral pathology. *Exp Neurol.* (2019) 316:39–51. doi: 10.1016/j.expneurol.2019.04.004
13. Doust YV, Rowe RK, Adelson PD, Lifshitz J, Ziebell JM. Age-at-injury determines the extent of long-term neuropathology and microgliosis after a diffuse brain injury in male rats. *Front Neurol.* (2021) 12:722526. doi: 10.3389/fneur.2021.722526
14. Streit WJ. Microglia and the response to brain injury. *Ernst Schering Res Found Workshop.* (2002) 39:11–24. doi: 10.1007/978-3-662-05073-6_2
15. Fu R, Shen Q, Xu P, Luo JJ, Tang Y. Phagocytosis of microglia in the central nervous system diseases. *Mol Neurobiol.* (2014) 49:1422–34. doi: 10.1007/s12035-013-8620-6
16. Sengupta P. The laboratory rat: relating its age with human's. *Int J Prev Med.* (2013) 4:624–30.
17. Anthony DC, Bolton SJ, Fearn S, Perry VH. Age-related effects of interleukin-1 beta on polymorphonuclear neutrophil-dependent increases in blood-brain barrier permeability in rats. *Brain.* (1997) 120:435–44. doi: 10.1093/brain/120.3.435
18. Webster KM, Sun M, Crack PJ, O'brien TJ, Shultz SR, Semple BD. Age-dependent release of high-mobility group box protein-1 and cellular neuroinflammation after traumatic brain injury in mice. *J Comp Neurol.* (2019) 527:1102–17. doi: 10.1002/cne.24589
19. Bianchi ME, Crippa MP, Manfredi AA, Mezzapelle R, Rovere Querini P, Venereau E. High-mobility group box 1 protein orchestrates responses to tissue damage via inflammation, innate and adaptive immunity, tissue repair. *Immunol Rev.* (2017) 280:74–82. doi: 10.1111/imr.12601
20. Claus CP, Tsuru-Aoyagi K, Adwanikar H, Walker B, Manvelyan H, Whetstone W, et al. Age is a determinant of leukocyte infiltration and loss of cortical volume after traumatic brain injury. *Dev Neurosci.* (2010) 32:454–65. doi: 10.1159/000316805
21. Anthony D, Dempster R, Fearn S, Clements J, Wells G, Perry VH, et al. CXC chemokines generate age-related increases in neutrophil-mediated brain inflammation and blood-brain barrier breakdown. *Curr Biol.* (1998) 8:923–6. doi: 10.1016/S0960-9822(07)00373-9
22. R Core Team. *R: A Language and Environment for Statistical Computing*. Vienna: R Foundation for Statistical Computing. (2021). Available online at: https://www.R-project.org/
23. Rowe RK, Harrison JL, Ellis TW, Adelson PD, Lifshitz J. Midline (central) fluid percussion model of traumatic brain injury in pediatric and adolescent rats. *J Neurosurg Pediatr.* (2018) 22:22–30. doi: 10.3171/2018.1.PEDS17449
24. Rowe RK, Ziebell JM, Harrison JL, Law LM, Adelson PD, Lifshitz J. Aging with traumatic brain injury: effects of age at injury on behavioral outcome following diffuse brain injury in rats. *Dev Neurosci.* (2016). 38:195–205. doi: 10.1159/000446773
25. Hosseini AH, Lifshitz J. Brain injury forces of moderate magnitude elicit the fencing response. *Med Sci Sports Exerc.* (2009) 41:1687–97. doi: 10.1249/MSS.0b013e31819fcd1b
26. Green TRF, Ortiz JB, Harrison JL, Lifshitz J, Rowe RK. Simultaneous cryosectioning of multiple rodent brains. *J Vis Exp.* (2018). 139:e58513. doi: 10.3791/58513
27. Beitchman J, Lifshitz J, Harris N, Currier-Thomas T, Lafrenaye A, Hanell A, et al. Spatial distribution of neuropathology and neuroinflammation elucidate the biomechanics of fluid percussion injury. *Neuro Rep.* (2021) 2:59–75. doi: 10.1089/neur.2020.0046
28. Morrison H, Young K, Qureshi M, Rowe RK, Lifshitz J. Quantitative microglia analyses reveal diverse morphologic responses in the rat cortex after diffuse brain injury. *Sci Rep.* (2017) 7:13211. doi: 10.1038/s41598-017-13581-z

29. Young K, Morrison H. Quantifying microglia morphology from photomicrographs of immunohistochemistry prepared tissue using imageJ. *J Vis Exp*. (2018). doi: 10.3791/57648
30. Ferrari SLP, Cribari-Neto F. Beta regression for modelling rates and proportions. *J Appl Stat*. (2004) 31:799–815. doi: 10.1080/0266476042000214501
31. Figueroa-Zuniga JI, Arellano-Valle RB, Ferrari SLP. Mixed beta regression: a Bayesian perspective. *Comput Stat Data Anal.* (2013) 61:137–47. doi: 10.1016/j.csda.2012.12.002
32. Hilbe JM. Negative binomial regression. *Mod Count Data.* (2014) 126–61. doi: 10.1017/CBO9781139236065.006
33. Cameron AC, Trivedi PK. Regression-based tests for overdispersion in the poisson model. *J Eco.* (1990) 46:347–64. doi: 10.1016/0304-4076(90)90014-K
34. Kleiber C, Zeileis A. *Applied Econometrics With R*. New York, NY: Springer-Verlag (2008).
35. Aarts E, Verhage M, Veenvliet JV, Dolan CV, Van Der Sluis S. A solution to dependency: using multilevel analysis to accommodate nested data. *Nat Neurosci.* (2014) 17:491–6. doi: 10.1038/nn.3648
36. Aarts E, Dolan CV, Verhage M, Van Der Sluis S. Multilevel analysis quantifies variation in the experimental effect while optimizing power and preventing false positives. *Bmc Neuroscience.* (2015) 16:94. doi: 10.1186/s12868-015-0228-5
37. Saber M, Giordano KR, Hur Y, Ortiz JB, Morrison H, Godbout JP, et al. Acute peripheral inflammation and post-traumatic sleep differ between sexes after experimental diffuse brain injury. *Eur J Neurosci.* (2020) 52:2791–814. doi: 10.1111/ejn.14611
38. Saber M, Murphy SM, Cho Y, Lifshitz J, Rowe RK. Experimental diffuse brain injury and a model of Alzheimer's disease exhibit disease-specific changes in sleep and incongruous peripheral inflammation. *J Neurosci Res.* (2021) 99:1136–60. doi: 10.1002/jnr.24771
39. Zhang Z, Hamagami F, Wang L, Grimm KJ, Nesselroade JR. Bayesian analysis of longitudinal data using growth curve models. *Int J Behav Dev.* (2007) 31:374–83. doi: 10.1177/0165025407077764
40. Lazic SE, Mellor JR, Ashby MC, Munafo MR. A bayesian predictive approach for dealing with pseudoreplication. *Sci Rep.* (2020) 10:2366. doi: 10.1038/s41598-020-59384-7
41. Van De Schoot R, Depaoli S. Bayesian analysis: where to start and what to report. *Eur Health Psychol.* (2014) 16:75–84.
42. Gelman A. Prior distributions for variance parameters in heirarchical models. *Bayesian Anal.* (2006) 1:515–34. doi: 10.1214/06-BA117A
43. Carpenter B, Gelman A, Hoffman MD, Lee D, Goodrich B, Betancourt M, et al. Stan: a probabilistic programming language. *J Stat Softw.* (2017). 76:1–32. doi: 10.18637/jss.v076.i01
44. Burkner PC. Brms: an r package for bayesian multilevel models using stan. *J Stat Software.* (2017) 80:1–28. doi: 10.18637/jss.v080.i01
45. Burkner PC. Advanced bayesian multilevel modeling with the r package brms. *R Journal.* (2018) 10:395–411. doi: 10.32614/RJ-2018-017
46. Team R. *RStudio: Integrated development for R. RStudio*. Boston: RStudio, PBC (2020).
47. Gelman A, Rubin DB. Inference from iterative simulation using multiple sequences. *Stat Sci.* (1992) 7:457–72. doi: 10.1214/ss/1177011136
48. Gelman A, Shirlet K. *Inference From Simulations Monitoring Convergence*. Boca Raton, FL: CRC Press (2011).
49. Gelman A, Carlin JB, Stern HS, Dunson DB, Vehtari A, Rubin DB. *Bayesian Data Analysis: Model Checking Improvement*. Boca Raton: CRC Press (2013).
50. Gabry J, Mahr. *Bayesplot: Plotting for Bayesian Models. R Package Version 1.7.0 ed.* (2019). Available online at: https://mc-stan.org/bayesplot/
51. Gabry J, Simpson D, Vehtari A, Betancourt M, Gelman A. Visualization in bayesian workflow. *J Royal Stat Soc Series A Stat Soc.* (2019) 182:389–402. doi: 10.1111/rssa.12378
52. Brambor T, Clark WR, Golder M. Understanding interaction models: improving empirical analyses. *Polit Anal.* (2006) 14:63–82. doi: 10.1093/pan/mpi014
53. Cohen J. *Statistical Power Analysis for the Behavioral Sciences*. Hillsdale, NJ: L. Erlbaum Associates (1988).
54. Sawilowsky SS. New effect size rule of thumb. *J Mod Appl Stat Meth.* (2009) 8:597–9. doi: 10.22237/jmasm/1257035100
55. Olejnik S, Algina J. Measures of effect size for comparative studies: applications, interpretations and limitations. *Contem Educ Psychol.* (2000) 25:241–86. doi: 10.1006/ceps.2000.1040
56. Kass RE, Raftery AE. Bayes factors. *J Am Stat Assoc.* (1995) 90:773–95. doi: 10.1080/01621459.1995.10476572
57. Kruschke JK, Liddell TM. The bayesian new statistics: hypothesis testing, estimation, meta-analysis, and power analysis from a bayesian perspective. *Psychon Bull Rev.* (2018) 25:178–206. doi: 10.3758/s13423-016-1221-4
58. Van De Schoot R, Kaplan D, Denissen J, Asendorpf JB, Neyer FJ, Van Aken M, et al. A gentle introduction to bayesian analysis: applications to developmental research. *Child Dev.* (2014) 85:842–60. doi: 10.1111/cdev.12169
59. Holloway OG, Canty AJ, King AE, Ziebell JM. Rod microglia and their role in neurological diseases. *Semin Cell Dev Biol.* (2019) 94:96–103. doi: 10.1016/j.semcdb.2019.02.005
60. Giordano KR, Denman CR, Dubisch PS, Akhter M, Lifshitz J. An update on the rod microglia variant in experimental and clinical brain injury and disease. *Brain Commun.* (2021) 3:fcaa227. doi: 10.1093/braincomms/fcaa227
61. Smith NM, Giacci MK, Gough A, Bailey C, Mcgonigle T, Black AMB, et al. Inflammation and blood-brain barrier breach remote from the primary injury following neurotrauma. *J Neuroinflammation.* (2018) 15:201. doi: 10.1186/s12974-018-1227-0
62. Loane DJ, Kumar A. Microglia in the TBI brain: the good, the bad, the dysregulated. *Exp Neurol 275 Pt.* (2016) 3:316–27. doi: 10.1016/j.expneurol.2015.08.018
63. Lier J, Ondruschka B, Bechmann I, Dreßler J. Fast microglial activation after severe traumatic brain injuries. *Int J Legal Med.* (2020) 134:2187–93. doi: 10.1007/s00414-020-02308-x
64. Ramlackhansingh AF, Brooks DJ, Greenwood RJ, Bose SK, Turkheimer FE, Kinnunen KM, et al. Inflammation after trauma: microglial activation and traumatic brain injury. *Ann Neurol.* (2011) 70:374–83. doi: 10.1002/ana.22455
65. Loane DJ, Kumar A, Stoica BA, Cabatbat R, Faden AI. Progressive neurodegeneration after experimental brain trauma: association with chronic microglial activation. *J Neuropathol Exp Neurol.* (2014) 73:14–29. doi: 10.1097/NEN.0000000000000021
66. Cattelani R, Lombardi F, Brianti R, Mazzucchi A. Traumatic brain injury in childhood: intellectual, behavioural and social outcome into adulthood. *Brain Inj.* (1998) 12:283–96. doi: 10.1080/026990598122584
67. Kamper JE, Pop V, Fukuda AM, Ajao DO, Hartman RE, Badaut J. Juvenile traumatic brain injury evolves into a chronic brain disorder: behavioral and histological changes over 6months. *Exp Neurol.* (2013) 250:8–19. doi: 10.1016/j.expneurol.2013.09.016
68. Witcher KG, Eiferman DS, Godbout JP. Priming the inflammatory pump of the CNS after traumatic brain injury. *Trends Neurosci.* (2015) 38:609–20. doi: 10.1016/j.tins.2015.08.002
69. Muccigrosso MM, Ford J, Benner B, Moussa D, Burnsides C, Fenn AM, et al. Cognitive deficits develop 1month after diffuse brain injury and are exaggerated by microglia-associated reactivity to peripheral immune challenge. *Brain Behav Immun.* (2016) 54:95–109. doi: 10.1016/j.bbi.2016.01.009
70. Chevignard M, Câmara-Costa H, Dellatolas G. Pediatric traumatic brain injury and abusive head trauma. *Handb Clin Neurol.* (2020) 173:451–84. doi: 10.1016/B978-0-444-64150-2.00032-0
71. Dalmau I, Vela JM, González B, Finsen B, Castellano B. Dynamics of microglia in the developing rat brain. *J Comp Neurol.* (2003) 458:144–57. doi: 10.1002/cne.10572
72. Paolicelli RC, Bolasco G, Pagani F, Maggi L, Scianni M, Panzanelli P, et al. Synaptic pruning by microglia is necessary for normal brain development. *Science.* (2011) 333:1456–8. doi: 10.1126/science.1202529
73. Schafer DP, Stevens B. Microglia function in central nervous system development and plasticity. *Cold Spring Harb Perspect Biol.* (2015) 7:a020545. doi: 10.1101/cshperspect.a020545
74. Chung WS, Barres BA. The role of glial cells in synapse elimination. *Curr Opin Neurobiol.* (2012) 22:438–45. doi: 10.1016/j.conb.2011.10.003
75. Lenz KM, Nelson LH. Microglia and beyond: innate immune cells as regulators of brain development and behavioral function. *Front Immunol.* (2018) 9:698. doi: 10.3389/fimmu.2018.00698

76. Taylor SE, Morganti-Kossmann C, Lifshitz J, Ziebell JM. Rod microglia: a morphological definition. *PLoS ONE.* (2014) 9:e97096. doi: 10.1371/journal.pone.0097096
77. Streit WJ, Graeber MB, Kreutzberg GW. Functional plasticity of microglia: a review. *Glia.* (1988) 1:301–7. doi: 10.1002/glia.440010502
78. Cao T, Thomas TC, Ziebell JM, Pauly JR, Lifshitz J. Morphological and genetic activation of microglia after diffuse traumatic brain injury in the rat. *Neuroscience.* (2012) 225:65–75. doi: 10.1016/j.neuroscience.2012.08.058
79. Tozaki-Saitoh H, Miyata H, Yamashita T, Matsushita K, Tsuda M, Inoue K. P2Y12 receptors in primary microglia activate nuclear factor of activated T-cell signaling to induce C-C chemokine 3 expression. *J Neurochem.* (2017) 141:100–10. doi: 10.1111/jnc.13968
80. Bolte AC, Lukens JR. Neuroimmune cleanup crews in brain injury. *Trends Immunol.* (2021) 42:480–94. doi: 10.1016/j.it.2021.04.003
81. Ziebell JM, Ray-Jones H, Lifshitz J. Nogo presence is inversely associated with shifts in cortical microglial morphology following experimental diffuse brain injury. *Neuroscience.* (2017) 359:209–23. doi: 10.1016/j.neuroscience.2017.07.027
82. Witcher KG, Bray CE, Chunchai T, Zhao F, O'neil SM, Gordillo AJ, et al. Traumatic brain injury causes chronic cortical inflammation and neuronal dysfunction mediated by microglia. *J Neurosci.* (2021) 41:1597–616. doi: 10.1523/JNEUROSCI.2469-20.2020
83. Dos Santos SE, Medeiros M, Porfirio J, Tavares W, Pessôa L, Grinberg L, et al. Similar microglial cell densities across brain structures and mammalian species: implications for brain tissue function. *J Neurosci.* (2020) 40:4622–43. doi: 10.1523/JNEUROSCI.2339-19.2020
84. Burda JE, Bernstein AM, Sofroniew MV. Astrocyte roles in traumatic brain injury. *Exp Neurol.* (2016) 3:305–15. doi: 10.1016/j.expneurol.2015.03.020
85. Li Y, Chopp M. Temporal profile of nestin expression after focal cerebral ischemia in adult rat. *Brain Res.* (1999) 838:1–10. doi: 10.1016/S0006-8993(99)01502-4
86. Pekny M, Johansson CB, Eliasson C, Stakeberg J, Wallén A, Perlmann T, et al. Abnormal reaction to central nervous system injury in mice lacking glial fibrillary acidic protein and vimentin. *J Cell Biol.* (1999) 145:503–14. doi: 10.1083/jcb.145.3.503
87. Karve IP, Taylor JM, Crack PJ. The contribution of astrocytes and microglia to traumatic brain injury. *Br J Pharmacol.* (2016) 173:692–702. doi: 10.1111/bph.13125
88. Agoston DV, Shutes-David A, Peskind ER. Biofluid biomarkers of traumatic brain injury. *Brain Inj.* (2017) 31:1195–203. doi: 10.1080/02699052.2017.1357836
89. Shahim P, Politis A, Van Der Merwe A, Moore B, Ekanayake V, Lippa SM, et al. Time course and diagnostic utility of NfL, tau, GFAP, and UCH-L1 in subacute and chronic TBI. *Neurology.* (2020) 95:e623–36. doi: 10.1212/WNL.0000000000009985
90. Olude MA, Mustapha OA, Aderounmu OA, Olopade JO, Ihunwo AO. Astrocyte morphology, heterogeneity, and density in the developing African giant rat (Cricetomys gambianus). *Front Neuroanat.* (2015) 9:67. doi: 10.3389/fnana.2015.00067
91. Kettenmann H, Verkhratsky A. [Neuroglia–living nerve glue]. *Fortschr Neurol Psychiatr.* (2011) 79:588–97. doi: 10.1055/s-0031-1281704

Conflict of Interest: The authors declare that the research was conducted in the absence of any commercial or financial relationships that could be construed as a potential conflict of interest.

frontiers in Neurology

MINI REVIEW
published: 25 January 2022
doi: 10.3389/fneur.2021.819613

Analgesia in the Neurosurgical Intensive Care Unit

Slavica Kvolik[1,2]*, *Nenad Koruga*[1,3] *and Sonja Skiljic*[1,2]*

[1] Faculty of Medicine, Josip Juraj Strossmayer University of Osijek, Osijek, Croatia, [2] Department of Anesthesiology and Critical Care, Osijek University Hospital, Osijek, Croatia, [3] Department of Neurosurgery, Osijek University Hospital, Osijek, Croatia

Acute pain in neurosurgical patients is an important issue. Opioids are the most used for pain treatment in the neurosurgical ICU. Potential side effects of opioid use such as oversedation, respiratory depression, hypercapnia, worsening intracranial pressure, nausea, and vomiting may be problems and could interfere with neurologic assessment. Consequently, reducing opioids and use of non-opioid analgesics and adjuvants (N-methyl-D-aspartate antagonists, α2 -adrenergic agonists, anticonvulsants, corticosteroids), as well as non-pharmacological therapies were introduced as a part of a multimodal regimen. Local and regional anesthesia is effective in opioid reduction during the early postoperative period. Among non-opioid agents, acetaminophen and non-steroidal anti-inflammatory drugs are used frequently. Adverse events associated with opioid use in neurosurgical patients are discussed. Larger controlled studies are needed to find optimal pain management tailored to neurologically impaired neurosurgical patients.

Keywords: analgesia, pain, intensive care units, neurosurgery, opioids, drug side effects, constipation, gastroparesis

OPEN ACCESS

Edited by:
Mårten Risling,
Karolinska Institutet (KI), Sweden

Reviewed by:
Katherine N. Theken,
University of Pennsylvania,
United States

***Correspondence:**
Slavica Kvolik
skvolik@mefos.hr
Sonja Skiljic
skiljicsonja@gmail.com

Specialty section:
This article was submitted to Neurotrauma, a section of the journal Frontiers in Neurology

Received: *21 November 2021*
Accepted: *23 December 2021*
Published: *25 January 2022*

Citation:
Kvolik S, Koruga N and Skiljic S (2022) Analgesia in the Neurosurgical Intensive Care Unit. Front. Neurol. 12:819613. doi: 10.3389/fneur.2021.819613

INTRODUCTION

Acute pain following acute brain injury could be substantial, but commonly it is not the primary consideration of the neurosurgical intensive care (NSICU) patients. The main reason for this is a priority of preventing secondary brain damage after trauma or surgical procedure (1, 2). Preservation of adequate cerebral perfusion and oxygenation while managing systemic intracranial pressure, mechanical ventilation, stabilization of circulation, fluid balance, temperature, and glycemic control in neurosurgical patients is complex and demanding but adequate pain control could improve outcome and patient satisfaction (3).

Several ERAS protocols (enhanced recovery after surgery) were recently developed for postoperative patients and perioperative pain treatment is included in them (4). Reduced preoperative fasting, maltodextrin fructose solution 2 h preoperatively, local infiltration of the surgical incision, and non-opioid analgesia are some of the maneuvers that were proven as efficient in awake patients (5). In addition to faster mobilization, these procedures also aim to reduce the use of opioids in the perioperative period, the side effect of which may be chronic opioid use and opioid dependence (6). It is usually easy to assess pain and administer appropriate pain medications in conscious patients, but it could be challenging in sedated, drowsy, or non-cooperative patients (7).

In this review, we will present the pain assessment and the most common modalities of analgesia in NSICU patients. We will discuss the problems associated with analgesia in patients with impaired consciousness, and complications of opioid use in patients with acute brain injury. Respiratory depression, gastrointestinal dysmotility, delirium, and addiction with possibilities to reduce them will be highlighted.

MULTIMODAL ANALGESIA POST-CRANIOTOMY

Acute pain after craniotomy is considered moderate to severe during the first two postoperative days. It is often underrated and hard to estimate, potentially becoming chronic (8, 9). No analgesic regimen for post-craniotomy pain was proven as efficient for all patients (1, 10), although opioids provided superior acute pain relief compared to other drugs in small clinical studies (11). Despite their efficiency in pain control, potential side effects such as (over) sedation, respiratory depression, hypercapnia with worsening intracranial pressure, nausea, and vomiting may be problematic in neurosurgical patients and can interfere with neurologic assessment (12). The risk of opioid dependence limits safe opioid use for only a few days.

The introduction of the ERAS protocol in neurosurgery aims to accelerate postoperative recovery and length of stay in the ICU, and analgesia with fewer opioids in the early post-craniotomy period is crucial in achieving these goals. By adhering to these protocols, Elayat and co-workers reduced the length of stay in the ICU, reduced the number of episodes with VAS >4, and reduced opioid consumption in the patients undergoing elective craniotomy for supratentorial neurosurgery (5). Consequently, non-opioid analgesics as a part of a multimodal regimen with fewer side effects became standard of care in the postoperative pain treatment in the NSICU (3).

Local and regional anesthesia techniques, such as local scalp infiltration/block seem to be effective in the early postoperative period (13). Postoperative scalp infiltration was associated with a significant reduction in pain scores and the reduction of the opioid requirement over the 24 h postoperatively. No adverse events of the regional techniques were reported in a meta-analysis of the 7 RCTs with a total of 320 patients (13).

Among non-opioid agents, acetaminophen and non-steroidal anti-inflammatory drugs are used most frequently in the first postoperative days to reduce the dose of opioids (11, 14). Recently various adjuvants were added as a part of preemptive, intraoperative and early postoperative analgesia for craniotomy pain. These include non-steroidal analgesics: N-methyl-D-aspartate (NMDA) antagonists (ketamine), α2 -adrenergic agonists (dexmedetomidine) (10, 15, 16), as well as anticonvulsants (gabapentin and pregabalin) (17), corticosteroids, an intravenous local anesthetic (lidocaine), and non-pharmacological interventions, such as multipoint electro-acupuncture (3, 10, 11).

Analgesia in NSICU patients with acute brain injury must not be a simple extension of post-craniotomy analgesia.

PAIN ASSESSMENT TOOLS AND PATIENTS WITH ALTERED MENTAL STATUS

Pain treatment in patients who have altered mental status before and after craniotomy is challenging. In NSICU patients, pain may be postoperative, e.g., after a craniotomy. It can be caused by intubation, mechanical ventilation, insufficient mobilization, as well as placement of nasogastric tube, urinary catheter, or central venous catheter. Several factors including sepsis, use of vasopressors, multiple comorbidities, previous (18), or new neurological deficiencies may influence pain assessment and treatment (19).

There are several tools adopted for the pain assessment in mechanically ventilated ICU patients, and patients with altered mental status. Behavioral Pain Scale (BPS), Critical Care Pain Observation Tool (CPOT) (20), or Nociception Coma Scale-Revised (NCS-R) (21) are some of the tools widely used. The parameters evaluated by these tools are physiologic parameters, verbal response, motor response, or facial mimic, which may be irreversibly impaired by brain damage. A study conducted by Nazari and coworkers showed that most of the behaviors that have been observed during painful stimulation in patients with traumatic brain injury included facial expressions, sudden eye-opening, frowning, lip changes, clear movements of extremities, neck stiffness, and sighing or moaning (22). Using these tools may be helpful, but also misleading in patients with brain edema after hypoxic brain injury, or in patients with intracranial hemorrhage and hypertension.

Severgnini et coworkers compared CPOT and BPS to examine their applicability in awake and sedated patients. They confirmed that both scales correlate with pain. In the comparison, CPOT was more sensitive (BPS 62.7%, CPOT 76.5%), and BPS was found to be more specific (BPS 91.7%, CPOT 70.8%) for pain assessment. The best results were obtained by combining both scales (23). In another study, Ribeiro and coworkers have studied psychometric properties of the BPS in traumatic brain injury. They found that BPS had good internal consistency, good discriminant validity, moderate to excellent reliability, and high responsiveness, but also that deep sedation affected the increase of grading during painful procedures (24).

Currently, none of the above rating scales can be considered the gold standard for pain assessment in neurocritical patients. As with other ICU patients, pain should be routinely assessed using validated behavioral scales and documented, especially before invasive procedures and physical therapy (24).

Implementation of standardized pain assessment protocols for the NSICU patients is important, but the actual implementation and adherence to these protocols remains an area for improvement and further investigations. Vital signs should not be used as a sole measurement, and surrogates for pain assessment (24). Using these tools may be helpful and misleading in patients with brain edema after hypoxic brain injury, or in patients with intracranial hemorrhage and hypertension.

The implementation of clinical assessment tools may lead to reduced use of analgesic and sedative agents, as observed in the nurses' study carried by Gelinas and coworkers (25). In the study of Phillips and coworkers, the implementation of the CPOT led to increased frequency of the pain assessment and a significant increase in the administration of paracetamol, opiates, propofol, patient-controlled analgesia, modified-release opiates, and neuropathic pain agents (26). A similar observation that implementation of pain assessment tools led to the more liberal administration of opioid-based pain relief was observed in Mascarenhas' study. Nurses in their study have increased opioid

administration by 100% (27). The administration of opioids may decrease the pain experience, but may increase respiratory depression, have an impact on alertness and vigilance, and may impair neuropsychological evaluation.

The situation is more complicated when patients' condition dictates prolonged sedation, mechanical ventilation, and when other invasive and painful procedures are routinely performed in NSICU. In such situations, a protocol called "analgesia first sedation" may be useful by increasing compliance with the ventilator but may lead to increased opioid use (27). In neurologically impaired patients, it may mask their neurologic assessment.

ACUTE BRAIN INJURY AND PAIN CONTROL

In patients with acute brain injury, intracranial pressure oscillations are associated with hemodynamic instability and are treated with a reduction in intracranial pressure by continuous use of sedatives, such as propofol and opiates. Sedatives and opioids are given commonly, based on the blood pressure and pulse values to maintain smooth circulation and mechanical ventilation (28). Different opioids may be used like fentanyl, sufentanil, remifentanil, and morphine. Opioids are beneficial for analgesia, but their bolus administration may increase ICP with associated decreases in MAP and CPP, and should be avoided (29). In the systematic review Wiener and coworkers have found no consistent results between different opioids, and between opioid and non-opioid analgesia in the management of traumatic brain injury regarding their effects on MAP, ICP, or CPP (29). Opioid consumption can be reduced by the use of dexmedetomidine for sedation without affecting neurological function (30).

Paroxysmal Sympathetic Hyperactivity

Paroxysmal sympathetic hyperactivity (PSH) is a syndrome resulting usually from traumatic brain injury (79.4% of the patients), and rarely from hypoxia (9.7%) or cerebrovascular accident (5.4%) (31). Since these conditions are commonly accompanied by severe brain swelling or blood extravasation, pain could be very strong although it is rarely reported and/or observed. PSH is characterized by simultaneous, paroxysmal transient increases in sympathetic (elevated heart rate, blood pressure, respiratory rate, temperature, sweating) and motor activity (31). Analgesia is particularly demanding in patients with impaired mental status and in those who have developed PSH (18). In patients with PSH, these symptoms may resemble withdrawal syndrome or acute pain (**Table 1**) and are very often treated with opioids (32–34). Until now, there are no studies reporting pain scores using any of the pain assessment tools in PSH patients.

Common problems with PSH are difficult mechanical ventilation, difficult maintenance of fluid and electrolyte balance, management of increased body temperature, increased number of blood specimens, and unresponsiveness of the symptoms to treatment.

TABLE 1 | The most common symptoms of paroxysmal sympathetic hyperactivity, withdrawal syndrome, and acute pain in neurosurgical patients.

	Paroxysmal sympathetic hyperactivity	Opioid withdrawal syndrome	Acute pain
Tachycardia	++	++	++
Hypertension	++	++	++
Hyperventilation	++	+	+
Fever	++	+ (or hypothermia)	–
Profuse sweating	++	+	++
Restlessness	+	++	+
Muscle rigidity and hypertonus	++	Movement disorders, tremor	+/–
Agitation, insomnia	–	++	+
Other symptoms	Typical posturing	Rhinorrhoea, lacrimation, nausea, vomiting, diarrhea	↑ ICP

Note: ++ present, + sometimes present, +/– not always present, – not registered, ↑ increase.

One of the treatment goals in brain-injured patients is symptoms prevention and reduction (15). The symptoms of PSH are usually treated with various drugs, including morphine, non-selective β-blockers, short-acting benzodiazepines, baclofen, clonidine, non-steroidal anti-inflammatory drugs, α2 agonists, and GABA agonists. Although opioids and benzodiazepines are capable to control breakthrough episodes, due to their sedative effects and the possibility of addiction, other drug classes are gaining more popularity (35).

Currently, dexmedetomidine and gabapentin are used for both symptom and opioid reduction. In a recent study, Peng and coworkers have confirmed that dexmedetomidine reduces paroxysmal hypertension, average time for normalization of body temperature, heart rate, and respiratory rate below 25 breaths per minute, but does not protect against the recurrence of PSH (36). In the patients with severe traumatic brain injury and symptoms of paroxysmal sympathetic hyperactivity who underwent surgery, dexmedetomidine was not capable of either reducing ICU and hospital stay or of improving Glasgow outcome score (37).

Gabapentin is a promising drug for the treatment of PSH. Godo and colleagues reported a case series of patients who were resistant to benzodiazepines, opioids, and non-steroidal anti-inflammatory drugs. Initial gabapentin doses of 200 mg 3 times a day increased to 400 mg 3 times a day resulted in a reduction of PSH symptoms (32). To achieve wider use of gabapentin for PSH treatment, its effects observed in the single institution must be confirmed in a larger placebo-controlled study.

ADVERSE EVENTS OF OPIOIDS IN NEUROSURGICAL PATIENTS

Although some preclinical studies have suggested that opioid receptor agonists may be beneficial in brain injury, capable of

reducing brain edema as well as of providing neuroprotection during a stroke (38), these preclinical observations were not confirmed in clinical studies. Moreover, the use of opioids as an analgesic regimen in neurosurgical patients is associated with several clinical problems (side effects) such as oversedation, respiratory depression, prolonged mechanical ventilation, truncal rigidity, inappropriate immune modulation, development of opioid tolerance, opioid-induced hyperalgesia, ICU addiction, and delirium (39). Opioids also have direct cardiovascular effects, decreasing blood pressure, causing vasodilation, and decreasing cardiac work (40). Gastrointestinal-related side effects, which include constipation, nausea, vomiting, dry mouth, gastro-esophageal reflux, abdominal cramping, spasms, and bloating, are well-known as opioid-induced bowel dysfunction. Opioid-induced constipation (OIC) in patients receiving opioids is persistent and the most frequently reported side effect (41, 42).

Respiratory Depression

Respiratory depression with consequent hypoxia and permanent brain injury has often been described after acute opioid intoxication (43). The outcomes of these patients are associated with the duration and severity of hypoxia. There are fewer studies correlating outcomes of the patients with acute brain trauma regarding opioid use and the duration of mechanical ventilation. Dexmedetomidine and propofol allow patients to wake up faster and breathe easier, although they are usually used with opioids in patients with acute brain injury. In the patients with acute brain injury, both dexmedetomidine and dexmedetomidine with propofol were associated with a significantly higher rate of hypotension as compared to propofol only or no sedation (44).

Gastroparesis and Constipation

Gastrointestinal dysmotility, i.e., gastroparesis and bowel paralysis are commonly observed in the acute phase of injury in neurosurgical patients (45, 46). Both disorders are a complication of opioid use and brainstem lesions (**Table 2**). In 139 mechanically ventilated patients in general ICU, the incidence of opioid-induced constipation (OIC) was 63%, and gastric retention was 49% (53). Guerra and coworkers found OIC in 72% of critically ill patients (54). In their paper, by the study protocol patients on the parenteral nutrition therapy were excluded. The incidence of constipation would probably be even higher if such patients were accounted.

Kieninger and coworkers studied a promotility protocol in adult NSICU patients with acute severe brain injury and anticipated mechanical ventilation for more than 3 days (55). All patients received sufentanil and sedation. Promotility procedures were colon massage, physical therapy, and early peroral lactulose, followed by naloxone 4 mg p.o. 3x/day. In the study group, an adequate defecation pattern was observed in 9 out of 37 (24.3%) compared to only 9 out of 109 (8.3%) in the control group (55). Opioid antagonists are considered a logical approach to treat OIC. In a recent study, both enteral naloxone and subcutaneous methylnaltrexone were effective for the treatment of OIC in medical ICU. The median times to first bowel movement were 30 and 24 h for naloxone and methylnaltrexone patients, respectively (56).

Schmittner and coworkers reported no difference in the time period until full enteral nutrition or first defecation between patients receiving opioid fentanyl and S(+)-ketamine in neurosurgical patients (57). This suggests that brain damage, *per se*, may influence gut dysfunction via unknown mechanisms. Larger prospective studies are needed to answer the true OIC incidence and optimal treatment in NSICU patients with brain injury.

Hypotension

A decrease in the mean arterial blood pressure is well-known during fentanyl, remifentanil, or alfentanil administration (58), as well as during prolonged sedation in mechanically ventilated patients and it is accompanied by increased use of vasopressors in the medical ICU (59). The total amount of propofol and fentanyl correlated with vasopressor use and prolonged sedation. Patients who underwent analgesia with S(+)-ketamine showed a trend to lower demand for norepinephrine compared with the fentanyl group without an increase of ICP and CPP (57).

Addiction in the ICU

Addicted patients are a growing category in ICU. Analyzing toxicological samples taken from 44 patients admitted to the Intensive Care Unit Ruiz-García and coworkers confirmed the use of $\geq$1 substance in 74% of patients. The most consumed substances were alcohol and tobacco (> 55%), and cannabis, amphetamines (> 11%), and cocaine (9%). Discontinuation of each of these substances can lead to withdrawal syndrome (60).

Opioid addiction is reflected in an individual pathologically pursuing reward and/or relief by substance use and other behaviors. Usually, they need a special approach while on opioid maintenance treatment during the ICU stay, since the opioid restriction is not recommended during the acute illness (61). The toxic effect of opioids and other substances of abuse may lead to ischemic brain damage and ICU admission in youth and younger adults (62). Non-traumatic hypoxic brain injury was observed in a total of 8% of the patients admitted into the ICU with opioid overdose with mortality of 10% (63). In the period after hypoxic brain injury, during the recovery in ICU, these patients may develop symptoms of withdrawal syndrome (**Table 1**) (64).

Withdrawal syndrome may be a serious complication during ICU treatment (33). The most severe symptoms can be experienced in patients who have discontinued opioid therapy at the NSICU, regardless of whether the patient was taking opioids before admission to the NSICU, or opioid therapy as part of analgesia during NSICU treatment. Risk factors associated with iatrogenic withdrawal syndrome include duration of therapy and cumulative drug dose (65). Critically ill patients with preexisting cognitive or functional

TABLE 2 | Frequency of the most common gastrointestinal motility disorders in the neurosurgical intensive care unit and their association with risk factors.

References	Postinjury phase	GI motility disorder (%)	Risk factors
Lim et al. (47)	Acute poststroke	Constipation 39%	Immobility, bedpan use, a longer length of stay
Vieira et al. (48)	Traumatic brain injury- acute postinjury phase	Diarrhea 69.6%	Critical illness, enteral nutrition, antibiotics usage
Makkar et al. (49)	Traumatic brain injury- acute postinjury phase	Gastroparesis, gastric aspirate volume (GAV) 60.5%	Raised intracranial pressure, sympathetic stimulation, hyperglycemia, use of opioids.
Pinto et al. (45)	Traumatic brain injury- acute postinjury phase	Feeding intolerance 75.0%	Brain-gut dysfunction
Berry et al. (50)	Traumatic brain injury- acute postinjury phase	No bowel movement between 48 and 72 h 45.6%	Autonomic disturbances, hyper-sympathetic response, damage of hypothalamus, narcotic analgesics
Cai et al. (51)	Acute recovery sequelae phase	Constipation 41.6% Constipation 31.5 % Constipation 22.6%	Incidence higher with acute phase, basal ganglia inclusion, and cerebral hemorrhage
Robain et al. (52)	Rehabilitation after recent vascular hemiplegia	Constipation 60%	Brain lesions, functional status of patients (assessed by Barthel Index)
Cheng et al. (46)	Chronic	Constipation	Brainstem lesions, the desire for defecation threshold, physical activity level

impairment are at special risk to develop opioid withdrawal syndrome (66).

In NSICU where opioids are commonly used, withdrawal may be difficult to recognize. Its recognition could be even poorer because no valid tools were developed for ICU patients. Opioid withdrawal syndrome may mimic PSH or other manifestations of brain damage (**Table 1**). Opioid doses should be kept at a minimum, and non-opioid drugs are preferred, whenever their use is effective. There are several strategies for opioid weaning, including scheduled enteral opioids after continuous opioid infusions (66) and the use of non-opioid drugs like dexmedetomidine and clonidine.

Promoting non-opioid analgesics and reducing opioid use is important to minimize the use of opioids in previously opioid-naïve patients after discharge from the NSICU. To date, there are no studies to confirm the frequency of opioid use in neurosurgical patients after discharge from the ICU. Data from other fields of intensive care confirm that this proportion is significant. Based on the recent cohort studies 40.8% (346 in 848) medical ICU patients and 45% (32 of the 71 surgical) opiate-naïve patients were discharged with a new opioid prescription (67, 68). A shorter inpatient opioid therapy decreased the risk of post-discharge opioid therapy (68).

In clinical situations where opioid use cannot be avoided, nor can opioids be replaced by other drugs, opioid rotation may be useful. It can reduce both risks of opioid dependence and of opioid tolerance, i.e., increase the opioid dose to maintain equianalgesic effects (39, 69).

ICU Delirium

Patients may develop delirium as a consequence of opioid administration in the ICU. Pisani and coworkers reported patients who received opioids had a longer duration of delirium (70). The incidence of delirium in neurosurgical patients may be as high as 42.2% as observed by Wang and coworkers (71), but a correlation between delirium and opioid use was not analyzed in the study. Opioid use in NSICU is a modifiable risk factor for delirium.

UNANSWERED QUESTIONS IN THE FIELD

There are numerous unresolved questions in the field of analgesic use in acute brain injury, such as whether the choice of analgesics may influence neurological recovery in acute brain injury. In the *in vivo* study tramadol was able to minimize perivascular edema, neuronal necrosis, inflammatory cell infiltration in acute and chronic ischemia/reperfusion injury (72). The comparable neuroprotective effect was observed with dexmedetomidine in *in vitro* and *in vivo* studies. Possible mechanisms are signaling pathways for inflammatory response, oxidative stress, neurotransmitter regulation, mitochondrial function, apoptotic pathway, and autophagy (73). This effect was not confirmed in human studies. It is also unknown whether opioid rotation can reduce the incidence of ICU withdrawal syndrome, and post-discharge opioid use. It has been confirmed that the use of multimodal treatment under the ERAS protocol, such as the combination of non-opioid analgesics, and gabapentin, reduces opioid use in postoperative general surgical patients (74). While decreasing pain scores, it decreased the level of consciousness in a dose-dependent fashion, and prolonged stay in the post-anesthesia care unit, too (74). There are no such studies in the patients who suffered an acute brain injury. It is particularly unknown whether the neurological outcome may be modified in the patients who have received such a multimodal treatment. This should be confirmed by future studies.

CONCLUSION

Both pain assessment and pain control are challenging in neurosurgical patients with altered consciousness. Opioid use is common in NSICU but can lead to respiratory depression

and difficult neurological evaluation from oversedation. Avoiding opioids and the use of alternative medications and therapies are recommended. Multimodal postoperative analgesia and proper drug selection in the ICU may reduce the side effects of opioid treatment. Further studies should confirm whether the choice of analgesia and opioid restriction in patients with severe brain injury may influence outcomes.

AUTHOR CONTRIBUTIONS

SS and SK each wrote sections of the paper and performed the literature review. SK and NK have prepared tables for publication. SK, NK, and SS have approved a final version of the manuscript. All authors contributed to the article and approved the submitted version.

FUNDING

This manuscript was supported by IP16-20 and IP1-21 by J.J. Strossmayer University, Medical Faculty, Osijek, Croatia.

ACKNOWLEDGMENTS

The authors acknowledge Branko Bulovic (Library, University of New South Wales, Sydney, Australia) for help with language editing.

REFERENCES

1. Bösel J. Moderne prinzipien der neurologischen intensivmedizin. *Nervenarzt.* (2018) 89:1411–27. doi: 10.1007/s00115-018-0634-x
2. Borsook D, Upadhyay J, Chudler EH, Becerra L. A key role of the basal ganglia in pain and analgesia–insights gained through human functional imaging. *Mol Pain.* (2010) 6:27. doi: 10.1186/1744-8069-6-27
3. Morad A, Farrokh S, Papangelou A. Pain management in neurocritical care; an update. *Curr Opin Crit Care.* (2018) 24:72–79. doi: 10.1097/MCC.0000000000000480
4. Ali ZS, Ma TS, Ozturk AK, Malhotra NR, Schuster JM, Marcotte PJ, et al. Pre-optimization of spinal surgery patients: development of a neurosurgical enhanced recovery after surgery (ERAS) protocol. *Clin Neurol Neurosurg.* (2018) 164:142–53. doi: 10.1016/j.clineuro.2017.12.003
5. Elayat A, Jena SS, Nayak S, Sahu RN, Tripathy S. Enhanced recovery after surgery - ERAS in elective craniotomies-a non-randomized controlled trial. *BMC Neurol.* (2021) 21:127. doi: 10.1186/s12883-021-02150-7
6. Seal KH, Bertenthal D, Barnes DE, Byers AL, Gibson CJ, Rife TL, et al. Traumatic brain injury and receipt of prescription opioid therapy for chronic pain in iraq and afghanistan veterans: do clinical practice guidelines matter? *J Pain.* (2018) 19:931–41. doi: 10.1016/j.jpain.2018.03.005
7. Maier J, Fröhlich MR, Spirig R. [Standardized impartial assessment of pain in unconscious patients with the Zurich observation pain assessment on a neurosurgical intensive care unit - a case report]. *Pflege.* (2015) 28:19–31. doi: 10.1024/1012-5302/a000401
8. Lutman B, Bloom J, Nussenblatt B, Romo V. A contemporary perspective on the management of post-craniotomy headache and pain. *Curr Pain Headache Rep.* (2018) 22:69. doi: 10.1007/s11916-018-0722-4
9. Grodofsky S. Chronic pain in neurosurgery. *Anesthesiol Clin.* (2016) 34:479–95. doi: 10.1016/j.anclin.2016.04.003
10. Tsaousi GG, Logan SW, Bilotta F. Postoperative pain control following craniotomy: a systematic review of recent clinical literature. *Pain Pract.* (2017) 17:968–81. doi: 10.1111/papr.12548
11. Zeiler FA, AlSubaie F, Zeiler K, Bernard F, Skrobik Y. Analgesia in neurocritical care: an international survey and practice audit*. *Crit Care Med.* (2016) 44:973–80. doi: 10.1097/CCM.0000000000001602
12. Dunn LK, Naik BI, Nemergut EC, Durieux ME. Post-Craniotomy pain management: beyond opioids. *Curr Neurol Neurosci Rep.* (2016) 16:93. doi: 10.1007/s11910-016-0693-y
13. Guilfoyle MR, Helmy A, Duane D, Hutchinson PJA. Regional scalp block for postcraniotomy analgesia: a systematic review and meta-analysis. *Anesth Analg.* (2013) 116:1093–102. doi: 10.1213/ANE.0b013e3182863c22
14. Puntis M, Garner A. Management of pain following craniotomy. *Br J Nurs.* (2015) 24:740–4. doi: 10.12968/bjon.2015.24.14.740
15. Peng K, Jin X, Liu S, Ji F. Effect of intraoperative dexmedetomidine on post-craniotomy pain. *Clin Ther.* (2015) 37:1114–21.e1. doi: 10.1016/j.clinthera.2015.02.011
16. Vallapu S, Panda N, Samagh N, Bharti N. Efficacy of dexmedetomidine as an adjuvant to local anesthetic agent in scalp block and scalp infiltration to control postcraniotomy pain: a double-blind randomized trial. *J Neurosci Rural Pract.* (2018) 9:73–9. doi: 10.4103/jnrp.jnrp_310_17
17. Shay JE, Kattail D, Morad A, Yaster M. The postoperative management of pain from intracranial surgery in pediatric neurosurgical patients. *Pediatr Anesth.* (2014) 24:724–33. doi: 10.1111/pan.12444
18. Naro A, Bramanti P, Bramanti A, Calabrò RS. Assessing pain in patients with chronic disorders of consciousness: are we heading in the right direction? *Conscious Cogn.* (2017) 55:148–55. doi: 10.1016/j.concog.2017.08.009
19. Booth CM, Boone RH, Tomlinson G, Detsky AS. Is this patient dead, vegetative, or severely neurologically impaired?assessing outcome for comatose survivors of cardiac arrest. *JAMA.* (2004) 291:870–9. doi: 10.1001/jama.291.7.870
20. Chanques G, Pohlman A, Kress JP, Molinari N, de Jong A, Jaber S, et al. Psychometric comparison of three behavioural scales for the assessment of pain in critically ill patients unable to self-report. *Crit Care.* (2014) 18:R160. doi: 10.1186/cc14000
21. Chatelle C, Thibaut A, Whyte J, De Val MD, Laureys S, Schnakers C. Pain issues in disorders of consciousness. *Brain Inj.* (2014) 28:1202–8. doi: 10.3109/02699052.2014.920518
22. Nazari R, Pahlevan Sharif S, Allen KA, Sharif Nia H, Yee B-L, Yaghoobzadeh A. Behavioral pain indicators in patients with traumatic brain injury admitted to an intensive care unit. *J Caring Sci.* (2018) 7:197–203. doi: 10.15171/jcs.2018.030
23. Severgnini P, Pelosi P, Contino E, Serafinelli E, Novario R, Chiaranda M. Accuracy of critical care pain observation tool and behavioral pain scale to assess pain in critically ill conscious and unconscious patients: prospective, observational study. *J Inten Care.* (2016) 4:68. doi: 10.1186/s40560-016-0192-x
24. Ribeiro CJN, Lima AGCF, de Araújo RAS, Nunes M da S, Alves JAB, Dantas DV, et al. Psychometric properties of the behavioral pain scale in traumatic brain injury. *Pain Manag Nurs Off J Am Soc Pain Manag Nurses.* (2019) 20:152–7. doi: 10.1016/j.pmn.2018.09.004
25. Gélinas C, Arbour C, Michaud C, Vaillant F, Desjardins S. Implementation of the critical-care pain observation tool on pain assessment/management nursing practices in an intensive care unit with nonverbal critically ill adults: a before and after study. *Int J Nurs Stud.* (2011) 48:1495–504. doi: 10.1016/j.ijnurstu.2011.03.012
26. Phillips ML, Kuruvilla V, Bailey M. Implementation of the critical care pain observation tool increases the frequency of pain assessment for noncommunicative ICU patients. *Aust Crit Care.* (2019) 32:367–72. doi: 10.1016/j.aucc.2018.08.007
27. Mascarenhas M, Beattie M, Roxburgh M, MacKintosh J, Clarke N, Srivastava D. Using the model for improvement to implement the critical-care pain observation tool in an adult intensive care unit. *BMJ open Qual.* (2018) 7:e000304. doi: 10.1136/bmjoq-2017-000304
28. Roberts DJ, Hall RI, Kramer AH, Robertson HL, Gallagher CN, Zygun DA. Sedation for critically ill adults with severe traumatic brain injury: a

systematic review of randomized controlled trials. *Crit Care Med.* (2011) 39:2743–51. doi: 10.1097/CCM.0b013e318228236f
29. Wiener J, McIntyre A, Janzen S, Mirkowski M, MacKenzie HM, Teasell R. Opioids and cerebral physiology in the acute management of traumatic brain injury: a systematic review. *Brain Inj.* (2019) 33:559–66 doi: 10.1080/02699052.2019.1574328
30. Humble SS, Wilson LD, Leath TC, Marshall MD, Sun DZ, Pandharipande PP, et al. ICU sedation with dexmedetomidine after severe traumatic brain injury. *Brain Inj.* (2016) 30:1266–70. doi: 10.1080/02699052.2016.1187289
31. Perkes I, Baguley IJ, Nott MT, Menon DK. A review of paroxysmal sympathetic hyperactivity after acquired brain injury. *Ann Neurol.* (2010) 68:126–35. doi: 10.1002/ana.22066
32. Godo S, Irino S, Nakagawa A, Kawazoe Y, Fujita M, Kudo D, et al. Diagnosis and management of patients with paroxysmal sympathetic hyperactivity following acute brain injuries using a consensus-based diagnostic tool: a single institutional case series. *Tohoku J Exp Med.* (2017) 243:11–8. doi: 10.1620/tjem.243.11
33. Taesotikul S, Dilokpattanamongkol P, Tangsujaritvijit V, Suthisisang C. Incidence and clinical manifestation of iatrogenic opioid withdrawal syndrome in mechanically ventilated patients. *Curr Med Res Opin.* (2021) 37:1213–9. doi: 10.1080/03007995.2021.1928616
34. Peng Y, Zhang W, Kass IS, Han R. Lidocaine reduces acute postoperative pain after supratentorial tumor surgery in the pacu: a secondary finding from a randomized, controlled trial. *J Neurosurg Anesthesiol.* (2016) 28:309–15. doi: 10.1097/ANA.0000000000000230
35. Raithel DS, Ohler KH, Porto I, Bicknese AR, Kraus DM. Morphine: an effective abortive therapy for pediatric paroxysmal sympathetic hyperactivity after hypoxic brain injury. *J Pediatr Pharmacol Ther.* (2015) 20:335–40. doi: 10.5863/1551-6776-20.4.335
36. Peng Y, Zhu H, Chen H, Zhu Z, Zhou H, Zhang S, et al. Dexmedetomidine attenuates acute paroxysmal sympathetic hyperactivity. *Oncotarget.* (2017) 8:69012–9. doi: 10.18632/oncotarget.16920
37. Tang Q, Wu X, Weng W, Li H, Feng J, Mao Q, et al. The preventive effect of dexmedetomidine on paroxysmal sympathetic hyperactivity in severe traumatic brain injury patients who have undergone surgery: a retrospective study. *PeerJ.* (2017) 5:e2986. doi: 10.7717/peerj.2986
38. Yang L, Wang H, Shah K, Karamyan VT, Abbruscato TJ. Opioid receptor agonists reduce brain edema in stroke. *Brain Res.* (2011) 1383:307–16. doi: 10.1016/j.brainres.2011.01.083
39. Martyn JAJ, Mao J, Bittner EA. Opioid tolerance in critical illness. *N Engl J Med.* (2019) 380:365–78. doi: 10.1056/NEJMra1800222
40. *LiverTox: Clinical and Research Information on Drug-Induced Liver Injury*. Bethesda, MD: National Institute of Diabetes and Digestive and Kidney Diseases (2012).
41. Müller-Lissner S, Bassotti G, Coffin B, Drewes AM, Breivik H, Eisenberg E, et al. Opioid-induced constipation and bowel dysfunction: a clinical guideline. *Pain Med.* (2017) 18:1837–63. doi: 10.1093/pm/pnw255
42. Streicher JM, Bilsky EJ. Peripherally acting μ-opioid receptor antagonists for the treatment of opioid-related side effects: mechanism of action and clinical implications. *J Pharm Pract.* (2018) 31:658–69. doi: 10.1177/0897190017732263
43. Oladunjoye AO, Oladunjoye OO, Olubiyi O, Yee MR, Espiridion ED. Predictors and outcomes of invasive mechanical ventilation in opioid overdose hospitalization in the United States. *Cureus.* (2020) 12:e9788. doi: 10.7759/cureus.9788
44. Pajoumand M, Kufera JA, Bonds BW, Devabhakthuni S, Boswell S, Hesselton K, et al. Dexmedetomidine as an adjunct for sedation in patients with traumatic brain injury. *J Trauma Acute Care Surg.* (2016) 81:345–51. doi: 10.1097/TA.0000000000001069
45. Pinto TF, Rocha R, Paula CA, de Jesus RP. Tolerance to enteral nutrition therapy in traumatic brain injury patients. *Brain Inj.* (2012) 26:1113–7. doi: 10.3109/02699052.2012.666369
46. Cheng J, Li L, Xu F, Xu Y, Lin L, Chen JDZ. Poststroke constipation is associated with impaired rectal sensation. *Am J Gastroenterol.* (2020) 115:105–14. doi: 10.14309/ajg.0000000000000479
47. Lim S-F, Ong SY, Tan YL, Ng YS, Chan YH, Childs C. Incidence and predictors of new-onset constipation during acute hospitalisation after stroke. *Int J Clin Pract.* (2015) 69:422–8. doi: 10.1111/ijcp.12528
48. Vieira LV, Pedrosa LAC, Souza VS, Paula CA, Rocha R. Incidence of diarrhea and associated risk factors in patients with traumatic brain injury and enteral nutrition. *Metab Brain Dis.* (2018) 33:1755–60. doi: 10.1007/s11011-018-0287-2
49. Makkar JK, Gauli B, Jain K, Jain D, Batra YK. Comparison of erythromycin versus metoclopramide for gastric feeding intolerance in patients with traumatic brain injury: a randomized double-blind study. *Saudi J Anaesth.* (2016) 10:308–13. doi: 10.4103/1658-354X.174902
50. Berry JAD, Ogunlade J, Kashyap S, Berry DK, Wacker M, Miulli DE, et al. Clinical efficacy of mesenteric lift to relieve constipation in traumatic brain injury patients. *J Am Osteopath Assoc.* (2020) 597–600. doi: 10.7556/jaoa.2020.094
51. Cai W, Wang L, Guo L, Wang J, Zhang X, Cao W, et al. Correlation analysis between post-stroke constipation and brain injury. *Nan Fang Yi Ke Da Xue Xue Bao.* (2013) 33:117–20. Chinese.
52. Robain G, Chennevelle JM, Petit F, Piera JB. Incidence de la constipation dans une population de patients atteints d'hémiplégie vasculaire récente: étude prospective de 152 cas [Incidence of constipation after recent vascular hemiplegia: a prospective cohort of 152 patients]. *Rev Neurol (Paris).* (2002) 158:589–92.
53. Pérez-Sánchez J, Fernández-Boronat J, Martínez-Méndez E, Marín-Cagigas ML, Mota-Puerto D, Pérez-Román MC, et al. Evaluation and handling of constipation in critical patients. *Enferm Int.* (2017) 28:160–8. doi: 10.1016/j.enfie.2017.10.003
54. Guerra TL de S, Mendonça SS, Marshall NG. Incidence of constipation in an intensive care unit. *Rev Bras Ter intensiva.* (2013) 25:87–92. doi: 10.5935/0103-507X.20130018
55. Kieninger M, Sinner B, Graf B, Grassold A, Bele S, Seemann M, et al. Standardized application of laxatives and physical measures in neurosurgical intensive care patients improves defecation pattern but is not associated with lower intracranial pressure. *Crit Care Res Pract.* (2014) 2014:367251. doi: 10.1155/2014/367251
56. Merchan C, Altshuler D, Papadopoulos J. Methylnaltrexone versus naloxone for opioid-induced constipation in the medical intensive care unit. *Ann Pharmacother.* (2017) 51:203–8. doi: 10.1177/1060028016677310
57. Schmittner MD, Vajkoczy SL, Horn P, Bertsch T, Quintel M, Vajkoczy P, et al. Effects of fentanyl and s(+)-ketamine on cerebral hemodynamics, gastrointestinal motility, and need of vasopressors in patients with intracranial pathologies: a pilot study. *J Neurosurg Anesthesiol.* (2007) 19:257–62. doi: 10.1097/ANA.0b013e31811f3feb
58. Fodale V, Schifilliti D, Praticò C, Santamaria LB. Remifentanil and the brain. *Acta Anaesthesiol Scand.* (2008) 52:319–26. doi: 10.1111/j.1399-6576.2007.01566.x
59. Mukhopadhyay A, Tai BC, Remani D, Phua J, Cove ME, Kowitlawakul Y. Age related inverse dose relation of sedatives and analgesics in the intensive care unit. *PLoS ONE.* (2017) 12:e0185212. doi: 10.1371/journal.pone.0185212
60. Ruiz-García T, Nogué-Xarau S, Zavala-Zegarra E, Cirera-Guasch A, Ríos-Guillermo J. Need for sedation and analgesia in patients with a history of substance misuse admitted to an intensive care unit. *Nurs Crit Care.* (2016) 21:358–66. doi: 10.1111/nicc.12117
61. Vearrier L. The value of harm reduction for injection drug use: a clinical and public health ethics analysis. *Disease Month.* (2018) 65(5):119–41. doi: 10.1016/j.disamonth.2018.12.002
62. Chan V, Pole JD, Keightley M, Mann RE, Colantonio A. Children and youth with non-traumatic brain injury: a population based perspective. *BMC Neurol.* (2016) 16:110. doi: 10.1186/s12883-016-0631-2
63. Stevens JP, Wall MJ, Novack L, Marshall J, Hsu DJ, Howell MD. The critical care crisis of opioid overdoses in the United States. *Ann Am Thorac Soc.* (2017) 14:1803–9. doi: 10.1513/AnnalsATS.201701-022OC
64. Hamlin DW, Hussain N, Pathare A. Storms and silence: a case report of catatonia and paroxysmal sympathetic hyperactivity following cerebral hypoxia. *BMC Psychiatry.* (2020) 20:473. doi: 10.1186/s12888-020-02878-5
65. Best KM, Boullata JI, Curley MAQ. Risk factors associated with iatrogenic opioid and benzodiazepine withdrawal in critically ill pediatric patients: a systematic review and conceptual model. *Pediatr Crit Care Med.* (2015) 16:175–83. doi: 10.1097/PCC.0000000000000306
66. Best KM, Wypij D, Asaro LA, Curley MAQ. Patient, process, and system predictors of iatrogenic withdrawal syndrome in critically ill

children*. *Crit Care Med.* (2017) 45:e7–e15. doi: 10.1097/CCM.0000000000001953
67. Tollinche LE, Seier KP, Yang G, Tan KS, Tayban YD, Pastores SM, et al. Discharge prescribing of enteral opioids in opioid naïve patients following non-surgical intensive care: a retrospective cohort study. *J Crit Care.* (2021) 68:16–21. doi: 10.1016/j.jcrc.2021.10.021
68. Academia EC, Gabriel CJ, Mueller A, Schwarz KA, Bartels K, Valuck RJ, et al. Opioid prescribing after discharge in a previously mechanically ventilated, opioid-naïve cohort. *Ann Pharmacother.* (2020) 54:1065–72. doi: 10.1177/1060028020919122
69. Sanavia E, Mencía S, Lafever SN, Solana MJ, Garcia M, López-Herce J. Sedative and analgesic drug rotation protocol in critically ill children with prolonged sedation: evaluation of implementation and efficacy to reduce withdrawal syndrome. *Pediatr Crit care Med J Soc Crit Care Med World Fed Pediatr Int Crit Care Soc.* (2019) 20:1111–7. doi: 10.1097/PCC.0000000000002071
70. Pisani MA, Murphy TE, Araujo KLB, Slattum P, Van Ness PH, Inouye SK. Benzodiazepine and opioid use and the duration of intensive care unit delirium in an older population. *Crit Care Med.* (2009) 37:177–83. doi: 10.1097/CCM.0b013e318192fcf9
71. Wang J, Ji Y, Wang N, Chen W, Bao Y, Qin Q, et al. Risk factors for the incidence of delirium in cerebrovascular patients in a neurosurgery intensive care unit: a prospective study. *J Clin Nurs.* (2018) 27:407–15. doi: 10.1111/jocn.13943
72. Akkurt I, Cetin C, Erdogan AM, Dincel GC, Ceylan AF, Kisa U, et al. Cerebral ischaemia/reperfusion injury could be managed by using tramadol. *Neurol Res.* (2018) 40:774–84. doi: 10.1080/01616412.2018.1477556
73. Unchiti K, Leurcharusmee P, Samerchua A, Pipanmekaporn T, Chattipakorn N, Chattipakorn SC. The potential role of dexmedetomidine on neuroprotection and its possible mechanisms: evidence from *in vitro* and *in vivo* studies. *Eur J Neurosci.* (2021) 54:7006–47. doi: 10.1111/ejn.15474
74. Siddiqui NT, Yousefzadeh A, Yousuf M, Kumar D, Choudhry FK, Friedman Z. The effect of gabapentin on delayed discharge from the postanesthesia care unit: a retrospective analysis. *Pain Pract.* (2018) 18:18–22. doi: 10.1111/papr.12575

Conflict of Interest: The authors declare that the research was conducted in the absence of any commercial or financial relationships that could be construed as a potential conflict of interest.

Publisher's Note: All claims expressed in this article are solely those of the authors and do not necessarily represent those of their affiliated organizations, or those of the publisher, the editors and the reviewers. Any product that may be evaluated in this article, or claim that may be made by its manufacturer, is not guaranteed or endorsed by the publisher.

frontiers | Frontiers in Neurology

REVIEW
published: 06 May 2022
doi: 10.3389/fneur.2022.844497

The Glial Cells Respond to Spinal Cord Injury

*Ruideng Wang†, Rubing Zhou†, Zhengyang Chen, Shan Gao and Fang Zhou**

Department of Orthopedics, Peking University Third Hospital, Beijing, China

It is been over 100 years since glial cells were discovered by Virchow. Since then, a great deal of research was carried out to specify these further roles and properties of glial cells in central nervous system (CNS). As it is well-known that glial cells, such as astrocytes, microglia, oligodendrocytes (OLs), and oligodendrocyte progenitor cells (OPCs) play an important role in supporting and enabling the effective nervous system function in CNS. After spinal cord injury (SCI), these glial cells play different roles in SCI and repair. In this review, we will discuss in detail about the role of glial cells in the healthy CNS and how they respond to SCI.

Keywords: spinal cord injury, glial cells, reactive astrocytes, microglia, neuroinflammation, remyelination

OPEN ACCESS

Edited by:
Mårten Risling,
Karolinska Institutet (KI), Sweden

Reviewed by:
Andrew David Gaudet,
University of Texas at Austin, United States
Aminata Coulibaly,
University of Virginia, United States

***Correspondence:**
Fang Zhou
zhouf@bjmu.edu.cn

†These authors have contributed equally to this work

Specialty section:
This article was submitted to Neurotrauma, a section of the journal Frontiers in Neurology

Received: *28 December 2021*
Accepted: *08 March 2022*
Published: *06 May 2022*

Citation:
Wang R, Zhou R, Chen Z, Gao S and Zhou F (2022) The Glial Cells Respond to Spinal Cord Injury. Front. Neurol. 13:844497. doi: 10.3389/fneur.2022.844497

INTRODUCTION

Spinal cord injury (SCI) is a devastating and debilitating neurological and pathological condition with temporary or permanent major motor, sensory and autonomic dysfunctions. It is estimated that there are about 250,000∼500,000 people suffering from SCI around the world every year. Besides, ∼90% of these cases are caused by traumatic factors, despite the proportion of non-traumatic SCI appears to be growing (1). People with SCI are 2–5 times more likely to die prematurely than people without SCI. Meanwhile, these people with SCI have worse survival rates in low- and middle-income countries. In recent years, more and more studies have begun to reveal the pathophysiology, molecular mechanisms, and possible therapeutic strategies of spinal cord injury. Over the past 50 years, it is gradually realized that glial cells have critical roles in health and disease. Glial cells were first postulated by Virchow in the 19th century and called this unique tissue "Nervenkitt" (2). With time, scientists have been committed to specify these further roles and properties of glial cells in the central nervous system (CNS). The glial cells include four major groups: astrocytes, microglia, oligodendrocytes (OLs), and oligodendrocyte progenitor cells (OPCs). A large number of studies show that these glial cells play an important role in SCI. In this review, we will discuss how these glial cells function in the healthy CNS and respond to SCI.

GLIAL CELLS ARE VITAL IN HEALTHY CNS

Glial cells play a vital role in supporting and enabling effective nervous system function in the healthy CNS. During the development of the CNS, glial cells can constitute a cellular framework that contributes to the development of the nervous system, and induce the survival and differentiation of neuron. The main glial cells types include astrocytes, microglial, OLs, and OPCs. They cooperate with each other and perform different important functions in CNS (**Table 1**).

ASTROCYTES IN THE HEALTHY CNS

Astrocytes are the most abundant glial cells in CNS that have a large amount of complicated and fundamental functions in the healthy CNS. According to the differences in their cellular

TABLE 1 | Function of glial cells in the healthy CNS.

Glial cells types	Function in CNS
Astrocytes	Construction of BBB and BSB, regulating blood flow (1)
	Formation, function, and connection of synapses (2)
	Synthesis and maintenance of the ECM (3)
	Neuronal development, migration and differentiation, function (4)
	Energy provision (5)
	Fluid and ion homeostasis (6)
Microglia	Guide neurons and axons in forming prenatal circuits (7)
	Control synaptic density, connectivity and plasticity (8)
	Phagocytose cellular and myelin components (9)
	Regulate development and responses of neuron and other glial cells (10)
OLs	Myelination of Axons and speed conduction velocity (11, 12)
	Support the function and survival of axons (13, 14)
	Information processing (15)
OPCs	Differentiate into oligodendrocytes (12)
	Modulate neuronal activity (16)
	Immunomodulatory capacity (12)

BBB, blood brain barrier; BSB, blood spinal barrier; ECM, extracellular matrix; OLs, oligodendrocytes; OPCs, oligodendrocyte progenitor cells.

morphologies and anatomical locations, astrocytes are divided into two types: protoplasmic astrocytes with the morphological feature of several stem branches are found in gray matter while fibrous astrocytes with the morphological feature of many long fiber-like processes are found in white matter (3). In addition, both astrocyte subtypes have critical roles in health and disease. Astrocytes contribute to the construction of blood-brain barrier (BBB) and blood-spinal barrier (BSB) by combining with endothelial cells and perivascular pericytes through astrocytic endfeet (4–6). Previous studies have indicated that astrocytic endfeet show specialized feature characteristic as the astrocytic endfeet membrane expresses a large number of water channel aquaporin 4 (AQP4) and the Kir4.1 K+ channel, which is important for the properties of BBB (7–9). The Kir4.1 and AQP4 both bind to α-Syntrophin that could contribute to the inductive influence on BBB (10). Astrocytes are proved to produce a series of humoral agents, such as glial cell line-derived neurotrophic factor (GDNF), transforming growth factor-β (TGFβ), and angiopoetin-1 that can induce the aspects of BBB phenotypes (11–13). What's more, it is now recognized that the control of blood flow in brain is mediated by astrocytes. Neuronal activities may result in releasing potassium ions from astrocytic endfeet, extracellular K+ concentration can dilate the vessels through hyperpolarizing smooth muscle cells (14). The rise of Ca^{2+} concentration in astrocytic endfeet can also constrict vessels (15).

Astrocytes contribute to the formation, function, and connection of synapses as astrocytes have a close connection with synapses. The "tripartite synapse" concept was first described by Alfonso Araque, it includes the classic pre- and post-synaptic neuronal structures and astrocytes which should be viewed as integral modulatory elements of tripartite synapses (16). The role of astrocytes in synapses formation was first studied in 1995. Meyer-Franke et al. observed that retinal ganglion cells (RGCs) make very few synapses by purifying and culturing RGC neurons, however, RGCs can make many synapses if they are cultured in an astrocyte feeder layer or a culture medium that is previously conditioned by astrocytes (17). On the basis of the RGC culture system, subsequent studies identified that multiple factors secreted by astrocytes could control the formation of synapses. Thrombospondins (TSPs), the extracellular matrix (ECM) proteins secreted by astrocytes, have been proved to contribute to the formation of synapses (18, 19). By adding purified TSPs to cultured neurons greatly increased the number of synapses. In addition, Cagla Eroglu et al. showed that the von Willebrand factor A (VWF-A) domain of the calcium channel subunit α2δ1 interacts with the EGF-like receptors common to all TSPs which enhanced synaptogenesis both *in vitro* and *in vivo* (20). Hevin, another synaptogenic protein secreted by astrocytes, also induces an increase in the number of structural synapses by bridging presynaptic neurexin-1alpha (NRX1α) (21). Astrocytes can control the specific aspects of synapses function through many different signals, such as positive [cholesterol, glypican 4,6, ECM, tumor necrosis factor a (TNF-a)] and negative (SPARC, TSP) signals (22–27). For example, astrocyte-secreted cholesterol plays an important role in regulating the glutamatergic presynaptic function by complexing to apolipoprotein E-containing lipoproteins (27). Besides, astrocyte-secreted glypican 4/6 has an ability to upregulate the surface level of alpha-amino-3-hydroxy-5-methyl isoxazole propionic acid (AMPA) receptors (AMPARs) at synapses and increase the synaptic activity in neurons (26). As we all know, synapses can undergo rapid formation and elimination under certain conditions. Recent studies have identified some potential mechanisms, such as direct and indirect role of astrocytes in mediating synapses elimination. Microglia have been shown to recognize and phagocytose C1q/C3-coated synapses (28), and astrocytes would express TGF-β to induce the C1q expression which is critical for the phagocytic functions of microglia, and finally astrocytes mediate microglial-dependent synapses elimination (29). Meanwhile, astrocytes contribute to synapses elimination through MEGF10 and MERTK pathways (30).

Astrocytes are actively involved in the synthesis and maintenance of the ECM by secreting various substances in CNS. Tenascin-C, a glycoprotein, is expressed by astrocytes which can regulate cell growth, adhesion, and migration (31). Besides, astrocytes produce a large number of proteoglycans, such as chondroitin sulfate proteoglycans (CSPGs), which are suited for regulating neural development (32).

Other aspects of the role in CNS, such as astrocytes can store glycogen granules and make important contributions to the metabolism in CNS (33). The astrocyte-neuron lactate shuttle hypothesis which explains how astrocytes support neurons energy metabolism in detail. Glutamate released by neurons during the neuronal activity can bind to glutamate transporters (GLT-1), expressed by astrocytes, which mediate astrocytes taking up glucose from the blood circulation *via* glucose transporters (GLUT1). Then, glucose is subsequently metabolized to lactate

and pyruvate. On the one hand, intracellular lactate can be shuttled to extracellular matrix *via* monocarboxylate transporter (MCT) 1 and MCT4 expressed by astrocytes and then could be absorbed by neurons through neuronal MCT2. Neuronal lactate can participate in the neuronal cell energy metabolism and promote ATP synthesis in the mitochondria directly or after conversion to pyruvate (34, 35). Similarly, ammonium (NH_4^+) released by neurons increase lactate levels in astrocytes which can be shuttled to neurons (36). In summary, as astrocytes possess unique cellular properties, they play a vital role in the function and integrity of CNS (**Table 1**).

MICROGLIA FUNCTIONS IN THE HEALTHY CNS

Debate on microglial origin still continues in this field, recent studies showed that microglia were derived from erythromyeloid precursors in the yolk sac through Pu.1- and Irf8-dependent pathways (37). Microglia are crucial for the development of CNS. They arise around the same time as neurons and critically contribute to the establishment of complex neuronal networks. During the early development of CNS, microglia act as guidepost cells to guide neurons and axons to form prenatal circuits (38). Moreover, microglia are involved in the regulation of surrounding cellular milieu by secreting trophic factors [brain-derived neurotrophic factor (BDNF) (39), insulin-like growth factor-1 (IGF-1) (40), and hepatocyte growth factor (HGF) (41)] which could promote the survival of neurons. For instance, the best-known trophic factors, IGF-1, can enhance the survival of cortical neurons. On contrary, inhibiting IGF-1 signaling (minocycline, CD11b-DTR, and $Cx3cr1^{GFP/GFP}$) would result in the cell death in layer V (40). Besides, microglia are the sensors of damage as they can phagocytose apoptotic neuron driven by both TAM receptor ligands Gas6 and protein S (42). Additionally, they engulf excess new born neural progenitor cells *via* primary phagocytosis which is beneficial to the homeostasis during the development of CNS (43).

Microglia play an important role in the control of synaptic density, connectivity, and plasticity. Microglia can selectively remove synapses from injured neurons which is termed "synaptic stripping" (44, 45). This process is identified to be mediated through several mechanisms. C3 receptors (CR3) expressed by microglia can bind to C1q and C3, the complement proteins expressed by damaged cells, which could lead the microglia to be involved in the active removal or "stripping" of these synaptic contacts and finally contribute to synaptic elimination (46). Microglia can also activate "synaptic stripping" through the fractalkine/CX3CR1 signaling pathway (47). Except for the receptor binding mode, microglia can also shape the strength and plasticity of synapses by releasing reactive oxygen species (ROS) (48), nitric oxide (NO) (49), TNF-α (50) as well as neurotrophic factors [BDNF (51)]. For example, microglia-derived BDNF activates Trk in spinal neurons that could impact synapse activity (52). Above all, microglia are vital for neuronal health and survival during the development of CNS (**Table 1**).

OLs AND OPCs FUNCTIONS IN THE HEALTHY CNS

Another major glial cell type is OLs, generated from OPCs, are fundamental to the myelin formation in CNS. The newborn OPCs can express DM-20 during embryonic development, and first appear in a restricted region of the embryonic ventral neural tube at embryonic day 12.5 in mice (53). Then, they finally differentiate into OLs through a complicated process. Importantly, OPCs are observed to differentiate into OLs throughout development and adulthood. Except for differentiating into OLs, OPCs can tile throughout the entire CNS and constitute ∼5% of all cells (54). The fate of OPCs to keep as precursor cells or differentiate into OLs is influenced by many factors, such as mechanical environment and extracellular matrix elasticity (55–57). OPCs continue to be precursor cells by self-renewal to achieve homeostasis in CNS. Besides, OPCs express GABA receptors, kainite glutamate receptors, and AMPA receptors to form neuron-OPC synapses which modulate the neuronal activity (58, 59).

Oligodendrocytes are crucial for maintaining the function and integrity of axons. The most important function of OLs is to generate myelin sheath, as we all know that myelin sheath is an extension structure of the OLs plasma membrane wrapping the nerve axons. Myelination is a complex and tightly regulated process: OLs in the growth zone of CNS undergo proliferation under certain factors, then contact and arrange along the axon, respectively. The inner and outer plasma membrane wrapping the nerve axons interact with each other through cytoplasmic channels which pushes the inner plasma membrane layer after layer to generate the compact myelin. Once the appropriate number of plasma membrane wrapping per axon is generated, this process is called myelination (60). Functionally, the myelin sheath enables fast and efficient nerve conduction in the nervous system and provides metabolic support to the axons (61).

Oligodendrocytes have a physiological role in supporting the function and survival of axons that is independent of myelination. In the absence of PLP and DM20, the membrane proteolipids of myelin sheath that are integral for myelinated axons, myelination is not disrupted but with subsequently widespread axonal dysfunction (62). Subsequent studies found that PLP/DM20 was important for OLs in supporting the axonal energy metabolism (63, 64). With the further study, it is now well-recognized that OLs are essential for supporting the axons energy metabolism (65). The mechanisms how OLs provide neuronal metabolic support are described in detail as following. OLs can express a large number of MCT1, which can mediate metabolic support to neurons by co-transporting lactate and pyruvate (66). OLs can take up glucose from the extracellular matrix *via* GLUT1 expressed by OLs and then convert glucose into lactate and pyruvate by glycolysis. Besides, glutamate released by neuron after neuronal activity can bind to NMDA receptors (NMDARs) expressed by OLs which subsequently result in an increased glucose uptake as well as more lactate and pyruvate production in OLs (67). Moreover, the gap junctions between astrocytes and OLs may contribute to OLs metabolic support as lactate and glucose derived from astrocytes could be shuttled into OLs

through gap junctions, such as Cx32-Cx30, Cx32-Cx26, Cx47-Cx30, and Cx47-Cx43 (68–70). All the functions of OLs and OPCs in healthy CNS are shown in **Table 1**.

GLIAL CELLS RESPOND TO SCI

As discussed above, glial cells, such as astrocytes, microglia, OLs, and OPCs all are crucial for the development of CNS and maintaining homeostasis in healthy CNS. They have different and vital physiological functions for the CNS due to their cytological properties and cellular interactions. After SCI, the noxious mechanical forces cause tissue damage, such as cells death and disrupt the homeostasis of local CNS, as a result, these events trigger diverse multi-cellular responses and can lead either to the neural repair or secondary cellular injury. Glial cells exhibit various pathophysiological functions to repair the damage and maintain local microenvironment homeostasis due to various internal and external factors after SCI. Next, we will describe in detail the response of various glial cells to SCI.

ASTROCYTES: REACTIVE ASTROCYTES AND GLIAL SCAR FORMATION

Astrocytes, as discussed above, are essential to maintain the homeostasis in healthy CNS. Similarly, astrocytes also play an important role after SCI. After SCI, various intrinsic and extrinsic factors subsequently regulate astrocytes into reactive astrocytes with significant morphological, phenotypical, and functional changes, such changes are mainly based on different factors, such as the injury severity, the injury time, and the distance of astrocytes to the lesion. Reactive astrocytes have characteristics in morphology, such as cellular hypertrophy, thicker processes, and increased expression of intermediate filament proteins. Besides, the degree of changes are proportional to the stimulus intensity (71). On the basis of discrete gene-expression identifiers and functions, different types of reactive astrocytes have been recognized, such as A1, A2, and scar-forming astrocytes (72, 73). For example, complement component 3 is highly expressed by A1 astrocytes, and S100A10 is a specific hallmark for A2 astrocytes while type I collagen for scar-forming astrocytes (73, 74). Compared with the normal astrocytes, accumulating evidence suggests that reactive astrocytes show various abnormal functions, such as releasing proinflammatory chemokines and cytokines (71).

Molecules and Signaling Pathways Implicated in Formation of Reactive Astrocytes

Mechanical forces usually cause direct damage to the normal tissue and disrupt local homeostasis when patients or animals undergo SCI, which on the other hand triggers multitudinous multi-cellular responses. Although it is incompletely understood how mechanical forces and damaged tissues initially trigger the activation of astrocytes after SCI. The previous study has identified that astrocytes are susceptible to membrane distortions and debris (75). Traumatic membrane deformation could activate mechanosensitive ion channels and result in the rapid influx of extracellular calcium and sodium in astrocytes (76–78). Other studies show that plasma membrane stretching can rise the release of intracellular calcium and ATP *via* extracellular signal-regulated protein kinase (ERK) and PKB/Akt signaling pathways (79, 80). Besides, astrocytes may also release endothelin-1 (ET-1), isoprostanes, and matrix metalloproteinases 9 (MMP-9) after stretch-induced injury (81, 82). More studies are needed to have a deeper understanding of these.

Accumulating studies have identified that a lot of molecules, such as chemokines, cytokines, transcription factors, and growth factors are the mediators for the activation of astrocytes (factors are shown in **Table 2**). For example, proinflammatory cytokines, such as TNF-α, interleukin (IL)-6, and IL-1β initially trigger the reactivity of astrocytes during the acute phase after SCI while other molecules maintain astrocytes reactivity in the later stages (83–85). Additionally, it is worth mentioning that reactive astrocytes can release triggering molecules, such as TNF-α, IL-6, and MMP-9, which in turn activate more astrocytes (86). Besides, other glial cells, such as activated microglia, are identified to induce the activation of astrocytes by secreting various factors, such as Il-1α, TNF, and C1q (87). Other related molecules involved in the activation of astrocytes are shown in **Table 2**.

TABLE 2 | The activation of astrocytes.

Factors	Signaling pathways	Molecules and gene expression
Membrane stretching (17–19) ATP (19), debris (20) IL-1β, IL-1α, IL-2, IL-6, IL-10, IL-17, TNF-α, IFN-γ, CNTF, TGFβ1, INFγ, IL-2, LIF, C1q, oncostatin M, SHH (21–26) Glutamate, norepinephrine (27) NO, ROS (26) MCP-1, FGF-2, IGF, MMP-9, Sox9 (4) Amyloid-beta (28), α-synuclein (29) Estrogens (30), glucocorticoids (31) LPS, Toll-like receptor ligands (32) Laminin, fibronectin (33) Erythropoietin, ET-1 (34)	STAT3 signaling (35) NFκB signaling (36) TGF-β signaling (37) JNK/c-Jun signaling (34) MAPK Signaling (38) Olig2 (39) SOC3 (40) RhoA (4) Smads (4) cAMP (41) IGF1-calcineurin (42)	CCL2, CCL3, CCL4, CCL5, CXCL1, CXCL2, CXCL10, CCL12, CXCL20 (37, 43, 44) VEGF, FGF-2, BDNF, GDNF (24, 45, 46) IL-1β, IL-6, IL-10, TNF-α, INF-γ, TGF-α, TGF-β, CNTF, LIF, CLCF1 (23, 37, 43, 47, 48) CSPGs, IGFBP6, BMP, connective tissue growth factor, collagen I, fibronectin, MMP-9 (49–52) ROS, NO, NOS (53–55) GABA, glutamate, d-serine (56–58) Nestin, vimentin, GFAP (49, 52) EGFR, KCa3.1, AQP4 (59–61) STAT3, NF-κB, Olig2, SOX9, mTOR, SOCS-1, SOCS-3 (40, 47, 48) Adenosine, glutathione (4)

IL, interleukin; CNTF, ciliary neurotrophic factor; LIF, leukemia inhibitory factor; SHH, Sonic hedgehog; MCP-1, Monocyte chemoattractant protein-1; FGF-2, fibroblast growth factor-2; NO, nitric oxide; ROS, reactive oxygen species; IGF, insulin-like growth factor; LPS, lipopolysaccharide; MMP-9, matrixmetalloproteinase-9; ET-1, endothelin-1; VEGF, vascular endothelial growth factor; BDNF, brain derived neurotrophic factor; GDNF, glial cell derived neurotrophic factor; CSPGs, chondroitin sulfate proteoglycans; BMF, bone morphogenetic protein; GFAP, glial fibrillary acidic protein; EGFR, epidermal growth factor receptor.

Many signaling pathways are closely involved in the activation of astrocytes, such as STAT3, TGF-β, NF-κB, JNK/c-Jun, and MAPK (more signaling ways are shown in **Table 2**). Here we will mainly introduce TGF-β and STAT3 signaling pathways. The STAT3 signaling pathway is one of the most important signaling pathways to mediate the formation of reactive astrocytes. Mice with STAT3 knock-out in astrocytes showed the attenuated upregulation of GFAP, unsuccessful cell hypertrophy, and failed scar formation after SCI (88). Other groups also identified that selective STAT3 deletion in mice could limit the migration of astrocytes and result in the widespread infiltration of inflammatory cells, degeneration of neurons, and demyelination of axons that can lead to severe motor deficits. However, by the activation of STAT3 signaling pathway, they observed that reactive astrocytes migrated rapidly around the lesion and secluded inflammatory cells that lead to a notable improvement in functional recovery (89). These results provided a potential intervention target of STAT3 signaling pathway in the treatment of SCI. TGF-β signaling pathway greatly contributes to the formation of reactive astrocytes. As discussed above, TGF-β is a key upstream trigger in the formation of reactive astrocytes. The previous study has shown that TGF-β could increase the expression of anti-regenerative molecules, such as CSPGs, laminin, and fibronectin by several-fold in reactive astrocytes (90). Interestingly, fibrinogen could act as a stimulating factor which can activate TGF-β signaling pathway, as a result, it could induce the activation of astrocytes and formation of CSPGs (91). In addition, it could induce astrogliosis by injecting fibrinogen into the mouse cortex (91). On contrary, with the genetical ablation of fibrinogen in mice, they found inhibited TGF-β activation and hampered glial scar formation (91). Other signaling pathways are shown in **Table 2**.

TABLE 3 | Positive and negative influence of reactive astrogliosis.

Positive influence of reactive astrocytes
Seclude inflammatory cells and limit the extent of inflammation (62)
Repair damaged BSB and modulate blood flow (62)
Clearance of debris, alleviation of glutamate excitotoxicity (53, 63)
Mediate neuroimmune response (32)
Formation of glial scar (64, 65)
Defend against oxidative stress (64)
Contribute to remyelination (66)
Negative influence of reactive astrocytes
Obstruct axon growth, facilitate axon degeneration (67)
Formation of glial scar (64)
Inhibition in NPCs and OPCs (68)
Contributes to the development and persistence of chronic pain (69)

Reactive Astrocytes Expression Change and Their Functions

Recent years, numerous studies have identified that the activation of astrocytes could lead to the change of functions with releasing a range of molecules, such as cytokines [TNF-α, IL-6, IL-10, IL-1β, etc. (85, 92, 93)], chemokines [CCL2, CCL3, etc. (94, 95)], growth factors [BDNF, GDNF, etc. (96, 97)], toxic amino acids [GABA and glutamate (98, 99)], extracellular matrix [CSPGs, collagen I, fibronectin, MMP-9, etc. (100–102)], and intermediate filaments [Nestin, vimentin, and GFAP (100, 102)], which would have a significant influence on the spinal cord microenvironment after SCI (**Table 2**). The molecules released by reactive astrocytes can activate more normal astrocytes into reactive astrocytes and contribute to glial scar forming. On the other hand, they also affect other cells, such as neurons, OPCs, and microglia through a variety of complexed effects (71).

Over the past years, reactive astrocytes were thought to be detrimental for recovery after SCI. However, recent studies have identified that reactive astrocytes also contribute to SCI repair. Here, we will discuss the beneficial and detrimental effects of reactive astrocytes after SCI (**Table 3**).

Reactive astrocytes are considered to be a defense mechanism of astrocytes responding to SCI. After SCI, BBB breaks down and becomes leaky to endogenous and exogenous blood-borne macromolecules that can result in disastrous consequence. These changes will mediate reactive astrocytes to upregulate Sonic hedgehog (SHH) and activate signaling cascades to repair the tight junctions of the BBB (103). Interestingly, with the absence of reactive astrocytes, it was failure in repairing the damaged BBB (104). At acute stage after SCI, reactive astrocytes migrate rapidly around the lesion to seclude inflammatory cells and limit the extent of inflammation that has a notable improvement in functional recovery (89). Further, Jill et al. found significantly increased and prolonged infiltration of inflammatory cells around the lesion with selective and conditional reactive astrocytes ablation in mice (104). Various endogenous and exogenous factors result in the release and accumulation of cell debris and neurotoxic factors in the extracellular spaces after SCI. Recently, reactive astrocytes were identified to play a crucial role in removing these cell debris and neurotoxic factors. More importantly, reactive astrocytes have the ability to phagocytose dead cells *in vitro* and *in vivo via* the upregulation of ABCA1 (105, 106). Reactive astrocytes can also reduce the impact of glutamate excitotoxicity on neurons and OPCs by clearing excess glutamate from the blood or necrotic neuronal cell death (107). Besides, reactive astrocytes can affect immune cells through releasing various molecules, such as TNF-α, TGF-β, and proteoglycans. CSPGs have a close relationship with immune activity as they can recruit chemokines and growth factors that enhances the connection of immune cells (71).

Glial scar formation has been recognized for many years. After SCI, inflammatory cells (macrophages, neutrophils, and lymphocytes), fibrotic cells, and other cells, such as pericytes, fibroblasts, and OPCs migrate rapidly into the lesion, and subsequently newly proliferated, elongated reactive astrocytes come around the lesion to form a border which could separate necrotic tissue from healthy tissue (108–110). The border formed by reactive astrocytes can limit further expansion of the lesion and restrict inflammatory cells within damaged tissue that will protect the surrounding viable neural tissue from secondary damage (111). Further, selective inhibition of astrocyte reactivity results in the widespread propagation of inflammatory cells beyond the lesion.

In addition to the above protective effects, reactive astrocytes also have detrimental effects. As discussed above, reactive astrocytes can form a physical barrier to confine the lesion, however, it can also obstruct axonal growth. Besides, reactive astrocytes secrete inhibitory proteins, such as CSPGs, which are considered to be the major inhibitors of axonal regeneration. CSPGs derived from reactive astrocytes inhibit the growth of axons *in vitro*, and axonal regeneration is observed to stop at CSPG-rich regions *in vivo*. On the contrary, Chondroitinase ABC, by removing CSPG glycosaminoglycan (GAG) chains, attenuates the inhibitory activity of CSPGs, which is shown to facilitate axonal regeneration and functional recovery (112). Further, Hyunjung Lee et al. found that using thermostabilized Chondroitinase ABC through a hydrogel-microtube scaffold system could enhance the axonal regrowth, sprouting, and improve functional recovery after SCI (113). Additionally, other studies have shown that CSPGs inhibited axonal regeneration while the inhibition of CSPGs could improve functional recovery (114).

Reactive astrocytes play a modulatory role in NPCs and OPCs post-SCI. OPCs have extremely powerful ability in remyelination as they can proliferate and differentiate into OLs that will replenish a large number of lost OLs after SCI. Recently, Justin R Siebert et al. have discovered that astrocytes-derived CSPGs highly inhibited the migration and differentiation of OPCs *in vitro*, and the number of OPCs surrounding the lesion significantly increased when treated with the enzyme chondroitinase ABC (115). Other study also proved that CSPGs had a dampening effect on the outgrowth and differentiation of OPCs, and treated with chondroitinase ABC could completely eliminate this inhibition (116). In addition to CSPGs, other molecules, such as BMP and ET-1 released by reactive astrocytes can also inhibit the differentiation of OPCs and finally influence remyelination (117, 118). Besides, reactive astrocytes have a role in inhibiting the neuronal differentiation of NPCs by expressing insulin-like growth factor binding protein 6 (IGFBP6) and CSPGs (119).

MICROGLIA/MACROPHAGES: NEUROINFLAMMATION

Microglia/macrophages maybe the most potent modulators to launch the innate immune response after SCI. As discussed above, we know that microglia are resident in CNS while macrophages derive from the periphery. However, activated microglia and macrophages are difficult to distinguish through the morphology or antigenic markers following CNS injury, so they are referred as microglia/macrophages. Over the past years, the studies have revealed that microglia/macrophages had both the detrimental and beneficial effects on neurological recovery due to their different phenotypes at different stages after SCI (120).

Microglia/Macrophages Phenotypes

Microglia/macrophages phenotypes are mainly determined by the focal lesion and new stimuli can change the phenotypes. It is now well-acknowledged that microglia/macrophages are activated into different functional phenotypes after SCI. M1/M2 dichotomy is the earliest and simplest concept. M1 macrophages (or 'classically' activated macrophages) are activated by the prototypical T helper 1 cytokine (TH1), interferon-γ (IFNγ), and lipopolysaccharide (LPS), which typically release inflammatory cytokines (IL-1, IL-6, TNFα, etc.), chemokines (CCL8, CCL 15, CXCL 10, CXCL 11, etc.), and the high levels of oxidative metabolites (ROS and NOS). On the contrast, M2 macrophages (or "alternatively" activated macrophages) are activated by the prototypic TH2 cytokine IL-4 and IL-13, which can produce numerous protective factors (TGFβ, IL-10, IL-1Ra, etc.) and clear cellular debris (120–122). However, the status and functional phenotypes of microglia/macrophages are much more complicated *in vivo*. Accumulating studies have identified the multiformity in M2 phenotype subpopulations, such as M2a, M2b, and M2c phenotypes, each phenotype is characterized by unique physiological features and distinct biological functions (121). Nowadays, microglia/macrophages in many other situations did not show a clear M1 or M2 phenotype or showed phenotypic plasticity during the disease progression. Single cell techniques and other new tools are, contributing to the understanding of polarization heterogeneity (123). By single-cell analysis, Lindsay M Milich at el. identified four microglial subtypes in the injured mouse spinal cord, which were labeled homeostatic, inflammatory, dividing, and migrating microglia. Homeostatic microglia were identified by several annotated markers of steady-state microglia, such as P2ry12, Siglech, and Tmem119. Inflammatory microglia were identified by the low expression of purinergic receptor P2ry12 and increased expression of Igf1. Dividing microglia expressed low levels of P2ry12, increased expression of Msr1, and high levels of cell cycle–related genes, such as Cdk1. Migrating microglia had the low levels of P2ry12, and the high levels of Msr1 and the growth factor Igf1 (124). Besides, two macrophage subtypes were named chemotaxis-inducing macrophages and inflammatory macrophages in addition to the border-associated macrophages based on their gene ontology terms. Both subtypes expressed the lysosomal gene Cd63, however, chemotaxis-inducing macrophages preferentially express heme oxygenase Hmox1 while inflammatory macrophages express *Apoe* (124, 125).

Microglia/Macrophages Respond to SCI

Activated microglia could release a large number of pro-inflammatory cytokines, chemokines, and other cytotoxic factors after SCI. They respond to SCI within minutes by producing pro-inflammatory molecules which can lead to the influx of multiple inflammatory cells from the circulation. Neutrophils are the first circulating leukocytes to infiltrate into the lesion and are prominently located in severely damaged site (126, 127). Besides, peripheral macrophages will infiltrate into the lesion and help clear apoptotic cells (127). However, these neutrophils and macrophages may be destructive to the lesion as they can produce various molecules, such as MMP-9 and disrupt the functions of the BSB (128). Besides, T and B lymphocytes are found to infiltrate into the injured lesion and cause a systemic autoimmune response (129). Here, we will mainly discuss the

harmful and beneficial effects of neuroinflammation induced by activated microglia/macrophages after SCI.

Activated M1 microglia/macrophages induce neurons death and contribute to the secondary damage by releasing pro-inflammatory factors, such as IL-1β, IL-6, TNF-α, CCL5, and iNOS. Here we mainly elaborate IL-1β and TNF-α that play a detrimental role after SCI. IL-1β expressed by astrocytes and microglia was detected to reach peak at 12 h after SCI in rodents (130). IL-1β and TNF-α were proved to involve in the recruitment and activation of peripheral immune cells and the activation of astrocytes and microglia. In rats, the infusion of IL-1β markedly enhanced the cortical neuronal loss, on the contrast, it could significantly inhibit neuronal damage by IL-1 receptor antagonist (IL-1ra) (131). Other study also identified that IL-1β contributed to ischemic brain damage while IL-1ra markedly protected the focal cerebral from ischemia in the rat (132). TNF-α, another proinflammatory cytokine, expressed mainly by activated microglia/macrophages, contributes to neuronal cells death after SCI by binding to TNFRI and TNFRII (133). In addition, soluble TNFRI, which can compete with TNF-α by binding to TNFR, eventually reduces the neuronal cells death (133). Tiziana Genovese et al. indicated that the genetic inhibition of TNF-α significantly reduced the degree of inflammation, tissue injury, and apoptosis in an experimental model of spinal cord trauma (134). Besides, overexpressing TNF-α was shown to mediate OLs, OPCs death, and myelin vacuolization which could finally result in spontaneous demyelination (135).

Activated M2 microglia/macrophages have anti-inflammatory and neuroprotective effects by increasing the expression of anti-inflammatory molecules, such as IL-10, TGF-β, IGF-1, and BNDF. For example, IL-10 shows a wide range of regulatory activities in response to SCI. Tiziana Genovese et al. found that there was a significant augmentation of TNF-α, IL-1β and S100β which worsened the recovery of limb function in IL-10 KO mice (136). Recently, the group of Jessica Y Chen delivered IL-10 into mice SCI model by loading an implantable biomaterial scaffold. They observed that IL-10 could significantly reduce damage to tissue and improve subsequent motor deficits (137). IGF-I is a potent neurotrophic factor released by activated microglia/macrophages with anti-inflammatory response. The previous study showed that IGF-I gene transfer after SCI could inhibit the loss of neurons and significantly improve the neurological dysfunction (138). Besides, other study showed that BDNF and IGF-I could significantly enhance neuroprotective effects, such as repairing BSCB damage, alleviating edema, and cells injury by the downregulation of nNOS after SCI in rat model (139).

OLs AND OPCs: DEMYELINATION AND REMYELINATION

OLs and Demyelination

In addition to the immediate trauma damage, there is a prolonged secondary damage after SCI. OLs are quite susceptible to changes in the surrounding microenvironment after SCI which can result in the necrosis, apoptosis, and autophagy of OLs (140–142). Acute OLs death has previously been investigated to occur within 15 min after injury and the number of OLs steadily declined by 7 days post-injury (143, 144). Previous studies have identified several aspects of subsequent damage that can lead to the death of OLs. Ischemia is an apparent reason to result in OLs death in the damaged areas of white matter (145). Ischemia and reperfusion contribute to the formation of free radical, such as reactive oxygen and nitrogen species, and OLs are particularly vulnerable to the oxidative stress. After SCI, ROS (hydroxyl radicals and superoxide) and RNS (nitric oxide, peroxynitrite, and nitrated protein) were detected to be at the increased levels (146–148). By oxidizing protein, lipids and nuclear material, ROS and NOS damage OLs which results in the necrosis and apoptosis of OLs. Besides, excitotoxicity is another major factor leading to the OLs death after SCI. The glutamate will reach a toxic level after SCI that can lead to the OLs death *in vitro* and *in vivo*. Glutamate binding to AMPA/kainate glutamate receptors expressed in OLs leads to OLs death *via* receptor overactivation and the specific inhibitors of AMPA receptors can block OLs death (149). As discussed above, extracellular ATP released by multiple cell types after SCI can also contribute to OLs death. ATP is proved to cause OLs death *via* an activation of calcium-permeable P2X(7) and treatment with P2X(7) antagonists reduces demyelination and improve neurological symptoms (150). In addition, recent studies reveal that proinflammatory cytokines potentially contribute to OLs cell death. An overexpression of TNF-α was observed to induce OLs apoptosis which could contribute to the degenerative change and demyelination *via* TNFR1 and TNFR2 expressed in OLs (151). Other cytokines, such as IL-2, IL-1, IFNγ, and proNGF, all contribute to OLs apoptosis (142). In addition to apoptosis and necrosis, autophagy is activated in SCI, and Beclin1, a promoter of autophagy, is highly expressed in OLs (152).

Oligodendrocytes are fundamental to myelin formation as described earlier. The injury or death of OLs results in the degeneration of myelin sheaths and the support of axons by OLs would be disrupted after SCI which eventually lead to the widespread demyelination of spared axons. As a matter of fact, accumulating studies have demonstrated that demyelination indeed occurred in animal models and human after SCI (153, 154). For example, demyelinated axons were seen within 2 weeks after injury in paraplegic domestic animals in previous study (153). More interestingly, the extent of demyelination mainly contingents on the type and severity of injury. The normal myelinated axons are characterized by the regular distribution of sodium and potassium channels, after demyelination, the distribution of sodium and potassium channels is disrupted that contributes to an axonal conduction block (155). Besides, demyelination is identified to increase voltage-gated Na+ channels, which may result in Na^+ influx during action potential propagation. To eliminate the excess Na^+, more ATP is required which can disrupt the axonal internal energy balance. Additionally, the excess Na^+ may lead to axonal Ca^{2+} overload *via* the $Na^+/Ca2^+$ exchangers. These events eventually result in axonal degeneration (156, 157). Besides, the demyelinated axons are vulnerable to damage in the microenvironment after SCI and ultimately lead to axonal degeneration (158).

TABLE 4 | Factors regulate remyelination via different effects on OPCs.

Classifications	Factors	Effect on OPCs
Growth factors	PDGF-A; EGF; FGF-2; IGF; Nrg-1 (70–72)	Survival ↑
Neurotrophins	BDNF; NT-3 (73, 74)	Proliferation↑
Chemokines	CXCL1; CXCL12 (74)	Migration ↑
Cytokines	CNTF; LIF; IFN-γ; IL-17A; IL-1β (66, 75, 76)	Differentiation ↑
Transcription factors	OLIG1; OLIG2 (77)	
	SOX5; SOX6; SOX8; SOX9; SOX10 (78, 79)	
	ZFP191; ZFP488 (80)	
	MYT1; MASH1; NKX family; YY1 (81–83)	

PDGF-A, platelet-derived growth factor; Nrg-1, neuregulin-1; IL, interleukin; BDNF, brain derived neurotrophic factor; FGF-2, fibroblast growth factor-2; IGF, insulin-like growth factor; EGF, epidermal growth factor; NT-3, neurotrophin-3; LIF, leukemia inhibitory factor.

OPCs and Remyelination

After SCI, OPCs are multipotential stem cells which can differentiate into remyelinated cells to involve in axonal remyelination and contribute to the glial scar formation. McTigue et al. assessed the proliferation of NG^{2+} cells and OLs by bromodeoxyuridine incorporation and they found increased proliferation of NG^{2+} cells persisting throughout the first 4 weeks post-injury while the number of OLs continuously reduced by 7 days post-injury. However, they detected an increased number of OLs at 14 days post-injury. These results showed that proliferated NG^{2+} cells may differentiate into OLs after injury (159). Besides, the study using fate mapping confirmed that 30% of new OLs responsible for myelin regeneration were derived from OPCs while OPCs differentiate into the majority of myelinating Schwann cells (160). Other group also revealed that OPCs from the PDGFRα-expressing lineage could be transformed into functional myelinating Schwann cells after SCI (161). Moreover, by using genetic fate mapping, Hackett et al. found that ∼25% of astrocytes were derived from NG^{2+} cells in the glial scar by 4 weeks after SCI (162). It is worth mentioning that the functions of OPCs are intricately modulated by a complex network including various factors (**Table 4**). We will not go into further discussion here. In addition to OPCs, the endogenous NPCs can also contribute to OLs replacement as they will be activated and migrate into the lesion after SCI (163, 164).

Remyelination occurs spontaneously on residual axons after SCI. Remyelination is difficult to detect until genetic fate mapping approaches are applied, the scientists can distinguish new myelin from preexisted myelin *via* labeling new myelination. Assinck et al. found that spontaneous remyelination was induced by OLs and myelinating Schwann cells in mice after SCI (160). Besides, other group detected remarkably clear visualization of spontaneously regenerated myelin *in vivo* (165). However, endogenous remyelination was limited due to multi-factors (166). Nashmi et al. found that the spontaneous remyelination in the injured white matter was non-optimal and incomplete because the newly formed myelin around the injured axons was thinner than normal myelinated axons (167). Recent studies have uncovered that multiple factors affected remyelination, such as (1) the myelinating OLs derived from OPCs are inadequate (168), (2) OLs maturation and myelination are limited (142), (3) axonal ensheathment and remyelination is influenced (169), and (4) OPCs, neural progenitor cells (NPCs) are affected by the unfriendly microenvironment (166). Therefore, more endogenous mechanisms of remyelination are needed to be explored.

CONCLUSIONS

Glial cells play a crucial role in maintaining the function and homeostasis of the CNS. Once the homeostasis of the CNS is disrupted, glial cells will respond to the different kinds of damage by multiplying, differentiating, activating, and so on. Nowadays, based on the animal models of SCI, we have gained a better understanding of the pathophysiological changes of glial cells after SCI. For example, after SCI, various factors lead to the activation of astrocytes, which can secrete various molecules, such as cytokines and chemokines in response to SCI. Besides, multicellular and multi-molecular components are involved in forming glial scar that has beneficial and detrimental effects in axonal regeneration and neuro-inflammation. Therefore, an in-depth exploration of the role of glial cells in SCI is conducive to the development of SCI repair strategies. Further studies should develop novel targets and strategies that contribute to the post-SCI reparative responses of glial cells.

AUTHOR CONTRIBUTIONS

RW and RZ contributed to the writing of the manuscript. ZC and SG contributed to a systematic literature search. All authors discussed the results and contributed to the final manuscript.

FUNDING

This work was supported by the National Natural Science Foundation of China (No. 81971160).

REFERENCES

1. Quadri SA, Farooqui M, Ikram A, Zafar A, Khan MA, Suriya SS, et al. Recent update on basic mechanisms of spinal cord injury. *Neurosur Rev.* (2020) 43:425–41. doi: 10.1007/s10143-018-1008-3
2. Letterer E. [Virchow's contribution to modern pathology; on the 100th anniversary of cellular pathology, August 20, 1858]. *Hippokrates.* (1958) 29:505–11.
3. Sofroniew MV, Vinters HV. Astrocytes: biology and pathology. Acta *Neuropathol.* (2010) 119:7–35. doi: 10.1007/s00401-009-0619-8

4. Wolburg H, Noell S, Mack A, Wolburg-Buchholz K, Fallier-Becker P. Brain endothelial cells and the glio-vascular complex. *Cell Tissue Res*. (2009) 335:75–96. doi: 10.1007/s00441-008-0658-9
5. Abbott NJ. Astrocyte-endothelial interactions and blood-brain barrier permeability. *J Anat*. (2002) 200:629–38. doi: 10.1046/j.1469-7580.2002.00064.x
6. Abbott NJ, Patabendige AA, Dolman DE, Yusof SR, Begley DJ. Structure and function of the blood-brain barrier. *Neurobiol Dis*. (2010) 37:13–25. doi: 10.1016/j.nbd.2009.07.030
7. Wolburg H. Orthogonal arrays of intramembranous particles: a review with special reference to astrocytes. *J Hirnforsch*. (1995) 36:239–58.
8. Verbavatz JM, Ma T, Gobin R, Verkman AS. Absence of orthogonal arrays in kidney, brain and muscle from transgenic knockout mice lacking water channel aquaporin-4. *J Cell Sci*. (1997) 110(Pt 22):2855–60. doi: 10.1242/jcs.110.22.2855
9. Nielsen S, Nagelhus EA, Amiry-Moghaddam M, Bourque C, Agre P, Ottersen OP. Specialized membrane domains for water transport in glial cells: high-resolution immunogold cytochemistry of aquaporin-4 in rat brain. *J Neurosci*. (1997) 17:171–80. doi: 10.1523/JNEUROSCI.17-01-00171.1997
10. Abbott NJ, Rönnbäck L, Hansson E. Astrocyte-endothelial interactions at the blood-brain barrier. *Nat Rev Neurosci*. (2006) 7:41–53. doi: 10.1038/nrn1824
11. Igarashi Y, Utsumi H, Chiba H, Yamada-Sasamori Y, Tobioka H, Kamimura Y, et al. Glial cell line-derived neurotrophic factor induces barrier function of endothelial cells forming the blood-brain barrier. *Biochem Biophys Res Commun*. (1999) 261:108–12. doi: 10.1006/bbrc.1999.0992
12. Haseloff RF, Blasig IE, Bauer HC, Bauer H. In search of the astrocytic factor(s) modulating blood-brain barrier functions in brain capillary endothelial cells *in vitro*. *Cell Mol Neurobiol*. (2005) 25:25–39. doi: 10.1007/s10571-004-1375-x
13. Lee SW, Kim WJ, Choi YK, Song HS, Son MJ, Gelman IH, et al. SSeCKS regulates angiogenesis and tight junction formation in blood-brain barrier. *Nat Med*. (2003) 9:900–6. doi: 10.1038/nm889
14. Paulson OB, Newman EA. Does the release of potassium from astrocyte endfeet regulate cerebral blood flow? *Science*. (1987) 237:896–8. doi: 10.1126/science.3616619
15. Mulligan SJ, MacVicar BA. Calcium transients in astrocyte endfeet cause cerebrovascular constrictions. *Nature*. (2004) 431:195–9. doi: 10.1038/nature02827
16. Araque A, Parpura V, Sanzgiri RP, Haydon PG. Tripartite synapses: glia, the unacknowledged partner. *Trends Neurosci*. (1999) 22:208–15. doi: 10.1016/S0166-2236(98)01349-6
17. Meyerfranke A, Kaplan MR, Pfrieger FW, Barres BA. Characterization of the signaling interactions that promote the survival and growth of developing retinal ganglion-cells in culture. *Neuron*. (1995) 15:805–19. doi: 10.1016/0896-6273(95)90172-8
18. Christopherson KS, Ullian EM, Stokes CCA, Mullowney CE, Hell JW, Agah A, et al. Thrombospondins are astrocyte-secreted proteins that promote CNS synaptogenesis. *Cell*. (2005) 120:421–33. doi: 10.1016/j.cell.2004.12.020
19. Liauw J, Hoang S, Choi M, Eroglu C, Choi M, Sun GH, et al. Thrombospondins 1 and 2 are necessary for synaptic plasticity and functional recovery after stroke. *J Cerebr Blood F Met*. (2008) 28:1722–32. doi: 10.1038/jcbfm.2008.65
20. Eroglu C, Allen NJ, Susman MW, O'Rourke NA, Park CY, Ozkan E, et al. Gabapentin receptor alpha2delta-1 is a neuronal thrombospondin receptor responsible for excitatory CNS synaptogenesis. *Cell*. (2009) 139:380–92. doi: 10.1016/j.cell.2009.09.025
21. Kucukdereli H, Allen NJ, Lee AT, Feng A, Ozlu MI, Conatser LM, et al. Control of excitatory CNS synaptogenesis by astrocyte-secreted proteins Hevin and SPARC. *Proc Natl Acad Sci USA*. (2011) 108:E440–9. doi: 10.1073/pnas.1104977108
22. Chung W-S, Allen NJ, Eroglu C. Astrocytes control synapse formation, function, and elimination. *Cold Spring Harb Perspect Biol*. (2015) 7:a020370. doi: 10.1101/cshperspect.a020370
23. Goritz C, Mauch DH, Pfrieger FW. Multiple mechanisms mediate cholesterol-induced synaptogenesis in a CNS neuron. *Mol Cell Neurosci*. (2005) 29:190–201. doi: 10.1016/j.mcn.2005.02.006
24. Albrecht D, Lopez-Murcia FJ, Perez-Gonzalez AP, Lichtner G, Solsona C, Llobet A. SPARC prevents maturation of cholinergic presynaptic terminals. *Mol Cell Neurosci*. (2012) 49:364–74. doi: 10.1016/j.mcn.2012.01.005
25. Beattie EC, Stellwagen D, Morishita W, Bresnahan JC, Ha BK, Von Zastrow M, et al. Control of synaptic strength by glial TNFalpha. *Science*. (2002) 295:2282–5. doi: 10.1126/science.1067859
26. Allen NJ, Bennett ML, Foo LC, Wang GX, Chakraborty C, Smith SJ, et al. Astrocyte glypicans 4 and 6 promote formation of excitatory synapses via GluA1 AMPA receptors. *Nature*. (2012) 486:410–4. doi: 10.1038/nature11059
27. Mauch DH, Nagler K, Schumacher S, Goritz C, Muller EC, Otto A, et al. CNS synaptogenesis promoted by glia-derived cholesterol. *Science*. (2001) 294:1354–7. doi: 10.1126/science.294.5545.1354
28. Schafer DP, Lehrman EK, Kautzman AG, Koyama R, Mardinly AR, Yamasaki R, et al. Microglia sculpt postnatal neural circuits in an activity and complement-dependent manner. *Neuron*. (2012) 74:691–705. doi: 10.1016/j.neuron.2012.03.026
29. Bialas AR, Stevens B. TGF-beta signaling regulates neuronal C1q expression and developmental synaptic refinement. *Nat Neurosci*. (2013) 16:1773–82. doi: 10.1038/nn.3560
30. Chung W-S, Clarke LE, Wang GX, Stafford BK, Sher A, Chakraborty C, et al. Astrocytes mediate synapse elimination through MEGF10 and MERTK pathways. *Nature*. (2013) 504:394–400. doi: 10.1038/nature12776
31. Joester A, Faissner A. The structure and function of tenascins in the nervous system. *Matrix Biol*. (2001) 20:13–22. doi: 10.1016/S0945-053X(00)00136-0
32. Wiese S, Karus M, Faissner A. Astrocytes as a source for extracellular matrix molecules and cytokines. *Front Pharmacol*. (2012) 3:120. doi: 10.3389/fphar.2012.00120
33. Brown AM, Ransom BR. Astrocyte glycogen and brain energy metabolism. *Glia*. (2007) 55:1263–71. doi: 10.1002/glia.20557
34. Pellerin L, Magistretti PJ. Glutamate uptake into astrocytes stimulates aerobic glycolysis: a mechanism coupling neuronal activity to glucose utilization. *Proc Natl Acad Sci USA*. (1994) 91:10625–9. doi: 10.1073/pnas.91.22.10625
35. Kasischke KA, Vishwasrao HD, Fisher PJ, Zipfel WR, Webb WW. Neural activity triggers neuronal oxidative metabolism followed by astrocytic glycolysis. *Science*. (2004) 305:99–103. doi: 10.1126/science.1096485
36. Lerchundi R, Fernández-Moncada I, Contreras-Baeza Y, Sotelo-Hitschfeld T, Mächler P, Wyss MT, et al. NH4(+) triggers the release of astrocytic lactate via mitochondrial pyruvate shunting. *Proc Natl Acad Sci USA*. (2015) 112:11090–5. doi: 10.1073/pnas.1508259112
37. Kierdorf K, Erny D, Goldmann T, Sander V, Schulz C, Perdiguero EG, et al. Microglia emerge from erythromyeloid precursors via Pu.1- and Irf8-dependent pathways. *Nat Neurosci*. (2013) 16:273–80. doi: 10.1038/nn.3318
38. Squarzoni P, Thion MS, Garel S. Neuronal and microglial regulators of cortical wiring: usual and novel guideposts. *Front Neurosci*. (2015) 9:248. doi: 10.3389/fnins.2015.00248
39. Trang T, Beggs S, Salter MW. Brain-derived neurotrophic factor from microglia: a molecular substrate for neuropathic pain. *Neuron Glia Biol*. (2011) 7:99–108. doi: 10.1017/S1740925X12000087
40. Ueno M, Fujita Y, Tanaka T, Nakamura Y, Kikuta J, Ishii M, et al. Layer V cortical neurons require microglial support for survival during postnatal development. *Nat Neurosci*. (2013) 16:543–51. doi: 10.1038/nn.3358
41. Yamagata T, Muroya K, Mukasa T, Igarashi H, Momoi M, Tsukahara T, et al. Hepatocyte growth factor specifically expressed in microglia activated Ras in the neurons, similar to the action of neurotrophic factors. *Biochem Biophys Res Commun*. (1995) 210:231–7. doi: 10.1006/bbrc.1995.1651
42. Fourgeaud L, Través PG, Tufail Y, Leal-Bailey H, Lew ED, Burrola PG, et al. TAM receptors regulate multiple features of microglial physiology. *Nature*. (2016) 532:240–4. doi: 10.1038/nature17630
43. Luo C, Koyama R, Ikegaya Y. Microglia engulf viable newborn cells in the epileptic dentate gyrus. *Glia*. (2016) 64:1508–17. doi: 10.1002/glia.23018
44. Blinzinger K, Kreutzberg G. Displacement of synaptic terminals from regenerating motoneurons by microglial cells. *Z Zellforsch Mikrosk Anat*. (1968) 85:145–57. doi: 10.1007/BF00325030
45. Perry VH, O'Connor V. The role of microglia in synaptic stripping and synaptic degeneration: a revised perspective. *ASN Neuro*. (2010) 2:e00047. doi: 10.1042/AN20100024

46. Stevens B, Allen NJ, Vazquez LE, Howell GR, Christopherson KS, Nouri N, et al. The classical complement cascade mediates CNS synapse elimination. *Cell*. (2007) 131:1164–78. doi: 10.1016/j.cell.2007.10.036
47. Hoshiko M, Arnoux I, Avignone E, Yamamoto N, Audinat E. Deficiency of the microglial receptor CX3CR1 impairs postnatal functional development of thalamocortical synapses in the barrel cortex. *J Neurosci*. (2012) 32:15106–11. doi: 10.1523/JNEUROSCI.1167-12.2012
48. Zhang J, Malik A, Choi HB, Ko RWY, Dissing-Olesen L, MacVicar BA. Microglial CR3 activation triggers long-term synaptic depression in the hippocampus via NADPH oxidase. *Neuron*. (2014) 82:195–207. doi: 10.1016/j.neuron.2014.01.043
49. Vezzani A, Viviani B. Neuromodulatory properties of inflammatory cytokines and their impact on neuronal excitability. *Neuropharmacology*. (2015) 96:70–82. doi: 10.1016/j.neuropharm.2014.10.027
50. Stellwagen D, Malenka RC. Synaptic scaling mediated by glial TNF-alpha. *Nature*. (2006) 440:1054–9. doi: 10.1038/nature04671
51. Tong L, Prieto GA, Kramár EA, Smith ED, Cribbs DH, Lynch G, et al. Brain-derived neurotrophic factor-dependent synaptic plasticity is suppressed by interleukin-1β via p38 mitogen-activated protein kinase. *J Neurosci.* (2012) 32:17714–24. doi: 10.1523/JNEUROSCI.1253-12.2012
52. Coull JA, Beggs S, Boudreau D, Boivin D, Tsuda M, Inoue K, et al. BDNF from microglia causes the shift in neuronal anion gradient underlying neuropathic pain. *Nature*. (2005) 438:1017–21. doi: 10.1038/nature04223
53. Timsit S, Martinez S, Allinquant B, Peyron F, Puelles L, Zalc B. Oligodendrocytes originate in a restricted zone of the embryonic ventral neural tube defined by DM-20 mRNA expression. *J Neurosci.* (1995) 15:1012–24. doi: 10.1523/JNEUROSCI.15-02-01012.1995
54. Chang A, Nishiyama A, Peterson J, Prineas J, Trapp BD. NG2-positive oligodendrocyte progenitor cells in adult human brain and multiple sclerosis lesions. *J Neurosci.* (2000) 20:6404–12. doi: 10.1523/JNEUROSCI.20-17-06404.2000
55. Jagielska A, Norman AL, Whyte G, Vliet KJV, Guck J, Franklin RJM. Mechanical environment modulates biological properties of oligodendrocyte progenitor cells. *Stem Cells Dev*. (2012) 21:2905–14. doi: 10.1089/scd.2012.0189
56. Lourenço T, Paes de Faria J, Bippes CA, Maia J, Lopes-da-Silva JA, Relvas JB, et al. Modulation of oligodendrocyte differentiation and maturation by combined biochemical and mechanical cues. *Sci Rep*. (2016) 6:21563. doi: 10.1038/srep21563
57. Urbanski MM, Kingsbury L, Moussouros D, Kassim I, Mehjabeen S, Paknejad N, et al. Myelinating glia differentiation is regulated by extracellular matrix elasticity. *Sci Rep*. (2016) 6:33751. doi: 10.1038/srep33751
58. Lin S-c, Bergles DE. Synaptic signaling between GABAergic interneurons and oligodendrocyte precursor cells in the hippocampus. *Nat Neurosci*. (2004) 7:24–32. doi: 10.1038/nn1162
59. Bergles DE, Roberts JD, Somogyi P, Jahr CE. Glutamatergic synapses on oligodendrocyte precursor cells in the hippocampus. *Nature*. (2000) 405:187–91. doi: 10.1038/35012083
60. Bercury KK, Macklin WB. Dynamics and mechanisms of CNS myelination. *Dev Cell*. (2015) 32:447–58. doi: 10.1016/j.devcel.2015.01.016
61. Stadelmann C, Timmler S, Barrantes-Freer A, Simons M. Myelin in the central nervous system: structure, function, and pathology. *Physiol Rev*. (2019) 99:1381–431. doi: 10.1152/physrev.00031.2018
62. Griffiths I, Klugmann M, Anderson T, Yool D, Thomson C, Schwab MH, et al. Axonal swellings and degeneration in mice lacking the major proteolipid of myelin. *Science.* (1998) 280:1610–3. doi: 10.1126/science.280.5369.1610
63. Ferreirinha F, Quattrini A, Pirozzi M, Valsecchi V, Dina G, Broccoli V, et al. Axonal degeneration in paraplegin-deficient mice is associated with abnormal mitochondria and impairment of axonal transport. *J Clin Invest*. (2004) 113:231–42. doi: 10.1172/JCI200420138
64. Tarrade A, Fassier C, Charvin D, Charvin D, Vitte J, Peris L, et al. A mutation of spastin is responsible for swellings and impairment of transport in a region of axon characterized by changes in microtubule composition. *Hum Mol Genet*. (2006) 15:3544–58. doi: 10.1093/hmg/ddl431
65. Philips T, Rothstein JD. Oligodendroglia: metabolic supporters of neurons. *J Clin Invest*. (2017) 127:3271–80. doi: 10.1172/JCI90610
66. Lee Y, Morrison BM, Li Y, Lengacher S, Farah MH, Hoffman PN, et al. Oligodendroglia metabolically support axons and contribute to neurodegeneration. *Nature*. (2012) 487:443–8. doi: 10.1038/nature11314
67. Saab AS, Tzvetavona ID, Trevisiol A, Baltan S, Dibaj P, Kusch K, et al. Oligodendroglial NMDA receptors regulate glucose import and axonal energy metabolism. *Neuron*. (2016) 91:119–32. doi: 10.1016/j.neuron.2016.05.016
68. Magnotti LM, Goodenough DA, Paul DL. Functional heterotypic interactions between astrocyte and oligodendrocyte connexins. *Glia*. (2011) 59:26–34. doi: 10.1002/glia.21073
69. Niu J, Li T, Yi C, Huang N, Koulakoff A, Weng C, et al. Connexin-based channels contribute to metabolic pathways in the oligodendroglial lineage. *J Cell Sci*. (2016) 129:1902–14. doi: 10.1242/jcs.178731
70. Orthmann-Murphy JL, Abrams CK, Scherer SS. Gap junctions couple astrocytes and oligodendrocytes. *J Mol Neurosci*. (2008) 35:101–16. doi: 10.1007/s12031-007-9027-5
71. Li X, Li M, Tian L, Chen J, Liu R, Ning B. Reactive astrogliosis: implications in spinal cord injury progression and therapy. *Oxid Med Cell Longev*. (2020) 2020:9494352. doi: 10.1155/2020/9494352
72. Zamanian JL, Xu L, Foo LC, Nouri N, Zhou L, Giffard RG, et al. Genomic analysis of reactive astrogliosis. *J Neurosci*. (2012) 32:6391–410. doi: 10.1523/JNEUROSCI.6221-11.2012
73. Hara M, Kobayakawa K, Ohkawa Y, Kumamaru H, Yokota K, Saito T, et al. Interaction of reactive astrocytes with type I collagen induces astrocytic scar formation through the integrin-N-cadherin pathway after spinal cord injury. *Nat Med.* (2017) 23:818–28. doi: 10.1038/nm.4354
74. Boghdadi AG, Teo L, Bourne JA. The neuroprotective role of reactive astrocytes after central nervous system injury. *J Neurotrauma*. (2020) 37:681–91. doi: 10.1089/neu.2019.6938
75. Cullen DK, Vernekar VN, LaPlaca MC. Trauma-induced plasmalemma disruptions in three-dimensional neural cultures are dependent on strain modality and rate. *J Neurotrauma*. (2011) 28:2219–33. doi: 10.1089/neu.2011.1841
76. Bowman CL, Ding JP, Sachs F, Sokabe M. Mechanotransducing ion channels in astrocytes. *Brain Res*. (1992) 584:272–86. doi: 10.1016/0006-8993(92)90906-P
77. Islas L, Pasantes-Morales H, Sanchez JA. Characterization of stretch-activated ion channels in cultured astrocytes. *Glia.* (1993) 8:87–96. doi: 10.1002/glia.440080204
78. Floyd CL, Gorin FA, Lyeth BG. Mechanical strain injury increases intracellular sodium and reverses Na+/Ca2+ exchange in cortical astrocytes. *Glia*. (2005) 51:35–46. doi: 10.1002/glia.20183
79. Neary JT, Kang Y, Willoughby KA, Ellis EF. Activation of extracellular signal-regulated kinase by stretch-induced injury in astrocytes involves extracellular ATP and P2 purinergic receptors. *J Neurosci.* (2003) 23:2348–56. doi: 10.1523/JNEUROSCI.23-06-02348.2003
80. Neary JT, Kang Y, Tran M, Feld J. Traumatic injury activates protein kinase B/Akt in cultured astrocytes: role of extracellular ATP and P2 purinergic receptors. *J Neurotrauma*. (2005) 22:491–500. doi: 10.1089/neu.2005.22.491
81. Hoffman SW, Rzigalinski BA, Willoughby KA, Ellis EF. Astrocytes generate isoprostanes in response to trauma or oxygen radicals. *J Neurotrauma*. (2000) 17:415–20. doi: 10.1089/neu.2000.17.415
82. Ostrow LW, Suchyna TM, Sachs F. Stretch induced endothelin-1 secretion by adult rat astrocytes involves calcium influx via stretch-activated ion channels (SACs). *Biochem Biophys Res Commun.* (2011) 410:81–6. doi: 10.1016/j.bbrc.2011.05.109
83. Giulian D, Lachman LB. Interleukin-1 stimulation of astroglial proliferation after brain injury. *Science*. (1985) 228:497–9. doi: 10.1126/science.3872478
84. Selmaj KW, Farooq M, Norton WT, Raine CS, Brosnan CF. Proliferation of astrocytes *in vitro* in response to cytokines. A primary role for tumor necrosis factor. *J Immunol*. (1990) 144:129–35.
85. Balasingam V, Tejada-Berges T, Wright E, Bouckova R, Yong VW. Reactive astrogliosis in the neonatal mouse brain and its modulation by cytokines. *J Neurosci.* (1994) 14:846–56. doi: 10.1523/JNEUROSCI.14-02-00846.1994
86. Ridet JL, Malhotra SK, Privat A, Gage FH. Reactive astrocytes: cellular and molecular cues to biological function. *Trends Neurosci*. (1997) 20:570–7. doi: 10.1016/S0166-2236(97)01139-9

87. Liddelow SA, Guttenplan KA, Clarke LE, Bennett FC, Bohlen CJ, Schirmer L, et al. Neurotoxic reactive astrocytes are induced by activated microglia. *Nature*. (2017) 541:481–7. doi: 10.1038/nature21029
88. Herrmann JE, Imura T, Song B, Qi J, Ao Y, Nguyen TK, et al. STAT3 is a critical regulator of astrogliosis and scar formation after spinal cord injury. *J Neurosc*. (2008) 28:7231–43. doi: 10.1523/JNEUROSCI.1709-08.2008
89. Okada S, Nakamura M, Katoh H, Miyao T, Shimazaki T, Ishii K, et al. Conditional ablation of Stat3 or Socs3 discloses a dual role for reactive astrocytes after spinal cord injury. *Nat Med*. (2006) 12:829–34. doi: 10.1038/nm1425
90. Gris P, Tighe A, Levin D, Sharma R, Brown A. Transcriptional regulation of scar gene expression in primary astrocytes. *Glia*. (2007) 55:1145–55. doi: 10.1002/glia.20537
91. Schachtrup C, Ryu JK, Helmrick MJ, Vagena E, Galanakis DK, Degen JL, et al. Fibrinogen triggers astrocyte scar formation by promoting the availability of active TGF-beta after vascular damage. *J Neurosci*. (2010) 30:5843–54. doi: 10.1523/JNEUROSCI.0137-10.2010
92. Winter CG, Saotome Y, Levison SW, Hirsh D. A role for ciliary neurotrophic factor as an inducer of reactive gliosis, the glial response to central nervous system injury. *Proc Natl Acad Sci USA*. (1995) 92:5865–9. doi: 10.1073/pnas.92.13.5865
93. Rabchevsky AG, Weinitz JM, Coulpier M, Fages C, Tinel M, Junier MP. A role for transforming growth factor alpha as an inducer of astrogliosis. *J Neurosci*. (1998) 18:10541–52. doi: 10.1523/JNEUROSCI.18-24-10541.1998
94. Lo U, Selvaraj V, Plane JM, Chechneva OV, Otsu K, Deng W. p38α (MAPK14) critically regulates the immunological response and the production of specific cytokines and chemokines in astrocytes. *Sci Rep*. (2014) 4:7405. doi: 10.1038/srep07405
95. Ambrosini E, Remoli ME, Giacomini E, Rosicarelli B, Serafini B, Lande R, et al. Astrocytes produce dendritic cell-attracting chemokines *in vitro* and in multiple sclerosis lesions. *J Neuropathol Exp Neurol*. (2005) 64:706–15. doi: 10.1097/01.jnen.0000173893.01929.fc
96. Saba J, Turati J, Ramírez D, Carniglia L, Durand D, Lasaga M, et al. Astrocyte truncated tropomyosin receptor kinase B mediates brain-derived neurotrophic factor anti-apoptotic effect leading to neuroprotection. *J Neurochem*. (2018) 146:686–702. doi: 10.1111/jnc.14476
97. Duarte Azevedo M, Sander S, Tenenbaum GDNF L. a neuron-derived factor upregulated in glial cells during disease. *J Clin Med*. (2020) 9:456. doi: 10.3390/jcm9020456
98. Oh S-J, Han K-S, Park H, Woo DH, Kim HY, Traynelis SF, et al. Protease activated receptor 1-induced glutamate release in cultured astrocytes is mediated by Bestrophin-1 channel but not by vesicular exocytosis. *Mol Brain*. (2012) 5:38. doi: 10.1186/1756-6606-5-38
99. Jo S, Yarishkin O, Hwang YJ, Chun YE, Park M, Woo DH, et al. GABA from reactive astrocytes impairs memory in mouse models of Alzheimer's disease. *Nat Med*. (2014) 20:886–96. doi: 10.1038/nm.3639
100. McKeon RJ, Schreiber RC, Rudge JS, Silver J. Reduction of neurite outgrowth in a model of glial scarring following CNS injury is correlated with the expression of inhibitory molecules on reactive astrocytes. *J Neurosci*. (1991) 11:3398–411. doi: 10.1523/JNEUROSCI.11-11-03398.1991
101. Hsu JYC, Bourguignon LYW, Adams CM, Peyrollier K, Zhang H, Fandel T, et al. Matrix metalloproteinase-9 facilitates glial scar formation in the injured spinal cord. *J Neurosci*. (2008) 28:13467–77. doi: 10.1523/JNEUROSCI.2287-08.2008
102. Liddelow SA, Barres BA. Reactive astrocytes: production, function, therapeutic potential. *Immunity*. (2017) 46:957–67. doi: 10.1016/j.immuni.2017.06.006
103. Pitter KL, Tamagno I, Feng X, Ghosal K, Amankulor N, Holland EC, et al. The SHH/Gli pathway is reactivated in reactive glia and drives proliferation in response to neurodegeneration-induced lesions. *Glia*. (2014) 62:1595–607. doi: 10.1002/glia.22702
104. Faulkner JR, Herrmann JE, Woo MJ, Tansey KE, Doan NB, Sofroniew MV. Reactive astrocytes protect tissue and preserve function after spinal cord injury. *J Neurosci*. (2004) 24:2143–55. doi: 10.1523/JNEUROSCI.3547-03.2004
105. Lööv C, Hillered L, Ebendal T, Erlandsson A. Engulfing astrocytes protect neurons from contact-induced apoptosis following injury. *PLoS ONE*. (2012) 7:e33090. doi: 10.1371/journal.pone.0033090
106. Morizawa YM, Hirayama Y, Ohno N, Shibata S, Shigetomi E, Sui Y, et al. Reactive astrocytes function as phagocytes after brain ischemia via ABCA1-mediated pathway. *Nat Commun*. (2017) 8:28. doi: 10.1038/s41467-017-00037-1
107. Liang J, Takeuchi H, Doi Y, Kawanokuchi J, Sonobe Y, Jin S, et al. Excitatory amino acid transporter expression by astrocytes is neuroprotective against microglial excitotoxicity. *Brain Res*. (2008) 1210:11–9. doi: 10.1016/j.brainres.2008.03.012
108. Anjum A, Yazid Di M, Fauzi Daud M, Idris J, Ng AMH, Selvi Naicker A, et al. Spinal cord injury: pathophysiology, multimolecular interactions, and underlying recovery mechanisms. *Int J Mol Sci*. (2020) 21:7533. doi: 10.3390/ijms21207533
109. Cooper JG, Jeong SJ, McGuire TL, Sharma S, Wang W, Bhattacharyya S, et al. Fibronectin EDA forms the chronic fibrotic scar after contusive spinal cord injury. *Neurobiol Dis*. (2018) 116:60–8. doi: 10.1016/j.nbd.2018.04.014
110. Hawkins LA, Devitt A. Current understanding of the mechanisms for clearance of apoptotic cells-a fine balance. *J Cell Death*. (2013) 6:57–68. doi: 10.4137/JCD.S11037
111. Yuan Y-M, He C. The glial scar in spinal cord injury and repair. *Neurosci Bull*. (2013) 29:421–35. doi: 10.1007/s12264-013-1358-3
112. Bradbury EJ, Moon LDF, Popat RJ, King VR, Bennett GS, Patel PN, et al. Chondroitinase ABC promotes functional recovery after spinal cord injury. *Nature*. (2002) 416:636–40. doi: 10.1038/416636a
113. Lee H, McKeon RJ, Bellamkonda RV. Sustained delivery of thermostabilized chABC enhances axonal sprouting and functional recovery after spinal cord injury. *Proc Natl Acad Sci USA*. (2010) 107:3340–5. doi: 10.1073/pnas.0905437106
114. Smith-Thomas LC, Stevens J, Fok-Seang J, Faissner A, Rogers JH, Fawcett JW. Increased axon regeneration in astrocytes grown in the presence of proteoglycan synthesis inhibitors. *J Cell Sci*. (1995) 108(Pt 3):1307–15. doi: 10.1242/jcs.108.3.1307
115. Siebert JR, Stelzner DJ, Osterhout DJ. Chondroitinase treatment following spinal contusion injury increases migration of oligodendrocyte progenitor cells. *Exp Neurol*. (2011) 231:19–29. doi: 10.1016/j.expneurol.2011.05.002
116. Siebert JR, Osterhout DJ. The inhibitory effects of chondroitin sulfate proteoglycans on oligodendrocytes. *J Neurochem*. (2011) 119:176–88. doi: 10.1111/j.1471-4159.2011.07370.x
117. Wang Y, Cheng X, He Q, Zheng Y, Kim DH, Whittemore SR, et al. Astrocytes from the contused spinal cord inhibit oligodendrocyte differentiation of adult oligodendrocyte precursor cells by increasing the expression of bone morphogenetic proteins. *J Neurosci*. (2011) 31:6053–8. doi: 10.1523/JNEUROSCI.5524-09.2011
118. Hammond TR, Gadea A, Dupree J, Kerninon C, Nait-Oumesmar B, Aguirre A, et al. Astrocyte-derived endothelin-1 inhibits remyelination through notch activation. *Neuron*. (2014) 81:588–602. doi: 10.1016/j.neuron.2013.11.015
119. Barkho BZ, Song H, Aimone JB, Smrt RD, Kuwabara T, Nakashima K, et al. Identification of astrocyte-expressed factors that modulate neural stem/progenitor cell differentiation. *Stem Cells Dev*. (2006) 15:407–21. doi: 10.1089/scd.2006.15.407
120. David S, Kroner A. Repertoire of microglial and macrophage responses after spinal cord injury. *Nat Rev Neurosci*. (2011) 12:388–99. doi: 10.1038/nrn3053
121. Mosser DM, Edwards JP. Exploring the full spectrum of macrophage activation. *Nat Rev Immunol*. (2008) 8:958–69. doi: 10.1038/nri2448
122. Hu X, Leak RK, Shi Y, Suenaga J, Gao Y, Zheng P, et al. Microglial and macrophage polarization—new prospects for brain repair. *Nat Rev Neurol*. (2015) 11:56–64. doi: 10.1038/nrneurol.2014.207
123. Murray PJ. Macrophage polarization. *Annu Rev Physiol*. (2017) 79:541–66. doi: 10.1146/annurev-physiol-022516-034339
124. Milich LM, Choi JS, Ryan C, Cerqueira SR, Benavides S, Yahn SL, et al. Single-cell analysis of the cellular heterogeneity and interactions in the injured mouse spinal cord. *J Exp Med*. (2021) 218:e20210040. doi: 10.1084/jem.20210040
125. Van Hove H, Martens L, Scheyltjens I, De Vlaminck K, Pombo Antunes AR, De Prijck S, et al. A single-cell atlas of mouse brain macrophages reveals unique transcriptional identities shaped by ontogeny and tissue environment. *Nat Neurosci*. (2019) 22:1021–35. doi: 10.1038/s41593-019-0393-4

126. Carlson SL, Parrish ME, Springer JE, Doty K, Dossett L. Acute inflammatory response in spinal cord following impact injury. *Exp Neurol*. (1998) 151:77–88. doi: 10.1006/exnr.1998.6785
127. Stirling DP, Yong VW. Dynamics of the inflammatory response after murine spinal cord injury revealed by flow cytometry. *J Neurosci Res*. (2008) 86:1944–58. doi: 10.1002/jnr.21659
128. Scholz M, Cinatl J, Schädel-Höpfner M, Windolf J. Neutrophils and the blood-brain barrier dysfunction after trauma. *Med Res Rev*. (2007) 27:401–16. doi: 10.1002/med.20064
129. Ankeny DP, Lucin KM, Sanders VM, McGaughy VM, Popovich PG. Spinal cord injury triggers systemic autoimmunity: evidence for chronic B lymphocyte activation and lupus-like autoantibody synthesis. *J Neurochem*. (2006) 99:1073–87. doi: 10.1111/j.1471-4159.2006.04147.x
130. Pineau I, Lacroix S. Proinflammatory cytokine synthesis in the injured mouse spinal cord: multiphasic expression pattern and identification of the cell types involved. *J Comp Neurol*. (2007) 500:267–85. doi: 10.1002/cne.21149
131. Lawrence CB, Allan SM, Rothwell NJ. Interleukin-1beta and the interleukin-1 receptor antagonist act in the striatum to modify excitotoxic brain damage in the rat. *Eur J Neurosci*. (1998) 10:1188–95. doi: 10.1046/j.1460-9568.1998.00136.x
132. Loddick SA, Rothwell NJ. Neuroprotective effects of human recombinant interleukin-1 receptor antagonist in focal cerebral ischaemia in the rat. *J Cereb Blood Flow Metab*. (1996) 16:932–40. doi: 10.1097/00004647-199609000-00017
133. Ferguson AR, Christensen RN, Gensel JC, Miller BA, Sun F, Beattie EC, et al. Cell death after spinal cord injury is exacerbated by rapid TNF alpha-induced trafficking of GluR2-lacking AMPARs to the plasma membrane. *J Neurosci*. (2008) 28:11391–400. doi: 10.1523/JNEUROSCI.3708-08.2008
134. Genovese T, Mazzon E, Crisafulli C, Di Paola R, Muià C, Esposito E, et al. TNF-alpha blockage in a mouse model of SCI: evidence for improved outcome. *Shock*. (2008) 29:32–41. doi: 10.1097/shk.0b013e318059053a
135. Probert L, Eugster HP, Akassoglou K, Bauer J, Frei K H, Lassmann, et al. TNFR1 signalling is critical for the development of demyelination and the limitation of T-cell responses during immune-mediated CNS disease. *Brain*. (2000) 123(Pt 10):2005–19. doi: 10.1093/brain/123.10.2005
136. Genovese T, Esposito E, Mazzon E, Di Paola R, Caminiti R, Bramanti P, et al. Absence of endogenous interleukin-10 enhances secondary inflammatory process after spinal cord compression injury in mice. *J Neurochem*. (2009) 108:1360–72. doi: 10.1111/j.1471-4159.2009.05899.x
137. Chen JY, Fu EJ, Patel PR, Hostetler AJ, Sawan HA, Moss KA, et al. Lentiviral interleukin-10 gene therapy preserves fine motor circuitry and function after a cervical spinal cord injury in male and female mice. *Neurotherapeutics*. (2021) 18:503–14. doi: 10.1007/s13311-020-00946-y
138. Hung K-S, Tsai S-H, Lee T-C, Lin J-W, Chang C-K, Chiu W-T. Gene transfer of insulin-like growth factor-I providing neuroprotection after spinal cord injury in rats. *J Neurosurg Spine*. (2007) 6:35–46. doi: 10.3171/spi.2007.6.1.35
139. Sharma HS, Nyberg F, Westman J, Alm P, Gordh T, Lindholm D. Brain derived neurotrophic factor and insulin like growth factor-1 attenuate upregulation of nitric oxide synthase and cell injury following trauma to the spinal cord. An immunohistochemical study in the rat. *Amino Acids*. (1998) 14:121–9. doi: 10.1007/BF01345252
140. Crowe MJ, Bresnahan JC, Shuman SL, Masters JN, Beattie MS. Apoptosis and delayed degeneration after spinal cord injury in rats and monkeys. *Nat Med*. (1997) 3:73–6. doi: 10.1038/nm0197-73
141. Kanno H, Ozawa H, Sekiguchi A, Yamaya S, Itoi E. Induction of autophagy and autophagic cell death in damaged neural tissue after acute spinal cord injury in mice. *Spine*. (2011) 36:E1427–34. doi: 10.1097/BRS.0b013e3182028c3a
142. Almad A, Sahinkaya FR, McTigue DM. Oligodendrocyte fate after spinal cord injury. *Neurotherapeutics*. (2011) 8:262–73. doi: 10.1007/s13311-011-0033-5
143. Grossman SD, Rosenberg LJ, Wrathall JR. Temporal-spatial pattern of acute neuronal and glial loss after spinal cord contusion. *Exp Neurol*. (2001) 168:273–82. doi: 10.1006/exnr.2001.7628
144. Lytle JM, Wrathall JR. Glial cell loss, proliferation and replacement in the contused murine spinal cord. *Eur J Neurosci*. (2007) 25:1711–24. doi: 10.1111/j.1460-9568.2007.05390.x
145. Griffiths IR, McCulloch MC. Nerve fibres in spinal cord impact injuries. Part 1. Changes in the myelin sheath during the initial 5 weeks. *J Neurol Sci*. (1983) 58:335–49. doi: 10.1016/0022-510X(83)90093-X
146. Bao F, Liu D. Hydroxyl radicals generated in the rat spinal cord at the level produced by impact injury induce cell death by necrosis and apoptosis: protection by a metalloporphyrin. *Neuroscience*. (2004) 126:285–95. doi: 10.1016/j.neuroscience.2004.03.054
147. Liu D, Sybert TE, Qian H, Liu J. Superoxide production after spinal injury detected by microperfusion of cytochrome c. *Free Radic Biol Med*. (1998) 25:298–304. doi: 10.1016/S0891-5849(98)00055-0
148. Liu D, Ling X, Wen J, Liu J. The role of reactive nitrogen species in secondary spinal cord injury: formation of nitric oxide, peroxynitrite, nitrated protein. *J Neurochem*. (2000) 75:2144–54. doi: 10.1046/j.1471-4159.2000.0752144.x
149. McDonald JW, Althomsons SP, Hyrc KL, Choi DW, Goldberg MP. Oligodendrocytes from forebrain are highly vulnerable to AMPA/kainate receptor-mediated excitotoxicity. *Nat Med. (*1998) 4:291–7. doi: 10.1038/nm0398-291
150. Matute C, Torre I, Perez-Cerda F, Perez-Samartin A, Alberdi E, Etxebarria E, et al. P2X(7) receptor blockade prevents ATP excitotoxicity in oligodendrocytes and ameliorates experimental autoimmune encephalomyelitis. *J Neurosci*. (2007) 27:9525–33. doi: 10.1523/JNEUROSCI.0579-07.2007
151. Inukai T, Uchida K, Nakajima H, Yayama T, Kobayashi S, Mwaka ES, et al. Tumor necrosis factor-alpha and its receptors contribute to apoptosis of oligodendrocytes in the spinal cord of spinal hyperostotic mouse (twy/twy) sustaining chronic mechanical compression. *Spine*. (2009) 34:2848–57. doi: 10.1097/BRS.0b013e3181b0d078
152. Kanno H, Ozawa H, Sekiguchi A, Itoi E. Spinal cord injury induces upregulation of Beclin 1 and promotes autophagic cell death. *Neurobiol Dis*. (2009) 33:143–8. doi: 10.1016/j.nbd.2008.09.009
153. Smith PM, Jeffery ND. Histological and ultrastructural analysis of white matter damage after naturally-occurring spinal cord injury. *Brain Pathol*. (2006) 16:99–109. doi: 10.1111/j.1750-3639.2006.00001.x
154. Guest JD, Hiester ED, Bunge RP. Demyelination and Schwann cell responses adjacent to injury epicenter cavities following chronic human spinal cord injury. *Exp Neurol*. (2005) 192:384–93. doi: 10.1016/j.expneurol.2004.11.033
155. Plemel JR, Keough MB, Duncan GJ, Sparling JS, Yong VW, Stys PK, et al. Remyelination after spinal cord injury: is it a target for repair? *Prog Neurobiol*. (2014) 117:54–72. doi: 10.1016/j.pneurobio.2014.02.006
156. Stys PK, Waxman SG, Ransom BR. Ionic mechanisms of anoxic injury in mammalian CNS white matter: role of Na+ channels and Na(+)-Ca2+ exchanger. *J Neurosci*. (1992) 12:430–9. doi: 10.1523/JNEUROSCI.12-02-00430.1992
157. Li S, Stys PK. Na(+)-K(+)-ATPase inhibition and depolarization induce glutamate release via reverse Na(+)-dependent transport in spinal cord white matter. *Neuroscience*. (2001) 107:675–83. doi: 10.1016/S0306-4522(01)00385-2
158. Irvine KA, Blakemore WF. Remyelination protects axons from demyelination-associated axon degeneration. *Brain*. (2008) 131:1464–77. doi: 10.1093/brain/awn080
159. McTigue DM, Wei P, Stokes BT. Proliferation of NG2-positive cells and altered oligodendrocyte numbers in the contused rat spinal cord. *J Neurosci*. (2001) 21:3392–400. doi: 10.1523/JNEUROSCI.21-10-03392.2001
160. Assinck P, Duncan GJ, Plemel JR, Lee MJ, Stratton JA, Manesh SB, et al. Myelinogenic plasticity of oligodendrocyte precursor cells following spinal cord contusion injury. *J Neurosci*. (2017) 37:8635–54. doi: 10.1523/JNEUROSCI.2409-16.2017
161. Bartus K, Burnside ER, Galino J, James ND, Bennett DLH, Bradbury EJ. ErbB receptor signaling directly controls oligodendrocyte progenitor cell transformation and spontaneous remyelination after spinal cord injury. *Glia*. (2019) 67:1036–46. doi: 10.1002/glia.23586
162. Hackett AR, Yahn SL, Lyapichev K, Dajnoki A, Lee DH, Rodriguez M, et al. Injury type-dependent differentiation of NG2 glia into heterogeneous astrocytes. *Exp Neurol*. (2018) 308:72–9. doi: 10.1016/j.expneurol.2018.07.001
163. Horky LL, Galimi F, Gage FH, Horner PJ. Fate of endogenous stem/progenitor cells following spinal cord injury. *J Comp Neurol*. (2006) 498:525–38. doi: 10.1002/cne.21065

164. Karimi-Abdolrezaee S, Schut D, Wang J, Fehlings MG. Chondroitinase and growth factors enhance activation and oligodendrocyte differentiation of endogenous neural precursor cells after spinal cord injury. *PLoS ONE*. (2012) 7:e37589. doi: 10.1371/journal.pone.0037589
165. Powers BE, Sellers DL, Lovelett EA, Cheung W, Aalami SP, Zapertov N, et al. Remyelination reporter reveals prolonged refinement of spontaneously regenerated myelin. *Proc Natl Acad Sci USA*. (2013) 110:4075–80. doi: 10.1073/pnas.1210293110
166. Alizadeh A, Dyck SM, Karimi-Abdolrezaee S. Myelin damage and repair in pathologic CNS: challenges and prospects. *Front Mol Neurosci*. (2015) 8:35. doi: 10.3389/fnmol.2015.00035
167. Nashmi R, Fehlings MG. Changes in axonal physiology and morphology after chronic compressive injury of the rat thoracic spinal cord. *Neuroscience*. (2001) 104:235–51. doi: 10.1016/S0306-4522(01)00009-4
168. Mothe AJ, Tator CH. Proliferation, migration, and differentiation of endogenous ependymal region stem/progenitor cells following minimal spinal cord injury in the adult rat. *Neuroscience*. (2005) 131:177–87. doi: 10.1016/j.neuroscience.2004.10.011
169. Lampron A, Larochelle A, Laflamme N, Prefontaine P, Plante MM, Sanchez MG, et al. Inefficient clearance of myelin debris by microglia impairs remyelinating processes. *J Exp Med*. (2015) 212:481–95. doi: 10.1084/jem.20141656

Conflict of Interest: The authors declare that the research was conducted in the absence of any commercial or financial relationships that could be construed as a potential conflict of interest.

Publisher's Note: All claims expressed in this article are solely those of the authors and do not necessarily represent those of their affiliated organizations, or those of the publisher, the editors and the reviewers. Any product that may be evaluated in this article, or claim that may be made by its manufacturer, is not guaranteed or endorsed by the publisher.

frontiers | Frontiers in Neurology

BRIEF RESEARCH REPORT
published: 13 May 2022
doi: 10.3389/fneur.2022.865969

Decline in the Incidence of Chronic Subdural Hematoma During the Coronavirus Disease 2019 Pandemic: A Retrospective Single-Center Descriptive Study

Ryosuke Maeoka[1,2]*, *Ichiro Nakagawa*[2], *Keigo Saeki*[3], *Hiroyuki Nakase*[2] and *Hideyuki Ohnishi*[1]

[1] Department of Neurosurgery, Ohnishi Neurological Center, Hyogo, Japan, [2] Department of Neurosurgery, Nara Medical University, Nara, Japan, [3] Department of Epidemiology, Nara Medical University School of Medicine, Nara, Japan

The coronavirus disease 2019 (COVID-19) pandemic has forced restrictions on social activities in some areas. There has also been a decrease in the number of trauma patients in the United States during the COVID-19 pandemic. Chronic subdural hematoma (CSDH) is a traumatic disorder that often develops following head injury. We therefore investigated the impact of the COVID-19 pandemic on CSDH. In this retrospective single-center descriptive study from April 2018 through September 2021, there were 5,282 head trauma patients and 196 patients with CSDH in the pre-pandemic group compared to 4,459 head trauma patients and 140 patients with CSDH in the intra-pandemic group. Significant decreases in the incidence rate (IR) of head trauma (951/100,000 vs. 795/100,000 person-years; IR ratio (IRR): 0.836, 95% confidence interval (CI): 0.803–0.870, $p < 0.001$) and also in the IR of CSDH (35.0/100,000 vs. 24.8/100,000 person-years, IRR: 0.708, 95% CI: 0.570–0.879, $p = 0.002$) were seen in the intra-pandemic group compared to the pre-pandemic group. In this study, the COVID-19 pandemic was associated with significant decreases in the IRs of head trauma and CSDH due to forced restrictions on social activities. Besides, the IR of mild cases of CSDH was significantly lower in the intra-pandemic group than in the pre-pandemic group (IRR: 0.68, 95% CI: 0.51–0.89, $p = 0.006$). Fewer people being out in communities should result in fewer chances for head trauma and CSDH. On the other hand, forced restrictions on social activities due to the COVID-19 pandemic should aggravate CSDH.

Keywords: head trauma, chronic subdural hematoma, coronavirus disease 2019, pandemic, stay-at-home

OPEN ACCESS

Edited by:
Mårten Risling,
Karolinska Institutet (KI), Sweden

Reviewed by:
Tor Brommeland,
Oslo University Hospital, Norway
Mathew Joseph,
Christian Medical College & Hospital, India

***Correspondence:**
Ryosuke Maeoka
r.maeoka@naramed-u.ac.jp

Specialty section:
This article was submitted to Neurotrauma, a section of the journal Frontiers in Neurology

Received: *30 January 2022*
Accepted: *12 April 2022*
Published: *13 May 2022*

Citation:
Maeoka R, Nakagawa I, Saeki K, Nakase H and Ohnishi H (2022) Decline in the Incidence of Chronic Subdural Hematoma During the Coronavirus Disease 2019 Pandemic: A Retrospective Single-Center Descriptive Study. Front. Neurol. 13:865969. doi: 10.3389/fneur.2022.865969

INTRODUCTION

Chronic subdural hematoma (CSDH) is a common neurosurgical disorder that mainly affects elderly individuals (1). With the demographic shift toward an aging population, incidence rates (IRs) of CSDH have been rising (2). The IR of CSDH among United States veterans and elderly individuals between 2000 and 2012 was reported as 79.4/100,000 person-years (3). Recently, the initial trauma has been considered as the first step in the pathogenesis of CSDH (2, 4). CSDH is therefore considered a traumatic disorder that often develops after head injury. In Japan, the first

patient with coronavirus disease 2019 (COVID-19) was reported on January 16, 2020. To control the viral spread, numerous government agencies across several areas of many prefectures enforced restrictions with stay-at-home orders, impacting social activities, including travel, going out, eating out, and drinking outside. Government agencies in Japan implemented stay-at-home orders for some prefectures, including Akashi city, Hyogo, from April 7, 2020. The COVID-19 pandemic has resulted in a restructuring of the healthcare systems worldwide and has forced restrictions on social activities, and declines in trauma have been reported at local, regional, and national levels (5–8). In fact, significant declines in physical activity during the COVID-19 pandemic have been reported among the elderly in Japan (9, 10). Moreover, some researchers have reported that regular physical activity is associated with an increased incidence of activity-related injury (11–13). We therefore hypothesized that social restrictions would be associated with a significantly lower IR of head trauma and would have resulted in a decline in the IR of CSDH. On the other hand, CSDH patients were reported to present with a longer interval from the initial head injury to the final diagnosis in the lockdown period than in the same period the previous year (14). We also hypothesized that social restrictions would change the severity of CSDH.

METHODS

This retrospective single-center descriptive study in the Akashi city, Hyogo, Japan involved a total of 303,899 inhabitants in the Akashi region as population in the pre-pandemic period. This study also involved a total of 304,553 in the Akashi region as population in the intra-pandemic period. In this study, all patients who presented with head trauma and all CSDH treated with burr hole evacuation in our institution in Akashi city, Hyogo, Japan, from April 1, 2018 through September 30, 2021, were reviewed. The electronic medical records of each patient were reviewed, and data were obtained regarding patient's age, sex, use of anticoagulants and antiplatelet medicines, date of surgery, and preoperative modified Rankin Scale (mRS) score to evaluate whether the severity of CSDH had exacerbated because of patients refraining from seeing doctors (15). We defined preoperative mRS score of 1–3 as mild cases and score of 4–5 as severe cases. During the study period, three institutions in Akashi had a department of neurosurgery. According to the information provided by the Akashi City Fire Department, about 70% of patients with head traumas were transported to our institution every month. We conducted a retrospective review of 9,741 consecutive patients with head trauma and 390 patients with CSDH. Inclusion criteria for head trauma were a diagnosis of head trauma with or without head imaging. Inclusion criteria for CSDH were: (1) new diagnosis of CSDH; and (2) radiological findings of CSDH from computed tomography (CT) of the head. Exclusion criteria included: (1) patients with CSDH from other secondary causes, such as post-craniotomy or intracranial hypotension; (2) patients with recurrent CSDH; and (3) patients with initial imaging showing acute subdural hematoma. Preoperative severity was measured by the mRS score. We compared the IRs of CSDH and head trauma and preoperative mRS score between the 21 months prior to the pandemic (April 1, 2018 to December 31, 2019; pre-pandemic group) and the first 21 months of the pandemic (January 1, 2020 to September 30, 2021; intra-pandemic group). Each patient was examined by fellowship-trained neurosurgeons. Written informed consent was obtained from each patient, their nearest relative, or a person who had been given authority to provide consent for admission and surgery for the patient. The institutional ethics committee of the institution approved this study (approval no. 211101).

Categorical variables are provided as numbers (percentage) and continuous variables are reported as median with interquartile range (IQR). Statistical analysis was performed with the chi-squared test for categorical variables and Wilcoxon's rank-sum test for continuous variables. Trends in the IR of CSDH and head trauma were reported as IR ratios (IRRs) with 95% confidence intervals (CIs). Log-linear Poisson regression models have been used to estimate age-adjusted IRRs in each age strata, as crude estimates may give biased results. Two-sided p -values of less than 0.05 were considered to indicate statistical significance. Descriptive and frequency analyses were performed, and comparisons were made using JMP version 14.0.0 software (SAS Institute, Cary, NC, USA).

RESULTS

A total of 9,741 patients presented with head trauma at our hospital during the study period; 5,282 patients (median age, 54 years; IQR: 10–76 years; 2,719 [51.5%] men) were in the pre-pandemic group and 4,459 patients (median age, 57 years; IQR: 10–78 years; 2,304 [51.7%] men) were in the intra-pandemic group. Significant declines in numbers (5,282 vs. 4,459 cases) and IR (951/100,000 vs. 795/100,000 person-years) were seen in the intra-pandemic group compared to the pre-pandemic group. The IRR of head trauma was 0.836 (95% CI: 0.803–0.870; $p < 0.001$) (**Table 1**). Although no significant difference was seen in sex ($p = 0.85$), the median age of head trauma patients was significantly higher in the intra-pandemic group than in the pre-pandemic group ($p = 0.02$). The IRR of head trauma patients was significantly higher among patients over the age of 70 years than among patients under the age of 20 years or 20–70 years ($p < 0.001$) (**Table 1**).

A total of 390 patients with CSDH underwent burr hole evacuation during the study period. Fifty-four patients were excluded, comprising 43 patients with recurrent CSDH, 9 patients with iatrogenic CSDH, and 2 patients with CSDH related to cerebrospinal fluid hypovolemia. A final total of 336 patients were included in this study. Following the exclusion criteria, 196 patients (median age, 80 years; IQR: 72.5–85 years; 135 [68.9%] men) in the pre-pandemic group and 140 patients (median age, 80 years; IQR: 74–85 years; 90 [64.3%] men) in the intra-pandemic group were included for analysis. Significant declines in numbers (196 vs. 140 cases) and IR of CSDH (35.0/100,000 vs. 24.8/100,000 person-years) were seen in the intra-pandemic group compared to the pre-pandemic group. The IRR of CSDH

TABLE 1 | Incidence of head trauma according to pre- and intra-pandemic status in Akashi city, Japan.

	Pre-pandemic status Apr 1, 2018 – Dec 31, 2019			Intra-pandemic status Jan 1,2020 – Sep 30, 2021				
	Cases	Person-years	IR[a,†]	Cases	Person-years	IR[a,†]	IRR[b,§] (95%CI[c])	*P* value
All	5,282	555,488	950.9	4,459	561,207	794.5	0.84 (0.80–0.87)	<0.001
0–19 years	1,780	100,606	1,769.3	1,464	101,348	1,444.5	0.82 (0.76–0.87)	<0.001
20–69 years	1,551	356,773	434.7	1,219	353,876	344.5	0.79 (0.74–0.85)	<0.001
70+ years	1,951	98,110	1,988.6	1,776	105,983	1,675.7	0.84 (0.79–0.90)	<0.001

[a]*IR, incidence rate;* [b]*IRR, incidence rate ratio;* [c]*CI, confidence interval.* [†]*per 100,000 person-year.* [§]*IR in intra-pandemic status/ IR in pre-pandemic status.*

TABLE 2 | Incidence of chronic subdural hematoma according to pre- and intra-pandemic status in Akashi city, Japan.

	Pre-pandemic status Apr 1, 2018 – Dec 31, 2019			Intra-pandemic status Jan 1, 2020 – Sep 30, 2021				
Characteristics	Cases	Person-years	IR[a,†]	Cases	Person-years	IR[a,†]	IRR[b,§] (95%CI[c])	*P* value
All	196	559,914	35.0	140	564,969	24.8	0.71 (0.57–0.88)	0.002
0–19 years	1	102,161	1.0	3	102,624	2.9	2.99 (0.31–28.7)	0.34
20–69 years	31	358,076	8.7	18	354,912	5.1	0.59 (0.33–1.05)	0.071
70+ years	164	99,525	164.8	119	107,210	111.0	0.67 (0.53–0.85)	0.001
Preoperative mRS [d]								
1	18	559,914	3.2	14	564,969	2.5	0.77 (0.38–1.55)	0.47
2	43	559,914	7.7	34	564,969	6.0	0.78 (0.50–1.23)	0.29
3	62	559,914	11.1	36	564,969	6.4	0.58 (0.38–0.87)	0.008
4	47	559,914	8.4	40	564,969	7.1	0.84 (0.55–1.29)	0.43
5	26	559,914	4.6	16	564,969	2.8	0.61 (0.33–1.14)	0.12
1–3	123	559,914	22.0	84	564,969	14.9	0.68 (0.51–0.89)	0.006
4–5	73	559,914	13.0	56	564,969	9.9	0.76 (0.54–1.08)	0.12

[a]*IR, incidence rate;* [b]*IRR, incidence rate ratio;* [c]*CI, confidence interval;* [d]*mRS, modified Rankin scale.* [†]*per 100,000 person-year.* [§]*IR in intra-pandemic status/ IR in pre-pandemic status.*

was 0.708 (95% CI: 0.570–0.879, $p = 0.002$) (**Table 2**). However, we saw no significant differences in age ($p = 0.66$), sex ($p = 0.38$), and rates of taking anticoagulants (15 patients [7.7%] vs. 15 patients [10.7%]; $p = 0.33$) and antiplatelet medicines (31 patients [15.8%] vs. 22 patients [15.7%]; $p = 0.98$) between the pre- and intra-pandemic groups. No significant difference was seen in the median preoperative mRS score (3 [IQR: 2–4] vs. 3 [IQR: 2–4]; $p = 0.87$) between the pre- and intra-pandemic groups. The IR for each mRS strata of patients with mRS score of 3 was significantly lower in the intra-pandemic group than in the pre-pandemic group (IRR: 0.58, 95% CI: 0.38–0.87, $p = 0.008$). Declines in IR were seen in both mild and severe cases of CSDH. Although the IR in the mild cases of CSDH was significantly lower in the intra-pandemic group than in the pre-pandemic group (IRR: 0.68, 95% CI: 0.51–0.89, $p = 0.006$), for the severe cases of CSDH, the 95% CI for the IRR included 1 (**Table 2**).

DISCUSSION

This retrospective single-center descriptive study revealed that the COVID-19 pandemic correlated with significant declines in both the number and IR for hospital presentation due to head trauma (−16.4%) and CSDH (−29.2%) during the intra-pandemic period, compared to the pre-pandemic period. Although there are some reports of declines in trauma at local, regional, and national levels during the COVID-19 pandemic period, this represents the first study to examine associations between the COVID-19 pandemic and CSDH, as far as we know (5–8).

The IR of head trauma in all three age strata declined significantly. The IRR of head trauma (adjusted to age under 20 years) for patients aged more than 70 years was highest among the three age strata. Although the forced restrictions on social activities, such as stay-at-home orders and lockdowns, were enacted, resulting in unprecedented limitations on public and commercial interactions, the effects of these restrictions on head trauma appear particularly prominent in the lower age strata of under 70 years. As a result, a significant increase in the median age of head trauma patients was seen during the intra-pandemic period. In addition, a significant decline in physical activity during the COVID-19 pandemic period has been reported among the elderly in Japan (9, 10). Regular physical activity has been associated with an increased incidence of activity-related injuries (11–13). Although declines in physical activity could result in declining head trauma among the elderly, the effects of restricting social activities on head trauma were relatively small in the population aged over 70 years. We attribute this to head trauma occurring at places unrelated to social activities, such as

indoors, particularly in the elderly (16). We consider that this is why the effects of restricted social activities on head trauma were small among the elderly.

CSDH is considered a traumatic disorder that often develops after head injury. Association between CSDH and minor head trauma, such as whiplash trauma and indirect trauma to the cranium, have been reported in elderly individuals with brain atrophy (2, 17). We observed significant declines in the number and IR of CSDHs between pre- and intra-pandemic groups. As more than three-quarters of CSDH cases in both pre- and intra-pandemic groups occurred in patients over the age of 72 years, no major difference in the age of CSDH patients was identified between groups. Declines in the number of head traumas may result in declines in the number of CSDHs in the elderly. Chan et al. reported that CSDH patients presented with longer interval, from the initial head injury to the final diagnosis, in the lockdown period than in the same period in the previous year (14). On the other hand, they also found no difference in the severity of CSDH between the lockdown period and the same period in the previous year (14). However, this study found that the IR in preoperative mRS score of only the mild cases of CSDH in the intra-pandemic period was significantly lower than that in the pre-pandemic period. Consequently, the IR of the severe cases of CSDH in intra-pandemic relatively increased. We consider that the forced restrictions on social activities due to COVID-19 pandemic result in CSDH patients refraining from seeing doctors and hence aggravates CSDH.

The present study has some limitations. First, we did not include outpatients with CSDH, who had not undergone burr hole evacuation. Second, this study focused on a single center. There is a certainty that patients who were treated in other health systems and trauma centers were excluded. This study also included a small number of patients. The results of this analysis may not reflect a global decline in the IR of CSDH. Finally, trauma by its nature often shows wide variations from month to month, and so other factors may have affected declines in the numbers of head traumas and CSDHs.

We identified significant associations between the COVID-19 pandemic and declines in the numbers and IRs of head traumas and CSDHs. Fewer people being out in their communities may result in fewer chances for head trauma and CSDH. According to this study, forced restrictions on social activities due to COVID-19 pandemic results in CSDH patients refraining from seeing doctors, and aggravates CSDH. We would like to raise alarm for this situation, and clinicians must consider this insidious and curable neurosurgical disorder.

DATA AVAILABILITY STATEMENT

The raw data supporting the conclusions of this article will be made available by the authors, without undue reservation.

ETHICS STATEMENT

The studies involving human participants were reviewed and approved by the Institutional Ethics Committee of the Ohnishi Neurological Center (Approval No. 211101). Written informed consent to participate in this study was provided by the participants' legal guardian/next of kin.

AUTHOR CONTRIBUTIONS

RM and IN contributed to the study design and conception, drafting the manuscript, and editing of the manuscript. RM and HO collected the clinical data. RM, IN, and KS contributed to clinical data analysis and interpretation. KS conducted the statistical analysis. HN and HO supervised all aspects of this study. RM took responsibility for the study as a whole. All authors contributed to the article and approved the submitted version.

ACKNOWLEDGMENTS

We would like to thank FORTE (https://www.forte-science.co.jp) for English language editing.

REFERENCES

1. Weigel R, Schmiedek P, Krauss JK. Outcome of contemporary surgery for chronic subdural haematoma- evidence based review. *J Neurol Neurosurg Psychiat.* (2003) 74:937–43. doi: 10.1136/jnnp.74.7.937
2. Feghali J, Yang W, Huang J. Updates in chronic subdural hematoma: epidemiology, etiology, pathogenesis, treatment, and outcome. *World Neurosurg.* (2020) 141:339–45. doi: 10.1016/j.wneu.2020.06.140
3. Balser D, Farooq S, Mehmood T, Reyes M, Samadani U. Actual and projected incidence rates for chronic subdural hematomas in united states veterans administration and civilian populations. *J Neurosurg.* (2015) 123:1209–15. doi: 10.3171/2014.9.JNS141550
4. Lee KS. Natural History of Chronic Subdural Haematoma. *Brain Inj.* (2004) 18:351–8. doi: 10.1080/02699050310001645801
5. DiFazio LT, Curran T, Bilaniuk JW, Adams JM, Durling-Grover R, Kong K, et al. The impact of the Covid-19 pandemic on hospital admissions for trauma and acute care surgery. *Am Surg.* (2020) 86:901–3. doi: 10.1177/0003134820939904
6. Ghafil C, Matsushima K, Ding L, Henry R, Inaba K. Trends in trauma admissions during the COVID-19 pandemic in Los Angeles county, California. *JAMA Netw Open.* (2021) 4:e211320. doi: 10.1001/jamanetworkopen.2021.1320
7. Leichtle SW, Rodas EB, Procter L, Bennett J, Schrader R, Aboutanos MB. The influence of a statewide "stay-at-home" order on trauma volume and patterns at a level 1 trauma center in the United States. *Injury.* (2020) 51:2437–41. doi: 10.1016/j.injury.2020.08.014
8. Christey G, Amey J, Campbell A, Smith A. Variation in volumes and characteristics of trauma patients admitted to a level one trauma centre during national level 4 lockdown for Covid-19 in New Zealand. *New Zeal Med J.* (2020) 133:81–8.
9. M Yamada, Y Kimura, D Ishiyama, Y Otobe, M Suzuki, S Koyama, et al. Effect of the Covid-19 epidemic on physical activity in community-dwelling older adults in japan- a cross-sectional online survey. *J Nutr Health Aging.* (2020) 24:948–50. doi: 10.1007/s12603-020-1501-6
10. M Yamada, Y Kimura, D Ishiyama, Y Otobe, M Suzuki, S Koyama, et al. The influence of the Covid-19 pandemic on physical activity and new incidence

of frailty among initially non-frail older adults in japan- a follow-up online survey. *J Nutr Health Aging.* (2021) 25:751–6. doi: 10.1007/s12603-021-1634-2
11. Carlson SA, Hootman JM, Powell KE, Macera CA, Heath GW, Gilchrist J, et al. Self-reported injury and physical activity levels: United States 2000 to 2002. *Ann Epidemiol.* (2006) 16:712–9. doi: 10.1016/j.annepidem.2006.01.002
12. Parkkari J, Kannus P, Natri A, Lapinleimu I, Palvanen M, Heiskanen M, et al. Active living and injury risk. *Int J Sports Med.* (2004) 25:209–16. doi: 10.1055/s-2004-819935
13. J Conn, J Annest, Gilchrist J. Sports and recreation related injury episodes in the us population, 1997-99. *Injury Prevent.* (2003) 9:117–23. doi: 10.1136/ip.9.2.117
14. Chan DYC, Poon WS, Chan DTM, Mak WK, Wong GKC. Chronic subdural haematoma during the COVID-19 lockdown period: late presentation with a longer interval from the initial head injury to the final presentation and diagnosis. *Chin Neurosurg J.* (2021) 7:4. doi: 10.1186/s41016-020-00229-7
15. Banks JL, Marotta CA. Outcomes validity and reliability of the modified rankin scale: implications for stroke clinical trials: a literature review and synthesis. *Stroke.* (2007) 38:1091–6. doi: 10.1161/01.STR.0000258355.23810.c6
16. Hruska K, Ruge T. The tragically hip: trauma in elderly patients. *Emerg Med Clin North Am.* (2018) 36:219–35. doi: 10.1016/j.emc.2017.08.014
17. Ommaya AK, Yarnell P. Subdural haematoma after whiplash injury. *Lancet.* (1969) 2:237–9. doi: 10.1016/S0140-6736(69)90005-1

Conflict of Interest: The authors declare that the research was conducted in the absence of any commercial or financial relationships that could be construed as a potential conflict of interest.

Publisher's Note: All claims expressed in this article are solely those of the authors and do not necessarily represent those of their affiliated organizations, or those of the publisher, the editors and the reviewers. Any product that may be evaluated in this article, or claim that may be made by its manufacturer, is not guaranteed or endorsed by the publisher.

frontiers | Frontiers in Neurology

SYSTEMATIC REVIEW
published: 20 May 2022
doi: 10.3389/fneur.2022.872261

Research Hotspots and Trends of Peripheral Nerve Injuries Based on Web of Science From 2017 to 2021: A Bibliometric Analysis

Shiwen Zhang[1], *Meiling Huang*[1], *Jincao Zhi*[1], *Shanhong Wu*[1], *Yan Wang*[2]* *and Fei Pei*[2]*

[1] *Department of Rehabilitation Medicine and Physical Therapy, Graduate School, Heilongjiang University of Traditional Chinese Medicine, Harbin, China,* [2] *Rehabilitation Center, The Second Affiliated Hospital of Heilongjiang University of Traditional Chinese Medicine, Heilongjiang University of Traditional Chinese Medicine, Harbin, China*

Background: Peripheral nerve injury (PNI) is very common in clinical practice, which often reduces the quality of life of patients and imposes a serious medical burden on society. However, to date, there have been no bibliometric analyses of the PNI field from 2017 to 2021. This study aimed to provide a comprehensive overview of the current state of research and frontier trends in the field of PNI research from a bibliometric perspective.

Methods: Articles and reviews on PNI from 2017 to 2021 were extracted from the Web of Science database. An online bibliometric platform, CiteSpace, and VOSviewer software were used to generate viewable views and perform co-occurrence analysis, co-citation analysis, and burst analysis. The quantitative indicators such as the number of publications, citation frequency, h-index, and impact factor of journals were analyzed by using the functions of "Create Citation Report" and "Journal Citation Reports" in Web of Science Database and Excel software.

Results: A total of 4,993 papers was identified. The number of annual publications in the field remained high, with an average of more than 998 publications per year. The number of citations increased year by year, with a high number of 22,272 citations in 2021. The United States and China had significant influence in the field. Johns Hopkins University, USA had a leading position in this field. JESSEN KR and JOURNAL OF NEUROSCIENCE were the most influential authors and journals in the field, respectively. Meanwhile, we found that hot topics in the field of PNI focused on dorsal root ganglion (DRG) and satellite glial cells (SGCs) for neuropathic pain relief and on combining tissue engineering techniques and controlling the repair Schwann cell phenotype to promote nerve regeneration, which are not only the focus of research now but is also forecast to be of continued focus in the future.

Conclusion: This is the first study to conduct a comprehensive bibliometric analysis of publications related to PNI from 2017 to 2021, whose bibliometric results can provide a reliable source for researchers to quickly understand key information in this field and identify potential research frontiers and hot directions.

Keywords: peripheral nerve injuries, CiteSpace, VOSviewer, bibliometric analysis, Web of Science

OPEN ACCESS

Edited by:
Mårten Risling,
Karolinska Institutet (KI), Sweden

Reviewed by:
Jaspreet Kaur,
University of Copenhagen, Denmark
Mengchen Yin,
Shanghai University of Traditional Chinese Medicine, China

***Correspondence:**
Yan Wang
swallow-1113@163.com
Fei Pei
peifeihyd@163.com

Specialty section:
This article was submitted to Neurotrauma, a section of the journal Frontiers in Neurology

Received: *09 February 2022*
Accepted: *19 April 2022*
Published: *20 May 2022*

Citation:
Zhang S, Huang M, Zhi J, Wu S, Wang Y and Pei F (2022) Research Hotspots and Trends of Peripheral Nerve Injuries Based on Web of Science From 2017 to 2021: A Bibliometric Analysis. Front. Neurol. 13:872261. doi: 10.3389/fneur.2022.872261

INTRODUCTION

Peripheral nerve injuries (PNI) are mainly caused by surgery and trauma and are common in clinical practice, with 13 to 23 per 1,00,000 people typically suffering from PNI (1–4). PNI is characterized by complex regeneration mechanisms, poor prognosis, and slow recovery (5–9), often leading to sensory and motor dysfunction and even lifelong disability, which not only seriously reduces the quality of life of patients but also brings a more serious health care burden to society (10–14). However, despite the increased understanding of the mechanisms of injury and regeneration, full functional recovery remains unsatisfactory in most patients (15, 16). With the rapid increase in the number of publications, it is becoming increasingly difficult for researchers to keep up with the latest findings (17, 18). It has been noted that researchers can benefit from an overview analysis of the domain knowledge structure and current hotspots (19). Therefore, bibliometric techniques are becoming increasingly popular as a quantitative analysis method by obtaining the above parameters (20). Currently, there is only one bibliometric analysis on PNI, with a review of publications that increased substantially during the First World War (21). Thus, a comprehensive bibliometric analysis of PNI is still very much lacking. In this study, a comprehensive bibliometric analysis was conducted in the field of PNI from 2017 to 2021, to help researchers quickly understand the knowledge structure and current hotspots in the field, to provide new ideas for developing new research topics, and to contribute to improving the quality of articles on PNI.

MATERIALS AND METHODS

Data Acquisition and Search Strategy

The literature source was selected as the Science Citation Index Expanded (SCI-expanded) in Core Collection Indices of Web of Science (WoS). The literature search strategy was presented as follows: TOPIC: (peripheral nerve injury) OR TITLE: (peripheral nerve injury) OR TOPIC: (peripheral nerve injuries) OR TITLE: (peripheral nerve injuries). The time span was selected for the period from 2017 to 2021. The language was limited to "English". The document type was "articles" and "review" and other types, such as early access, editorial material, meeting abstract, proceedings paper, book chapter, letter, correction, data paper, book review, were excluded. A total of 4,993 publications was retrieved. The last deadline was January 23, 2022.

Data Extraction

Annual publication counts, citation frequency, country, institution, author, journal, keywords, and references were extracted from the data exported as "Full Record and Citation References". The H-index and the average citations per item (ACI) for countries and institutions are extracted through the "Create Citation Report" function in the Web of Science database. Journal Impact Factor (JIF) and quartile categories Q1, Q2, Q3, and Q4 were extracted from the Journal Citation Reports in the Web of Science database.

Data Analysis

Three bibliometric tools were used in this study. The online bibliometric platform was used in this study for country collaboration analysis and analysis of different country publications over the years (https://bibliometric.com/). CiteSpace, free software developed by Chen, is often used as a bibliometric tool to determine the structure and distribution of knowledge in a given field (22, 23). In our study, CiteSpace was used to perform collaborative analysis of institutions, co-citation relationships of authors, analysis of keywords, and analysis of references. It is worth noting that the nodes represent a type of project, such as country, institution, or author. The size and color of the node circles indicate the number or frequency of articles issued and the year of the appearance of these items, respectively, and the connecting lines between the nodes reflect the cooperation between different items (24). VOSviewer, another bibliometric software developed by Prof. van Eck and Waltman, with the ability to construct and view bibliometric maps, provides three types of maps, including

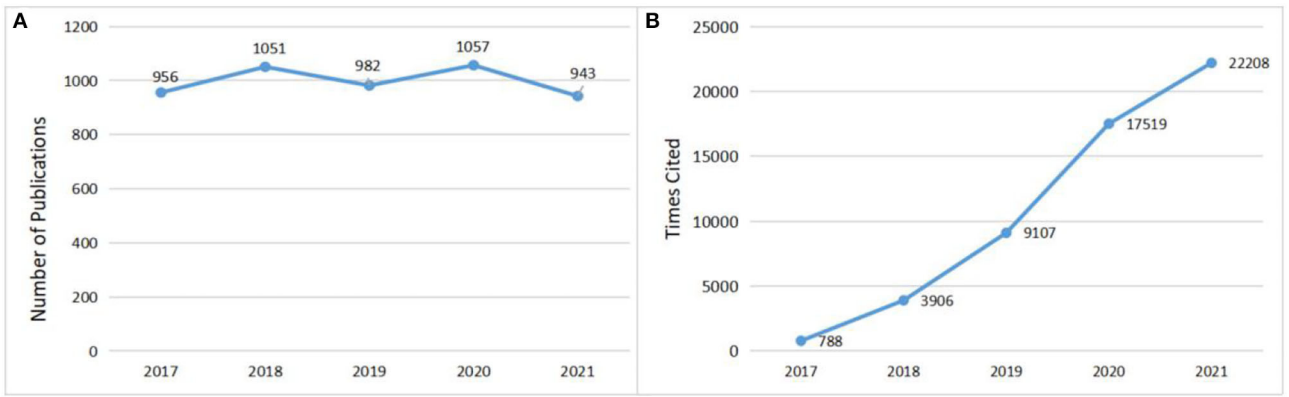

FIGURE 1 | (A) The number of annual publications. **(B)** The annual times cited.

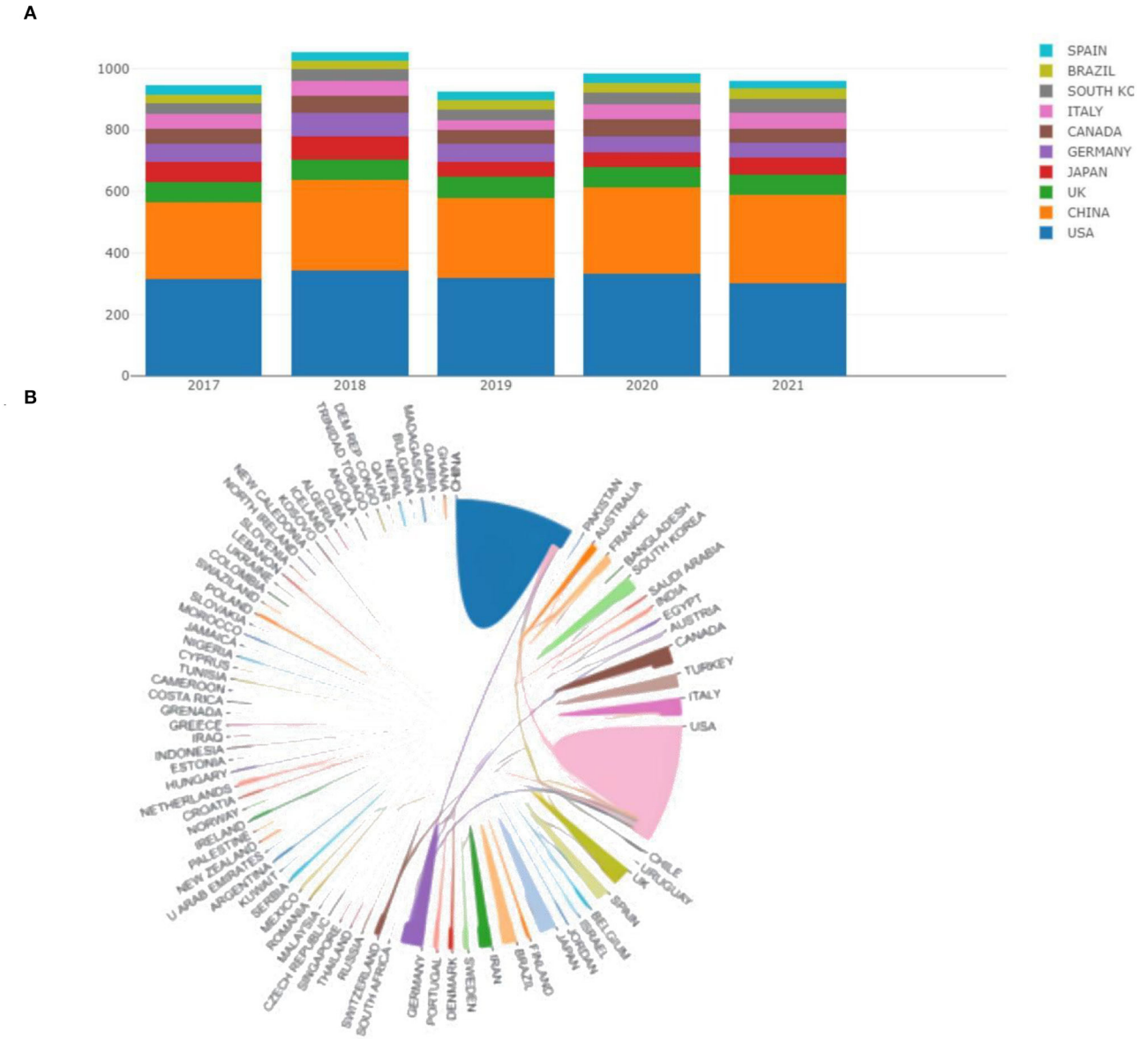

FIGURE 2 | (A) The annual publication counts of the top 10 countries from 2017 to 2021. **(B)** Collaboration analysis among different countries.

network visualization maps, coverage visualization maps, and density visualization maps, each of which emphasizes a different aspect of the map, a detailed description of which can be found on the website (https://www.vosviewer.com/documentation) (25, 26). This study mainly applied the software for the author's co-authorship analysis and journal co-citation analysis.

RESULTS AND DISCUSSION

Publication Outputs and Citation Trends

The annual publications and times cited can reflect directly the trends of scientific knowledge in a particular field. After the above literature screening, a total of 4,993 papers was included in the final analysis, of which 4,120 were original articles and 873 were reviews. The specific distribution of annual publications was shown in **Figure 1A**. As can be seen, despite small fluctuations, the number of annual publications had been high, with an average of more than 998 publications per year, indicating that PNI has been hot and has received continued attention from research scholars during the 5 years, and the field is expected to remain a research hotspot in 2022. In terms of citations, the cumulative total number of citations for these publications was 54,719 (43,332 after removal self-citations), with average citations per item of 10.92. The distribution of the number of citations per year can be seen in **Figure 1B**, with the number increasing year by year and a large increase in the number of citations between

TABLE 1 | The top 10 most productive countries from 2017 to 2021.

RANK	Country	Contribution	% of 4,993	h-index	ACI
1	USA	1,641	32.87%	54	14.84
2	China	1,307	26.18%	44	12.2
3	England	318	6.37%	37	17.63
4	Germany	302	6.05%	33	15.24
5	Japan	297	5.95%	26	10.81
6	Canada	257	5.15%	28	13.37
7	Italy	234	4.69%	24	11.87
8	South Korea	195	3.91%	22	8.91
9	Brazil	159	3.18%	17	9.11
10	Spain	146	2.92%	23	13.56

19 and 20, with the highest number of citations in 2021 at 22,272. The heat of research on PNI remained high from 2017 to 2021 and attracted gradually the attention of annual publications and citations.

Country

The top 10 countries in terms of publications were presented in **Figure 2A**. According to the different color gradients, We can observe that the majority of the articles are from the United States and China. In specific, as shown in **Table 1**, we can understand that the US has the most publications in this field with 1,641 (32.87%), followed by China 1,307 (26.18%), UK 318 (6.37%), and Germany 302 (6.05%). The h-index, a new parameter for quantifying scientific achievement proposed by Jorge Hirsch, is defined as the number of papers with citation number $\geq$ h (27–29). It was evident from the Table that the USA and China still occupied the first and second positions in the h-index. ACI is another indicator to measure scientific contribution. The top 5 countries in ACI were England (17.56), Germany (15.19), the USA (14.8), Spain (13.52), and China (12.14). Overall, the US and China were significant influencers in all aspects including volume of publications, H-index, and ACI. Furthermore, as can be seen from **Figure 2B**, the cooperation between different countries was clearly shown. The thicker the line between the two countries indicates the more cooperative exchanges. It can be seen that the cooperation between the United States and China was closer.

Institution

The publication counts, h-index, and ACI of the top 10 most prolific institutions were shown in detail in **Figure 3A**. Among them, Nantong University in China ranked first with 148 articles, Johns Hopkins University in the United States ranked second with 117 papers, and Shanghai Jiao Tong University in China ranked third with 98 papers. In addition, Johns Hopkins also had the top H-index ranking at 27 and the ACI (18.7) ranking at Johns Hopkins was also in the higher position. As such, Johns Hopkins University had a leading position in this field. This study also conducted an institutional cooperation analysis using CiteSpace software (**Figure 3B**). The betweenness centrality (BC) of a node in a network reflects the importance of the node's position in the network, and BC is an indicator of the centrality of a node (30–32). In general, nodes with BC values of more than 0.1 have a purple outer ring, which also indicates that the node occupies a key position connecting a large number of nodes. Of all these institutions, 36 institutions had BC values above 0.1. The top five institutions with the highest BC values were, Rutgers State Univ (0.66), Mayo Clin (0.6), Ohio State Univ (0.54), Washington Univ (0.46), Univ Toronto (0.42). It can be seen that most of these institutions were from the United States, again indicating the influence of the United States in the field. In parallel to the CiteSpace software, we also conducted a collaborative institutional analysis of organizations through VOSviewer. As displayed in the overlay visualization in **Figure 3C**, the nodes representing institutions were marked with different colors depending on the average year of appearance (AAY) of each institution, where institutions with relatively early average years of appearance were closer to blue or dark blue, e.g., Gunma University, University of Strasbourg, Kitasato University, in contrast, many institutions marked in red or dark red may be relatively new participants in the field, e.g., Queens University, Chinese People's Liberation Army General Hospital, Ewha Womans University, etc.

Co-authorship and Co-citation Author

The analysis co-citation author is often used to reveal the key authors in the co-citation network of a particular field. The more citations an author receives, the more influence he or she has. The top five most-cited authors were, JESSEN KR (446), CHAPLAIN SR (335), JI RR (332), BENNETT GJ (328), and GORDON T (289). JESSEN KR is with the Department of Cell and Developmental Biology, University College London, where he focuses on Schwann cells as a fulcrum to explore the underlying mechanisms of peripheral nerve regeneration (33–36). As can be seen from **Figure 4A**, JESSEN KR collaborated closely with Arthur-Farraj P at the Department of Cell and Developmental Biology, University College London, and they had published more than 10 articles together. Of these, an article published in NEURON titled "c-Jun Reprograms Schwann Cells of Injured Nerves to Generate a Repair Cell Essential for Regeneration", which was cited 431 times for the study, found that the transcription factor c-Jun in Schwann cells can play a role in determining the expression of trophic factors and adhesion molecules, regenerative track formation, and myelin clearance, controlling the unique regenerative potential of peripheral nerves by activating repair programs in Schwann cells and creating cells that support regeneration, suggesting that a single glial transcription factor c-Jun is critical for the repair of damaged nerves (37). From the above results, it can be seen that JESSEN KR was one of the most influential authors in the field due to his high citation frequency and close communication with other authors in the field. The analysis of the authors' co-authorship relationships is beneficial in revealing the current collaborations within the field. In **Figure 4B**, the VOSviewer software generated a superimposed visualization of the author's co-authorship analysis. It can be observed that the group with Yi Sheng as the core was large, and there was more cooperation within the group. Yi Sheng worked at Nantong University, China,

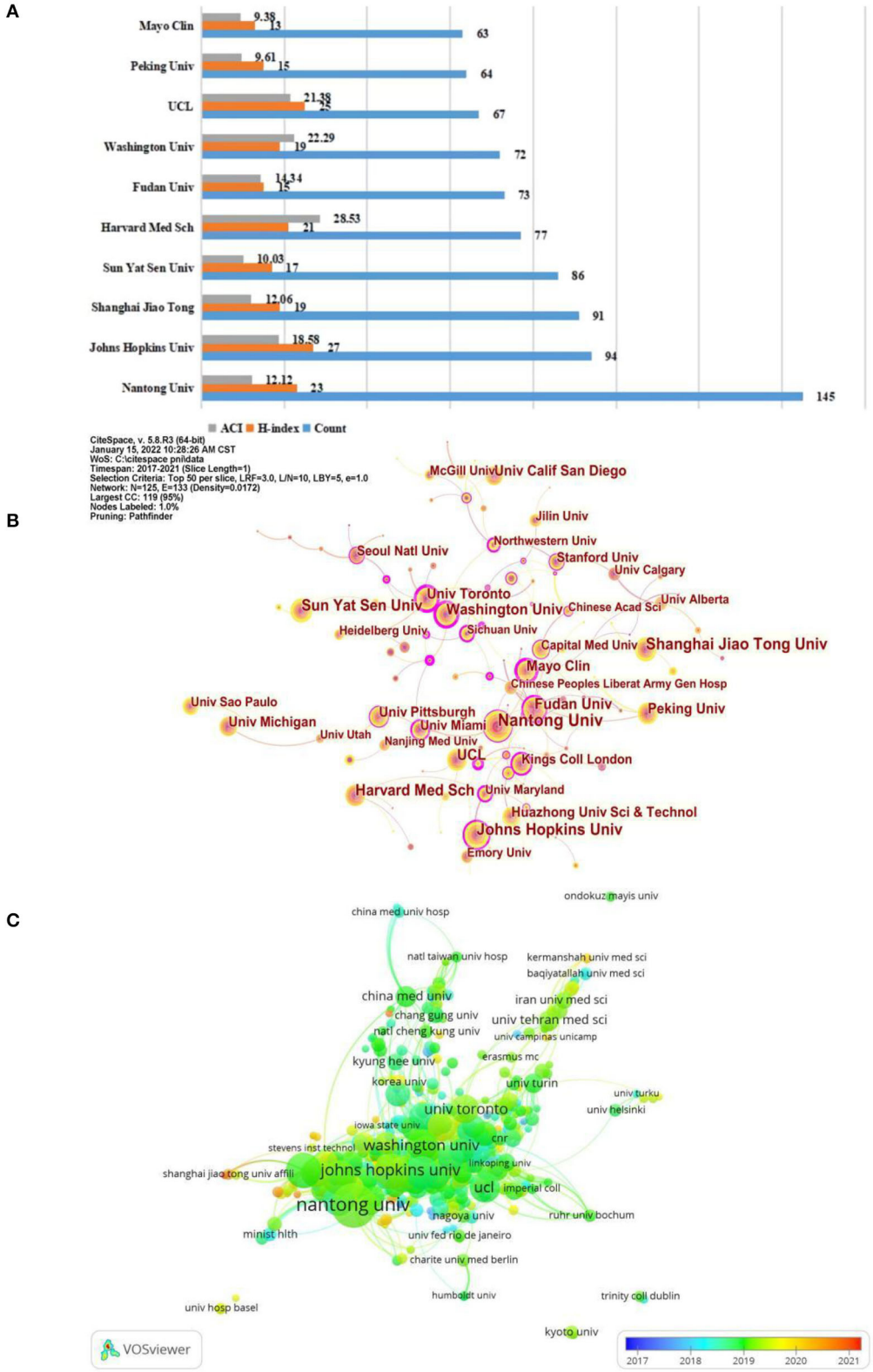

FIGURE 3 | (A) The publication counts, h-index, and ACI of the top 10 most prolific institutions. **(B)** Visualization map of institutions' cooperative relationship by using CiteSpace software. **(C)** Coverage visualization map of institutions co-authorship analysis by using VOSviewer software.

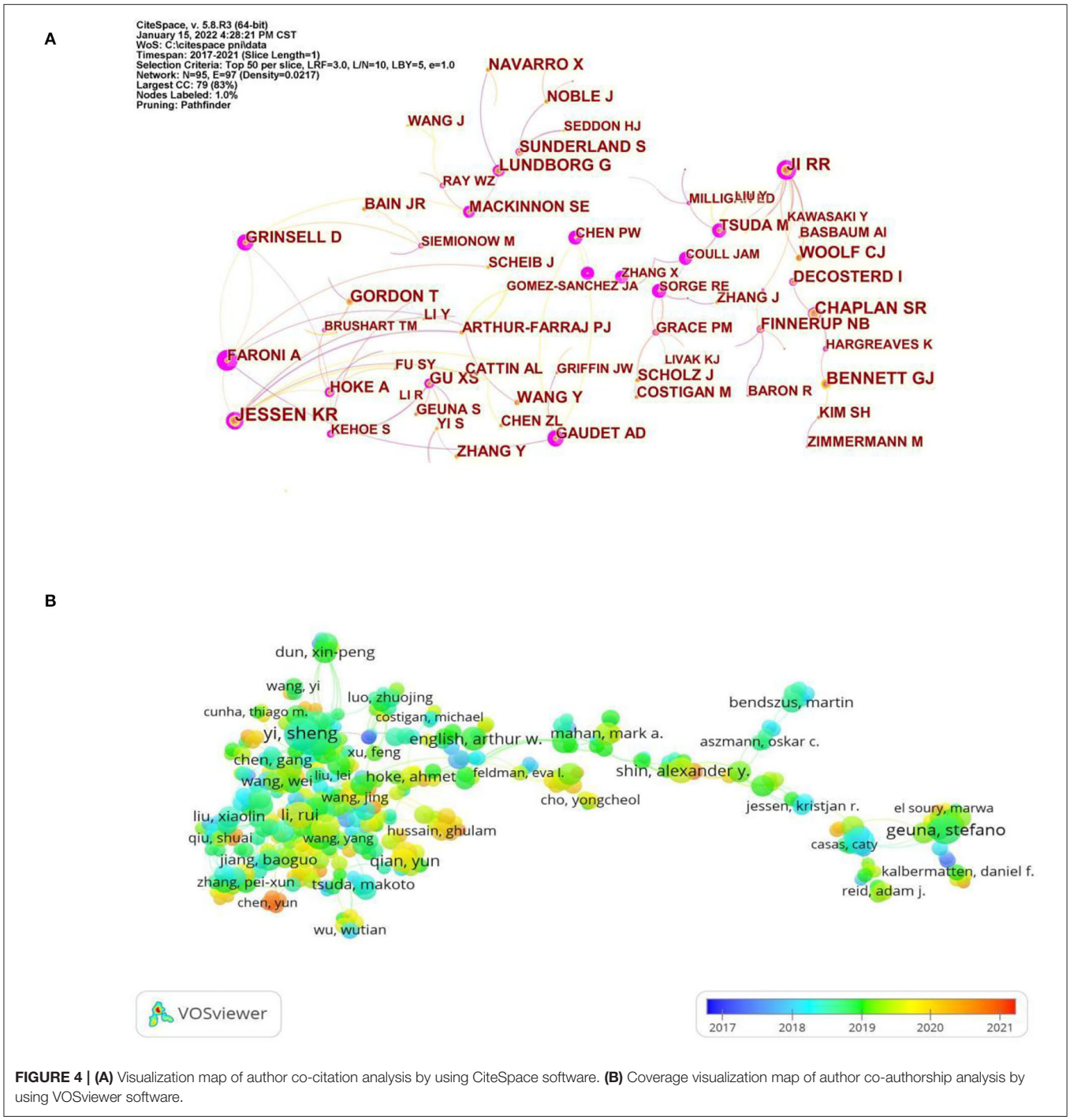

FIGURE 4 | (A) Visualization map of author co-citation analysis by using CiteSpace software. **(B)** Coverage visualization map of author co-authorship analysis by using VOSviewer software.

where he focused on microRNA (38, 39), and Schwann cells (40, 41). Notably, most of the authors in this group were from East Asia, and there was less collaboration with authors from Europe. In the future, authors in this field should strengthen cooperation and exchange to mutually improve their international influence. Following the color gradient shown in the bottom right corner, we can find that the authors represented by Chen Yun were relatively young researchers in the field.

Journal

In total, more than 1,000 journals appeared in this research area, according to statistics. The top 10 active journals published 817 papers on PNI, accounting for 16.36% of all 4,993 papers. Among them, as shown in **Table 2**, NEURAL REGENERATION RESEARCH (156 articles) published the most articles, SCIENTIFIC REPORTS (99 articles) ranked second, followed by PAIN (92 articles) and INTERNATIONAL

JOURNAL OF MOLECULAR SCIENCES (87 articles). In particular, the JIF of a journal is an important factor parameter in evaluating its value and the value of the publications it includes. Among the top 10 academic journals, JOURNAL OF NEUROSCIENCE had the highest JIF and was classified as Q1, which focused on neurophysiology (42, 43), neurodevelopment (44, 45), and brain imaging (46, 47). Interestingly, among the top 10 academic journals, 7 were in the neuroscience category, 1 called SCIENTIFIC REPORTS was a general journal, and the other 3, PAIN, INTERNATIONAL JOURNAL OF MOLECULAR SCIENCES, and MOLECULAR PAIN focused on the direction of pain and molecular biology. In addition to the number of publications, the impact of journals depends on the number of times they are co-cited in a particular field of study. For this study, CiteSpace software was used for co-citation journal analysis. As can be seen in **Figure 5**, the most cited journals were JOURNAL OF NEUROSCIENCE [2,681], followed by

EXPERIMENTAL NEUROLOGY (2,226), PLOS ONE (2,168), and P NATL ACAD SCI USA (1,898). In summary, JOURNAL OF NEUROSCIENCE was the most influential journal in this field.

TABLE 2 | The top 10 most productive journals from 2017 to 2021.

No.	Journal	Output	% of 4,993	JIF (2020)	Quartile in category (2020)
1	Neural regeneration research	156	3.13%	5.135	Q2
2	Scientific reports	99	1.98%	4.38	Q1
3	Pain	92	1.84%	5.135	Q2
4	International journal of molecular Sciences	87	1.74%	5.924	Q1/Q2
5	Molecular pain	68	1.36%	3.395	Q3
6	Experimental neurology	60	1.20%	5.33	Q2
7	Frontiers in cellular neuroscience	55	1.10%	5.505	Q1
8	Neuroscience	54	1.08%	3.59	Q3
9	Journal of neuroscience	50	1%	6.167	Q1
10	Neuroscience letters	50	1%	3.046	Q3

Analysis of Keywords Co-citation, Clustering, Timeline, and Burst

For bibliometrics, a useful method used to identify research hotspots is keyword co-occurrence analysis (48). **Figures 6A,B** showed the top 10 high-frequency keywords and high BC value keywords. After excluding the keywords "peripheral nerve", "peripheral nerve injury", "nerve injury", and "injury", other keywords "neuropathic pain", "Schwann cell", "regeneration", "expression", "sciatic nerve", "stem cell", "activation", "growth", and "conduit" were related to the study of mechanisms of peripheral nerve repair and regeneration and improvement of neuropathic pain. It should be noted that the modularity value (Q value) and the mean silhouette value (S value) are two important parameters to evaluate the effect of mapping. $Q > 0.3$ and $S > 0.7$ indicate significantly clustered (49, 50). In this present study, the

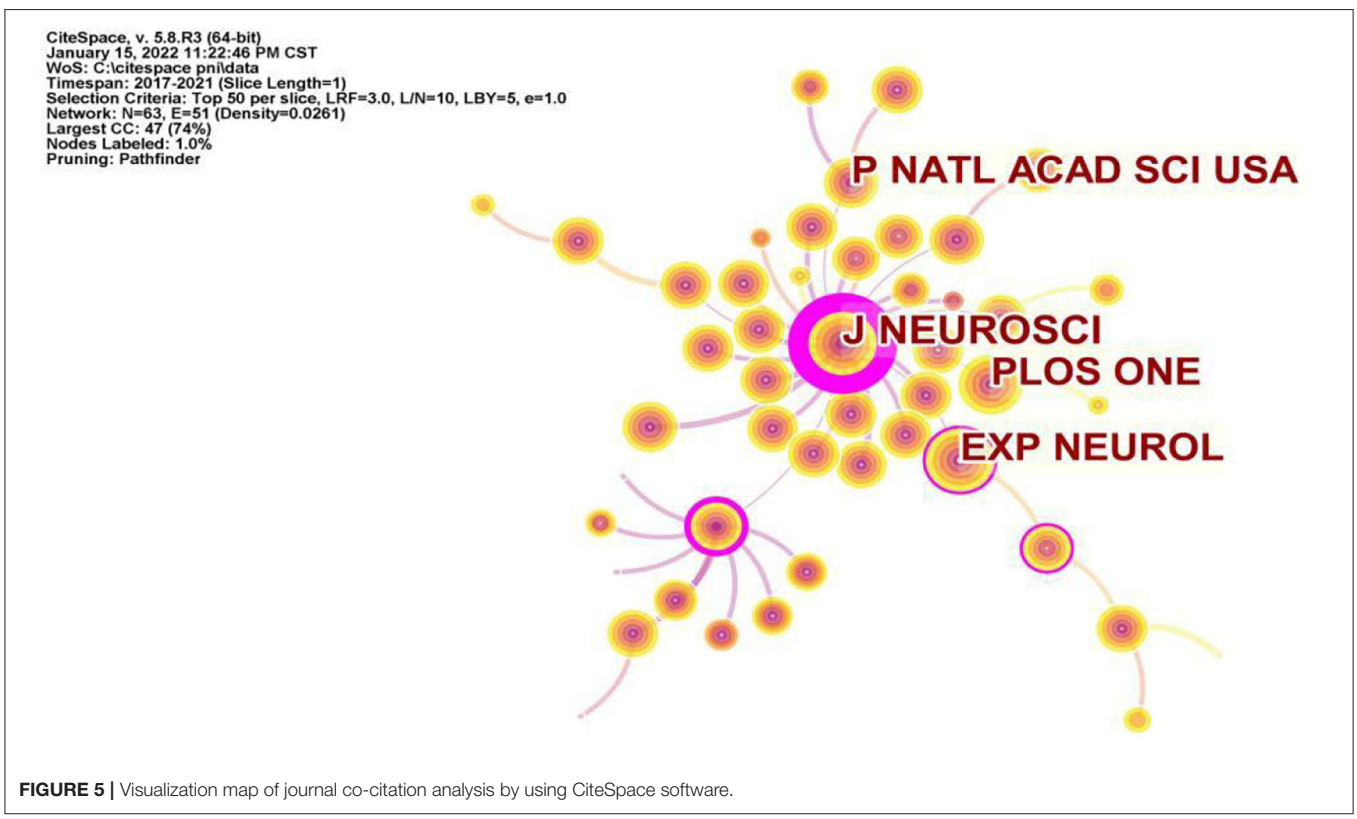

FIGURE 5 | Visualization map of journal co-citation analysis by using CiteSpace software.

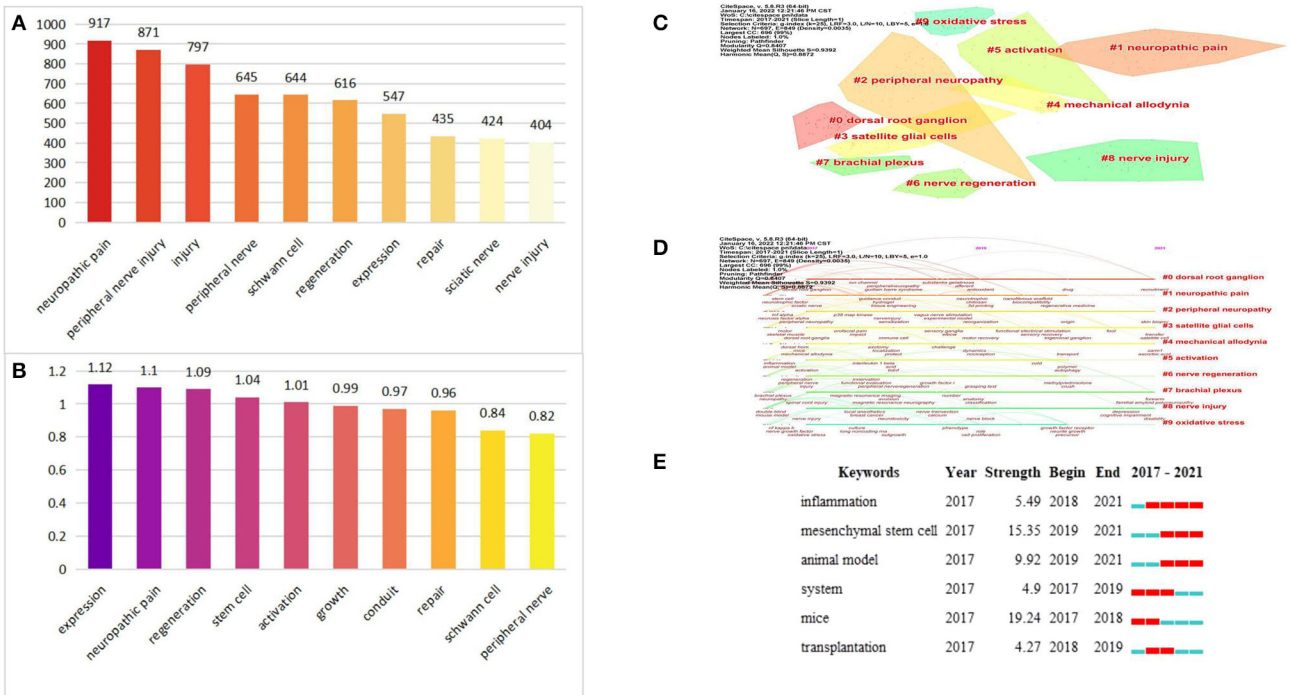

FIGURE 6 | (A) The top 10 high-frequency keywords. **(B)** The top 10 high BC value keywords. **(C)** The cluster view map by using CiteSpace software. **(D)** The timeline view map by using CiteSpace software. **(E)** Top 6 Keywords with the Strongest Citation Bursts.

TABLE 3 | Cluster analysis of keywords.

ID	Size	Sihouette	Year	Lable
0	50	0.909	2017	dorsal root ganglion
1	48	0.896	2017	neuropathic pain
2	38	0.934	2017	peripheral neuropathy
3	38	0.948	2018	satelite glial cells
4	33	0.968	2017	mechanical allodynia
5	31	0.94	2017	activation
6	31	1	2017	nerve regeneration
7	30	0.979	2017	brachial plexus
8	30	0.951	2018	nerve injury
9	30	0.964	2018	oxidative stress

Q value was 0.8407 and the mean S value was 0.9392, indicating that these clusters were effective and had good homogeneity. As shown in **Figure 6C** and **Table 3**, the top five clusters were, "dorsal root ganglion"(DRG) (#0), "neuropathic pain" (#1), "peripheral neuropathy" (#2), "satellite glial cells" (SGCs) (#3), and "mechanical allodynia" (#4). Meanwhile, we also provided a timeline view of the main clusters in **Figure 6D**, which can be used to understand the evolutionary characteristics of each cluster according to the timeline. It can be seen that "DRG" (#0), "peripheral neuropathy" (#2), "SGCs" (#3), "mechanical allodynia" (#4), "brachial plexus" (#7), and "nerve injury" (#8) were still the focus of research in 2021. Notably, neuropathic pain is one of the chronic pains which is often triggered by PNI and caused by damage to the somatosensory nervous system, with common clinical features such as mechanical allodynia. Neuropathic pain is challenging to cure, and there is currently no known cure (51, 52). DRG is widely recognized as a potential target for the treatment of chronic pain due to its ability to transmit harmful stimulus information to the cerebral cortex (53, 54). SGCs, a type of cell surrounding sensory neurons in the DRG, can communicate with sensory neurons through gap junctions and chemical signals to regulate chronic pain when activated after PNI (55). Recently, a new study revealed that DRG-SGCs show stem cell properties and can be effectively differentiated into sensory neurons, providing a basis for clinical treatment of chronic pain, suggesting that the potential of satellite glial cells is enormous (56). Mechanical allodynia, DRG and SGCs are some of the other hot keywords mentioned above, which means that exploring the pathophysiological mechanisms of neuropathic pain is a hot research topic. Keywords bursts refer to those that have been frequently cited within one period of time. From **Figure 6E**, we can find that blue represents 2017–2021, the left end of red indicates the start time of emergence, and the right end time of emergence, "inflammation", "MSCs", and "animal model" are important research directions and will continue to be focused on in the future. In addition, higher burst values indicate that they have received special attention and represent, to some extent, the research frontier in the field of study during the corresponding time interval. From the perspective of burst values, we can observe that the strongest burst strength among

TABLE 4 | The top 10 most cited references.

No.	Title	Author	count
1	The repair Schwann cell and its function in regenerating nerves	Jessen KR	229
2	Peripheral nerve regeneration: experimental strategies and future perspectives	Alessandro Faroni	116
3	Macrophage-Induced Blood Vessels Guide Schwann Cell-Mediated Regeneration of Peripheral Nerves	Anne-Laure Cattin	114
4	Pain regulation by non-neuronal cells and inflammation	Ru-Rong Ji	109
5	Peripheral nerve reconstruction after injury: a review of clinical and experimental therapies	D Grinsell	107
6	Neuropathic pain	Luana Colloca	105
7	Pharmacotherapy for neuropathic pain in adults: a systematic review and meta-analysis	Nanna B Finnerup	101
8	Role of macrophages in Wallerian degeneration and axonal regeneration after peripheral nerve injury	Peiwen Chen	94
9	Different immune cells mediate mechanical pain hypersensitivity in male and female mice	Robert E Sorge	88
10	Schwann Cells: Development and Role in Nerve Repair	Jessen KR	88

the three terms is MSCs. MSCs, a type of pluripotent stem cells from the mesoderm, can differentiate into neural cells to regulate the microenvironment of the injury zone. Currently, MSCs are often used in combination with tissue engineering, and it has been shown that nerve conduits loaded with bone marrow MSCs can both promote nerve growth and regulate the microenvironment of the injured area thereby effectively improving the regeneration and repair of PNI, which may be the reason why MSCs have been focused on in recent years, but so far, the differentiation mechanism and the ability of MSCs to secrete neurotransmitters are still unclear, which is an urgent issue to be addressed before MSC therapy can be applied clinically (57).

Analysis of References Co-citation, and Burst

The analysis of references is a significant factor in bibliometric studies (58). The top 10 most cited references were shown in **Table 4**, from which it can be found that the article written by Jessen KR has the highest number of co-citations, 229, and the article written by Jessen KR appears twice, indicating that Jessen KR has a certain social influence in this research area, which is consistent with the findings above. Furthermore, three articles with Schwann cells as a topic appeared in the top ten highly cited literature, indicating the key position of Schwann cells in the field of PNI. **Figure 6C** showed the top 25 references with the strongest citation bursts, which can be observed mainly in terms of both burst value and burst time. One of the references with the strongest burst values was written by Scheib et al. (59). In this study, they found that the rodent model of nerve injury, while adding to our understanding of peripheral nerve regeneration, does not adequately recapitulate the human situation, as human axons usually need to extend longer distances than mice after PNI, and due to the lack of proximal neuronal contact over time, distal hemopoietic cells and target tissues may atrophy and thus impede axon extension, and then suggested that the rodent model of chronic denervation can recapitulate an environment similar to that of human nerve injury, which would be more useful for the study of human nerve injury regeneration methods. In terms of burst timing, **Figure 7** showed that most of the reference bursts have ended, but some continue into 2021, mainly related to the themes of "a three-dimensional hierarchically aligned fibrin nanofiber hydrogel (AFG)" (60), "brief electric stimulation" (61, 62), and "Schwann cells" (63). Among them, AFG, prepared by electrospinning and molecular self-assembly, with the characteristics of hierarchically aligned topography and low elasticity, is utilized in the form of a combination of tissue engineering therapeutic techniques to build an effective microenvironment and facilitate the role of Schwann cells in promoting peripheral nerve regeneration (60). Combined with the burst keyword analysis, we can observe that the combination with tissue engineering technology to improve the functional recovery rate of PNI has now become a key topic of interest and is expected to be followed up continuously in the future. In addition, it is worth mentioning that whether from high-frequency keywords, highly cited literature, or burst citation literature we can find that the study of the physiopathological mechanism of PNI based on Schwann cell has been the focus of attention of related scholars, showing great potential to accelerate peripheral nerve regeneration. Jessen KR et al. (63, 64) reviewed the development of Schwann cells and their central role in reprogramming the repair of post-injury nerves, which provides a solid basis for the development of more effective therapeutic approaches. Schwann cells are glial cells in the peripheral nervous system that are reprogrammed into a series of specific repair phenotypes to promote nerve regeneration after nerve injury (10, 65). However, maintenance of the repair phenotype is often brief and unstable, which contributes to the undesirable neural regeneration outcome in humans. Therefore, the study of promoting and maintaining the repair Schwann cell phenotype is of great relevance for promoting peripheral nerve regeneration, which is one of the important reasons why Schwann cells are a hot topic. Currently, some strategies based on promoting and maintaining the repair Schwann cell phenotype have been revealed, including low-intensity ultrasound (66), histone deacetylases (67), superparamagnetic iron oxide nanoparticles mediated magnetic actuation (68), etc. However, although the exploration of more effective treatment strategies is indeed the focus of current research, as more innovative treatments increasingly emerge, we believe that optimizing treatment strategies and conducting clinical evaluation practices to translate them into reality as early as possible are more critical issues for future researchers to address.

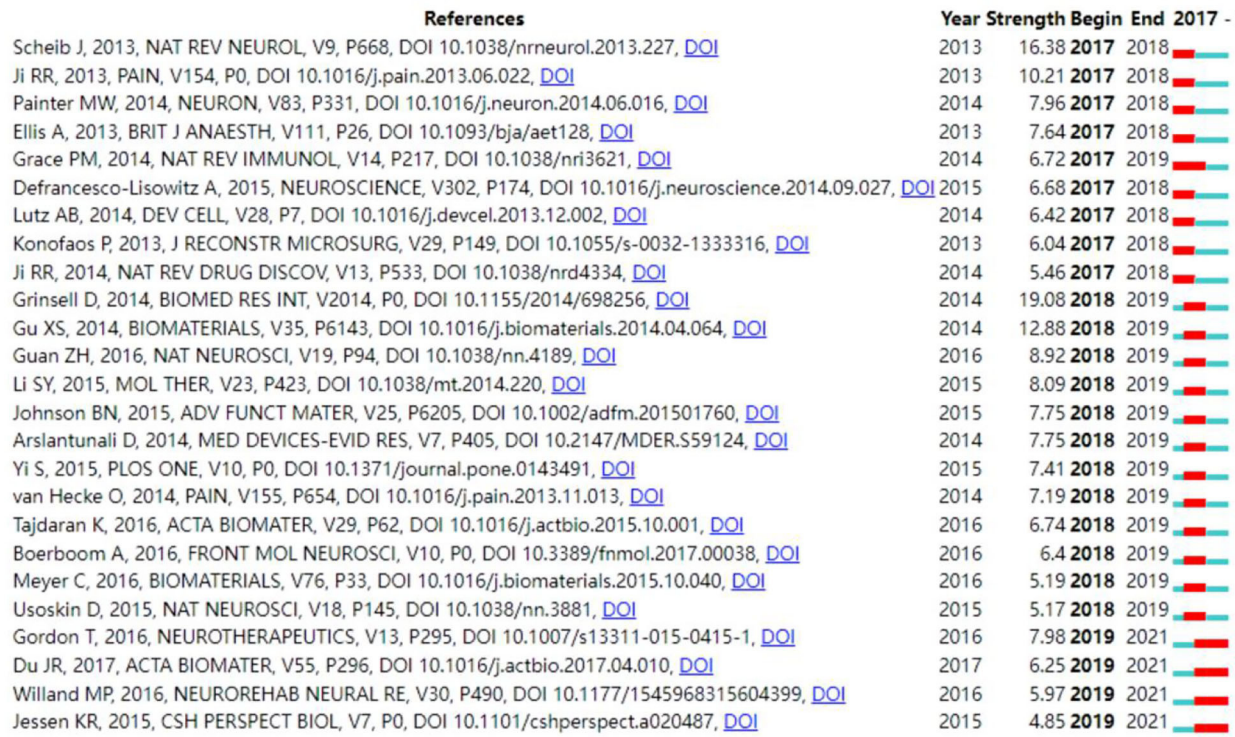

FIGURE 7 | TOP 25 References with the strongest citation bursts.

LIMITATION

First, only a single database, Web of Science Core Collection, was selected for analysis in this study, and other large medical databases such as PubMed, Scopus, and EMBASE were excluded and this study was limited to, language type, file type, and time span, which may lead to underrepresentation of potential research in this field and weaken its impact. In addition, some of the most recently published influential papers may not appear in our study due to the constant updating of databases. However, the amount of data collected in this study was large enough and adequate to reflect the current state of research in the field of PNI.

CONCLUSION

This is the first study to conduct a comprehensive bibliometric analysis of publications related to PNI from 2017 to 2021. Our findings indicated that the number of annual publications in the field of PNI remains high, with an average of more than 998 publications per year and an increasing number of citations yearly, up to 22,272 citations in 2021. Meanwhile, we found that hot topics in the field of PNI focused on DRG and SGCs for neuropathic pain relief and on combining tissue engineering techniques and controlling the repair Schwann cell phenotype to promote nerve regeneration, which are not only the focus of research now but will continue to be in the future. In summary, this bibliometric analysis will help researchers to quickly understand the knowledge structure and current hotspots in the field, provide new directions and ideas for research topics, and contribute to higher quality articles in the peripheral nerve field.

DATA AVAILABILITY STATEMENT

The original contributions presented in the study are included in the article/supplementary material, further inquiries can be directed to the corresponding authors.

AUTHOR CONTRIBUTIONS

These articles were retrieved and downloaded by SZ, MH, and JZ. Data were extracted from each article by SZ and SW. SZ, MH, JZ, and SW analyzed the data and wrote the manuscript. YW and FP were responsible for overseeing the project, revising drafts, and approving the final manuscript. All authors contributed significantly to the final article.

FUNDING

This research was supported by the National Natural Science Foundation of China (81973926), the Natural Science Foundation of Heilongjiang Province (LH2021H090), and the Heilongjiang University of Chinese Medicine Outstanding Innovative Talents Support Program research project (2018RCL10).

REFERENCES

1. Dong S, Feng S, Chen Y, Chen M, Yang Y, Zhang J, et al. Nerve suture combined with ADSCs injection under real-time and dynamic NIR-II fluorescence imaging in peripheral nerve regeneration in vivo. *Front Chem.* (2021) 9:676928. doi: 10.3389/fchem.2021.676928
2. Balog BM, Askew T, Lin DL, Kuang M, Hanzlicek B, Damaser MS. The pudendal nerve motor branch regenerates via a brain derived neurotrophic factor mediated mechanism. *Exp Neurol.* (2020) 334:113438. doi: 10.1016/j.expneurol.2020.113438
3. Al-Temimi MH, Chandrasekaran B, Phelan MJ, Pigazzi A, Mills SD, Stamos MJ, et al. Incidence, risk factors, and trends of motor peripheral nerve injury after colorectal surgery: analysis of the national surgical quality improvement program database. *Dis Colon Rectum.* (2017) 60:318–25. doi: 10.1097/DCR.0000000000000744
4. Babaei-Ghazani A, Eftekharsadat B, Samadirad B, Mamaghany V, Abdollahian S. Traumatic lower extremity and lumbosacral peripheral nerve injuries in adults: electrodiagnostic studies and patients symptoms. *J Forensic Leg Med.* (2017) 52:89–92. doi: 10.1016/j.jflm.2017.08.010
5. Zhang M, Li L, An H, Zhang P, Liu P. Repair of peripheral nerve injury using hydrogels based on self-Assembled peptides. *Gels.* (2021) 7:152. doi: 10.3390/gels7040152
6. Xu K, Liu X, Li X, Yin J, Wei P, Qian J, et al. Effect of electrical and electromechanical stimulation on pC12 cell proliferation and axon outgrowth. *Front Bioeng Biotechnol.* (2021) 9:757906. doi: 10.3389/fbioe.2021.757906
7. Chen SH, Zhang BY, Zhou B, Zhu CZ, Sun LQ, Feng YJ. Perineural invasion of cancer: a complex crosstalk between cells and molecules in the perineural niche. *Am J Cancer Res.* (2019) 9:1–21.
8. Zhong Y, Luo P, Gao J, Qi J, Li F, Yan L, et al. 3D reconstruction of peripheral nerves based on calcium chloride enhanced micro-CT images. *Anal Quant Cytopatho.* (2019) 41:159–68.
9. Badri O, Shahabi P, Abdolalizadeh J, Alipour M, Veladi H, Farhoudi M, et al. Combination therapy using evening primrose oil and electrical stimulation to improve nerve function following a crush injury of sciatic nerve in male rats. *Neural Regen Res.* (2017) 12:458. doi: 10.4103/1673-5374.202927
10. Balakrishnan A, Belfiore L, Chu T, Fleming T, Midha R, Biernaskie J, et al. Insights into the role and potential of schwann cells for peripheral nerve repair from studies of development and injury. *Front Mol Neurosci.* (2021) 13:608442. doi: 10.3389/fnmol.2020.608442
11. Chen S, Wu C, Lin S, Tseng W, Huang T, Yadav A, et al. Investigation of neuropathology after nerve release in chronic constriction injury of rat sciatic nerve. *Int J Mol Sci.* (2021) 22:4746. doi: 10.3390/ijms22094746
12. Hussain G, Wang J, Rasul A, Anwar H, Qasim M, Zafar S, et al. Current status of therapeutic approaches against peripheral nerve injuries: a Detailed story from injury to recovery. *Int J Biol Sci.* (2020) 16:116–34. doi: 10.7150/ijbs.35653
13. Bojanic C, To K, Zhang B, Mak C, Khan WS. Human umbilical cord derived mesenchymal stem cells in peripheral nerve regeneration. *World J Stem Cells.* (2020) 12:288–302. doi: 10.4252/wjsc.v12.i4.288
14. De la Rosa MB, Kozik EM, Sakaguchi DS. Adult stem cell-based strategies for peripheral nerve regeneration. (2018) 1119:41–71. doi: 10.1007/5584_2018_254
15. Maugeri G, D'Agata V, Trovato B, Roggio F, Castorina A, Vecchio M, et al. The role of exercise on peripheral nerve regeneration: from animal model to clinical application. *Heliyon.* (2021) 7:e8281. doi: 10.1016/j.heliyon.2021.e08281
16. Li M, Zhang PX, Zhang DY, PVDF. piezoelectric neural conduit incorporated pre-differentiated adipose derived stem cells may accelerate the repair of peripheral nerve injury. *Med Hypotheses.* (2018) 114:55–7. doi: 10.1016/j.mehy.2018.02.027
17. Yang K, Pei L, Wen K, Zhou S, Tao L. Investigating research hotspots and publication trends of spinal stenosis: a Bibliometric analysis during 2000–2018. *Front Med.* (2021) 8:556022. doi: 10.3389/fmed.2021.556022
18. Wu H, Cheng K, Guo Q, Yang W, Tong L, Wang Y, et al. Mapping knowledge structure and themes trends of osteoporosis in rheumatoid arthritis: a bibliometric analysis. *Front Med (Lausanne).* (2021) 8:787228. doi: 10.3389/fmed.2021.787228
19. Mattos FF, Perazzo MF, Vargas-Ferreira F, Martins-Junior PA, Paiva SM. Top 100 most-cited papers in core dental public health journals: bibliometric analysis. *Community Dent Oral Epidemiol.* (2021) 49:40–6. doi: 10.1111/cdoe.12572
20. Nakagawa S, Samarasinghe G, Haddaway NR, Westgate MJ. O Dea RE, Noble DWA, et al. Research weaving: visualizing the future of research synthesis trends. *Ecol Evol.* (2019) 34:224–38. doi: 10.1016/j.tree.2018.11.007
21. Koehler PJ. Publications on peripheral nerve injuries during world war i: a dramatic increase in knowledge. *Front Neurol Neurosci.* (2016) 38:43–55. doi: 10.1159/000442568
22. Chen CM. CiteSpace iI: detecting visualizing emerging trends transient patterns in scientific literature. *JASIST*. (2006) 57:359–77. doi: 10.1002/asi.20317
23. Synnestvedt MB, Chen C, Holmes JH. CiteSpace iI: visualization and knowledge discovery in bibliographic databases. *AMIA Annu Symp Proc.* (2005) 2005:724–8.
24. Hu S, Alimire A, Lai Y, Hu H, Chen Z, Li Y. Trends and Frontiers of research on cancer gene therapy from 2016 to 2020: a bibliometric analysis. *Front Med (Lausanne).* (2021) 8:740710. doi: 10.3389/fmed.2021.740710
25. van Eck NJ, Waltman L. Citation-based clustering of publications using citNetExplorer and vOSviewer. *Scientometrics.* (2017) 111:1053–70. doi: 10.1007/s11192-017-2300-7
26. van Eck NJ, Waltman L. Software survey: VOS viewer, a computer program for bibliometric mapping. *Scientometrics.* (2010) 84:523–38. doi: 10.1007/s11192-009-0146-3
27. Koltun V, Hafner D. The h-index is no longer an effective correlate of scientific reputation. *PLoS ONE.* (2021) 16:e253397. doi: 10.1371/journal.pone.0253397
28. Schreiber WE, Giustini DM. Measuring scientific impact with the h-index: a primer for pathologists. *Am J Clin Pathol.* (2019) 151:286–91. doi: 10.1093/ajcp/aqy137
29. Bertoli-Barsotti L, Lando T. The h-index as an almost-exact function of some basic statistics. *Scientometrics.* (2017) 113:1209–28. doi: 10.1007/s11192-017-2508-6
30. Lee J, Lee Y, Oh SM, Kahng B. Betweenness centrality of teams in social networks. *Chaos.* (2021) 31:61108. doi: 10.1063/5.0056683
31. Zaoli S, Mazzarisi P, Lillo F. Betweenness centrality for temporal multiplexes. *Sci Rep.* (2021) 11:4919. doi: 10.1038/s41598-021-84418-z
32. Li Y, Li W, Tan Y, Liu F, Cao Y, Lee KY. Hierarchical decomposition for betweenness centrality measure of complex networks. *Sci Rep.* (2017) 7:46491. doi: 10.1038/srep46491
33. Wagstaff LJ, Gomez-Sanchez JA, Fazal SV, Otto GW, Kilpatrick AM, Michael K, et al. Failures of nerve regeneration caused by aging or chronic denervation are rescued by restoring schwann cell c-Jun. *Elife.* (2021) 10:32. doi: 10.7554/eLife.62232
34. Jessen KR, Arthur-Farraj P. Repair schwann cell update: adaptive reprogramming, eMT, and stemness in regenerating nerves. *Glia.* (2019) 67:421–37. doi: 10.1002/glia.23532
35. Jessen KR, Mirsky R. Schwann cell precursors; multipotent glial cells in embryonic nerves. *Front Mol Neurosci.* (2019) 12:69. doi: 10.3389/fnmol.2019.00069
36. Jessen KR, Mirsky R. The success and failure of the schwann cell response to nerve injury. *Front Cell Neurosci.* (2019) 13:33. doi: 10.3389/fncel.2019.00033
37. Arthur-Farraj PJ, Latouche M, Wilton DK, Quintes S, Chabrol E, Banerjee A, et al. C-jun reprograms schwann cells of injured nerves to generate a repair cell essential for regeneration. *Neuron.* (2012) 75:633–47. doi: 10.1016/j.neuron.2012.06.021
38. Chen S, Zhu J, Zhang Y, Cai X, Yi S, Wang X. MiR-328a-3p stimulates endothelial cell migration and tubulogenesis. *Exp Ther Med.* (2021) 22:1104. doi: 10.3892/etm.2021.10538
39. Wang X, Chen Q, Yi S, Liu Q, Zhang R, Wang P, et al. The microRNAs let-7 and miR-9 down-regulate the axon-guidance genes ntn1 and dcc during peripheral nerve regeneration. *J Biol Chem.* (2019) 294:6695. doi: 10.1074/jbc.AAC119.008724
40. Chen Q, Liu Q, Zhang Y, Li S, Yi S. Leukemia inhibitory factor regulates schwann cell proliferation and migration and affects peripheral nerve regeneration. *Cell Death Dis.* (2021) 12:417. doi: 10.1038/s41419-021-03706-8
41. Wang Y, Zhang F, Zhang Y, Shan Q, Liu W, Zhang F, et al. Betacellulin regulates peripheral nerve regeneration by affecting

schwann cell migration and axon elongation. *Mol Med.* (2021) 27:27. doi: 10.1186/s10020-021-00292-5
42. Verkest C, Diochot S, Lingueglia E, Baron A. C-Jun n-terminal kinase post-translational regulation of pain-related acid-sensing ion channels 1b and 3. *J Neurosci.* (2021) 41:8673–85. doi: 10.1523/JNEUROSCI.0570-21.2021
43. Ramakrishna S, Jhaveri V, Konings SC, Nawalpuri B, Chakraborty S, Holst B, et al. APOE4 affects basal and nMDAR-mediated protein synthesis in neurons by perturbing calcium homeostasis. *J Neurosci.* (2021) 41:8686–709. doi: 10.1523/JNEUROSCI.0435-21.2021
44. Stevens SR, van der Heijden ME, Ogawa Y, Lin T, Sillitoe RV. Rasband MN. Ankyrin-R links kv33 to the spectrin cytoskeleton and is required for purkinje neuron survival. *J Neurosci.* (2022) 42:2–15. doi: 10.1523/JNEUROSCI.1132-21.2021
45. Wen W, Turrigiano GG. Developmental regulation of homeostatic plasticity in mouse primary visual cortex. *J Neurosci.* (2021) 41:9891–905. doi: 10.1523/JNEUROSCI.1200-21.2021
46. Marques DB, Ruggiero RN, Bueno-Junior LS, Rossignoli MT, Leite JP. Prediction of learned resistance or helplessness by hippocampal-prefrontal cortical network activity during stress. *J Neurosci.* (2022) 42:81–96. doi: 10.1523/JNEUROSCI.0128-21.2021
47. Gillis M, Vanthornhout J, Simon JZ, Francart T, Brodbeck C. Neural markers of speech comprehension: measuring EEG tracking of linguistic speech representations, controlling the speech acoustics. *J Neurosci.* (2021) 41:10316–29. doi: 10.1523/JNEUROSCI.0812-21.2021
48. Goncalves MP, Kieckbusch TG, Perna RF, Fujimoto JT, Morales S, Romanelli JP. Trends on enzyme immobilization researches based on bibliometric analysis. *Process Biochem.* (2019) 76:95–110. doi: 10.1016/j.procbio.2018.09.016
49. Zheng J, Zhou R, Meng B, Li F, Liu H, Wu X. Knowledge framework and emerging trends in intracranial aneurysm magnetic resonance angiography: a scientometric analysis from 2004 to (2020). *Quant Imaging Med Surg.* (2021) 11:1854–69. doi: 10.21037/qims-20-729
50. Okhovati M, Arshadi H. COVID-19 research progress: bibliometrics and visualization analysis. *Med J Islam Repub Iran.* (2021) 35:20. doi: 10.47176/mjiri.35.20
51. Bravo-Caparrós I, Ruiz-Cantero MC, Perazzoli G, Cronin S, Vela JM, Hamed MF, et al. Sigma-1 receptors control neuropathic pain macrophage infiltration into the dorsal root ganglion after peripheral nerve injury. *Faseb J.* (2020) 34:5951–66. doi: 10.1096/fj.201901921R
52. Yokoyama H, Hirai T, Nagata T, Enomoto M, Kaburagi H, Leiyo L, et al. DNA microarray analysis of differential gene expression in the dorsal root ganglia of four different neuropathic pain mouse models. *J Pain Res.* (2020) 13:3031–43. doi: 10.2147/JPR.S272952
53. Avraham O, Feng R, Ewan EE, Rustenhoven J, Zhao G, Cavalli V. Profiling sensory neuron microenvironment after peripheral and central axon injury reveals key pathways for neural repair. *Elife.* (2021) 1:10. doi: 10.7554/eLife.68457
54. Meyer K, Kaspar BK. Making sense of pain: are pluripotent stem cell-derived sensory neurons a new tool for studying pain mechanisms? *Mol Ther.* (2014) 22:1403–5. doi: 10.1038/mt.2014.123
55. Belzer V, Hanani M. Nitric oxide as a messenger between neurons and satellite glial cells in dorsal root ganglia. *Glia.* (2019) 67:1296–307. doi: 10.1002/glia.23603
56. Wang D, Lu J, Xu X, Yuan Y, Zhang Y, Xu J, et al. Satellite glial cells give rise to nociceptive sensory neurons. *Stem Cell Rev Rep.* (2021) 17:999–1013. doi: 10.1007/s12015-020-10102-w
57. Zhang RC, Du WQ, Zhang JY, Yu SX, Lu FZ, Ding HM, et al. Mesenchymal stem cell treatment for peripheral nerve injury: a narrative review. *Neural Regen Res.* (2021) 16:2170–6. doi: 10.4103/1673-5374.310941
58. Li KL, Chen YM, Wang XQ, Hu HY. Bibliometric analysis of studies on neuropathic pain associated with depression or anxiety published from 2000 to (2020). *Front Hum Neurosci.* (2021) 15:729587. doi: 10.3389/fnhum.2021.729587
59. Scheib J, Höke A. Advances in peripheral nerve regeneration. *Nat Rev Neurol.* (2013) 9:668–76. doi: 10.1038/nrneurol.2013.227
60. Du J, Liu J, Yao S, Mao H, Peng J, Sun X, et al. Prompt peripheral nerve regeneration induced by a hierarchically aligned fibrin nanofiber hydrogel. *Acta Biomater.* (2017) 55:296–309. doi: 10.1016/j.actbio.2017.04.010
61. Gordon T. Electrical stimulation to enhance axon regeneration after peripheral nerve injuries in animal models and humans. *Neurotherapeutics.* (2016) 13:295–310. doi: 10.1007/s13311-015-0415-1
62. Willand MP, Nguyen M, Borschel GH, Gordon T. Electrical stimulation to promote peripheral nerve regeneration. *Neurorehab Neural Re.* (2015) 30:490–6. doi: 10.1177/1545968315604399
63. Jessen KR, Mirsky R, Lloyd AC. Schwann cells: development and role in nerve repair. *Cold Spring Harb Perspect Biol.* (2015) 7:a20487. doi: 10.1101/cshperspect.a020487
64. Jessen KR, Mirsky R. The repair schwann cell and its function in regenerating nerves. *J Physiol.* (2016) 594:3521–31. doi: 10.1113/JP270874
65. Jeanette H, Marziali LN, Bhatia U, Hellman A, Herron J, Kopec AM, et al. YAP and TAZ regulate schwann cell proliferation and differentiation during peripheral nerve regeneration. *Glia.* (2021) 69:1061–74. doi: 10.1002/glia.23949
66. Acheta J, Stephens S, Belin S, Poitelon Y. Therapeutic low-Intensity ultrasound for peripheral nerve regeneration - a schwann cell perspective. *Front Cell Neurosci.* (2021) 15:812588. doi: 10.3389/fncel.2021.812588
67. Gomez-Sanchez JA, Patel N, Martirena F, Fazal SV, Mutschler C, Cabedo H. Emerging role of hDACs in regeneration and ageing in the peripheral nervous system: repair schwann cells as pivotal targets. *Int J Mol Sci.* (2022) 23:2996. doi: 10.3390/ijms23062996
68. Liu T, Wang Y, Lu L, Liu Y. SPIONs mediated magnetic actuation promotes nerve regeneration by inducing and maintaining repair-supportive phenotypes in schwann cells. *J Nanobiotechnology.* (2022) 20:159. doi: 10.1186/s12951-022-01337-5

Conflict of Interest: The authors declare that the research was conducted in the absence of any commercial or financial relationships that could be construed as a potential conflict of interest.

Publisher's Note: All claims expressed in this article are solely those of the authors and do not necessarily represent those of their affiliated organizations, or those of the publisher, the editors and the reviewers. Any product that may be evaluated in this article, or claim that may be made by its manufacturer, is not guaranteed or endorsed by the publisher.

frontiers | Frontiers in Neurology

OPINION
published: 11 July 2022
doi: 10.3389/fneur.2022.941151

Opinion: The Potential Role of Amyloid Beta Peptides as Biomarkers of Subconcussion and Concussion

Angela M. Boutté[1]*, *Bharani Thangavelu*[2] and *John Anagli*[3]

[1] *Aries Biotechnologies, Oakland, CA, United States,* [2] *Independent Researcher, Silver Spring, MD, United States,* [3] *NeuroTheranostics, Inc., Detroit, MI, United States*

Keywords: concussion, subconcussion, mild traumatic brain injury, amyloid beta, biomarker, blast

INTRODUCTION

Concussion, often referred to as mild traumatic brain injury (mTBI), is a bump or blow to the head that causes damage to the brain. An invisible wound is often not observed (https://www.cdc.gov/headsup/basics/concussion_whatis.html) (1). Concussed patients may experience loss of consciousness, dizziness, headaches, blurred vision or tired eyes (2, 3), ringing in the ears, bad taste in the mouth, fatigue or lethargy, a change in sleep patterns, behavioral or mood changes, trouble with memory, and slowed reaction time (4, 5). These symptoms may occur acutely or persist for years.

Subconcussion or concussion may occur as the result of high impact sports, like soccer (6), football (7), rugby (8), and gymnastics (9). This injury also occurs due to falls, automobile accidents, and domestic abuse (10, 11), which is vastly understudied. Another source of subconcussion is due to low level overpressure (LLOP) exposure, which occurs when the pressure in air exceeds that of normal atmospheric levels. Exposure is common among specially trained military or law enforcement personnel due to explosives or weapons use within controlled environments. LLOP exposure may also occur within civilian populations who are victims of terrorist bombings (12).

Symptoms reported after concussion or sub-concussive events, e.g., LLOP exposure or a light head hit, are often subjective or under-reported. When symptoms are reported, they often dissipate and are considered a metric of recovery. Subconcussion, in particular, leads to few, low grade, or fleeting symptoms that do not meet the threshold for diagnosis during clinical examination [https://concussionfoundation.org/cte-resources/subconcussive-impacts]. Long-term effects of subconcussion (e.g., per LLOP exposure history and service records) include increased risk of a definitive TBI diagnosis. Subconcussive event history and diagnosed concussion are associated with higher likelihood of neurodegenerative diseases, such as chronic traumatic encephalopathy (CTE) (13), Alzheimer's Disease (AD) (14), and Parkinson's Disease (PD) (15, 16).

Recent Findings Infer Aβ Has Utility as a Biomarker of Subconcussion and Concussion

Injured persons are frequently characterized as recovered and healthy to resume life activities, rendering identification of long-term effects challenging. Objective classification of sub-concussion before clinical manifestation or neurodegenerative disease diagnosis may offer a pre-text for monitoring. To address this gap, several blood-based protein biomarkers have been evaluated in the context of diagnosed concussion then successfully applied to subconcussive states (17).

Among the milieu of peripheral biomarkers, the most prolifically studied are glial fibrillary acidic protein (GFAP)—an abundant intermediate filament protein enriched in astrocytes; and ubiquitin carboxy hydrolase (UCH)-L1–a cell body enzyme found in neurons. GFAP and UCH-L1 were the first blood-based biomarkers to be approved by the FDA for monitoring TBI (18).

OPEN ACCESS

Edited by:
Mårten Risling,
Karolinska Institutet (KI), Sweden

Reviewed by:
Yushan Wang,
Defence Research and Development Canada (DRDC), Canada

***Correspondence:**
Angela M. Boutté
ariesbiotech.consult@gmail.com

Specialty section:
This article was submitted to Neurotrauma, a section of the journal Frontiers in Neurology

Received: *11 May 2022*
Accepted: *10 June 2022*
Published: *11 July 2022*

Citation:
Boutté AM, Thangavelu B and Anagli J (2022) Opinion: The Potential Role of Amyloid Beta Peptides as Biomarkers of Subconcussion and Concussion. Front. Neurol. 13:941151. doi: 10.3389/fneur.2022.941151

Increased levels of GFAP is well-documented among concussed patients (19). However, it offers poor specificity for detection of subconcussive injury, for which damage to the brain is not evident *via* high resolution medical imaging (20).

Amyloid beta peptides (Abeta)−40 and −42 peptides are toxic cleavage products of amyloid precursor protein (APP) enriched within neuronal cell populations. These toxic monomers are crucial to pathogenesis of chronic neurodegenerative diseases (21) and a pathological hallmark of the Alzheimer's disease (AD)-afflicted brain (22). Similar to neurodegenerative disease, severe TBI leads to APP loss with generation of Abeta. APP processing occurs through two major pathways. Non-amyloidogenic processing occurs *via* alpha (α)-secretase and the ADAM family of proteases (23). Whereas, the amyloidogenic pathway relies upon protease activity lent by β-secretase (BACE1) and the gamma (γ)-secretase complex (24–26). Recent studies have indicated cathepsin B beta-secretase activity also leads to APP loss with concomitant Abeta peptide generation in the brain, followed by efflux into cerebrospinal fluid (CSF) and blood (27, 28).

Abeta production and efflux has been reported to occur after subconcussion and concussion. A ProQuest search of publicly available data using the key words, "amyloid beta," "blood," "biomarker" and "concussion," resulted in 1,171 publications, 236 of which were peer-reviewed, from 2017–2022. Peptide quantitation in peripheral blood has become an increasingly popular research tool as an outcome measure of subconcussion, as well as diagnosed concussion.

Hours or days after concussion, Abeta peptides accumulate in increase exorbitantly in peripheral blood. For example, quantitation of Abeta-42 within neuronal exosomes isolated from plasma revealed that was this biomarker elevated among patients who had a history of TBI with impaired cognition (29). This effect was also observed among student athletes who were diagnosed with an mTBI, or concussion. Further, exosomal Abeta-42 nearly doubled compared to controls measured within acute (7 days) and chronic (3 months) time frames (30). Military personnel who suffered an mTBI within <2 years prior to blood collection, showed that Abeta was increased by nearly two-fold within purified exosomes, without association with chronic symptoms (30). In patients or among persons exposed to a subconcussive event, e.g., LLOP, Abeta levels persist in blood for months after the injury incident (31).

High serum Abeta−40 and −42 concentrates were recently associated with subconcussion as demonstrated within several successive reports conducted with military personnel exposed to LLOP. Abeta−40 and −42 were both increased within hours, after daily LLOP exposure from high caliber weapons usage (32). Abeta peptide levels were consistently elevated after LLOP exposure among personnel who reported symptomology either acutely (33) or chronically (34). Serum Abeta levels were nearly 50 times higher among study participants compared to controls who did not endure LLOP exposure in their history. Notably, reports of long-term dizziness, tinnitus (ear-ringing) and memory problems were common among the subconcussion cohort who had the highest Abeta levels in blood. These observations were unambiguous, but did not meet the threshold for clinical diagnosis.

Abeta is associated with concussion, subconcussion and presence of symptoms. However, it is not yet known if discrete quantitative levels, or relative changes over time, are directly proportional to symptom severity or act as prognostic indicators of long-term health outcomes. Large scale, longitudinal studies would address this knowledge gap and offer greater clinical utility.

DISCUSSION

Abeta measurements as a consequence of subconcussion and diagnosed concussion are evident. However, this feature is not without a few caveats. First, the sample size in most observational studies is fairly small, and the patient and human subject volunteers populations studied are largely composed of Caucasian males. Relevance of Abeta as a biomarker for subconcussion and concussion would be vastly strengthened by analysis of blood from women and a broader mixture of persons from various ethnic or cultural backgrounds. This approach would potentially provide a means to justify clinical imaging and medical monitoring for those who may suffer an accidental fall, or those who may be victims of short and long-term physical abuse. Additionally, monitoring amyloid beta among military personnel or law enforcement may offer a means to modify training guidelines that allow improved health among veterans later in life.

Second, recent studies utilized digital enzyme-linked immunosorbent assays (ELISA) provided by the SiMoA platform as a singular digital technology, which offers broad dynamic range and low limits of detection and quantitation for blood biomarkers. Reported differences in blood Abeta peptide concentrations have been generally reproducible relative to controls. Yet, Abeta concentrations may differ in plasma, compared to serum as well as exosomes (35). Cross-validation has yet to be conducted using these three biological sources of Abeta within the same cohorts. Additionally, validation in comparison other platforms, such as mass spectrometry (36), prior to adaptation for clinical use is needed.

Lastly, L1-CAM is commonly used to enrich exosomes of neuronal origin, since it is enriched within the cerebral cortex and cerebellum. However, this receptor is also detectable within the kidney and epidermis (https://www.proteinatlas.org/ENSG00000198910-L1CAM/tissue). Subconcussion and concussion affect multiple organs. Thus, greater specificity for neuronal exosome isolation and exclusion of damage to other organs, such as the kidney or skin, may offer improved utility of exosomal Abeta as it relates to the subconcussed or concussed brain.

CONCLUSIONS

An uptick in Abeta peptide concentrations, from plasma, serum or exosomes after subconcussion or clinically diagnosed concussion has generally been consistent across studies. Data collectively infer that Abeta−40 and −42 may be more sensitive than that of self-reported symptoms, which are underreported or may dissipate over time.

AUTHOR CONTRIBUTIONS

All authors listed have made a substantial, direct, and intellectual contribution to the work and approved it for publication.

ACKNOWLEDGMENTS

The authors thank patients, study volunteers, and military service members for their participation in the referenced studies.

REFERENCES

1. Sussman ES, Pendharkar AV, Ho AL, Ghajar J. Mild traumatic brain injury and concussion: terminology and classification. *Handb Clin Neurol.* (2018) 158:21–24. doi: 10.1016/B978-0-444-63954-7.00003-3
2. Ciuffreda KJ, Kapoor N, Rutner D, Suchoff IB, Han ME, Craig S. Occurrence of oculomotor dysfunctions in acquired brain injury: a retrospective analysis. *Optometry.* (2007) 78:155–161. doi: 10.1016/j.optm.2007.05.011
3. Goodrich GL, Flyg HM, Kirby JE, Chang CY, Martinsen GL. Mechanisms of TBI and visual consequences in military and veteran populations. *Optom Vis Sci.* (2013) 90:105–112. doi: 10.1097/OPX.0b013e31827f15a1
4. Lathan C, Spira JL, Bleiberg J, Vice J, Tsao JW. Defense Automated Neurobehavioral Assessment (DANA)-psychometric properties of a new field-deployable neurocognitive assessment tool. *Mil Med.* (2013) 178:365–71. doi: 10.7205/MILMED-D-12-00438
5. Carr W, Polejaeva E, Grome A, Crandall B, LaValle C, Eonta SE. Relation of repeated low-level blast exposure with symptomology similar to concussion. *J Head Trauma Rehabil.* (2015) 30:47–55. doi: 10.1097/HTR.0000000000000064
6. Levy ML, Kasasbeh AS, Baird LC, Amene C, Skeen J, Marshall L. Concussions in soccer: a current understanding. *World Neurosurg.* (2012) 78:535–44. doi: 10.1016/j.wneu.2020.09.032
7. Abraham KJ, Casey J, Subotic A, Tarzi C, Zhu A, Cusimano MD. Medical assessment of potential concussion in elite football: video analysis of the 2016 UEFA European championship. *BMJ Open.* (2019) 9:e024607. doi: 10.1136/bmjopen-2018-024607
8. Underhill LA, Barbarita C, Collis S, Tucker R, Lechner BE. Sport Concussion Assessment Tool: baseline and clinical reference limits for concussion diagnosis and management in elite Rugby Union. *J Sci Med Sport.* (2021) 24:122–8. doi: 10.1016/j.jsams.2017.11.006
9. Veliz P, Eckner JT, Zdroik J, Schulenberg JE. Lifetime Prevalence of Self-Reported Concussion Among Adolescents Involved in Competitive Sports: a National US Study. *J Adolesc Health.* (2019) 64:272–5. doi: 10.1016/j.jadohealth.2011.11.023
10. Zieman G, Bridwell A, Cárdenas JF. Traumatic Brain Injury in Domestic Violence Victims: a Retrospective Study at the Barrow Neurological Institute. *J Neurotrauma.* (2017) 34:876–80. doi: 10.1089/neu.2016.4579
11. Rowe RK, Murphy SM, Handmaker H, Lifshitz J. Population-level epidemiology of concussion concurrent with domestic violence in Arizona. *USA. J Neurotrauma.* (2021) 38:2301–10. doi: 10.1089/neu.2021.0022
12. Cooper GJ, Maynard RL, Cross NL, Hill JF. Casualties from terrorist bombings. *J Trauma.* (1983) 23:955–67. doi: 10.1097/00005373-198311000-00001
13. Danielsen T, Hauch C, Kelly L, White CL. Chronic Traumatic Encephalopathy (CTE)-Type neuropathology in a young victim of domestic abuse. *J Neuropathol Exp Neurol.* (2021) 80:624–27. doi: 10.1093/jnen/nlab015
14. Dams-O'Connor K, Guetta G, Hahn-Ketter AE, Fedor A. Traumatic brain injury as a risk factor for Alzheimer's disease: current knowledge and future directions. *Neurodegener Dis Manag.* (2016) 6:417–29. doi: 10.2217/nmt-2016-0017
15. Gardner RC, Byers AL, Barnes DE, Li Y, Boscardin J, Yaffe K. Mild TBI and risk of Parkinson disease: a chronic effects of neurotrauma consortium study. *Neurology.* (2018) 90:e1771–e1779. doi: 10.1212/WNL.0000000000005522
16. Kornblith E, Peltz CB, Xia F, Plassman B, Novakovic-Apopain T, Yaffe K. Sex race, and risk of dementia diagnosis after traumatic brain injury among older veterans. *Neurology.* (2020) 95:e1768–75. doi: 10.1212/WNL.0000000000010617
17. Hier DB, Obafemi-Ajayi T, Thimgan MS, Olbricht GR, Azizi S, Allen B. Blood biomarkers for mild traumatic brain injury: a selective review of unresolved issues. *Biomark Res.* (2021) 9:70. doi: 10.1186/s40364-021-00325-5
18. Bazarian JJ, Biberthaler P, Welch RD, Lewis LM, Barzo P, Bogner-Flatz V, et al. Serum GFAP and UCH-L1 for prediction of absence of intracranial injuries on head CT (ALERT-TBI): a multicentre observational study. *Lancet Neurol.* (2018) 17:782–89. doi: 10.1016/S1474-4422(18)30231-X
19. Yue JK, Yuh EL, Korley FK, Winkler EA, Sun X, Puffer RC, et al. Association between plasma GFAP concentrations and MRI abnormalities in patients with CT-negative traumatic brain injury in the TRACK-TBI cohort: a prospective multicentre study. *Lancet Neurol.* (2019) 18:953–61. doi: 10.1016/S1474-4422(19)30282-0
20. Posti JP, Hossain I, Takala RS, Liedes H, Newcombe V, Outtrim J. Glial fibrillary acidic protein and ubiquitin C-terminal hydrolase-L1 are not specific biomarkers for mild CT-negative traumatic brain injury. *J Neurotrauma.* (2017) 34:7. doi: 10.1089./neu.2016.4442
21. Schonrock N, Matamales M, Ittner LM, Götz J. MicroRNA networks surrounding APP and amyloid-β metabolism–implications for Alzheimer's disease. *Exp Neurol.* (2012) 235:447–54. doi: 10.1016/j.expneurol.2014.03.013
22. He Z, Guo JJ, McBride S, Narasimhan H, Kim L, Changolkar B, et al. Amyloid-β plaques enhance Alzheimer's brain tau-seeded pathologies by facilitating neuritic plaque tau aggregation. *Nat Med.* (2018) 24:29–38. doi: 10.1038/nm.4443
23. Parvathy S, Hussain I, Karran EH, Turner AJ, Hooper NM. Cleavage of Alzheimer's amyloid precursor protein by alpha-secretase occurs at the surface of neuronal cells. *Biochemistry.* (1999) 38:9728–34. doi: 10.1021/bi9906827
24. Vassar R, Bennett BD, Babu-Khan S, Kahn S, Mendiaz EA, Denis P, et al. Beta-secretase cleavage of Alzheimer's amyloid precursor protein by the transmembrane aspartic protease BACE. *Science.* (1999) 286:735–41. doi: 10.1126/science.286.5440.735
25. Hook V, Schechter I, Demuth HU, Hook G. Alternative pathways for production of beta-amyloid peptides of Alzheimer's disease. *Biol Chem.* (2008) 389:993–1006. doi: 10.1515/BC.2008.124
26. Chow VW, Mattson MP, Wong PC, Gleichmann M. An overview of APP processing enzymes and products. *Neuromolecular Med.* (2010) 12:1–12. doi: 10.1007/s12017-009-8104-z
27. Cartagena CM, Mountney A, Hwang H, Swiercz A, Rammelkamp Z, Boutte AM, et al. Subacute Changes in Cleavage Processing of Amyloid Precursor Protein and Tau following Penetrating Traumatic Brain Injury. *PLoS One.* (2016) 11:e0158576. doi: 10.1371/journal.pone.0158576
28. Thangavelu B, Wilfred BS, Johnson D, Gilsdorf JS, Shear DA, Boutté AM. Penetrating Ballistic-Like Brain Injury Leads to MicroRNA Dysregulation, BACE1 Upregulation, and Amyloid Precursor Protein Loss in Lesioned Rat Brain Tissues. *Front Neurosci.* (2020)b 14:915. doi: 10.3389/fnins.2020.00915
29. Goetzl EJ, Peltz CB, Mustapic M, Kapogiannis D, Yaffe K. Neuron-Derived Plasma Exosome Proteins after Remote Traumatic Brain Injury. *J Neurotrauma.* (2020) 37, 382–388. doi: 10.1089/neu.2019.6711
30. Goetzl EJ, Elahi FM, Mustapic M, Kapogiannis D, Pryhoda M, Gilmore A. Altered levels of plasma neuron-derived exosomes and their cargo proteins characterize acute and chronic mild traumatic brain injury. *FASEB J.* (2019) 33:5082–88. doi: 10.1096/fj.201802319R
31. Bogoslovsky T, Wilson D, Chen Y, Hanlon D, Gill J, Jeromin A. Increases of plasma levels of glial fibrillary acidic protein, tau, and amyloid β up to 90 days after traumatic brain injury. *J Neurotrauma.* (2017) 34:66–73. doi: 10.1089/neu.2015.4333
32. Thangavelu B, Boutté AM. Overpressure Exposure From.50-Caliber Rifle Training Is Associated With Increased Amyloid Beta Peptides in Serum. *Front Neurol.* (2020)a 11:620. doi: 10.3389/fneur.2020.00620

33. Boutté AM, Thangavelu B, LaValle CR, Nemes J, Gilsdorf J, Shear DA. Brain-related proteins as serum biomarkers of acute, subconcussive blast overpressure exposure: a cohort study of military personnel. *PLoS one.* (2019) 14:e0221036. doi: 10.1371/journal.pone.0221036
34. Boutté AM, Thangavelu B, Nemes J, LaValle CR, Egnoto M, Carr W, et al. Neurotrauma Biomarker Levels and Adverse Symptoms Among Military and Law Enforcement Personnel Exposed to Occupational Overpressure Without Diagnosed Traumatic Brain Injury. *JAMA Netw Open.* (2021) 4:e216445. doi: 10.1001/jamanetworkopen.2021.6445
35. O'Connell GC, Alder ML, Webel AR, Moore SM. Neuro biomarker levels measured with high-sensitivity digital ELISA differ between serum and plasma. *Bioanalysis.* (2019) 11:2087–94. doi: 10.4155/bio-2019-0213
36. Kirmess KM, Meyer MR, Holubasch MS, Knapik SS, Hu Y, Jackson EN, et al. The PrecivityAD® test: Accurate and reliable LC-MS/MS assays for quantifying plasma amyloid beta 40 and 42 and apolipoprotein E proteotype for the assessment of brain amyloidosis. *Clin Chim Acta.* (2021) 519:267–75. doi: 10.1016/j.cca.2021.05.011

Conflict of Interest: AB is the founder and owner of Aries Biotechnologies, Oakland, CA and an employee of renegade.bio, Berkeley, CA. BT is an employee of Novavax Inc., Gaithersburg, MD. JA is the founder and owner of Neurotheranostics, Inc., Detroit, MI. Neither renegade.bio or Novavax, Inc. had a role in this work.

frontiers | Frontiers in Neurology

TYPE Original Research
PUBLISHED 26 July 2022
DOI 10.3389/fneur.2022.898813

OPEN ACCESS

EDITED BY
Mårten Risling,
Karolinska Institutet (KI), Sweden

REVIEWED BY
Shyam Gajavelli,
University of Florida, United States
Fredrik Clausen,
Uppsala University, Sweden
Robson Luis Amorim,
University of São Paulo, Brazil
Huaqiu Zhang,
Huazhong University of Science and Technology, China

*CORRESPONDENCE
Zengguang Wang
wzgforrest@163.com
Weidong Yang
yangweidongshine@sina.com

†These authors have contributed equally to this work and share first authorship

SPECIALTY SECTION
This article was submitted to Neurotrauma, a section of the journal Frontiers in Neurology

RECEIVED 17 March 2022
ACCEPTED 30 June 2022
PUBLISHED 26 July 2022

CITATION
Liu Y, Liu X, Chen Z, Wang Y, Li J, Gong J, He A, Zhao M, Yang C, Yang W and Wang Z (2022) Evaluation of decompressive craniectomy in mice after severe traumatic brain injury. *Front. Neurol.* 13:898813. doi: 10.3389/fneur.2022.898813

Evaluation of decompressive craniectomy in mice after severe traumatic brain injury

Yuheng Liu[1,2†], Xuanhui Liu[1,2†], Zhijuan Chen[1†], Yuanzhi Wang[2,3], Jing Li[1,2], Junjie Gong[1,2], Anqi He[1,2], Mingyu Zhao[1,2], Chen Yang[1,2], Weidong Yang[1*] and Zengguang Wang[1,2*]

[1]Department of Neurosurgery, Tianjin Medical University General Hospital, Tianjin, China, [2]Tianjin Neurological Institute, Key Laboratory of Post-Neuroinjury Neuro-repair and Regeneration in Central Nervous System, Ministry of Education and Tianjin, Tianjin, China, [3]Department of Pharmacy, Tianjin Medical University General Hospital, Tianjin, China

Decompressive craniectomy (DC) is of great significance for relieving acute intracranial hypertension and saving lives after traumatic brain injury (TBI). In this study, a severe TBI mouse model was created using controlled cortical impact (CCI), and a surgical model of DC was established. Furthermore, a series of neurological function assessments were performed to better understand the pathophysiological changes after DC. In this study, mice were randomly allocated into three groups, namely, CCI group, CCI+DC group, and Sham group. The mice in the CCI and CCI+DC groups received CCI after opening a bone window, and after brain injury, immediately returned the bone window to simulate skull condition after a TBI. The CCI+DC group underwent DC and contused tissue removal 6 h after CCI. The mice in the CCI group underwent the same anesthesia process; however, no further treatment of the bone window and trauma was performed. The mice in the Sham group underwent anesthesia and the process of opening the skin and bone window, but not in the CCI group. Changes in Modified Neurological Severity Score, rotarod performance, Morris water maze, intracranial pressure (ICP), cerebral blood flow (CBF), brain edema, blood–brain barrier (BBB), inflammatory factors, neuronal apoptosis, and glial cell expression were evaluated. Compared with the CCI group, the CCI+DC group had significantly lower ICP, superior neurological and motor function at 24 h after injury, and less severe BBB damage after injury. Most inflammatory cytokine expressions and the number of apoptotic cells in the brain tissue of mice in the CCI+DC group were lower than in the CCI group at 3 days after injury, with markedly reduced astrocyte and microglia expression. However, the degree of brain edema in the CCI+DC group was greater than in the CCI group, and neurological and motor functions, as well as spatial cognitive and learning ability, were significantly poorer at 14 days after injury.

KEYWORDS

traumatic brain injury, decompressive craniectomy, controlled cortical impact (CCI), animal model, severe traumatic brain injury (sTBI)

Introduction

Traumatic brain injury (TBI) is an important cause of morbidity and mortality worldwide (1–3). It accounts for an estimated 37% of all injury-related deaths in the EU and 30.5% in the USA, and the mortality is estimated to be ∼13 cases per 100,000 people in China (4, 5). The complex pathophysiological changes that occur after TBI, which result from primary and secondary injuries, can lead to increased intracranial pressure (ICP), brain contusion, brain edema, and blood–brain barrier (BBB) disruption (6–8). More importantly, TBI can induce temporary or permanent motor, sensory, cognitive, and emotional impairments that lead to poor prognosis (9, 10).

Decompressive craniectomy (DC) is an important treatment for patients with uncontrollable brain swelling, and is widely accepted for ICP reduction (11–14). Although DC is currently recognized as an effective means of reducing intracranial hypertension, whether it is beneficial for the treatment of moderate and severe TBI is still controversial, and there is no consensus on DC after moderate and severe TBI (15). Proponents believe that removal of a bone flap and the contused brain tissue can quickly relieve intracranial hypertension and reduce inflammation. However, those who prefer conservative treatment believe that, except in some emergency situations, surgery itself is traumatic to patients, excision of contused tissue will itself destroy surrounding brain tissues and aggravate neurological deficits, and overly aggressive surgical treatment is not conducive to good long-term prognosis.

Due to the paucity of clinical data, evaluations of DC after severe TBI are mostly retrospective. Moderate and severe TBI are emergencies; the injury mechanism, location, and degree of the injury vary greatly, and the surgical techniques of chief surgeons differ. All these factors substantially limit the evaluation of the effect of DC after TBI. Compared with clinical data, animal model evaluation has more consistency and broader evaluation indicators. However, despite its relevance, this issue has rarely been evaluated in experimental animals (16, 17).

This study established a stable animal model of DC in mice and compared the CCI+DC mice with the conservative CCI mice with regard to outcomes such as ICP, neurological function, inflammation, brain edema, and BBB function, providing references for clinical decision-making (Figure 1).

Methods and materials

Animals

Male C57BL/6 mice (aged 7–9 weeks, 22–24 g, Vital River Laboratory Animal Technology Co., Ltd., Beijing, China) were housed in the animal facility of Tianjin Medical University General Hospital under a 12-h light/dark cycle in a temperature-controlled room (20 ± 2°C) and were provided food and water *ad libitum*. All experimental procedures involving animals were approved by the Animal Ethics Committee of Tianjin Medical University (Tianjin, China).

TBI model

The TBI mouse model was induced using a controlled cortical impact (CCI) device (eCCI-6.3 device, Custom Design & Fabrication, USA) as follows (Figure 2A). The mouse was anesthetized with a mixture of ketamine (100 mg/kg) and xylazine (10 mg/kg) by an intraperitoneal injection. After the head was shaved and disinfected, a 10-mm median incision was made on the scalp, and the periosteum was removed. The mouse was held on a fixed frame, and a 4 mm round bone window was cut in the center of the parietal bone (Figure 2D). During the process, we aimed to maintain bone flap integrity and avoid damage to the dura mater and brain parenchyma. We adjusted the position of the impactor tip to fit only the exposed dura mater for a single impact with these specific parameters (18), namely, flat impactor tip diameter: 3.0 mm, depth: 2.0 mm, speed: 5 m/s, and dwell time: 200 ms.

The mouse was then quickly removed from the fixator. As previously described by Zweckberger et al., we closed the bone window immediately after CCI to simulate the clinical response of elevated ICP under a nearly closed bone window after trauma (19, 20). If the bone flap is not replaced, the open craniotomy defect will provide a release mechanism for the contused-swollen brain preventing the reproduction of a precise model (20). In our study, the complete bone flap was immediately placed back into the bone window before the lesion was completely swollen and edematous. The bone window was fixed with Type I glass ionomer cement (Shanghai Medical Instruments Co., Ltd., China) to completely cover the bone window and the surrounding 1 mm area (Figure 2B). After the cement was completely dried and solidified, the surgical field was disinfected, and the scalp incision was closed with 4-0 sutures. The animal was placed in a thermostatic cage to maintain body temperature for 45 min, and then placed in an ordinary cage for separate feeding. All mice were carefully observed for ≥4 h after surgery and then daily.

Experimental grouping and DC

Each mouse was randomly allocated to one of the three groups, namely, CCI+DC group, CCI group, and Sham group. Of these, the CCI+DC and CCI groups received CCI. The Sham group did not receive CCI; however, the other operations, including anesthesia, incision, bone window opening, and closure, were the same as in the CCI group. DC was performed in the CCI+DC group 6 h after CCI. After the mice were re-anesthetized and disinfected, the scalp and bone

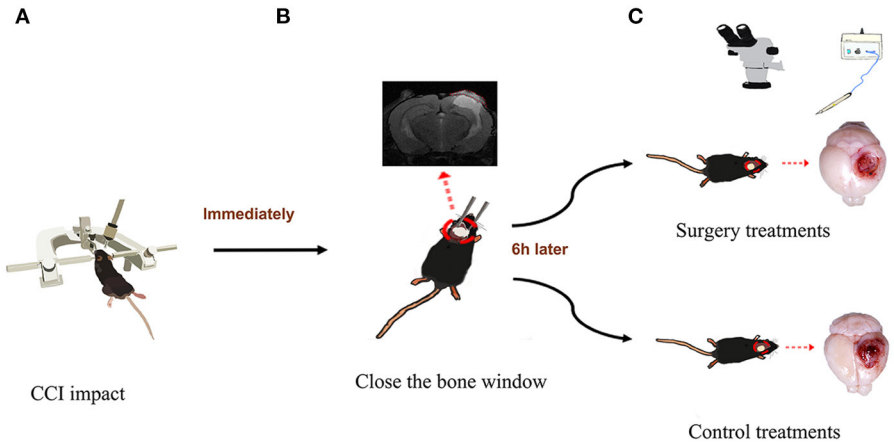

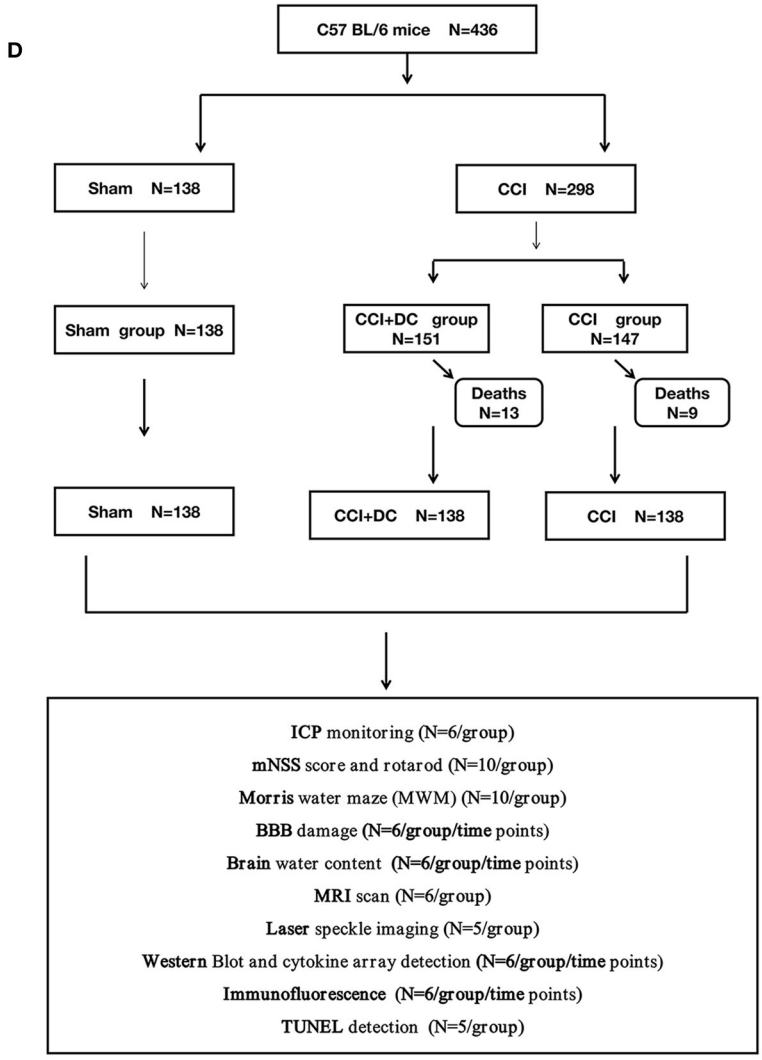

FIGURE 1
Experimental flow chart. **(A)** Mice in the CCI+DC group and CCI group were hit by CCI. **(B)** After the attack, the bone window was closed immediately. **(C)** 6 h after the attack, the mice in the CCI+DC group underwent bone window removal and contused tissue removal, the CCI group received the same anesthesia and skin incision. **(D)** Flow chart showing the experimental protocol with the number of animals used, died and included in the study.

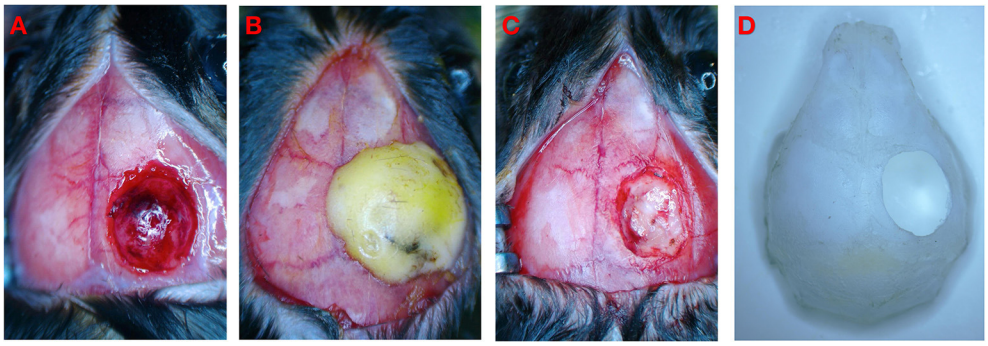

FIGURE 2
Schematic diagram of experimental operation. **(A)** Brain injury after CCI. **(B)** Close bone window after CCI. **(C)** CCI+DC group underwent bone window removal and contused tissue removal. **(D)** Schematic diagram of bone window.

window were opened and the wound focus and surrounding area were disinfected. Under the microscope, the dura mater was broken by micro-tweezers to expose the swollen brain tissue, and small tampons prepared in advance were used to gently staunch. Lesions with obvious contusion and necrosis were removed using unipolar electrocoagulation (Yangzhou Xiaguang Medical Instrument Co., Ltd China). During such an intervention, movements should be slow and careful, and attention should be paid to hemostasis. For a small amount of slow bleeding, monopolar electrocoagulation should be performed while avoiding contact with the normal brain tissue. Hemostatic yarn (SURGICEL, Absorbable Hemostat Johnson & Johnson, USA) was used to stop bleeding (Figure 2C). After disinfection, the scalp incision was sutured. Animals were placed in a thermostatic cage to maintain the body temperature for 45 min, and were then placed separately in a cage. The mice in the CCI group underwent the same anesthesia process; however, no further treatment of the bone window and trauma was performed.

ICP monitoring

Intracranial pressure was monitored at 1 h, 6 h, 24 h, 3 days, and 7 days after CCI using the Transonic Scisense SP200 Data Acquisition System (Transonic, USA). The mice were anesthetized and fixed on the stereotactic frame, and a bone aperture of 0.8 mm diameter was created at 2.5 mm to the right of midline and 2.5 mm anterior to lambda. After calibration of the ICP monitoring device, a 1.6F piezoelectric flexible pressure probe (Transonic FTH-1211B-0012) was inserted 2 mm below the cerebral cortex through the bone aperture (Figure 3A). Real-time ICP data were observed using LabScribe (iWorx Systems, Inc., Dover, NH, USA). ICP was recorded at a sampling speed of 1.0 sample/s. The data were recorded and saved, and the average value within the observation period was used as the recorded value. The burr hole for ICP monitoring was sealed with Vetbond Tissue Adhesive (3M Corp., Maplewood, MN, USA) before skin closure. For ICP measurements at 6 h, 24 h, 3 days, and 7 days after injury, the same burr hole was accessed again using the same 0.8 mm drill bit (16).

Modified neurological severity score and rotarod performance test

The Modified Neurological Severity Score (mNSS) and rotarod performance were evaluated as previously reported (21). The mNSS is a composite of the motor (muscle status and abnormal movement), sensory (visual, tactile, and proprioceptive sensibilities), beam balance, reflex absence, and abnormal movement tests, with a scoring standard between 0 and 18 points (normal score is 0 points; maximum score is 18 points). The higher is the score, the worse is the sensorimotor function. Mice were scored for mNSS on days 1, 3, 7, and 14 after CCI by the staff unaware of the experimental grouping.

Mouse exercise capacity was evaluated using rotarod, which is a rotating bar fatigue tester (YLS-4C; Yima Optoelec Co., Ltd., Beijing, China), at the same time as mNSS scoring. Mice were given 3 min for acclimation to the instrument rotating at 10 rpm. Acceleration from 0 to 40 rpm was then initiated for 5 min, and the fall time (or the time to complete five effortless spins) was recorded for each mouse. If mice could run in a normal posture for >5 min, the fall time was calculated as 300 s. A total of three tests were performed at each time point, with a 30-min interval, so that the mice could adequately rest. The average of the three trials was taken as the data of that time point.

Morris water maze

The Morris water maze (MWM) was applied 14 days after CCI. In brief, the mice in each group were randomly numbered and trained to locate the hidden platform for 6 days. They were

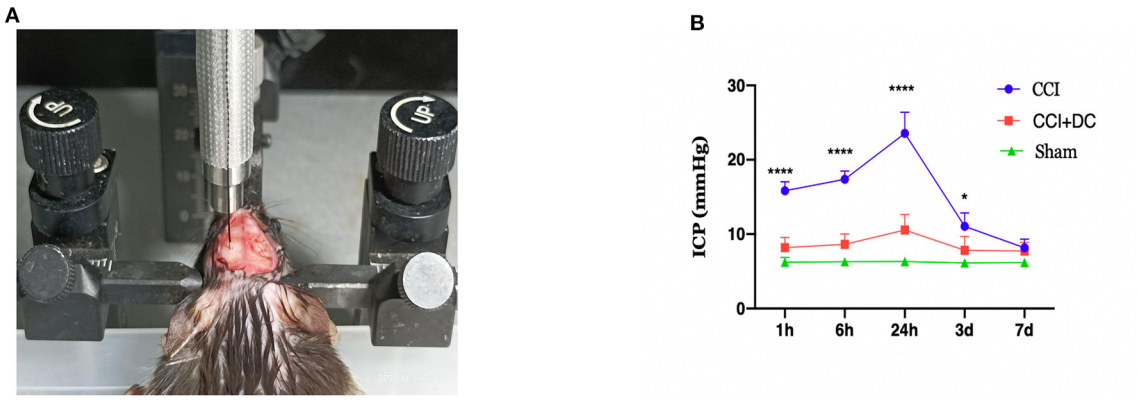

FIGURE 3
Intracranial pressure monitoring in mice. **(A)** Diagram for monitoring ICP in mouse. **(B)** Time-varying curves of ICP of mice in each group. Compared with the sham group, the ICP of the CCI+DC group and the CCI group was higher than that of the sham group after CCI, and the ICP of the CCI group was significantly higher than that of the CCI+DC group at 1, 6, and 24 h after attack ($n = 6$/group, $^{*}P < 0.05$, $^{****}P < 0.0001$ vs. CCI group).

trained four times a day with different starting positions, each time with an interval of ≥30 min, and the starting positions randomly changed daily. Whether the mice found the platform within 90 s or not, they were allowed to stay on the platform for 15 s to memorize the surrounding environment and the location of the markers on the wall. On day 7, the platform was removed and the mice were placed randomly for 90 s of free exploration. The operator of the experiment ensured that the specific mouse grouping was unknown to reduce bias. The latency to reach the platform and the target quadrant, the time spent in the target quadrant, and the number of times the platform was crossed were automatically determined by the software. After each experiment, the mice were dried with absorbent towels and placed in a constant-temperature cage with dry bedding to assure warmth.

Blood–brain barrier damage

Blood–brain barrier integrity was measured using Evans blue (EB) extravasation according to a previous study (22). The mice were anesthetized with 7% chloral hydrate and injected into the tail vein with 100 μl of 2% EB (E2129; Sigma-Aldrich, St. Louis, MO, USA) on days 1, 3, 7, and 14 after CCI. Two hours after injection, the mice were euthanized and immediately perfused with cold phosphate-buffered saline (PBS). Brain tissue samples from the injured side were cut into pieces in a tube. After adding 1 ml of formamide to each tube, samples were extracted in a 60°C water bath for 24 h. The tubes were then centrifuged at room temperature at a speed of 4,000 *g* for 15 min, and 200 μl of the supernatant was added to a 96-well plate. The scale was constructed by diluting EB with formamide in a concentration range of 25.6–0.4 μg/ml. The OD value of each well was detected by absorbance spectroscopy at 610 nm. The EB concentration of each supernatant was calculated.

Brain water content and MRI scan

The water content of brain tissue was detected as previously described (23, 24). In brief, mice were euthanized 1, 3, 7, and 14 days after CCI. Immediately thereafter, brain tissues were extracted, weighed, and recorded in a small dish as the wet weight, and then dried at 70°C for 48 h in the oven, weighed, and recorded as the dry weight. The degree of brain edema was evaluated as (wet weight – dry weight)/wet weight. The result is shown as a percentage.

T2-weighted imaging was performed on days 1, 3, 7, and 14 after CCI with a 9.4 T high-field MRI scanner (BioSpec 94/30 USR; Bruker, Billerica, MA, USA). The scanning parameters included 800 μm slice thickness. After MR scanning, the area of edema and necrosis was measured according to the T2 images, and a matching region of interest (ROI) was manually created using the RadiAnt DICOM Viewer (Medixant, Poznan, Poland). The total contusion volume and edema area are expressed as the sum of the ROI areas multiplied by the thickness in each scanning plane (25, 26).

Laser speckle imaging

On days 1, 3, 7, and 14 after CCI, the cortical blood flow of mice in each group was evaluated using the PeriCam PSI System (Perimed AB, Sweden). First, the mouse skull was fully exposed

under anesthesia. The cortical blood flow of the traumatic and contralateral sides was evaluated using a laser speckle imager (detection distance: 10 cm, laser irradiation area: 2 × 2 cm, 1,386 × 1,034 pixels, regional spatial contrast calculated by 3 × 3 secondary matrix), in a process lasting for 2 min. After detection, the skin was sutured and disinfected. PIMsoft 1.2 was used to analyze perfusion data. Each detection result selects the same ROI position and size and analyzes the average measured values at the same time.

Western blot and cytokine array detection

On days 1, 3, 7, and 14 after CCI, brain tissue proteins were extracted, and cytokines were detected by western blot and array. In brief, immediately after euthanasia, mice were perfused with cold PBS, and then, the injured lateral brain tissue was obtained. The total protein was extracted with RIPA protein lysis buffer and 1% PMSF. The protein sample was separated by 10% SDS-PAGE at 120 V for 90 min, and the separated proteins were transferred onto PVDF membranes. The PVDF membranes were then blocked, cut into bands, and incubated with primary antibodies {β-actin Proteintech 66009, 1:5,000; IL-1-β [CST (3A6) Mouse mAb #12242], 1:250; IL-6 (antibody ab9324), 1:1,000} overnight at 4°C on a shaker. After washing three times, the bands were incubated with an HRP-coupled secondary antibody (1:5,000, Zhongshanjinqiao China) for 1 h at room temperature. A ChemiDoc imaging system (Bio-Rad, Hercules, CA, USA) was used to detect the exposure by ECL chemiluminescence.

Cytokine array was performed as per manufacturer's instructions (ARY006; R&D Systems, Minneapolis, MN, USA). The brain tissue proteins of the abovementioned groups were mixed according to the proportion of total protein content (six mixed with one), and each protein detection chip membrane was incubated overnight at 4°C with 2,000 μg of the total protein content. First, after sufficient washing with 1× washing buffer, each chip protein was incubated with streptomycin-horseradish peroxidase for 30 min. After a new wash, each chip was immersed in ECL luminescent solution for 1 min and then exposed and detected by the ChemiDoc imaging system (Bio-Rad).

Immunofluorescence and TUNEL detection

After euthanasia and heart perfusion with cold PBS and 4% PFA, the intact brain tissue was obtained and fixed in 4% PFA at 4°C for 24 h. Next, the brain tissue was dehydrated in 15% and 30% sucrose, embedded with OCT, and cut into coronal sections with an 8 μm thickness using a microtome for sectioning frozen sections (CM 1950; Leica Biosystems, Deer Park, IL, USA). After rewarming, the OCT was washed away with PBS and the tissue was circled with a hydrophobic pen. Then, the brain sections were incubated with 2% BSA, 2% goat serum, 0.2% Triton X-100, and 0.05% Tween 20 in PBS for 1.5 h at room temperature. After removing the liquid, 30 μl of diluted primary antibody [anti-Neu N ab177487 (1:300), anti-GFAP ab4674 (1:1,000), and anti-Iba 1 ab5076 (1:200)] were added to each tissue and incubated overnight at 4°C. After rewarming and washing with PBS, the fluorescent-labeled secondary antibody was added and incubated at room temperature for 1 h, while avoiding exposure to light. Then, the sections were sealed with DAPI-containing sealing tablets. Once ready, the samples were observed with an inverted fluorescence microscope (Olympus, Shinjuku City, Tokyo, Japan).

After the incubation with Neu N primary antibody and fluorescent secondary antibody, the TDT enzyme from the TUNEL staining kit (Roche, 11684817910) was mixed with fluorescent labeling solution in a ratio of 1:9. After 10 min, 30 μl of the mixed solution was dripped onto each tissue, which was then incubated at 37°C for 1 h, washed with PBS, sealed with DAPI-containing sealing tablets, and imaged with an inverted fluorescence microscope (OLYMPUS). ImageJ software was used to calculate the gray values used for measuring staining intensity and nuclei in the observation area.

Data analysis

All data are expressed as mean ± standard error of the mean. Independent unpaired *t*-tests and two-way ANOVA were used to evaluate significance, and $p < 0.05$ was considered statistically significant. SPSS 22.0 software (IBM Corp., Armonk, NY, USA) and GraphPad Prism 9.0 (GraphPad Software, San Diego, CA, USA) were used for data analysis and plotting.

Results

DC can effectively reduce ICP in severe TBI

The ICP was dynamically monitored at 1 h, 6 h, 24 h, 3 days, and 7 days after CCI. Compared with that of the Sham group, ICP in the CCI group increased gradually over time, reached a peak at 24 h after CCI, and then slowly decreased. Compared with that of the CCI group, ICP in the CCI+DC group was significantly lower at each observation time point, and there were significant differences at 1 h, 6 h, 24 h, and 3 days ($p < 0.05$) (Figure 3B).

DC can improve neurological and motor function at 24 h after CCI, but weaken the spatial cognition and learning ability at late stages of CCI

At 24 h after CCI, the mNSS scores in the CCI+DC group were significantly lower than those in the CCI group ($p < 0.05$). However, there was no significant difference in mNSS scores between the CCI and CCI+DC groups at 3 and 7 days after CCI. By the 14th day after injury, compared with the CCI group, the mice in the CCI+DC group had significantly higher mNSS score ($p < 0.05$) (Figure 4A).

Similarly, in the rotarod test, compared with the CCI group, the CCI+DC group had a longer latency time before falling at 24 h after injury ($p < 0.05$). There was no significant difference in latency time between the two groups at 3 and 7 days after CCI. By the 14th day, the CCI group had a longer residence time ($p < 0.05$) (Figure 4B).

The MWM was used to evaluate spatial cognition and learning ability 14 days after CCI. After removing the hidden platform, compared with that of the CCI group, the platform latency period of the CCI+DC group was longer, and the residence time in the target quadrant and the number of times crossing the platform area were significantly lower ($p < 0.05$) (Figures 4C–E). Moreover, in the water maze experiment, on the 3rd, 5th, and 7th days, the movement distance in the CCI+DC group was longer than that of the CCI group, ((Figure 4G) and the total movement distances of the two groups were significantly statistically different ($p < 0.05$) (Figure 4F).

DC can reduce BBB damage in severe TBI

The EB leakage test was used to evaluate BBB damage in the CCI+DC and CCI groups at different time points after CCI (Figure 5A). On the 3rd day after CCI, the leakage of EB into the brain tissue of the CCI+DC and CCI groups reached a peak and gradually decreased over time. Compared with that of the CCI group, EB leakage in the CCI+DC group was significantly lower at 24 h, 3 days, 7 days, and 14 days after CCI ($p < 0.05$) (Figure 5B).

DC can reduce brain tissue edema and necrosis but can briefly aggravate whole-brain edema in severe TBI

The brain water content, measured to evaluate brain edema, showed obvious edema in the CCI and CCI+DC groups at 24 h after CCI, reaching its peak on the 3rd day, and then gradually subsiding, leaving only a liquefied focus on the 14th day after CCI. On the 3rd and 7th days after injury, the brain water content in the CCI+DC group was significantly higher than that in the CCI group ($p < 0.05$) (Figure 6C).

However, MRI results showed that the edema and necrotic zone of mice in the CCI+DC group were significantly smaller in size than that in the CCI group. Especially on the 1st, 3rd, and 14th days after CCI, there was a significant statistical difference between the two groups ($p < 0.05$) (Figures 6A,B).

DC can improve brain cortex perfusion in severe TBI

Perfusion in the cortex was evaluated by laser speckle imaging. Blood flow in the CCI+DC and CCI groups gradually increased over time. Compared with that of the CCI group, perfusion of the injured cortex in the CCI+DC group was greater on the 1st, 3rd, 7th, and 14th days after CCI, especially on the 3rd and 14th days ($p < 0.05$) (Figures 7A,B). Similarly, for the contralateral cerebral hemisphere, cortical blood flow in the CCI+DC group was higher than that in the CCI group on the 7th and 14th days, especially on the 14th day ($p < 0.05$) (Figures 7A,C).

DC can reduce inflammation, apoptosis, and glial cell expression after severe TBI

A cytokine array was used to detect the levels of inflammatory factors in the brain tissue of mice in each group. Compared with that of the Sham group, the expression of inflammatory factors in the brain tissue of TBI mice reached its peak 24 h after TBI, and then gradually decreased. On the 1st day after CCI, the levels of inflammatory cytokines, namely, C5/C5a, IL-16, CXCL1 (KC), M-CSF, CCL2 (MCP-1), and TIMP-1 were higher in the CCI+DC group than in the CCI group, while the levels of ICAM-1 (CD54) and CXCL10 (IP-10/CRG-2) were lower (Figures 8A,B). However, the levels of C5/C5a, ICAM-1 (CD54), IL-16, CXCL10 (IP-10/CRG-2), M-CSF, and TIMP-1 in the brain tissue of the CCI+DC group were significantly lower than those in the CCI group on the 3rd day after CCI (Figure 8C), and ICAM-1 (CD54), IL-16, and CXCL10 (IP-10/CRG-2) levels were lower than those in the CCI group on the 7th day after CCI (Figure 8D).

Meanwhile, western blotting was used to detect the expression levels of IL-1β and IL-6 in mouse brain tissue in each group. Compared with that of the CCI group, the expression level of IL-1β was significantly lower in the CCI+DC group, especially on the 3rd and 7th days ($p < 0.05$) (Figures 9A,B). However, the IL-6 expression level was significantly higher in the CCI+DC group than in the CCI group at maximum time points, especially on the 7th day ($p < 0.05$) (Figures 9A,C).

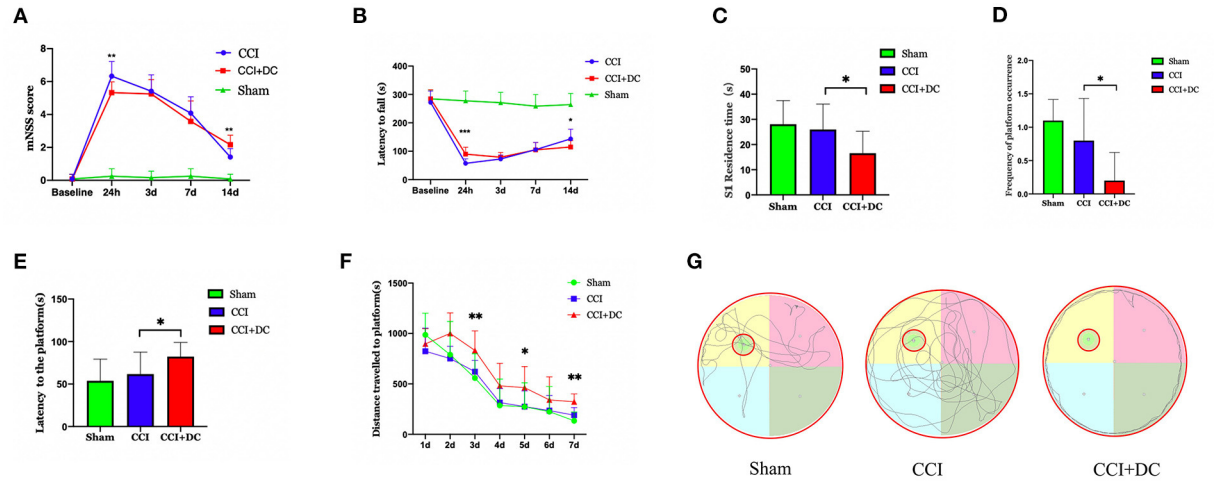

FIGURE 4
Functional results. **(A)** Comparison of results among all groups indicated that mNSS score of mice in the CCI+DC group improved 24 h after CCI compared with that in the CCI group, while functional score of mice in the CCI+DC group decreased significantly as time went by 14 days after CCI compared with that in the CCI group, and the difference was statistically significant. **(B)** The results of the rotarod indicated that the latency to fall in the CCI+DC group was significantly improved compared with that in the CCI group at 24 h after CCI, and the difference was statistically significant. However, on the 14th day after CCI, the motor function of mice in the CCI+DC group was worse than that in the CCI group, and the difference was statistically significant. **(C)** MWM results indicated that on 7th day of the MWM experiment, the time for mice in the CCI+DC group to pass S1 quadrant. **(D)** The number of platforms were significantly lower than those in the CCI group, and the differences were statistically significant. **(E)** MWM results indicated that the platform latency of mice in the CCI+DC group was significantly higher than that in the CCI group, and the difference was statistically significant. **(F)** The total movement distance of mice was counted in the MWM experiment. It was found that the movement distance of mice in the CCI+DC group was longer than that of mice in the CCI group on day 3, 5, and 7 of the water maze experiment, and the difference was statistically significant. **(G)** Movement route of mice on day 7 between different group ($n = 10$/group, $^{*}P < 0.05$, $^{**}P < 0.01$, vs. CCI group).

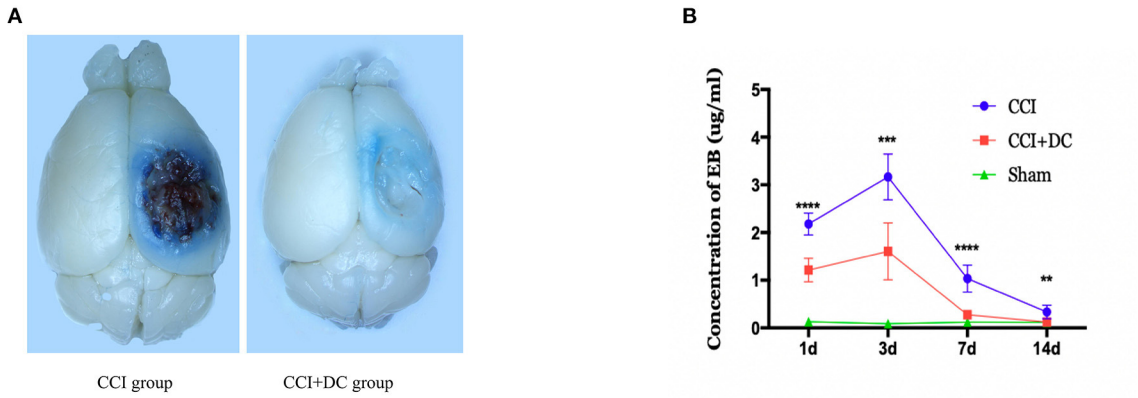

FIGURE 5
Effects on the blood-brain barrier. **(A)** General view of brain tissue after EB tail injection in rmice on 3 days after traumatic brain injury. **(B)** EB was extracted from the brain tissue to calculate the infiltration content of EB, and the results indicated that the infiltration amount of EB in the CCI+DC group was significantly reduced compared with the CCI group at each time point after CCI, with significant statistical difference ($n = 6$/group, $^{**}P < 0.01$, $^{***}P < 0.001$, $^{****}P < 0.0001$ vs. CCI group).

Immunofluorescence was used to compare the expression levels of glial cells (Figure 10C). Compared with that in the CCI group, the number of microglial cells in the CCI+DC group was significantly reduced on the 7th day ($p < 0.05$) (Figures 10A,B). Moreover, compared with that of the CCI group, the expression of astrocytes in the CCI+DC group was significantly reduced, and the difference was statistically significant on the 3rd day ($p < 0.05$) (Figures 11A,B).

Furthermore, TUNEL staining was performed on nerve cells in the ipsilateral hippocampus on the 3rd day after CCI. The

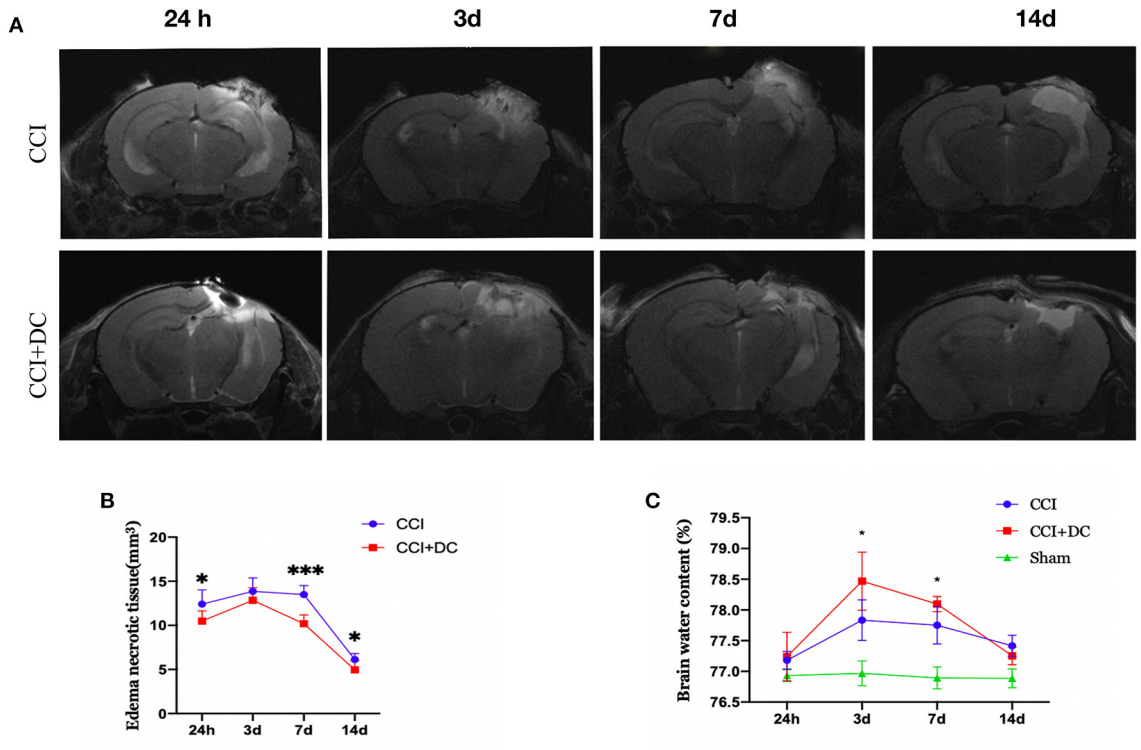

FIGURE 6
Effect on cerebral edema. **(A)** MR examination was performed at different time points after CCI. **(B)** The statistical results were shown intracranial edema and contusion tissues of mice in the CCI+DC group at each time point after CCI was lower than that of the CCI group, and the difference was statistically significant on the first, 7th and 14th day after CCI. **(C)** Brain water content was detected by extracting brain tissue, as shown in the **(C)** on the 3rd and 7th day after CCI, the degree of brain edema in the CCI+DC group was significantly worse than that in the CCI group, and the difference was statistically significant ($n = 6$/group, $^{*}P < 0.05$, $^{***}P < 0.001$ vs. CCI group).

results showed significantly lower neuron apoptosis near the lesion in the CCI+DC group than in the CCI group ($p < 0.05$) (Figures 12A,B).

Discussion

Decompressive craniectomy is widely used in clinical practice and plays a vital role in saving patients with life-threatening elevated ICP, and the use of DC will become increasingly common for severe head injuries and for other diseases such as stroke, subarachnoid hemorrhage, and infection. Thus, it is of great significance to establish a DC model and evaluate it systematically.

Although closed TBI models appear simpler, the depth and extent of the damage are not very reproducible. And most of the brain trauma caused by closed TBI is mild to moderate (17), in which case conservative treatments are usually used in the clinical process. At present, mouse models for weight drop injury (WDI), fluid percussion injury (FPI), and CCI have been created for studying severe brain trauma. Each model has several advantages and disadvantages. In WDI, the presence of the skull causes high variability in brain tissue changes. In addition, the mechanism of tissue damage associated with FPI is not similar to that observed in clinical TBI (27). The CCI model is an effective model to study TBI (28); this model uses an impactor resulting in significant neurological deficits as well as histopathological changes, including extensive cortical damage, hippocampal neuronal cell loss, extensive reactive gliosis, and breakdown of the BBB (18). And through closing the bone window after CCI, it can simulate the clinical situations of contused swollen tissues under a nearly closed bone window after trauma. Therefore, the CCI model is more consistent with the mechanism of clinical brain injury and can produce reproducible brain injury. Therefore, in our study, we chose to use the CCI mouse model to simulate patients with severe TBI who would need DC surgery in clinical practice. In our DC process, we chose a 4-mm bone window; this size can avoid the uncontrolled expansion of the brain caused by an excessively large bone flap, which may cause adverse neurological outcomes (29). In addition, compared with previous studies (16, 17), we cleared the apoptotic tissues to further release pressure in

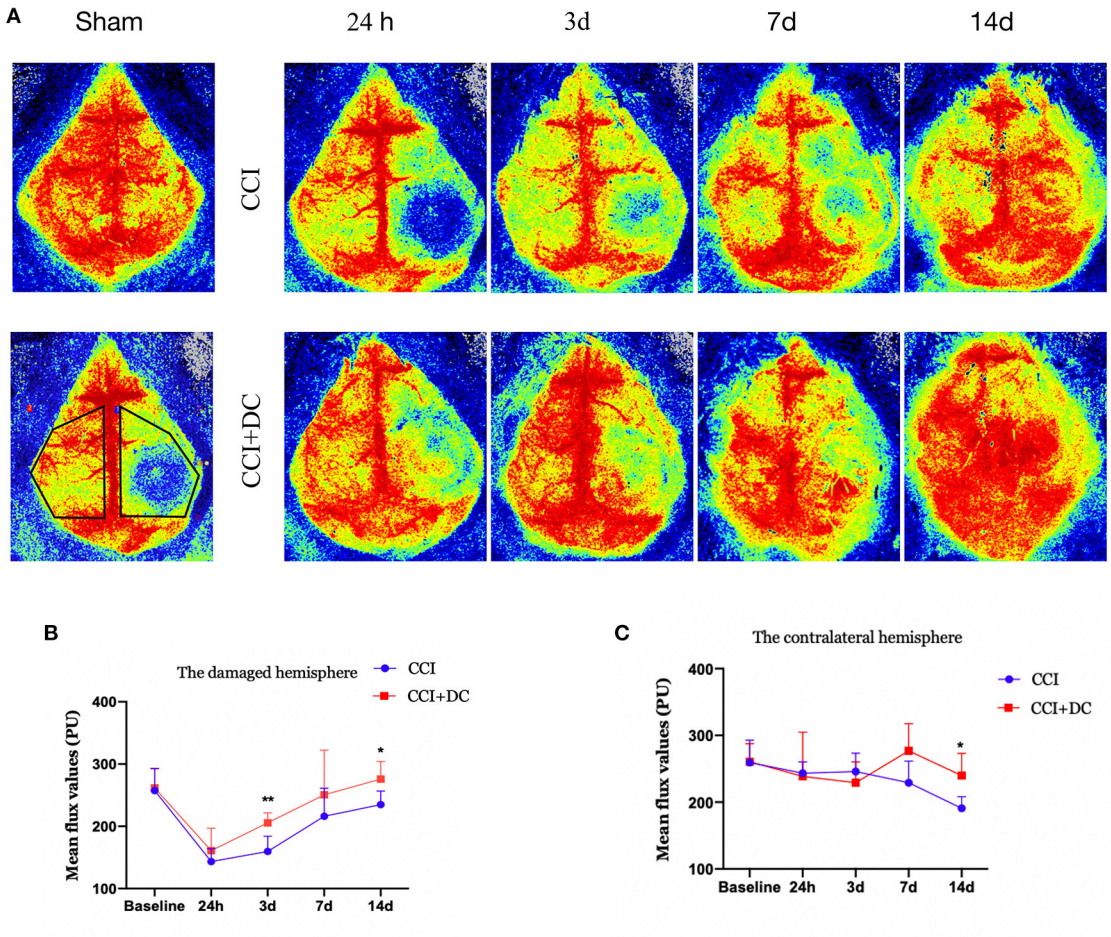

FIGURE 7
Effects on cerebral blood flow. **(A)** Laser speckle test was performed at different time points after CCI to evaluate cerebral blood flow, and the statistical results were shown in **(B,C)**. **(B)** It was statistically found that the cerebral blood flow on the injured side of the CCI+DC group after CCI was higher than that of the CCI group, and the results were statistically different on the 3rd and 14th day after CCI. **(C)** Statistically, cerebral blood flow in the healthy side of the CCI+DC group was higher than that in the CCI group on the 7th day after CCI, and the difference was statistically significant ($n = 5$/group, $^{*}P < 0.05$, $^{**}P < 0.01$, vs. CCI group).

the intracranial space. By monitoring ICP at different time points after the TBI onset, we showed that the DC with focal debridement model had a clear decompressive effect in mice with TBI, as compared with the control group.

Studies have shown different results for the effects of DC on neurological recovery after TBI. Early clinical studies showed that DC has a positive effect on the recovery of neurological function after TBI (30–32). However, other studies showed that DC exacerbates functional impairment (17). Currently, two important multicenter, clinical RCT trials of DC have been conducted. The randomized early decompressive craniectomy (DECRA) trial that included 155 adults with TBI showed that early bifrontotemporoparietal DC decreased ICP and the length of stay in the ICU but was associated with more unfavorable outcomes (29), and 12 months after severe diffuse TBI, DC did not improve outcomes and increased the proportion of vegetative survivors (33). The Randomized Evaluation of Surgery with Craniectomy for Uncontrollable Elevation of Intracranial Pressure (RESCUEicp) trial with 408 TBI patients showed that, at 6 months, DC resulted in a lower mortality rate, a higher proportion of vegetative outcomes, lower severe disability, and upper severe disability than medical care. The rates of moderate disability and good recovery were similar between the two groups (34). Possible explanations for the different results for neurological recovery include different injury locations, different mechanisms, focal vs. diffuse injuries, different surgical indications in different experiments, and different surgeons for the DC operations. The damage caused to the brain tissue during the DC process itself is also a factor that should be considered.

Studies have shown that the BBB is disrupted after TBI (8, 35). BBB disruption is an early event that occurs within hours

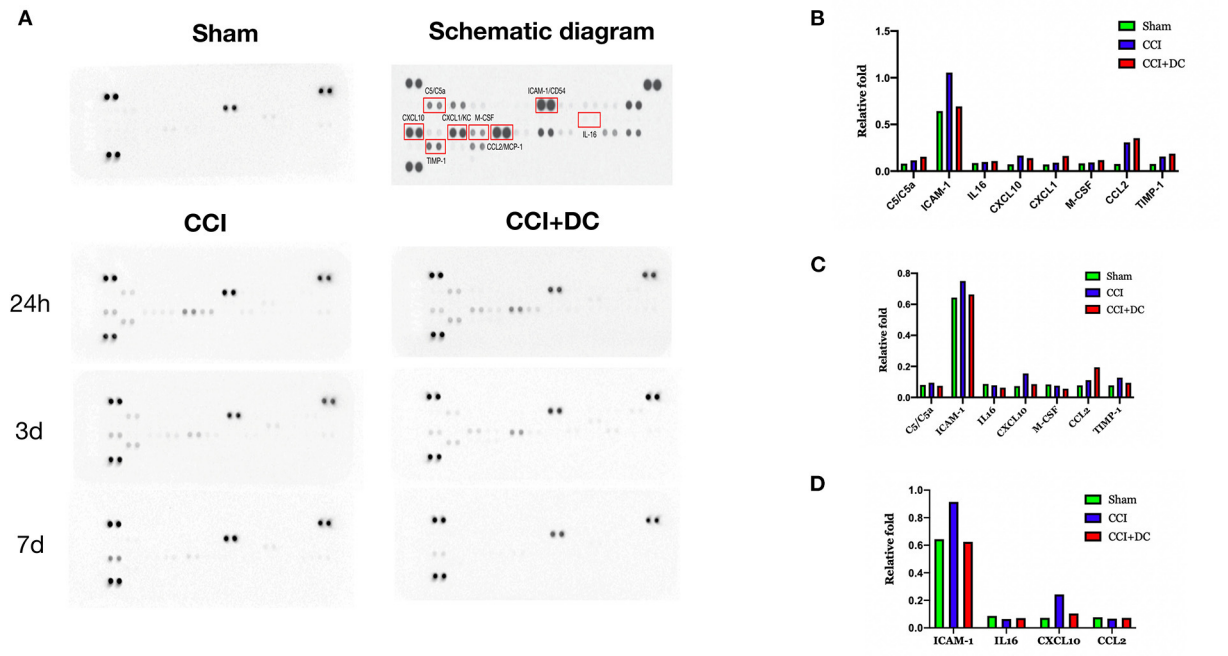

FIGURE 8
Changes in the expression of inflammatory factors. **(A)** Changes in the expression of inflammatory factors at 24 h, 3 d, and 7 d after brain trauma. **(B)** Expression levels of inflammatory factors in different groups of mice at 24 h after brain trauma. **(C)** Different groups of mice The expression level of inflammatory factors on the 3rd day after brain injury. **(D)** Expression levels of 7D inflammatory factors in mice in different groups of D after brain trauma.

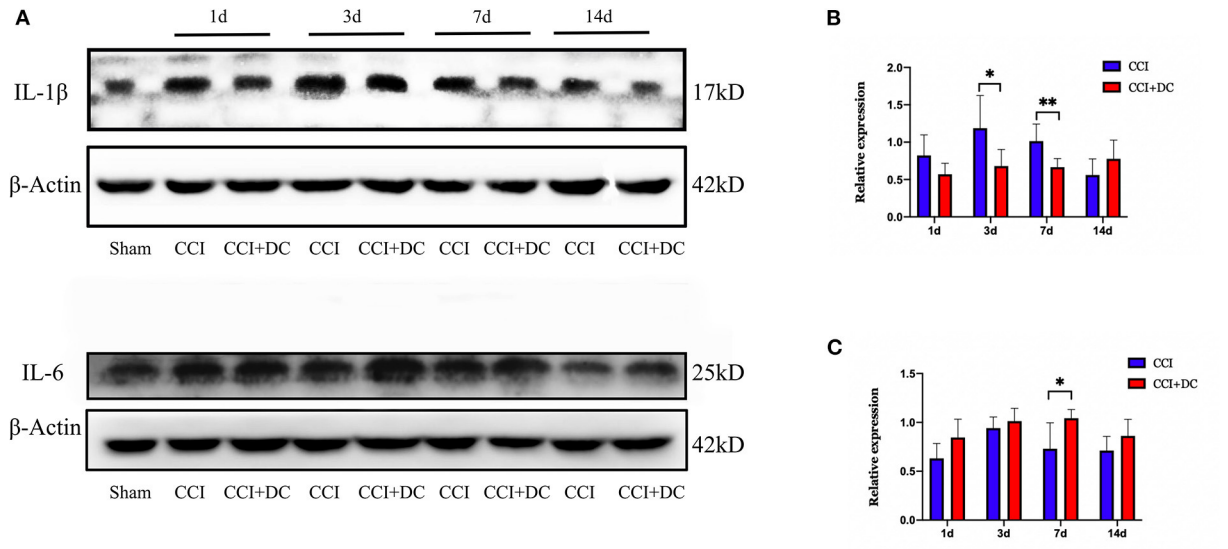

FIGURE 9
The effect on inflammatory factors. **(A)** Expression changes of inflammatory factors IL1β and IL6 on day 1, 3, 7, and 14 after CCI, and statistical results are shown in **(B,C)**. **(B)** ILIβ in the CCI+DC group was significantly higher than that in the CCI group on the 3rd and 7th day after CCI. **(C)** IL6 in the CCI group was lower than that in the CCI group on the 7th day after CCI, and the results were also statistically different ($n = 6$/group, $^{*}P < 0.05$, $^{**}P < 0.01$, vs. CCI group).

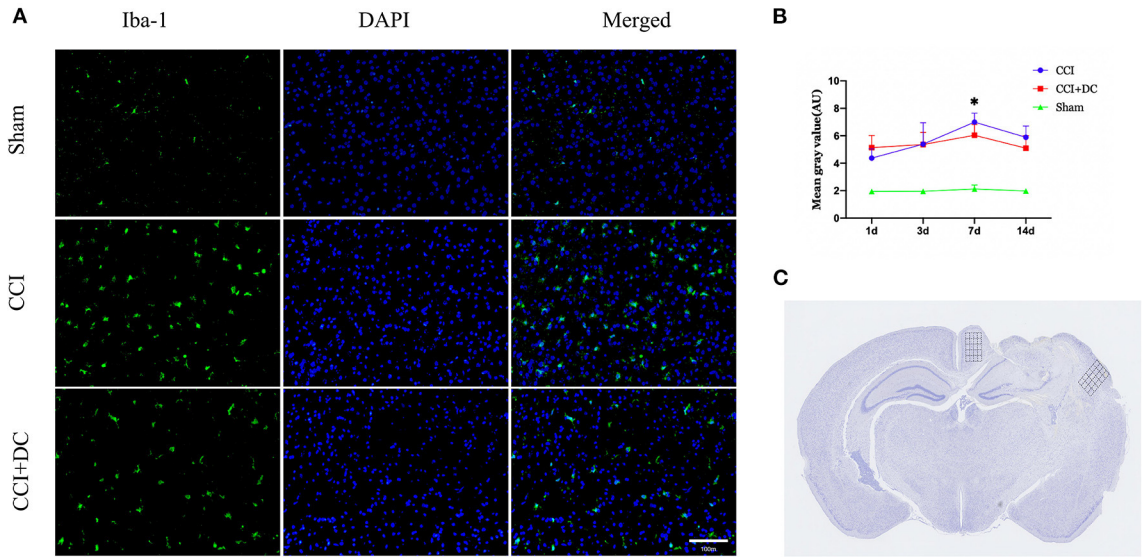

FIGURE 10
Effect on peri-contusional cortex microglia. **(A)** The expression of microglia in different groups on the 7th day after traumatic brain injury. **(B)** Expression of microglia in the CCI+DC group was significantly lower than that in the CCI group on the 7th day after CCI, the expression of cortical microglia was statistically different from that in the CCI group. **(C)** Detected areas of microglia and astrocytes. $n = 6$/group/time points, $^*P < 0.05$, vs. CCI group.

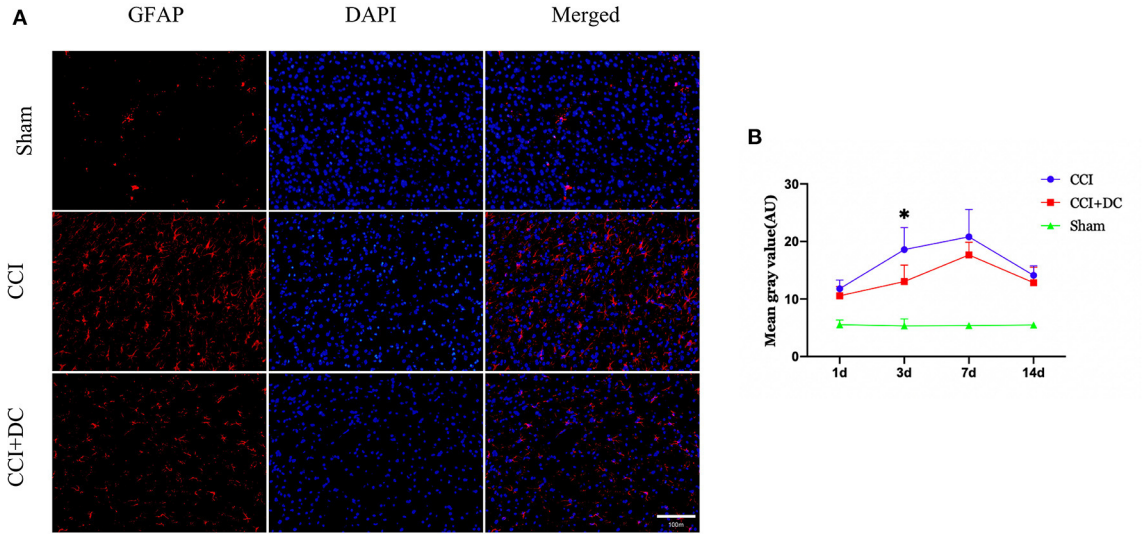

FIGURE 11
Effect on peri-contusional cortex astrocytes. **(A)** The expression of astrocytes in different groups on the 3rd day after brain injury. **(B)** On day 3 after CCI, the expression of microglia in the cortex of the CCI+DC group was significantly lower than that of the CCI group, and the expression of was statistically different from that in the CCI group ($n = 6$/group/time points, $^*P < 0.05$, vs. CCI group).

following injury but can persist for years (36). The destruction of the BBB can aggravate cerebral edema and increase ICP. After TBI, the increase in paracellular transport, indicated by a loss of tight junction proteins and an increase in transcytosis across the endothelium, contributes to BBB dysfunction; this leads to an influx of immune cells, such as neutrophils, and transport of large molecules and serum proteins that can exacerbate the inflammatory response (37, 38). In addition, intracranial astrocytes, endotheliocyte, and inflammatory factors play important roles in the destruction of the BBB (8, 39–41).

The early inflammatory response plays an important role in clearing tissue debris and repairing wounds. However, excessive

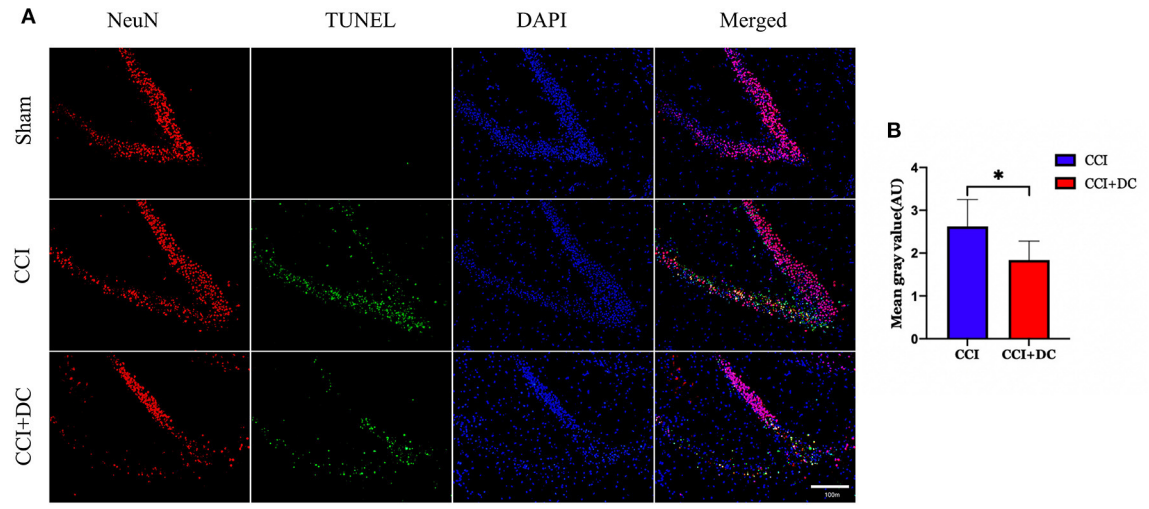

FIGURE 12
The effect of neuronal apoptosis in hippocampus on the third day after brain injury. **(A)** On the 3rd day after brain injury, the apoptosis of hippocampal neurons in different groups. **(B)** Hippocampal neurons apoptosis on the 3rd day after CCI. The results showed that the neuronal apoptosis of the CCI+DC group was less than that of the CCI group, and the difference was statistically significant ($n = 5$/group, $^*P < 0.05$, vs. CCI group).

inflammation can adversely affect neuronal function (42). For example, excessive inflammatory mediators such as IL-1β, IL-6, IL-18, and TNFα may lead to secondary injury after TBI (43). Although IL-1β alone does not seem to directly cause neuronal death in cell culture, in some cases, IL-1β can induce neuronal death, especially when other pro-inflammatory cytokines such as TNFα are present (44). Unlike the undesirable effects of IL-1β and TNFα in humans and animals, IL-6 appears to have neuroprotective effects in animal models (45).

Early studies have shown that after brain injury, cerebrovascular autoregulation is impaired or non-functional in many patients (46), and the brain blood volume decreases sharply after brain trauma (47). When cerebral edema occurs and ICP increases after TBI, the cerebral perfusion pressure will decrease, which leads to cerebral ischemia and hypoxia (48); DC can improve not only the ICP itself, but also cerebral blood flow and brain metabolism, as demonstrated in neuroimaging and multimodal studies (49, 50).

Early restoration of BBB integrity may aid in preventing the sequelae of other comorbidities associated with TBI, including post-traumatic epilepsy and neurodegenerative disease (51). During the DC process, the reduction of ICP and the clearance of contused necrotic tissue reduce oxidative stress and inflammation, thereby reducing post-TBI BBB damage and improving cerebral blood flow. However, during DC, the removal of severely contused and necrotic tissue aggravates the neurological injury. This change is associated with secondary injury caused by DC surgery.

Astrocytes and microglia have a dual effect on the recovery of brain tissue (52–56). Reactive astrocytes are capable of producing pro-inflammatory cytokines and chemokines that cause BBB disruption (57). However, astrocytes are also capable of producing factors that support repair and regeneration after CNS damage (58). At present, the role of astrocytes in TBI is unclear. The removal of proliferating astrocytes in mice has been shown to result in neuronal degeneration and inflammation, and play an essential role in preserving neuronal tissue after moderate (but not severe) TBI (59). In contrast, blocking astrocyte proliferation using agents that disrupt various stages of the cell cycle can lead to reduced neuronal cell death after FPI in rats (60). These actions may depend on the severity, stage, and affected brain area (61). Recent studies also show that astrocytes function as intracranial baroreceptors and play an important role in homeostatic control of arterial blood pressure and brain blood flow (62).

Although our study shows that DC can reduce the accumulation of astrocytes near the trauma site at day 3 and microglia at day 7 after TBI, it is difficult to determine the relationship between gliocytes and the post-TBI prognosis; therefore, more studies are needed to determine the role of gliocytes in DC after TBI.

Limitation

Traumatic brain injuries can be quite heterogeneous. There are limitations to our experimental design that must be considered before our findings can be translated into the clinical setting. It is difficult for animal models to truly simulate the pathophysiological changes that occur in human clinical

situations; there is no perfect animal model that can fully match the changes in human brain trauma. Accordingly, our DC model does not perfectly simulate the clinical features of human brain trauma.

Although this study utilized CCI to ensure that the TBI was standardized and used the same parameters, it does not encompass the full spectrum of TBIs. It is unclear whether DC in other TBI models would produce the same results. In addition, our study groups had limited sizes and comprised only male mice; therefore, the known sex-associated differences in TBI recovery and neuroplasticity could not be addressed. TBI in humans is usually caused by forces striking the frontal, occipital, or temporal areas of the skull. In contrast, TBI in the mouse model is usually induced *via* the skull vertex. A small diameter impactor tip in CCI models produces neither diffuse axonal injury (DAI) nor significant neurological functional deficits, and the CCI mouse model in our study often manifests with a focal injury; it is difficult to simulate diffuse lesions. And the damage to the meninges in CCI models is also not optimal for simulating the pathophysiological changes that occur in human clinical situations.

Functional evaluation of psychological and neurological parameters depends on a patient's verbal communication skills, which cannot be evaluated in mice. Animal experiments lack a scoring system such as the Glasgow Coma Scale (GCS), which evaluates the severity of brain trauma in human TBI patients. In addition, neurological recovery is more rapid and complete in mice. The ICP measurements in our study were performed under anesthesia, which is known to influence cerebrovascular hemodynamics.

Although there is evidence that a sustained elevation in ICP (> 20 mmHg) after severe TBI is associated with a poor outcome, the efficacy of threshold-targeted interventions has not been thoroughly established (16, 63). At the same time, due to the differences in mouse and human species, in our study, the surgical indications after CCI are mostly based on the personal opinions of our researchers, and it is difficult to simulate the surgical indications of DC after CCI in clinical situations.

Conclusion

In our study, we confirmed that DC and focal debridement can effectively attenuate the increase in ICP and improve cerebral blood flow in mice with severe TBI. Moreover, the removal of contused brain tissue alleviates the neurological dysfunction in the acute stage, reduces the expression of some pro-inflammatory factors [C5/C5a, ICAM-1 (CD54), IL-16, CXCL10 (IP-10/CRG-2), M-CSF, TIMP-1, IL-1 β, and IL-6], reduces neuron apoptosis, diminishes BBB disruption, and regulates the number of glial cells. However, DC and focal debridement negatively affected recovery of neurological function, motor function, and cognition in mice with TBI at intermediate and late stages. Thus, although surgical treatment of patients with TBI can relieve acute symptoms, it may not be conducive to the recovery of neurological function and improving quality of life.

Our mouse model provides an opportunity to systematically evaluate the changes that occur following DC for TBI; however, further research is needed before it can serve as a reference for making clinical decisions.

Data availability statement

The original contributions presented in the study are included in the article/supplementary material, further inquiries can be directed to the corresponding authors.

Ethics statement

The animal study was reviewed and approved by Tianjin Medical University General hospital.

Author contributions

WY and ZW conceived and designed the study. YL, XL, and ZC conducted the experiments and wrote the manuscript. YW, JL, JG, and AH analyzed the data and interpreted the results. All authors contributed to the article and approved the submitted version.

Funding

This work was supported by the Tianjin Science and Technology Support Key Project (Grant Number: 20YFZCSY00010). The authors are thankful for funding by Tianjin Key Medical Discipline (Specialty) Construction Project.

Acknowledgments

The authors are grateful to Lei Zhou, Hao Liang, Weiyun Cui, Fanglian Chen, Li Liu, Xiao Liu, and Guili Yang from the Tianjin Neurological Institute for their excellent technical support.

Conflict of interest

The authors declare that the research was conducted in the absence of any commercial or financial relationships that could be construed as a potential conflict of interest.

Publisher's note

References

1. Pearn ML, Niesman IR, Egawa J, Sawada A, Almenar-Queralt A, Shah SB, et al. Pathophysiology associated with traumatic brain injury: current treatments and potential novel therapeutics. *Cell Mol Neurobiol.* (2017) 37:571–85. doi: 10.1007/s10571-016-0400-1

2. Guo Z, Ding W, Cao D, Chen Y, Chen J. Decompressive craniectomy vs. craniotomy only for traumatic brain injury: a propensity-matched study of long-term outcomes in neuropsychology. *Front Neurol.* (2022) 13:813140. doi: 10.3389/fneur.2022.813140

3. Hubertus V, Finger T, Drust R, Al Hakim S, Schaumann A, Schulz M, et al. Severe Traumatic Brain Injury in children-paradigm of decompressive craniectomy compared to a historic cohort. *Acta Neurochir.* (2022) 164:1421–34. doi: 10.1007/s00701-022-05171-4

4. Maas AIR, Menon DK, Adelson PD, Andelic N, Bell MJ, Belli A, et al. Traumatic brain injury: integrated approaches to improve prevention, clinical care, and research. *Lancet Neurol.* (2017) 16:987–1048. doi: 10.1016/S1474-4422(17)30371-X

5. Jiang JY, Gao GY, Feng JF, Mao Q, Chen LG, Yang XF, et al. Traumatic brain injury in China. *Lancet Neurol.* (2019) 18:286–95. doi: 10.1016/S1474-4422(18)30469-1

6. Glover LE, Tajiri N, Lau T, Kaneko Y, Van Loveren H, Borlongan CV. Immediate, but not delayed, microsurgical skull reconstruction exacerbates brain damage in experimental traumatic brain injury model. *PLoS ONE.* (2012) 7:e33646. doi: 10.1371/journal.pone.0033646

7. Terpolilli NA, Kim SW, Thal SC, Kuebler WM, Plesnila N. Inhaled nitric oxide reduces secondary brain damage after traumatic brain injury in mice. *J Cereb Blood Flow Metab.* (2013) 33:311–8. doi: 10.1038/jcbfm.2012.176

8. Cash A, Theus MH. Mechanisms of blood-brain barrier dysfunction in traumatic brain injury. *Int J Mol Sci.* (2020) 21:3344. doi: 10.3390/ijms21093344

9. Capizzi A, Woo J, Verduzco-Gutierrez M. Traumatic brain injury: an overview of epidemiology, pathophysiology, and medical management. *Med Clin North Am.* (2020) 104:213–38. doi: 10.1016/j.mcna.2019.11.001

10. Brett BL, Gardner RC, Godbout J, Dams-O'connor K, Keene CD. Traumatic brain injury and risk of neurodegenerative disorder. *Biol Psychiatry.* (2022) 91:498–507. doi: 10.1016/j.biopsych.2021.05.025

11. Sahuquillo J, Arikan F. Decompressive craniectomy for the treatment of refractory high intracranial pressure in traumatic brain injury. *Cochrane Database Syst Rev.* (2006) 1:1–41. doi: 10.1002/14651858.CD003983.pub2

12. Vashu R, Sohail A. Decompressive craniectomy is indispensible in the management of severe traumatic brain injury. *Acta Neurochir.* (2011) 153:2065–6. doi: 10.1007/s00701-011-1101-7

13. Bor-Seng-Shu E, Figueiredo EG, Amorim RL, Teixeira MJ, Valbuza JS, De Oliveira MM, et al. Decompressive craniectomy: a meta-analysis of influences on intracranial pressure and cerebral perfusion pressure in the treatment of traumatic brain injury. *J Neurosurg.* (2012) 117:589–96. doi: 10.3171/2012.6.JNS101400

14. Stocchetti N, Maas AI. Traumatic intracranial hypertension. *N Engl J Med.* (2014) 370:2121–30. doi: 10.1056/NEJMra1208708

15. Hutchinson PJ, Timofeev I, Kolias AG, Corteen EA, Czosnyka M, Menon DK, et al. Decompressive craniectomy for traumatic brain injury: the jury is still out. *Br J Neurosurg.* (2011) 25:441–2. doi: 10.3109/02688697.2011.583366

16. Friess SH, Lapidus JB, Brody DL. Decompressive craniectomy reduces white matter injury after controlled cortical impact in mice. *J Neurotrauma.* (2015) 32:791–800. doi: 10.1089/neu.2014.3564

17. Szczygielski J, Mautes AE, Muller A, Sippl C, Glameanu C, Schwerdtfeger K, et al. Decompressive craniectomy increases brain lesion volume and exacerbates functional impairment in closed head injury in mice. *J Neurotrauma.* (2016) 33:122–31. doi: 10.1089/neu.2014.3835

18. Zhang YP, Cai J, Shields LB, Liu N, Xu XM, Shields CB. Traumatic brain injury using mouse models. *Transl Stroke Res.* (2014) 5:454–71. doi: 10.1007/s12975-014-0327-0

19. Zweckberger K, Stoffel M, Baethmann A, Plesnila N. Effect of decompression craniotomy on increase of contusion volume and functional outcome after controlled cortical impact in mice. *J Neurotrauma.* (2003) 20:1307–14. doi: 10.1089/089771503322686102

20. Zweckberger K, Erös C, Zimmermann R, Kim SW, Engel D, Plesnila N. Effect of early and delayed decompressive craniectomy on secondary brain damage after controlled cortical impact in mice. *J Neurotrauma.* (2006) 23:1083–93. doi: 10.1089/neu.2006.23.1083

21. Yuan J, Zhang J, Cao J, Wang G, Bai H. Geniposide alleviates traumatic brain injury in rats via anti-inflammatory effect and MAPK/NF-kB inhibition. *Cell Mol Neurobiol.* (2020) 40:511–20. doi: 10.1007/s10571-019-00749-6

22. O'connor CA, Cernak I, Vink R. Both estrogen and progesterone attenuate edema formation following diffuse traumatic brain injury in rats. *Brain Res.* (2005) 1062:171–4. doi: 10.1016/j.brainres.2005.09.011

23. Su Y, Fan W, Ma Z, Wen X, Wang W, Wu Q, et al. Taurine improves functional and histological outcomes and reduces inflammation in traumatic brain injury. *Neuroscience.* (2014) 266:56–65. doi: 10.1016/j.neuroscience.2014.02.006

24. Gao C, Qian Y, Huang J, Wang D, Su W, Wang P, et al. A three-day consecutive fingolimod administration improves neurological functions and modulates multiple immune responses of CCI mice. *Mol Neurobiol.* (2017) 54:8348–60. doi: 10.1007/s12035-016-0318-0

25. Sturiale CL, De Bonis P, Rigante L, Calandrelli R, D'arrigo S, Pompucci A, et al. Do traumatic brain contusions increase in size after decompressive craniectomy? *J Neurotrauma.* (2012) 29:2723–6. doi: 10.1089/neu.2012.2556

26. Szczygielski J, Hubertus V, Kruchten E, Muller A, Albrecht LF, Mautes AE, et al. Brain edema formation and functional outcome after surgical decompression in murine closed head injury are modulated by acetazolamide administration. *Front Neurol.* (2019) 10:273. doi: 10.3389/fneur.2019.00273

27. O'connor WT, Smyth A, Gilchrist MD. Animal models of traumatic brain injury: a critical evaluation. *Pharmacol Ther.* (2011) 130:106–13. doi: 10.1016/j.pharmthera.2011.01.001

28. Dixon CE, Clifton GL, Lighthall JW, Yaghmai AA, Hayes RL. A controlled cortical impact model of traumatic brain injury in the rat. *J Neurosci Methods.* (1991) 39:253–62. doi: 10.1016/0165-0270(91)90104-8

29. Cooper DJ, Rosenfeld JV, Murray L, Arabi YM, Davies AR, D'urso P, et al. Decompressive craniectomy in diffuse traumatic brain injury. *N Engl J Med.* (2011) 364:1493–502. doi: 10.1056/NEJMoa1102077

30. Ucar T, Akyuz M, Kazan S, Tuncer R. Role of decompressive surgery in the management of severe head injuries: prognostic factors and patient selection. *J Neurotrauma.* (2005) 22:1311–8. doi: 10.1089/neu.2005.22.1311

31. Aarabi B, Hesdorffer DC, Ahn ES, Aresco C, Scalea TM, Eisenberg HM. Outcome following decompressive craniectomy for malignant swelling due to severe head injury. *J Neurosurg.* (2006) 104:469–79. doi: 10.3171/jns.2006.104.4.469

32. Timofeev I, Kirkpatrick PJ, Corteen E, Hiler M, Czosnyka M, Menon DK, et al. Decompressive craniectomy in traumatic brain injury: outcome following protocol-driven therapy. *Acta Neurochir Suppl.* (2006) 96:11–6. doi: 10.1007/3-211-30714-1_3

33. Cooper DJ, Rosenfeld JV, Murray L, Arabi YM, Davies AR, Ponsford J, et al. Patient outcomes at twelve months after early decompressive craniectomy for diffuse traumatic brain injury in the randomized DECRA clinical trial. *J Neurotrauma.* (2020) 37:810–6. doi: 10.1089/neu.2019.6869

34. Hutchinson PJ, Kolias AG, Timofeev IS, Corteen EA, Czosnyka M, Timothy J, et al. Trial of decompressive craniectomy for traumatic intracranial hypertension. *N Engl J Med.* (2016) 375:1119–30. doi: 10.1056/NEJMoa1605215

35. Neuwelt E, Abbott NJ, Abrey L, Banks WA, Blakley B, Davis T, et al. Strategies to advance translational research into brain barriers. *Lancet Neurol.* (2008) 7:84–96. doi: 10.1016/S1474-4422(07)70326-5

36. Glushakova OY, Johnson D, Hayes RL. Delayed increases in microvascular pathology after experimental traumatic brain injury are associated with prolonged

inflammation, blood-brain barrier disruption, and progressive white matter damage. *J Neurotrauma.* (2014) 31:1180–93. doi: 10.1089/neu.2013.3080

37. Hawkins BT, Davis TP. The blood-brain barrier/neurovascular unit in health and disease. *Pharmacol Rev.* (2005) 57:173–85. doi: 10.1124/pr.57.2.4

38. Keaney J, Campbell M. The dynamic blood-brain barrier. *FEBS J.* (2015) 282:4067–79. doi: 10.1111/febs.13412

39. Rosenberg GA. Matrix metalloproteinases and their multiple roles in neurodegenerative diseases. *Lancet Neurol.* (2009) 8:205–16. doi: 10.1016/S1474-4422(09)70016-X

40. Ye L, Huang Y, Zhao L, Li Y, Sun L, Zhou Y, et al. IL-1β and TNF-α induce neurotoxicity through glutamate production: a potential role for neuronal glutaminase. *J Neurochem.* (2013) 125:897–908. doi: 10.1111/jnc.12263

41. Alves JL. Blood-brain barrier and traumatic brain injury. *J Neurosci Res.* (2014) 92:141–7. doi: 10.1002/jnr.23300

42. Hailer NP. Immunosuppression after traumatic or ischemic CNS damage: it is neuroprotective and illuminates the role of microglial cells. *Prog Neurobiol.* (2008) 84:211–33. doi: 10.1016/j.pneurobio.2007.12.001

43. Woodcock T, Morganti-Kossmann MC. The role of markers of inflammation in traumatic brain injury. *Front Neurol.* (2013) 4:18. doi: 10.3389/fneur.2013.00018

44. Dunn SL, Young EA, Hall MD, Mcnulty S. Activation of astrocyte intracellular signaling pathways by interleukin-1 in rat primary striatal cultures. *Glia.* (2002) 37:31–42. doi: 10.1002/glia.10010

45. Penkowa M, Giralt M, Lago N, Camats J, Carrasco J, Hernández J, et al. Astrocyte-targeted expression of IL-6 protects the CNS against a focal brain injury. *Exp Neurol.* (2003) 181:130–48. doi: 10.1016/S0014-4886(02)00051-1

46. Rangel-Castilla L, Gasco J, Nauta HJ, Okonkwo DO, Robertson CS. Cerebral pressure autoregulation in traumatic brain injury. *Neurosurg Focus.* (2008) 25:E7. doi: 10.3171/FOC.2008.25.10.E7

47. Immonen R, Heikkinen T, Tähtivaara L, Nurmi A, Stenius TK, Puoliväli J, et al. Cerebral blood volume alterations in the perilesional areas in the rat brain after traumatic brain injury–comparison with behavioral outcome. *J Cereb Blood Flow Metab.* (2010) 30:1318–28. doi: 10.1038/jcbfm.2010.15

48. Sorby-Adams AJ, Marcoionni AM, Dempsey ER, Woenig JA, Turner RJ. The role of neurogenic inflammation in blood-brain barrier disruption and development of cerebral oedema following acute central nervous system (CNS) injury. *Int J Mol Sci.* (2017) 18:1788. doi: 10.3390/ijms18081788

49. Ho CL, Wang CM, Lee KK, Ng I, Ang BT. Cerebral oxygenation, vascular reactivity, and neurochemistry following decompressive craniectomy for severe traumatic brain injury. *J Neurosurg.* (2008) 108:943–9. doi: 10.3171/JNS/2008/108/5/0943

50. Weiner GM, Lacey MR, Mackenzie L, Shah DP, Frangos SG, Grady MS, et al. Decompressive craniectomy for elevated intracranial pressure and its effect on the cumulative ischemic burden and therapeutic intensity levels after severe traumatic brain injury. *Neurosurgery.* (2010) 66:1111–8. doi: 10.1227/01.NEU.0000369607.71913.3E

51. Price L, Wilson C, Grant G. "Frontiers in neuroscience blood–brain barrier pathophysiology following traumatic brain injury," in *Translational Research in Traumatic Brain Injury*, eds D. Laskowitz and G. Grant (Boca Raton, FL: CRC Press/Taylor and Francis Group © 2016 by Taylor & Francis Group, LLC (2016).

52. Sofroniew MV. Molecular dissection of reactive astrogliosis and glial scar formation. *Trends Neurosci.* (2009) 32:638–47. doi: 10.1016/j.tins.2009.08.002

53. Colombo E, Farina C. Astrocytes: key regulators of neuroinflammation. *Trends Immunol.* (2016) 37:608–20. doi: 10.1016/j.it.2016.06.006

54. Karve IP, Taylor JM, Crack PJ. The contribution of astrocytes and microglia to traumatic brain injury. *Br J Pharmacol.* (2016) 173:692–702. doi: 10.1111/bph.13125

55. Loane DJ, Kumar A. Microglia in the TBI brain: the good, the bad, and the dysregulated. *Exp Neurol.* (2016) 275:316–27. doi: 10.1016/j.expneurol.2015.08.018

56. Zhou Y, Shao A, Yao Y, Tu S, Deng Y, Zhang J. Dual roles of astrocytes in plasticity and reconstruction after traumatic brain injury. *Cell Commun Signal.* (2020) 18:62. doi: 10.1186/s12964-020-00549-2

57. Kim HJ, Fillmore HL, Reeves TM, Phillips LL. Elevation of hippocampal MMP-3 expression and activity during trauma-induced synaptogenesis. *Exp Neurol.* (2005) 192:60–72. doi: 10.1016/j.expneurol.2004.10.014

58. Madathil SK, Carlson SW, Brelsfoard JM, Ye P, D'ercole AJ, Saatman KE. Astrocyte-specific overexpression of insulin-like growth factor-1 protects hippocampal neurons and reduces behavioral deficits following traumatic brain injury in mice. *PLoS ONE.* (2013) 8:e67204. doi: 10.1371/journal.pone.0067204

59. Myer DJ, Gurkoff GG, Lee SM, Hovda DA, Sofroniew MV. Essential protective roles of reactive astrocytes in traumatic brain injury. *Brain.* (2006) 129:2761–72. doi: 10.1093/brain/awl165

60. Di Giovanni S, Movsesyan V, Ahmed F, Cernak I, Schinelli S, Stoica B, et al. Cell cycle inhibition provides neuroprotection and reduces glial proliferation and scar formation after traumatic brain injury. *Proc Natl Acad Sci USA.* (2005) 102:8333–8. doi: 10.1073/pnas.0500989102

61. Michinaga S, Koyama Y. Pathophysiological responses and roles of astrocytes in traumatic brain injury. *Int J Mol Sci.* (2021) 22:6418. doi: 10.3390/ijms22126418

62. Marina N, Christie IN, Korsak A, Doronin M, Brazhe A, Hosford PS, et al. Astrocytes monitor cerebral perfusion and control systemic circulation to maintain brain blood flow. *Nat Commun.* (2020) 11:131. doi: 10.1038/s41467-019-13956-y

63. Chesnut RM, Temkin N, Carney N, Dikmen S, Rondina C, Videtta W, et al. A trial of intracranial-pressure monitoring in traumatic brain injury. *N Engl J Med.* (2012) 367:2471–81. doi: 10.1056/NEJMoa1207363

frontiers | Frontiers in Neurology

ORIGINAL RESEARCH
published: 05 August 2022
doi: 10.3389/fneur.2022.938076

A Novel Therapeutic Approach With Sodium Pyruvate on Vital Signs, Acid–Base, and Metabolic Disturbances in Rats With a Combined Blast and Hemorrhagic Shock

*Biswajit Saha, Geetaram Sahu and Pushpa Sharma**

Department of Anesthesiology, Uniformed Services University of the Health Sciences, Bethesda, MD, United States

OPEN ACCESS

Edited by:
Mårten Risling,
Karolinska Institutet (KI), Sweden

Reviewed by:
Brandon Peter Lucke-Wold,
University of Florida, United States
Mikulas Chavko,
Naval Medical Research Center,
United States

****Correspondence:***
Pushpa Sharma
pushpa.sharma@usuhs.edu

Specialty section:
This article was submitted to Neurotrauma, a section of the journal Frontiers in Neurology

Received: *06 May 2022*
Accepted: *21 June 2022*
Published: *05 August 2022*

Citation:
Saha B, Sahu G and Sharma P (2022) A Novel Therapeutic Approach With Sodium Pyruvate on Vital Signs, Acid–Base, and Metabolic Disturbances in Rats With a Combined Blast and Hemorrhagic Shock. Front. Neurol. 13:938076. doi: 10.3389/fneur.2022.938076

Background: Blast injuries from improvised explosive devices (IEDs) are known to cause blast traumatic brain injuries (bTBIs), hemorrhagic shock (HS), organ damage, mitochondrial dysfunction, and subsequent free radical production. A pre-citric acid cycle reagent, pyruvate, is suggested to improve mitochondrial ATP production through the activation of the mitochondrial gatekeeper enzyme "pyruvate dehydrogenase complex (PDH)." Our study aimed to investigate the role of physiologic, metabolic, and mitochondrial effects of hypertonic sodium pyruvate resuscitation in rats with a combined blast and HS injury.

Methods: A pre-clinical rat model of combined injury with repetitive 20 PSI blast exposure accompanied with HS and fluid resuscitation (sodium pyruvate as metabolic adjuvant or hypertonic saline as control), followed by transfusion of shed blood was used in this study. Control sham animals (instrumental and time-matched) received anesthesia and cannulation, but neither received any injury nor treatment. The mean arterial pressure and heart rate were recorded throughout the experiment by a computerized program. Blood collected at T0 (baseline), T60 (after HS), and T180 (end) was analyzed for blood chemistry and mitochondrial PDH enzyme activity.

Results: Sodium pyruvate resuscitation significantly improved the mean arterial pressure (MAP), heart rate (HR), pulse pressure (PP), hemodynamic stability (Shock index), and autonomic response (Kerdo index) after the HS and/or blast injury. Compared with the baseline values, plasma lactate and lactate/pyruvate ratios were significantly increased. In contrast, base excess BE/(HCO_3^-) was low and the pH was also acidotic <7.3, indicating the sign of metabolic acidosis after blast and HS in all animal groups. Sodium pyruvate infusion significantly corrected these parameters at the end of the experiment. The PDH activity also improved after the sodium pyruvate infusion.

Conclusion: In our rat model of a combined blast and HS injury, hypertonic sodium pyruvate resuscitation was significantly effective in hemodynamic stabilization by correcting the acid–base status and mitochondrial mechanisms *via* its pyruvate dehydrogenase enzyme.

Keywords: blast injury, hemorrhagic shock, sodium pyruvate resuscitation, shock index, metabolic acid-base disorder, pyruvate dehydrogenase complex (PDH) activity

INTRODUCTION

During modern wars and terrorist attacks, improvised explosive devices (IEDs) and roadside bombs are the leading causes of blast traumatic brain injuries (bTBI), death, and disabilities. Blast injury is typically encountered in the context of polytrauma, where multiple organs and body regions are injured from the sharp nails, frequently concomitant severe hemorrhage resulting in hemorrhagic shock (HS). The outcome of blast injury is therefore most often complicated. However, the patients with blast injuries are of particular concern, as there is evidence that the brains of blast-exposed casualties showed blood–brain barrier (BBB) breakdown, oxidative stress, and microglial activation (1), as well as subdural hemorrhage, cerebral contusion, and immunohistopathological changes in the brain (2). Most deaths in such scenarios occur in the pre-hospital (field) setting.

The hemorrhagic shock alone accounts for the preponderance (∼60%) of deaths in patients with potentially salvageable injuries (∼50%) (3). It may cause deleterious hemodynamic consequences and compromise the blood flow to some vital organs. Therefore, the combination of blast traumatic brain injury and HS is particularly onerous. Even brief episodes of hypotension and hypoxemia, clinical hallmarks of HS, double the mortality in patients with TBI. This is thought to be due to loss of cerebral autoregulation resulting in secondary ischemic insult to the already vulnerable brain. TBI, in turn, impairs neurologically mediated physiologic compensatory mechanisms that can be protective against mortality from HS.

The clinical consequences of hemodynamics and metabolic stress become evident shortly after blast injury and HS, while the complete response of secondary cellular injury takes longer due to the depleted cellular energy (ATP) stores and increased oxidative stress from the mitochondrial damage. Among the key mitochondrial metabolic enzymes, pyruvate dehydrogenase (PDH) is very sensitive to oxidative stress (4). This enzyme is especially important to the brain which relies mainly on carbohydrate metabolism. In the injured brain cells, PDH is believed to be inactive, leading to reduced glucose metabolism (5). Also, the mitochondrial dysfunction due to hypoxia after the injuries forces the cells into anaerobic metabolism, leading to the production of acid metabolites causing acidosis or acid–base disturbance. There remains a paucity of information on the nature of the acid–base disturbance and PDH activity in combined insults other than the blast injury or HS alone. There is also limited knowledge of the hemodynamic responses to a combined hemorrhage and blast injury, and their impact on the response to resuscitation in the prehospital setting. In light of this important knowledge gap regarding the distinct challenges associated with the treatment of a combined blast injury and HS in a prehospital setting, our designed study of combined injuries, therefore, cast light to answer the following questions: (1) What is the initial acid–base profile and physiological dysfunction from blast trauma and blood loss? (2) Can the degree of acid–base and physiological derangement be used to predict the mortality from the magnitude of blast injury and blood loss, or the time elapsed from injury to treatment? (3) How severe are the adverse hemodynamic and metabolic effects are from the acidosis? (4) What is the effect of combined injuries on the PDH activity used as an indicator of global oxidative stress?

From the discussion above, it is clear that optimal bTBI management often requires optimal HS management, especially during the pre-hospital phase. Recent studies have suggested that pyruvate, a natural product of the reaction in the last step of the glycolytic pathway, can improve the outcome in animal models with TBI or HS through mitochondrial mechanisms (6–9). In a pyruvate dose response study targeting the vital signs following hemorrhagic shock, our lab previously showed that sodium pyruvate 2.0 M was most effective in multiorgan failure and survival rate in HS (10). However, there is still a knowledge gap since the effects of this agent on a combined blast injury and HS have not been examined. It is, however, unclear if the combined insults are less or more amenable to novel therapies than TBI/HS alone. To address this important knowledge gap, this project, therefore, contributed to the goal of advancing the pre-hospital treatment of polytrauma casualties with blast injury and concomitant HS with the resuscitation of sodium pyruvate, and to check whether this antioxidant and an anti-inflammatory agent will improve the hemodynamics and metabolic derangements. Thus, the combined blast injury plus HS (blast injury + HS) is potentially an important new arena of therapy for use in civilian and blast polytrauma.

MATERIALS AND METHODS

All procedures were performed in accordance with the guidelines of the National Institutes of Health and were approved by the Institutional Animal Care and Use Committee (IACUC) of the Uniformed Services University of the Health Sciences (USUHS) at Bethesda, MD, USA.

Animal Preparation and Surgical Procedures

The procedures were performed according to our established protocol. Adult, male Sprague-Dawley rats (300–350 g) were

obtained from the Charles River Laboratories (Wilmington, MA, USA). The animals were anesthetized with 5% isoflurane in 100% oxygen in an anesthesia induction chamber, and the anesthesia was maintained *via* a nose cone (1.5–2% isoflurane + 100% oxygen). The depth of anesthesia was evaluated before surgery by the response to toe pinch. The spontaneously ventilating animals were instrumented by cannulating both femoral arteries and the right or left femoral vein with polyethylene tubing (PE50), secured with 4-0 silk ties. The cannulas were clamped and connected to closed stopcocks. The tail artery was cannulated to collect the baseline blood sample before any injury.

Blast Injury

We used a well-established rat blast injury model developed in our laboratory. The animals underwent three repeated blast injuries of 20PSI at 15 min interval. Exposure to blast overpressure (BOP) generated in a laboratory shock tube with the Mylar membranes rupturing at predetermined pressure thresholds will produce structural and functional changes in the brain.

Hemorrhagic Shock-Resuscitation Procedure

The instrumented, anesthetized, spontaneously ventilating animals underwent controlled arterial hemorrhage followed by volume/pressure limited resuscitation with hypertonic sodium pyruvate (2M) or hypertonic saline (7.5%) and then full resuscitation using the shed blood.

The right femoral artery was connected to a pressure transducer to monitor the mean arterial pressure (MAP). MAP and heart rate were monitored continuously and recorded every 5 min by computerized programming. The left femoral artery was connected with a catheter to a heparinized syringe to bleed the rat into hemorrhagic shock (HS). The left femoral vein was connected to an infusion pump for fluid/blood infusion. Core temperature was maintained at 37–37.5°C (measured with a rectal temperature probe) throughout the experiment using an electric heat pad.

Induction of Hemorrhagic Shock

Rats were allowed to acclimatize for 5 min and marked as experimental time 0 (**Figure 1**). After circulatory variables (MAP and pulse rate) and biochemical parameters were determined, controlled hemorrhage was induced. Rats were then bled for a 15-min period to a MAP of 40 mmHg. Blood was collected in pre-heparinized tubes. MAP was sustained at 40 mmHg for 40 min by withdrawal or infusion of shed blood.

Blood collected at T0 (baseline), T60 (after HS), and T180 (end) was analyzed for blood chemistry for acid–base balance and metabolites.

Mitochondria is a major subcellular target of ischemia/reperfusion injury, and blast injury/HS has been known to have altered mitochondrial function in various tissues. Oxidative stress has been linked to mitochondrial dysfunction and is thought to play a role in metabolic defects. As part of the mitochondrial metabolic test battery, biochemical analysis was also performed in our study to measure the plasma lactate and pyruvate levels and calculate the plasma lactate/pyruvate concentration ratio at different time-points in response to different injury and treatment groups.

Pyruvate Assay

A total of 100 μl of fresh whole blood was added to a chilled pyruvate collection tube containing 200 μl of 8% (W/V) perchloric acid to deproteinize the blood sample. The sample was mixed well for 30 s, then placed in ice for 10 min. Centrifugation was done for 10 min at 1,500 g. Plasma pyruvate concentration was determined using a kit from Sigma, Catalog no. MAK071.

Our study also rendered the blood mitochondrial enzymatic assay for Pyruvate dehydrogenase complex (PDH) that might suggest global reduction–oxidation (redox) status, aid in prognostication, and potentially guide in using mitochondrial-targeted therapies.

Blood-Based Dipstick Test for the Measurement of Mitochondrial Enzyme, PDH as Biomarker of Mitochondrial Damage

Blood PDH for the samples of different time-points were immunocaptured using a dipstick assay kit according to the manufacturer's guidelines (Abcam, MA, USA) using an immunologic sandwich assay. The intensity of the color band on the dipstick was measured using a flatbed scanner, and the results were analyzed by using the ImageJ software.

Experimental Groups

Group 1. Sham (eight animals): Instrumental and time-matched sham animals received only anesthesia and cannulation but did not undergo any injury or resuscitation except the withdrawal of blood for laboratory investigation.

Groups 2 and 3. Control (eight animals in each group): Control rats received HS+/− blast injury and resuscitation with hypertonic saline (HTS) at a rate of 5 ml/kg/h. The HTS was selected as the control infusion based on the volume and osmolality matched to the hypertonic sodium pyruvate.

Groups 4 and 5. Treatment (eight animals in each group): The treatment groups underwent the injury of HS+/− blast and resuscitation with sodium pyruvate at the same rate of 5 ml/kg/h.

RESULTS

In this study, our major goals were to (i) examine the effects of HS on blast injury and mitochondrial damage (mechanisms) and (ii) determine whether pharmacological protection of mitochondrial impairment with sodium pyruvate can improve the outcome of injury following HS+/− blast. However, the hemodynamic changes after HS+/− blast and infusion with either 2 M sodium pyruvate (NaPyr) or 7.5% saline (HTS) have been described below.

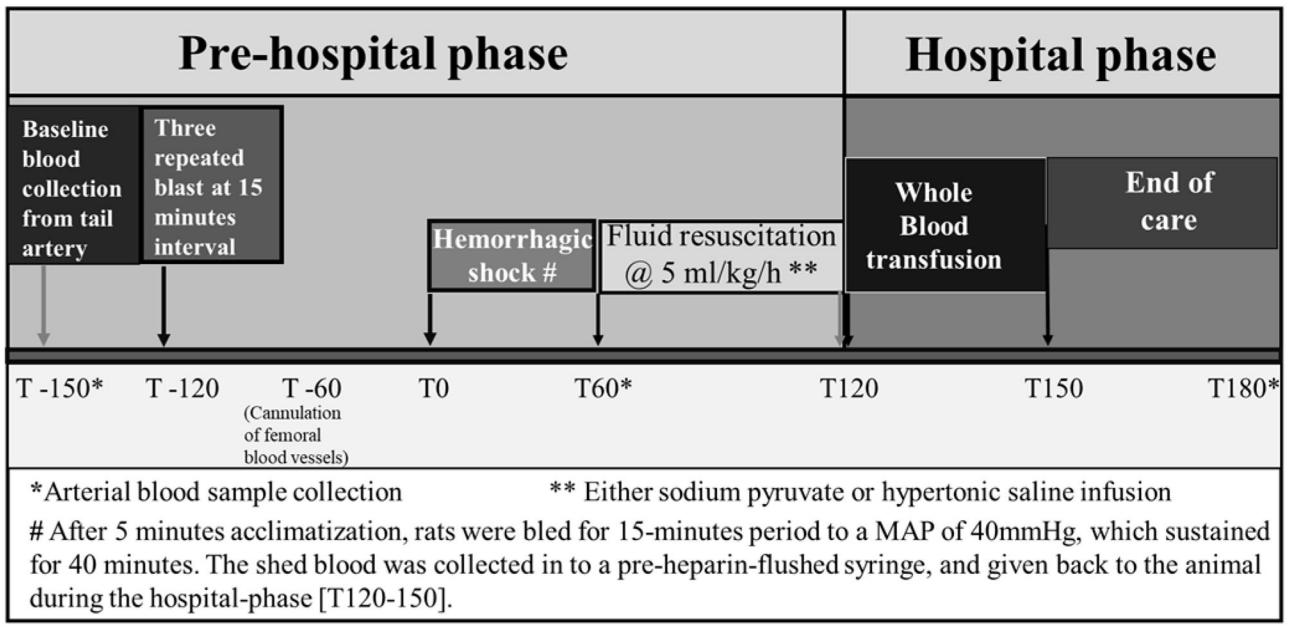

FIGURE 1 | Experimental design established to conduct the study protocol of hemorrhagic shock and/or blast injury.

Sodium Pyruvate Resuscitation Improves Mean Arterial Pressure in Response to a Combined Blast and HS Injury

Data depicted in **Figures 2**, **3** show that MAP was similar in all animals at the baseline (85–90 mmHg) and decreased to ∼40 mmHg in all hemorrhaged groups during the 15–20-min period that put them into HS. The HS was maintained for a total duration of 60 min. Because of the similar weights of the rats, the total shed blood volume did not differ significantly among the different rats (8.42 ± 0.15 mL of blood loss). Mean arterial pressure was measured at 0–180 min in all animals, and differences were noted among the different injury and treatment groups as follows: (i) *Sham animals:* the MAP of the sham group receiving no treatments remained stable between 80 and 92 mmHg throughout the experiment. (ii) *Sodium pyruvate or hypertonic saline infusion in the injured animals (T60–120):* Both pyruvate and hypertonic saline infusions were equally effective in increasing the MAP to or near the baseline value after the HS+/− blast injury. We found a statistically significant ($p < 0.0001$) increase in MAP after HS during the pyruvate or HTS resuscitation. MAP reached a maximum of 78 ± 5 mmHg in the blast + HS group and 88 ± 3 mmHg in the HS-alone group after the pyruvate infusion. Similarly, HTS infusion increased the MAP to the maximum of 87 ± 5 mmHg in the blast + HS animals and 89 ± 5 mmHg in the HS-alone animals. It was noticeable that in comparison to the single injury group with HS alone, the combined injury groups of blast and HS had less increase of MAP during the resuscitative period with sodium pyruvate or hypertonic saline solution. (iii) *Blood transfusion that followed either the sodium pyruvate or hypertonic saline infusion (T120–180):* In our study, we found that blood transfusion was effective in stabilizing the MAP above baseline till the end in all injury and treatment groups. Following both pyruvate and blood infusions, MAP overshot the baseline to 96 ± 5 mmHg in the blast + HS group and 105 ± 3 mmHg in the HS-alone group. Similarly, MAP reached a maximum of 104 ± 3 mmHg in the blast + HS animals and 101 ± 4 mmHg in the HS-alone group after both HTS and blood infusions.

Sodium Pyruvate Resuscitation Improves Heart Rate in Response to a Combined Blast and HS Injury

The baseline measurement (0–5 min) of HR was similar in all rats [345–375 beats per minute (bpm)]. HR decreased to approximately 325 ± 25 bpm during the 60-min period of HS. The HR of the sham animals remained stable between 350.0 ± 5 and 420 ± 5 bpm throughout the experiment. In the pyruvate-treated animals, HR increased to the maximum of 410 ± 12 bpm in the post-blast+HS group and 412 ± 10 bpm in the post-HS-alone group ($p < 0.0001$). Similarly, in the animals infused with HTS, HR reached a maximum of 378 ± 8 bpm in the post blast+HS group and 439 ± 25 bpm in the post-HS-alone group ($p < 0.0001$). However, *the blood transfusion that followed either the sodium pyruvate or hypertonic saline infusion (T120–180)* did not significantly change the HR from those associated with the intravenous fluid infusions.

Sodium Pyruvate Resuscitation Improves Pulse Pressure in Response to a Combined Blast and HS Injury

The compensatory increase in the heart rate in response to volume loss cannot be used alone to indicate the need for

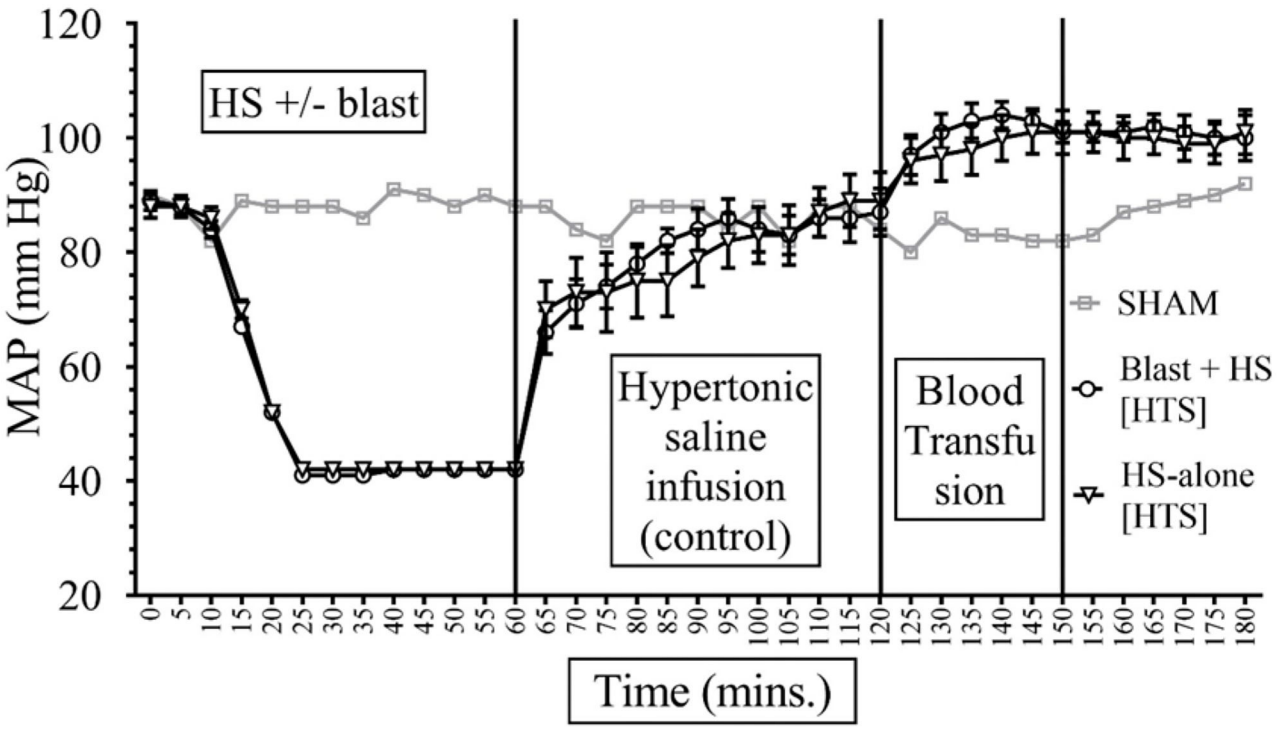

FIGURE 2 | Comparison of Mean Arterial Pressure (MAP) in Mean ± SE between the injury groups of Hypertonic Saline (7.5% saline) infusion ($n = 8$). Assuming that sham represents the normal MAP values for an anesthetized rodent. All rodents had similar MAP during the baseline and HS periods of the experiments. During the HS, the MAP was maintained within 40 s as intended. Intravenous fluid (IVF) infusion of HTS increased MAP toward the normal.

hemorrhage control since it varies widely and can be changed by other variables after injury, including stress and pain. Therefore, when the pulse pressure continues to narrow, it can be used additionally as an indicative of HS, which means that the stroke volume is low. Pulse pressure was similar in all animals in our experiments at the baseline (44–48 mmHg) and decreased to ∼22 ± 1 mmHg during the 60-min period of hemorrhage. Pulse pressure was measured at the T0-180-min mark and differences were noted among the different injury groups and fluid infusions. The PP of the sham group remained stable between 44 ± 1 and 50 ± 1 mmHg throughout the experiment. Sodium pyruvate solution increased the PP in the blast + HS group to the maximum of 42 ± 3 mmHg, while in the HS-alone group, it reached 47 ± 2 mmHg. After resuscitation with the HTS, PP increased to 47 ± 3 mmHg in the blast + HS animals and 48 ± 3 mmHg in the HS-alone injured animals. We found that the increase in PP after each fluid infusion was statistically significant ($p < 0.0001$) and inversely proportional to the severity of the injury, i.e., the combined injury group had less increase in comparison to the single injury group, though not statistically significant. With the blood infusion that followed either the sodium pyruvate or hypertonic saline infusion, the PP of all groups exceeded the baseline value. After both pyruvate and blood infusions, the PP increased to 57 ± 2 mmHg in the HS-alone group and 52 ± 3 mmHg in the blast + HS group. Pulse pressure increased to 55 ± 2 mmHg in the HS-alone group and 56 ± 2 mmHg in the blast+HS group after the HTS and blood infusions.

Sodium Pyruvate Resuscitation Improves Shock Index in Response to a Combined Blast and HS Injury

The formula of SI calculation is: [(HR in beats per minute)/(SBP in mmHg)]. In interpreting results, the normal is 0.5–0.7; elevated SI: (>0.9) was found helpful by Rady et al. to identify patients in the emergency care units requiring admission and/or intensive care despite apparently stable vital signs (11). In our study, data presented in **Figures 4**, **5** show that the baseline measurement (0–5 min) of SI was similar in all groups (2, 3). The highest increase of SI to 6 ± 1 was noticed in the combined injury of blast injury +HS group during the HS. We noticed that the increase in SI was directly proportional to the severity of the injury. The SI of the sham group remained stable between 2 and 3 throughout the experiment. Both sodium pyruvate and hypertonic saline infusions brought the SI to or near baseline value, which was statistically significant ($p < 0.0001$). The pyruvate infusion decreased the SI to 4 ± 0.65 in the blast injury +HS group and 3 ± 0.46 in the HS-alone group. Hypertonic saline infusion decreased the SI to 3 ± 0.6 in both blast injury +HS and HS-alone groups. The blood transfusion that followed

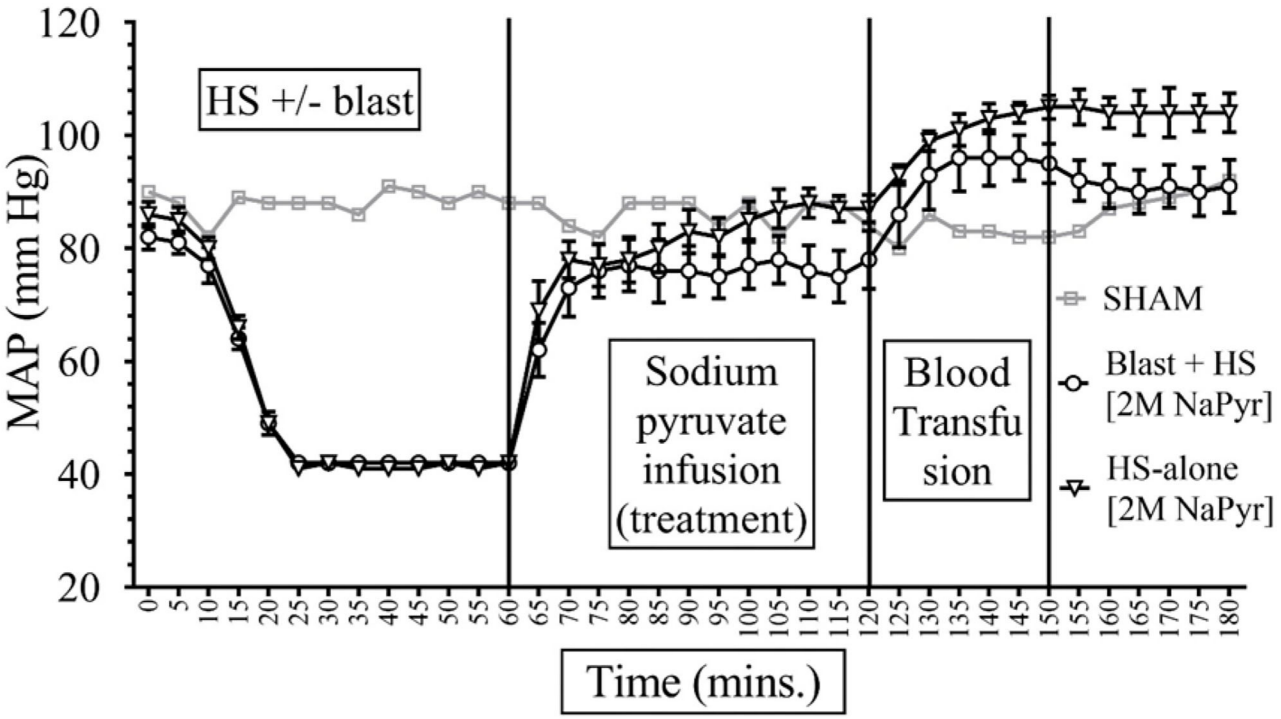

FIGURE 3 | Comparison of Mean Arterial Pressure (MAP) in Mean ± SE between the injury groups of 2M NaPyr infusion ($n = 8$). NaPyr infusion increased the MAP near the baseline. The most significant increase was seen in the HS-alone group in comparison to the combined injury of high-intensity blast+HS. Blood transfusion further increased the MAP above the baseline.

each solution further reduced or maintained the SI at the baseline value.

Sodium Pyruvate Resuscitation Improves the Kerdo Index in Response to a Combined Blast and HS Injury

The KI can be calculated by using the equation (1 – diastolic blood pressure/heart rate) + 100. The KI values above 100 indicate sympathicotonia and values below 100 indicate parasympathicotonia (12). In our study, KI was similar in all animals at the baseline (between 100.79 ± 0.004 and 100.81 ± 0.006) and increased to ∼100.92 ± 0.005 during the HS. The KI of the sham group remained stable between 100.77 ± 0.001 and 100.80 ± 0.001 throughout the experiment. After resuscitation either with the sodium pyruvate or hypertonic saline solution, the KI decreased to the near baseline value. Sodium pyruvate solution decreased the KI the most by −0.09 in the HS-alone group and −0.08 in the blast injury +HS group. Hypertonic saline solution decreased the KI by −0.08 in both blast injury +HS and HS-alone groups. With the blood infusion that followed either the sodium pyruvate or hypertonic saline infusion, all values further decreased at or below the baseline level.

Analysis of Blood Chemistry and Mitochondrial Enzyme

Sodium Pyruvate Resuscitation Improves Plasma Base Excess

Due to the volume deficit after the hemorrhagic shock, our results demonstrated a negative base excess (base deficit) https://www.sciencedirect.com/topics/medicine-and-dentistry/hypoxemia in all of the animals. We noticed an increasing severity of base deficit in the combined injury group of blast injury +HS in comparison to the HS-alone group. We found a decrease in BE/($sHCO_3^-$) associated with ongoing hemorrhage, which was more, i.e., a 6-fold decrease and statistically significant ($p < 0.001$) in the blast+HS group (**Table 1**). Along with the base deficit, the pH was also acidotic, which means that the primary process was metabolic acidosis. In addition, the PCO_2 value decreased from the baseline value during hemorrhage, which also means that the process was metabolic acidosis with compensatory respiratory alkalosis (**Table 2**). This metabolic acidosis was corrected at the end of the experiment after fluid infusion/blood transfusion. But when we compared the sodium pyruvate infusion groups with the hypertonic saline infusion, we noticed sodium pyruvate solution more effectively corrected that metabolic acidosis, which was a 2- to 4-fold increase in BE/($sHCO_3^-$) after HS and statistically significant ($p < 0.001$) too. Sham animals did not have any noticeable changes in the acid–base status during the experiment.

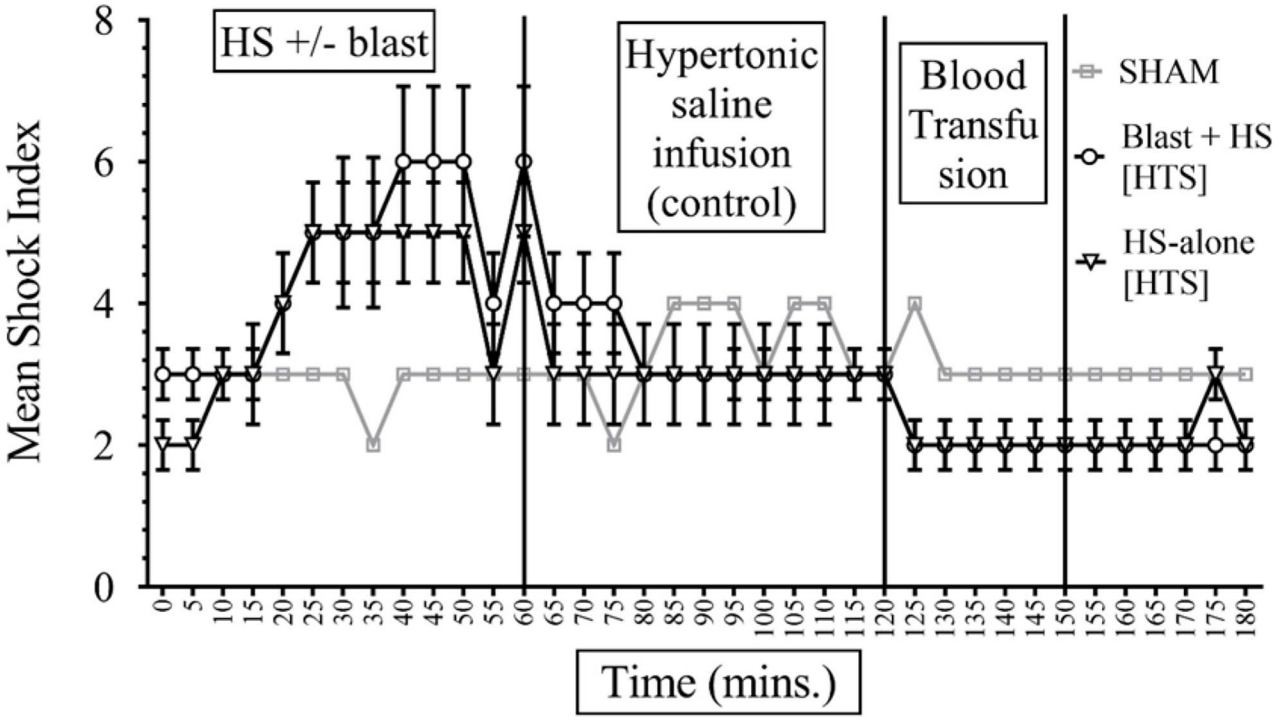

FIGURE 4 | Shock Index (SI) in HS+/− blast injury animals with hypertonic saline (7.5% saline) infusion. Results are in mean ± SE, eight animals per group. SI was higher in the combined injury group in comparison to the HS-alone group after the injury. Hypertonic saline resuscitation decreased the SI to or near the baseline value.

Sodium Pyruvate Resuscitation Improves Plasma Lactate

The changes in mitochondrial activity after the trauma and the possibilities of rapid progression through a secondary cell injury cascade necessitate different therapies to be studied to limit the mitochondrial damage and retain/restore its function after TBI/HS. As mentioned earlier, we aimed to demonstrate the potential therapeutic value of sodium pyruvate in our protocol, which will mediate mitochondrial protection in secondary brain injury. We noticed that the lactate concentration increased after the injury in all blast + HS and HS-alone groups, but when compared between the groups, this was more in the blast + HS animals. This lactate increase after HS was 5-fold and statistically significant ($p < 0.001$) from the baseline values in all blast + HS animal groups. The lactate concentration decreased at the end of experiments after both intravenous fluid infusions with no superiority to each other. So, the addition of pyruvate in this model resulted in less acidosis and lower lactate-level, indicating that the pyruvate was shunted toward aerobic respiration (**Table 3**).

Sodium Pyruvate Resuscitation Improves Lactate Clearance

In our experiments, lactate clearance was calculated using the following formula: lactate clearance = ($lactate_{afterHS} - lactate_{endvalue}$)/$lactate_{afterHS}$ × 100 (expressed as percentage change after the injury). We found a positive lactate clearance indicating a decrease of lactate over time in the surviving blast injury + HS and HS-alone groups after each fluid infusion/treatment, with the largest decrease in lactate (>60%) over 2 h. In animals with continuously increased lactate levels, there was no lactate clearance, which caused them to die early. So, we could conclude that lactate clearance may potentially be a useful tool to predict mortality, as lower lactate clearance is associated with increased mortality.

Sodium Pyruvate Resuscitation Improves Plasma Lactate/Pyruvate Ratio

Analysis of pyruvate along with lactate is of diagnostic importance that may suggest any error of metabolism as some present with lactic acidosis and/or a high lactate-to-pyruvate (L/P) ratio, a measure of NADH/NAD+ redox state in the circulation. In our experiments, we did not find any noticeable changes in the pyruvate levels at any time-points in different injury and treatment groups.

Usually, an L:P ratio >25 is considered increased and suggestive of a primary (or secondary) respiratory chain dysfunction and resultant production of the toxic reactive oxygen species (ROS). In our experiments, this condition occurred, i.e., the L/P ratio in blood was above 25 in all instances after the HS due to hypoxia, especially more and statistically significant ($p < 0.001$) changes from the baseline when this HS was combined with the highest intensity (20 PSI) blast injury (**Figure 6**). Here in our experiments, the increased L/P ratio was mainly due to

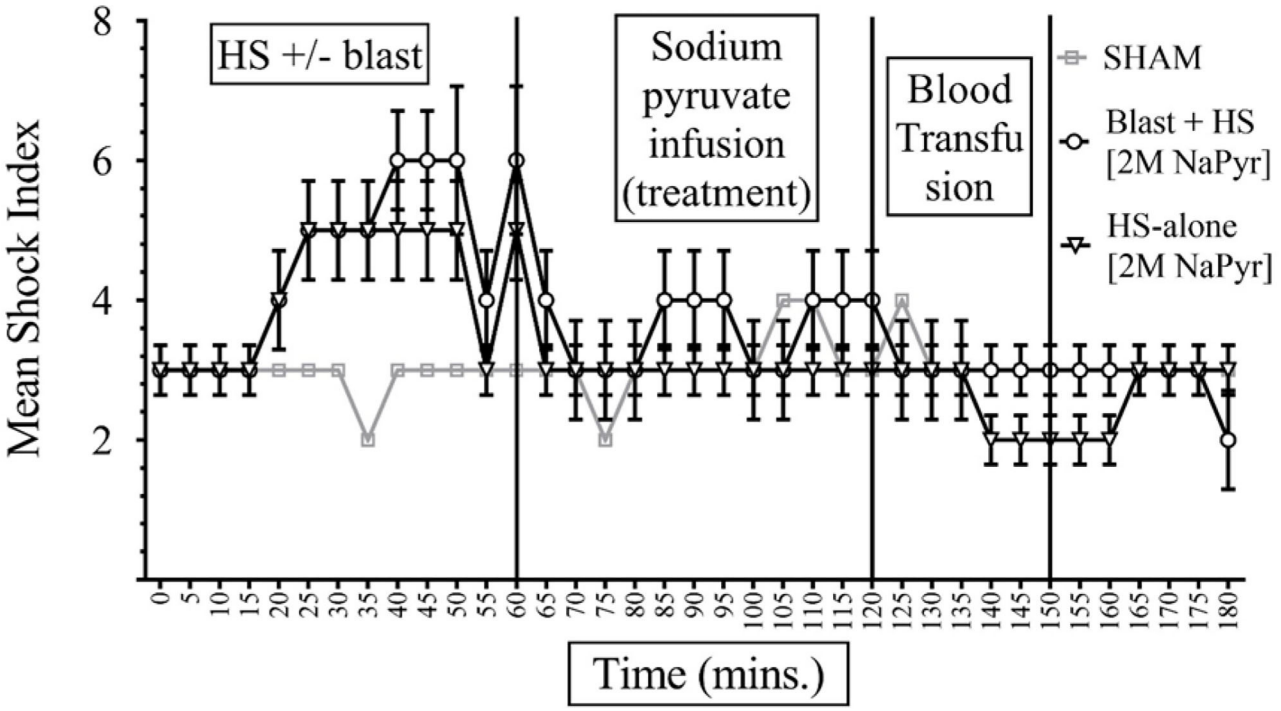

FIGURE 5 | Shock Index (SI) in HS+/− blast injury animals with 2M NaPyr infusion. Results are in Mean ± SE, eight animals per group. SI was higher in the combined injury group in comparison to the HS-alone group after the injury. After the sodium pyruvate resuscitation, SI decreased better near to the baseline value in the HS-alone group in comparison to the combined injury group.

the increased lactate levels as there were no noticeable changes in the plasma pyruvate levels. Fluid infusions of all treatment and control solutions effectively decreased the L/P ratio at the end of the experiment, indicating that the pyruvate was shunted toward aerobic respiration.

Sodium Pyruvate Resuscitation Improves Hyperglycemia

Our study showed an altered energy metabolism after the injury. We noticed an almost 2-fold increase in total blood glucose levels after the injuries of HS and/or blast because there was a limited amount of oxygen, and hence might promote the anaerobic glycolysis. In our experiments, after infusion of sodium pyruvate or hypertonic saline solution and blood transfusion, the increased blood glucose levels returned to the near baseline value at the end (**Table 3**).

Sodium Pyruvate Resuscitation Improves PDH Activity After the Injury

Our objective behind the use of PDH activity as a biomarker of blast injury/HS is that the dysfunctional mitochondria in the injured brain results in leakage of toxic free radicals into its matrix, cytosol, and subsequently into the circulation resulting in secondary cell injury and neuronal cell death. Therefore, the consequences of blast injury/HS on oxidative stress should reflect the PDH activity in blood.

In our experiments, we found a 62–76% decrease in PDH activity from the baseline value after the combined injury of blast and HS. In comparison to that, there was a 43–65% decrease in PDH activity in the single injury group of HS-alone. So, the decreased activity of PDH was inversely proportional to the severity of the injury and statistically significant ($p < 0.001$) too (**Figure 7**). The enzyme activity improved better after the sodium pyruvate infusion in comparison to the control hypertonic saline infusion.

DISCUSSION

As many as 50% of civilian urban, 80% of civilian rural, and 90% of military trauma fatalities occur before hospital arrival (3, 13). Consequently, most patients do not benefit from transformational improvements in hospital trauma care that have occurred over the last decades. These data show that improving pre-hospital resuscitation outcomes should be a key priority of traumatologists, representing a major unmet medical need.

Standard pre-hospital treatment includes basic life support, hemostasis efforts, and intravenous fluid resuscitation. The main objective of fluid resuscitation is volume replacement for the lost blood, restoration of vital signs, improvement of oxygen metabolism, prevention of cell death, organ damage, and enhancement of survival. The standard high-volume isosmotic resuscitation fluids restore intravascular volume but

TABLE 1 | Acid–base balance in mean ± SE.

Parameters	Groups	Time points		
		Baseline	End of hemorrhage	End of resuscitation
P H	Sham	7.41 ± 0.02	7.43 ± 0.01	7.38 ± 0.01
	Blast injury +HS ($n = 8$) (7.5% Saline infusion)	7.18 ± 0.03	7.02 ± 0.03	7.1 ± 0.02
	Blast injury + HS ($n = 8$) (2M NaPyr infusion)	7.18 ± 0.01	7.06 ± 0.02	7.22 ± 0.04
	HS-alone ($n = 8$) (7.5% Saline infusion)	7.1 ± 0.03	7.04 ± 0.03	7 ± 0.09
	HS-alone ($n = 8$) (2M NaPyr infusion)	7.03 ± 0.02	7.04 ± 0.02	7.27 ± 0.04
BE (mmol/L)	Sham	2.67 ± 0.93	−0.89 ± 0.72	5.44 ± 1.06
	Blast injury + HS ($n = 8$) (7.5% Saline infusion)	1 ± 0.73	−9.83 ± 1.11*	0.33 ± 0.76
	Blast injury + HS ($n = 8$) (2M NaPyr infusion)	2.25 ± 0.7	−10.13 ± 1.2*	12.63 ± 3.39∧
	HS-alone ($n = 8$) (7.5% Saline infusion)	−6.17 ± 0.83	−11 ± 2.14	0 ± 0.91
	HS-alone ($n = 8$) (2M NaPyr infusion)	−7 ± 1.52	−6.88 ± 1.23	19.14 ± 0.97∧
HCO3 (mmol/L)	Sham	27.22 ± 0.83	23.32 ± 0.57	31.71 ± 0.86
	Blast injury + HS ($n = 8$) (7.5% Saline infusion)	29.52 ± 0.73	20.87 ± 1.13*	29.82 ± 0.89
	Blast injury + HS ($n = 8$) (2M NaPyr infusion)	30.58 ± 0.53	20.24 ± 1.12*	40.46 ± 2.91∧
	HS-alone ($n = 8$) (7.5% Saline infusion)	23.47 ± 0.59	19.88 ± 2.01	29.82 ± 1.03
	HS-alone ($n = 8$) (2M NaPyr infusion)	23.66 ± 1.38	23.36 ± 1.32	45.81 ± 0.83∧

*Results indicated that there was metabolic acidosis in all animals after HS, especially more in the combined injury group. *$p < 0.001$, when compared with "baseline value" of the same group. ∧$p < 0.001$, when compared with the "end of hemorrhage" value of the same group.*

dilute O_2 content, further contributing to tissue hypoxia and anaerobic metabolism. Blood transfusions can be life-saving but are rarely available before hospital arrival as it requires refrigeration and typing. Consequently, mortality remains high for patients with severe HS (∼1 in 2) with current standard care. Therefore, one major issue with current standards for resuscitation of HS patients with concomitant blast injury appears to be providing adequate tissue (brain and other vital organs) oxygenation/cellular respiration without exacerbating cerebral edema with hypotonic volume overload.

In this study, using a rat model of HS+/− blast, we have demonstrated that infusion of low-volume hypertonic sodium pyruvate (HSP) solution as a metabolic adjuvant is significantly better in normalizing the physiologic measures while reducing cellular injury. Administration of sodium pyruvate during the pre-hospital phase of our study hastened restitution of hemodynamic and metabolic function. Our investigation was also the first to document the effects of sodium pyruvate infusion in the setting of combined brain trauma and hemorrhagic shock.

Intravenous Sodium Pyruvate Effects on Hemodynamics

Explosions can potentially cause massive hemorrhage, thus causing hemodynamic instability and putting a management challenge. Our study demonstrated that the hemodynamic triad of immediate bradycardia, hypotension, and increased Shock index was directly proportional to the severity of the injury, i.e., in the combined injury of blast + HS, there were more deleterious effects on hemodynamic parameters compared to the HS-alone trauma. In our hemorrhaging explosion-injured animals, after the start of the protocol infusions, both pyruvate and osmotic control groups significantly increased the MAP and HR, a measure of the myocardial contractile performance and ATP demand. These post-resuscitation improvements in hemodynamic parameters also depended on the severity of the injury. Pyruvate is a readily oxidized mitochondrial fuel that can be easily transported across the mitochondrial membrane. So, the post-resuscitation improvement in cardiac function could possibly be attributed to increased energy supply for cardiac work afforded by mitochondrial ATP production, thus resulting in enhanced myocardial energetic stability.

TABLE 2 | Blood gases in mean ± SE.

Parameters	Groups	Time points		
		Baseline	End of hemorrhage	End of resuscitation
PCO2 (mmHg)	Sham	43.56 ± 2.37	40.86 ± 1.62	54.88 ± 3.32
	Blast injury + HS ($n = 8$) (7.5% saline infusion)	81.05 ± 7.47	71.6 ± 8.8	95.97 ± 5.66
	Blast injury + HS ($n = 8$) (2M NaPyr infusion)	81.56 ± 2.06	72.19 ± 4.43	102.06 ± 7.69
	HS-alone ($n = 8$) (7.5% saline infusion)	75.77 ± 4.74	74.68 ± 9.35	104.08 ± 7.25
	HS-alone ($n = 8$) (2M NaPyr infusion)	89.26 ± 8.05	88.53 ± 5.49	102.93 ± 8.92
PO2 (mmHg)	Sham	360.17 ± 16.60	326.22 ± 19.81	414.89 ± 23.09
	Blast injury + HS ($n = 8$) (7.5% saline infusion)	305 ± 13.61	309.17 ± 14.25	408.83 ± 12
	Blast injury + HS ($n = 8$) (2M NaPyr infusion)	354.38 ± 14.87	298.38 ± 8.75	358.75 ± 14.89
	HS-alone ($n = 8$) (7.5% saline infusion)	308.17 ± 6.96	317 ± 15.67	410.67 ± 40.53
	HS-alone ($n = 8$) (2M NaPyr infusion)	313.75 ± 8.09	323.88 ± 19.6	397 ± 18.81
ETCO2 (mmol/L)	Sham	28.50 ± 0.87	24.44 ± 0.58	33.33 ± 0.92
	Blast injury + HS ($n = 8$) (7.5% saline infusion)	31.83 ± 0.87	23.33 ± 1.38	32.83 ± 1.05
	Blast injury + HS ($n = 8$) (2M NaPyr infusion)	33 ± 0.5	22.38 ± 1.32	43.38 ± 2.95
	HS-alone ($n = 8$) (7.5% saline infusion)	25.83 ± 0.65	22.17 ± 2.18	32.8 ± 1.17
	HS-alone ($n = 8$) (2M NaPyr infusion)	26 ± 1.49	26.38 ± 1.5	48.29 ± 0.67

The results are (Mean ± SE) of blood gases of eight animals per group in response to blast/HS and resuscitation. The PCO_2 value decreased from the baseline value after HS to compensate metabolic acidosis with compensatory respiratory alkalosis.

In this study, both the treatment and control solutions were efficacious in lowering the Shock index and the ratio of the HR to SBP. SI is a sensitive indicator of left ventricular dysfunction that can be elevated following a reduction in left ventricular stroke work (14). SI can display variability in critical patients displaying normal vital signs (15). Persistently elevated SI is also associated with poor outcomes in critically ill patients (16).

In this study, the shock induced in the combined injury of blast overpressure and hemorrhage might be multifactorial due to hemorrhagic and non-hemorrhagic causes. The severe TBI caused by repeated high-intensity (20 PSI) blast exposure might cause cardiovascular abnormalities in the animals. The hypotension might result from the disruption of brainstem centers for hemodynamic control associated with diffused axonal injury. However, hemorrhagic shock is a type of hypovolemic shock. This study developed as a result of intravascular volume loss due to bleeding out of the body, causing insufficient oxygen delivery to the cells. Restoration of intravascular volume was maintained in this study either with the sodium pyruvate or concentrated saline solution in an effort to stabilize the arterial blood pressure and protect the brain from secondary brain injury. In our study, the infusion of sodium pyruvate significantly ($P < 0.050$) increased the arterial blood pressure after the hemorrhagic shock.

The controlled resuscitation with the sodium pyruvate solution after the hemorrhagic shock introduces a potent, membrane-permeable antioxidant to the systemic circulation, which is thought to be capable of neutralizing the reactive oxygen and nitrogen species responsible for initiating the systemic inflammatory cascades (17–20). The antioxidant and anti-inflammatory capabilities of sodium pyruvate (17, 18), which is unique among the metabolic substrates, might have played a role in protecting the myocardium and possibly the vascular endothelium, thus stabilizing the systemic arterial pressure.

Acute hemorrhagic shock is known to reduce the contractility of the left ventricle. Pyruvate, a key intermediate of oxidative metabolism, has been shown to exert positive-inotropic effects on the heart and improves the contractile function as well as the hemodynamics both *in vivo* and *in vitro* (21–23). In this investigation, the improved arterial blood pressure, and, therefore, survival could probably be ascribed to (1) enhanced cardiac performance, and (2) increased cardiac tolerance to decreases in the MAP and ischemia.

Circulating pyruvate might also have helped maintain vascular performance by elevating the circulating HCO_3^- and base excess

TABLE 3 | Blood metabolites in mean ± SE.

Parameters	Groups	Time points		
		Baseline	End of hemorrhage	End of resuscitation
Glucose (mg/dL)	Sham	172 ± 4.88	139.75 ± 0.28	158.00 ± 4.63
	Blast injury + HS ($n = 8$) (7.5% saline infusion)	232.33 ± 11.37	354.33 ± 22.63*	191.5 ± 9.87∧
	Blast injury + HS ($n = 8$) (2M NaPyr infusion)	257.38 ± 10.53	345.13 ± 25.62*	178.5 ± 14.33∧
	HS-alone ($n = 8$) (7.5% saline infusion)	167.17 ± 10.2	271.33 ± 32.86*	148.67 ± 20.76∧
	HS-alone ($n = 8$) (2M NaPyr infusion)	158.75 ± 8.94	294.88 ± 20.14*	175.71 ± 7.94∧
Lactate (mmol/L)	Sham	1.01 ± 0.20	0.76 ± 0.04	1.17 ± 0.08
	Blast injury + HS ($n = 8$) (7.5% saline infusion)	0.62 ± 0.08	2.26 ± 0.18*	0.79 ± 0.18∧
	Blast injury + HS ($n = 8$) (2M NaPyr infusion)	0.54 ± 0.04	2.48 ± 0.55*	1.60 ±0.31
	HS-alone ($n = 8$) (7.5% saline infusi on)	0.59 ± 0.08	2.09 ± 0.60*	0.65 ± 0.18∧
	HS-alone ($n = 8$) (2M NaPyr infusion)	0.68 ± 0.11	1.66 ± 0.38	1.14 ± 0.17

*Data are presented as mean ± standard error of the mean (SEM), n = 8 animals in each group. Animals with combined blast and HS had both higher lactate and glucose levels compared with single injury. *$p < 0.001$, when compared with "baseline value" of the same group. ∧$p < 0.001$, when compared with the "end of hemorrhage" value of the same group.*

as evidenced in these experiments, thereby affording a more favorable acid–base chemistry profile to offset acidemia resulting from end-organ hypoxia.

Intravenous Sodium Pyruvate Effects on Blood Acid–Base Status, Lactate and Glucose Levels, and Lactate/Pyruvate Ratio

Metabolic Acidosis

The metabolic derangement is a key hallmark of major traumatic injury. As shown in this study, severe hemodynamic shifts were achieved due to the development of metabolic acidosis and some compensation after hemorrhagic shock. During shock, the decreased cardiac output, tachycardia, hypotension, and hypovolemic shock cause inadequate organ perfusion and oxygen delivery that interfere with aerobic metabolism. Increased anaerobic metabolism leads to the production of lactic acid and metabolic acidosis. The body's buffering capacity is reduced due to the loss of bicarbonate and hemoglobin during the hemorrhage. In our experiments, we observed statistically significant ($p < 0.05$) metabolic aberrations in plasma that were triggered by brain trauma and hemorrhagic shock, especially more in the combined injury groups in comparison to the single injury groups. This metabolic acidosis statistically significantly ($p < 0.05$) got corrected at the end of the experiment after pyruvate infusion.

Compensatory mechanisms for acid–base disturbances and blood gases: In the presence of metabolic acidosis after the hemorrhage, we noticed that the PCO_2 value decreased from the baseline value, which means that the process was metabolic acidosis with compensatory respiratory alkalosis. The respiratory system responds to metabolic acidosis quickly and predictably by hyperventilation, causing more CO_2 elimination through the stimulation of central chemoreceptors in the medulla and peripheral chemoreceptors in the carotid and aortic bodies. Over time, the respiratory compensation improved the acidosis after both fluid infusions/blood transfusion in our experiments, but to a greater extent in the pyruvate-treated animals.

Lactic Acidosis

For decades, lactate has been considered an excellent biomarker of oxygen limitation and organ hypoxia. This study aimed to evaluate the frequency of increased plasma lactate levels. We observed that lactic acidosis occurred at the setting of HS+/− blast, where oxygen deficiency is absolute or relative (hypoxia, ischemia, and hypotension). The combined hemorrhagic shock and blast-induced animals had a statistically significant ($p < 0.05$) higher production of lactic acid. After resuscitation with intravenous fluids, all solutions decreased the plasma lactate level near the baseline at T180.

In this study, to assess the metabolic stress after the injury, we also measured the global indexes of the cytosolic redox ratio [lactate/pyruvate (NADHc)/(NADc+)]. We noticed that the critical decreases in oxygen delivery after HS+/− blast injury caused an increase in the lactate/pyruvate ratio, and the pH dropped. These metabolic alterations were caused by both morphologic and enzymatic alterations of mitochondria in several organs. These cellular changes caused by a transient decrease in mitochondrial activity and cellular ATP could lead to secondary permanent mitochondrial damage, causing an irreversible inhibition of mitochondrial

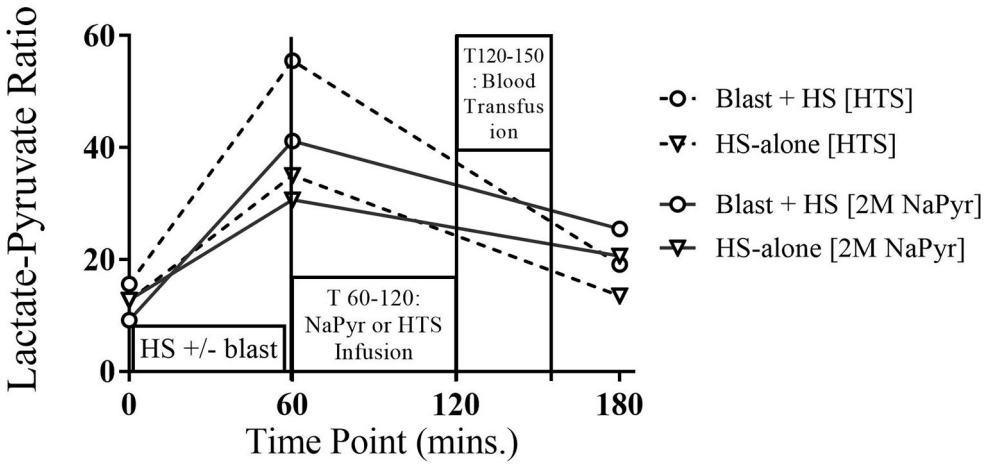

FIGURE 6 | Plasma lactate:pyruvate of 4-h survival animals at different time-points of HS and/or 20 PSI blast injury, and with either sodium pyruvate (treatment) or hypertonic saline (control) infusion. There was a statistically significant ($p < 0.001$) increase in the L:P ratio after the combined blast and HS injury (T60) from the baseline value. The condition greatly improved after both infusions.

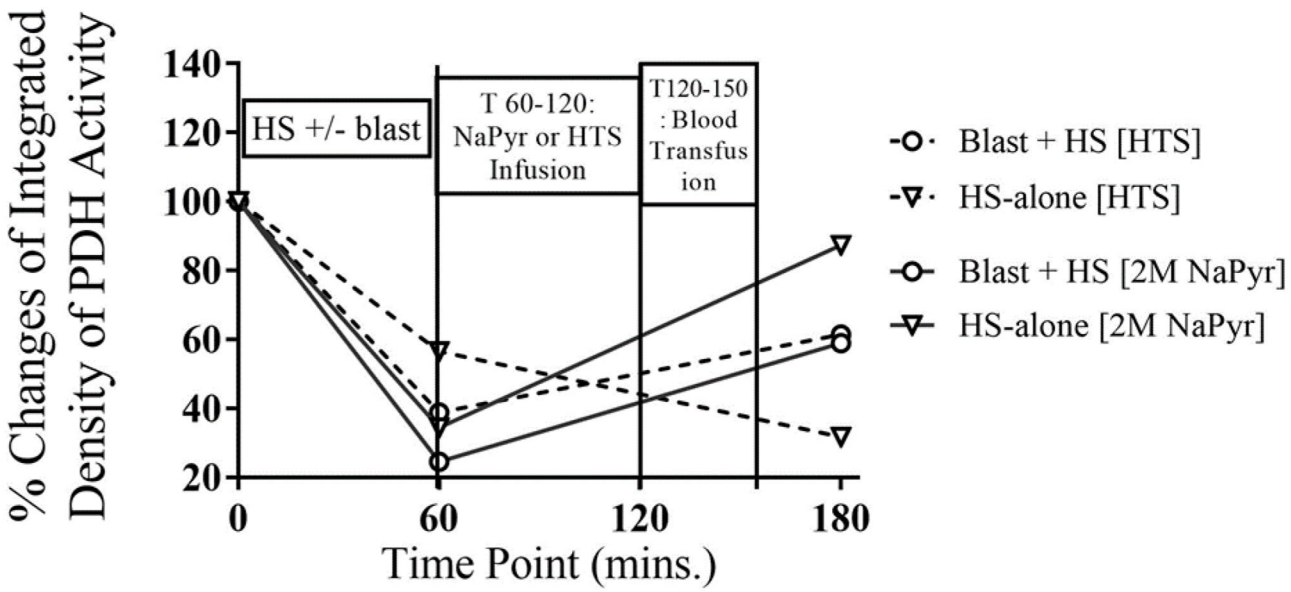

FIGURE 7 | PDH enzyme activity in whole blood at different time-points of HS and/or 20PSI blast injury, and sodium pyruvate (treatment) or hypertonic saline (control) infused animals ($n = 8$) surviving for 4 h. PDH activity decreased from the baseline value in all injury groups at T60, which was not statistically significant. The PDH enzyme activity greatly improved after sodium pyruvate infusion, which was dependent on the severity of the injury. Sham animals did not show any changes that has not been mentioned here.

function (24). Several *in vitro* studies on liver mitochondria indicated this possibility (25). The exogenous administration of sodium pyruvate in our study sharply lowered the arterial lactate/pyruvate ratio in the face of post-injury metabolic stress. The pyruvate-induced decrease in cytoplasmic redox potential [(NADHc)/(NADc+)] bolsters the cellular phosphorylation potential [(ATP)/(ADP)(Pi)] by coupling the cytoplasmic redox state to the phosphorylation potential through the glyceraldehyde-3-phosphate dehydrogenase/phosphoglycerate kinase system (26–28). Thus, maintaining the (ATP)/(ADP)(Pi) within the physiological limits is considered essential to improve cellular function by recovering from the ischemic stress (29, 30). Mongan et al. proposed that pyruvate, by reducing metabolic acidosis and stabilizing the ATP phosphorylation potentials, may suppress the opening of KATP channels, thereby preventing a decrease in intracellular Ca^{2+}, preserving the contractile function of vascular smooth muscle, and stabilizing the vasomotor tone (31–33).

Lactate/Pyruvate Ratio

In TBI patients, it is important to monitor the glucose delivery to the brain, and thus, using the L/P ratio as a marker of balance between the "aerobic" (referring to the TCA cycle) and "anaerobic" metabolism (referring to glycolysis culminating in lactate) (34). The best-known metabolic characteristics of an injured brain are a high lactate concentration and a high lactate/pyruvate (L/P) ratio, which are associated statistically with unfavorable clinical outcomes. When cellular respiration is impaired, as in hypoxia, pyruvate oxidation is reduced, resulting in lactic acidosis. In such situations, reduced forms of oxido-reduction coenzymes (NADH, FADH2) predominate and the L/P ratio increases. As expected, sodium pyruvate resuscitation in our experiments lowered the circulating lactate/pyruvate ratio. This can be considered to indicate the oxidation of NADH within the tissues, thus further protecting the tissue from increased oxidative stress.

Glucose Homeostasis

Mitochondrial dysfunction in HS+/− blast injury impairs the ability to utilize glucose effectively. Pyruvate dehydrogenase (PDH), a key enzyme to modulate glucose oxidation, significantly loses its activity during hypoxia. Sharma et al. demonstrated that TBI causes a significant reduction in PDH enzyme (5). Therefore, the altered glucose homeostasis manifested itself as initial hyperglycemia after the injury in this study. Pyruvate or hypertonic saline resuscitation improved glucose metabolism, and blood glucose levels returned to the near baseline value at the end of our experiments.

Pyruvate Dehydrogenase (PDH) Activity

Pyruvate dehydrogenase is a rate-limiting enzyme of the mitochondrial tri-carboxylic-acid cycle (TCA) and is an important bridge between aerobic and anaerobic respiration. The PDH is a target of oxidative stress, and its activity has been shown to undergo a significant decrease following ischemia (35). Our results demonstrated that PDH was susceptible to damage and inactivation by ROS during blast/HS.

Our study showed a statistically significant ($p < 0.001$) decrease in PDH activity after the HS+/− blast injury. Therefore, the impaired activity of PDH contributed to hyperglycemia and lactic acidosis due to reduced glucose metabolism. The sodium pyruvate treatment in our experiments after the injury improved the PDH activity. The possible mechanisms by which pyruvate was effective in preventing brain injury and loss of PDH activity may be (1) due to its antioxidant properties and (2) to optimize mitochondrial metabolism by providing substrate to PDH enzyme reaction and anaplerotic TCA cycle precursor (pyruvate carboxylase).

Here, in our experiments, the plasma pyruvate concentration did not change after the resuscitation as the improved PDH activity increased the conversion of pyruvate to acetyl-coenzyme A (acetyl-CoA), which serves as fuel for the tricarboxylic acid (TCA) cycle in the next stage of cellular respiration. In our study, we were not sure about the integrity of the electron transport chain (ETC) after the injury to be capable of generating adequate adenosine triphosphate (ATP). So, our future study direction warrants assessing the integrity of the ETC. However, our study had several limitations of not measuring the other physiological parameters [e.g., intracranial pressure (ICP)], and hence was unable to calculate the cerebral perfusion pressure (CPP). Our study also did not complement continuous brain tissue oxygen ($PbtO_2$) monitoring.

In conclusion, it is clear that the dysfunction of mitochondria is the main cause of energy failure and deleterious effects and might play a pivotal role in the secondary insult after bTBI and hemorrhagic shock. The mitochondrial-targeted multipotential therapeutic agent, sodium pyruvate, may provide new hope for the treatment of blast injury and hemorrhagic states. Administration of intravenous pyruvate during the pre-hospital rescue may have a major therapeutic potential for metabolic failure, cardiovascular decompensation, and death.

DATA AVAILABILITY STATEMENT

The original contributions presented in the study are included in the article/supplementary material, further inquiries can be directed to the corresponding author/s.

ETHICS STATEMENT

The animal study was reviewed and approved by the Institutional Animal Care and Use Committee (IACUC) of the Uniformed Services University of the Health Sciences (USUHS) at Bethesda, MD, USA.

AUTHOR CONTRIBUTIONS

PS contributed to the conception and design of the work, acquisition and interpretation of data, and substantial revisions. BS performed the experiments, contributed to data analysis, and significant contribution in writing the manuscript. GS performed biochemical analysis and contributed to animal experiments.

FUNDING

This research was supported by a CDMRP-DM167094 grant to PS.

REFERENCES

1. Readnower RD, Chavko M, Adeeb S, Conroy MD, Pauly JR, McCarron RM, et al. Increase in blood-brain barrier permeability, oxidative stress, and activated microglia in a rat model of blast-induced traumatic brain injury. *J Neurosci Res.* (2010) 88:3530–9. doi: 10.1002/jnr.22510
2. Ahlers ST, Vasserman-Stokes E, Shaughness MC, Hall AA, Shear DA, Chavko M, et al. Assessment of the effects of acute and repeated exposure to blast overpressure in rodents: toward a greater

understanding of blast and the potential ramifications for injury in humans exposed to blast. *Front Neurol.* (2012) 3:32. doi: 10.3389/fneur.2012.00032
3. Bellamy RF. The causes of death in conventional land warfare: implications for combat casualty care research. *Mil Med.* (1984) 149:55–62. doi: 10.1093/milmed/149.2.55
4. Cooper RH, Randle PJ, Denton RM. Stimulation of phosphorylation and inactivation of pyruvate dehydrogenase by physiological inhibitors of the pyruvate dehydrogenase reaction. *Nature.* (1975) 257:808–9. doi: 10.1038/257808a0
5. Sharma P, Benford B, Li ZZ, Ling GS. Role of pyruvate dehydrogenase complex in traumatic brain injury and measurement of pyruvate dehydrogenase enzyme by dipstick test. *J Emerg Trauma Shock.* (2009) 2:67–72. doi: 10.4103/0974-2700.50739
6. Sharma P, Walsh KT, Kerr-Knott KA, Karaian JE, Mongan PD. Pyruvate modulates hepatic mitochondrial functions and reduces apoptosis indicators during hemorrhagic shock in rats. *Anesthesiology.* (2005) 103:65–73. doi: 10.1097/00000542-200507000-00013
7. Mongan PD, Capacchione J, West S, Karaian J, Dubois D, Keneally R, et al. Pyruvate improves redox status and decreases indicators of hepatic apoptosis during hemorrhagic shock in swine. *Am J Physiol Heart Circ Physiol.* (2002) 283:H1634–44. doi: 10.1152/ajpheart.01073.2001
8. Zhou FQ. Pyruvate in the correction of intracellular acidosis: a metabolic basis as a novel superior buffer. *Am J Nephrol.* (2005) 25:55–63. doi: 10.1159/000084141
9. Sharma P, Benford B, Karaian JE, Keneally R. Effects of volume and composition of the resuscitative fluids in the treatment of hemorrhagic shock. *J Emerg Trauma Shock.* (2012) 5:309–15. doi: 10.4103/0974-2700.102372
10. Sharma P, Vyacheslav M, Carissa C, Vanessa R, Bodo M. Pyruvate dose response studies targeting the vital signs following hemorrhagic shock. *J Emerg Trauma Shock.* (2015) 8:159–66. doi: 10.4103/0974-2700.160729
11. Rady MY, Nightingale P, Little RA, Edwards JD. Shock index: a re-evaluation in acute circulatory failure. *Resuscitation.* (1992) 23:227–34. doi: 10.1016/0300-9572(92)90006-X
12. Kérdö I. [An index for the evaluation of vegetative tonus calculated from the data of blood circulation]. *Acta Neuroveg.* (1966) 29:250–68. doi: 10.1007/BF01269900
13. Meislin H, Criss EA, Judkins D, Berger R, Conroy C, Parks B, et al. Fatal trauma: the modal distribution of time to death is a function of patient demographics and regional resources. *J Trauma.* (1997) 43:433–40. doi: 10.1097/00005373-199709000-00008
14. Bodo M, Bothwell S, Dorsey J. Comparison of circulatory stress indicators in a swine model. *Kalokagathia.* (2010) 48:166–81. Available online at: http://drsiposkornel.com/publikaciok/comparison_of_circulatory_stress_indicators.pdf
15. Yealy DM, Delbridge TR. The shock index: all that glitters. *Ann Emerg Med.* (1994) 24:714–5.
16. Cancio LC, Wade CE, West SA, Holcomb JB. Prediction of mortality and of the need for massive transfusion in casualties arriving at combat support hospitals in Iraq. *J Trauma.* (2008) 64(Suppl. 2):S51–5; discussion S5–6. doi: 10.1097/TA.0b013e3181608c21
17. Mallet RT. Pyruvate: metabolic protector of cardiac performance. *Proc Soc Exp Biol Med.* (2000) 223:136–48. doi: 10.1046/j.1525-1373.2000.22319.x
18. Mallet RT, Sun J, Knott EM, Sharma AB, Olivencia-Yurvati AH. Metabolic cardioprotection by pyruvate: recent progress. *Exp Biol Med.* (2005) 230:435–43. doi: 10.1177/153537020523000701
19. Flaherty DC, Mallet RT, Yurvati A. Pyruvate: a physiologic energy substrate and antioxidant for cardiopulmonary bypass. Oxidative stress: clinical and biomedical implications. *Nova Sci Publ.* (2007) 85–102. Available online at: https://experts.unthsc.edu/en/publications/pyruvate-a-physiologic-energy-substrate-and-antioxidant-for-cardi
20. Mallet RT, Sun J. Antioxidant properties of myocardial fuels. *Mol Cell Biochem.* (2003) 253:103–11. doi: 10.1023/A:1026009519783
21. Torres CA, Varian KD, Canan CH, Davis JP, Janssen PM. The positive inotropic effect of pyruvate involves an increase in myofilament calcium sensitivity. *PLoS ONE.* (2013) 8:e63608. doi: 10.1371/journal.pone.0063608
22. Hermann HP, Zeitz O, Lehnart SE, Keweloh B, Datz N, Hasenfuss G, et al. Potentiation of beta-adrenergic inotropic response by pyruvate in failing human myocardium. *Cardiovasc Res.* (2002) 53:116–23. doi: 10.1016/S0008-6363(01)00437-0
23. Martin BJ, Valdivia HH, Bünger R, Lasley RD, Mentzer Jr RM. Pyruvate augments calcium transients and cell shortening in rat ventricular myocytes. *Am J Physiol.* (1998) 274:H8–17. doi: 10.1152/ajpheart.1998.274.1.H8
24. Logsdon AF, Lucke-Wold BP, Nguyen L, Matsumoto RR, Turner RC, Rosen CL, et al. Salubrinal reduces oxidative stress, neuroinflammation and impulsive-like behavior in a rodent model of traumatic brain injury. *Brain Res.* (2016) 1643:140–51. doi: 10.1016/j.brainres.2016.04.063
25. Cheng G, Kong RH, Zhang LM, Zhang JN. Mitochondria in traumatic brain injury and mitochondrial-targeted multipotential therapeutic strategies. *Br J Pharmacol.* (2012) 167:699–719. doi: 10.1111/j.1476-5381.2012.02025.x
26. Bünger R, Mukohara N, Kang YH, Mallet RT. Combined glyceraldehyde-3-phosphate dehydrogenase/phosphoglycerate kinase in catecholamine-stimulated guinea-pig cardiac muscle. Comparison with mass-action ratio of creatine kinase. *Eur J Biochem.* (1991) 202:913–21. doi: 10.1111/j.1432-1033.1991.tb16451.x
27. Scholz TD, Laughlin MR, Balaban RS, Kupriyanov VV, Heineman FW. Effect of substrate on mitochondrial nadh, cytosolic redox state, and phosphorylated compounds in isolated hearts. *Am J Physiol.* (1995) 268:H82–91. doi: 10.1152/ajpheart.1995.268.1.H82
28. Veech RL, Lawson JW, Cornell NW, Krebs HA. Cytosolic phosphorylation potential. *J Biol Chem.* (1979) 254:6538–47. doi: 10.1016/S0021-9258(18)50401-4
29. Bünger R, Mallet RT, Hartman DA. Pyruvate-Enhanced phosphorylation potential and inotropism in normoxic and postischemic isolated working heart. Near-complete prevention of reperfusion contractile failure. *Eur J Biochem.* (1989) 180:221–33. doi: 10.1111/j.1432-1033.1989.tb14637.x
30. Fiolet JW, Baartscheer A, Schumacher CA, Coronel R, ter Welle HF. The change of the free energy of atp hydrolysis during global ischemia and anoxia in the rat heart. Its possible role in the regulation of transsarcolemmal sodium and potassium gradients. *J Mol Cell Cardiol.* (1984) 16:1023–36. doi: 10.1016/S0022-2828(84)80015-2
31. Mongan PD, Fontana JL, Chen R, Bünger R. Intravenous pyruvate prolongs survival during hemorrhagic shock in swine. *Am J Physiol.* (1999) 277:H2253–63. doi: 10.1152/ajpheart.1999.277.6.H2253
32. do Nascimento P, Jr., Vaid SU, Hoskins SL, Espana JM, Kinsky MP, et al. Hypertonic 15% sodium pyruvate offers no initial resuscitation advantage compared with 8% hypertonic nacl in sheep with multiple hemorrhages. *Shock.* (2007) 27:565–71. doi: 10.1097/01.shk.0000245015.96419.73
33. Aalkjaer C, Peng HL. Ph and smooth muscle. *Acta Physiol Scand.* (1997) 161:557–66. doi: 10.1046/j.1365-201X.1997.00263.x
34. Carpenter KL, Jalloh I, Hutchinson PJ. Glycolysis and the significance of lactate in traumatic brain injury. *Front Neurosci.* (2015) 9:112. doi: 10.3389/fnins.2015.00112
35. Martin E, Rosenthal RE, Fiskum G. Pyruvate dehydrogenase complex: metabolic link to ischemic brain injury and target of oxidative stress. *J Neurosci Res.* (2005) 79:240–7. doi: 10.1002/jnr.20293

Author Disclaimer: The views expressed in this article are those of the authors and do not necessarily reflect the official policy or position of the Uniformed Services University, Department of the Navy, Department of Defense, nor the U.S. Government.

Conflict of Interest: The authors declare that the research was conducted in the absence of any commercial or financial relationships that could be construed as a potential conflict of interest.

Publisher's Note: All claims expressed in this article are solely those of the authors and do not necessarily represent those of their affiliated organizations, or those of the publisher, the editors and the reviewers. Any product that may be evaluated in this article, or claim that may be made by its manufacturer, is not guaranteed or endorsed by the publisher.

frontiers | Frontiers in Neurology

TYPE Original Research
PUBLISHED 17 August 2022
DOI 10.3389/fneur.2022.988854

OPEN ACCESS

EDITED BY
Darrin Jason Lee,
University of Southern California,
United States

REVIEWED BY
Guangzhi Ning,
Tianjin Medical University General Hospital, China
Benjamin Yim,
Stanford University, United States

*CORRESPONDENCE
Xian-Jian Huang
xjhuang@email.szu.edu.cn

†These authors have contributed equally to this work

SPECIALTY SECTION
This article was submitted to Neurotrauma,
a section of the journal
Frontiers in Neurology

RECEIVED 07 July 2022
ACCEPTED 01 August 2022
PUBLISHED 17 August 2022

CITATION
Su G-J, Zhang D, Wu J-N, Deng Y-H, Wu C-W, Zhang X-J and Huang X-J (2022) Immunoexpression of MMP-8 and MMP-9 in chronic subdural hematoma. *Front. Neurol.* 13:988854. doi: 10.3389/fneur.2022.988854

Immunoexpression of MMP-8 and MMP-9 in chronic subdural hematoma

Gao-Jian Su†, Di Zhang†, Jia-Nuo Wu, Yu-Hang Deng, Chu-Wei Wu, Xie-Jun Zhang and Xian-Jian Huang*

Department of Neurosurgery, Shenzhen Key Laboratory of Neurosurgery, The First Affiliated Hospital of Shenzhen University, Shenzhen Second People's Hospital, Shenzhen, China

To determine the possible role of matrix metallopeptidase (MMP)-8 and MMP-9 in the development of chronic subdural hematoma (CSDH), we investigated their expression in CSDH. In our previous study, we analyzed hematoma fluid and peripheral blood of 83 patients with CSDH, including 17 postoperative patients. Based on these results, we included 50 people in the normal group and analyzed 20 markers in the peripheral blood of each person. In order to identify representative markers, it was assessed by using overall differential gene expression. The concentration of MMP-8 was significantly higher in the normal group than that in the preoperative and postoperative groups. The concentration of MMP-9 was significantly lower in the normal group than in both preoperative and postoperative groups. Immunohistochemistry confirmed the expression of MMP-8 and MMP-9 in CSDH membranes. In conclusion, our results provide evidence of the expression of MMP-8 and MMP-9 in CSDH. In addition, the expression of MMP-8 and MMP-9 suggests angiogenesis in CSDH formation.

KEYWORDS

chronic subdural hematoma, matrix metallopeptidase, immunoexpression, differential gene expression, disease development

Introduction

As a common neurosurgical disease, chronic subdural hematoma (CSDH) involves the collection of blood in the subdural space (1). The incidence rates of CSDH have been rising on account of the aging population and the increasing use of anticoagulants and antiplatelet medications (2). However, the development of CSDH is still poorly understood (3, 4). Previous research has investigated the mechanisms underlying CSDH, including angiogenesis, fibrinolysis, and inflammation (5).

In a rat model, inflammation and angiogenesis were found to play important roles in the formation of CSDH (6, 7). Numerous biomarkers have been identified in patients with CSDH, including interleukin (IL)-1, IL-6, IL-8, IL-10, vascular endothelial growth factor (VEGF), matrix metallopeptidase (MMP)-2, and MMP-9 (5, 8–10). In our previous study, we found that MMP-8 and MMP-9 may play a key role in the pathophysiology of CSDH (11).

MMPs are a family of zinc-dependent proteolytic enzymes that contribute to pathological inflammation and endothelial dysfunction (12). This appears to be related to CSDH formation. However, there have been few studies on the expression and activity of MMPs in CSDH. Based on our previous study, we used immunohistochemistry to analyze CSDH membranes to determine the possible role of MMP-8 and MMP-9 in the development of CSDH (11).

Materials and methods

Patients and tissue samples

We recruited 50 individuals to the normal group based on our previous study (11). In addition, the membranes of CSDHs were obtained from 10 patients (eight males and two females) who underwent surgeries at the Shenzhen Second People's Hospital. The patients ranged from 35 to 84 years of age (mean: 65.3 years) and had not been previously treated for CSDH. This clinical study was approved by the Ethics Committee of the Shenzhen Second People's Hospital (20200422003-XZ2021-XZ2021). Informed consent was obtained from all the participants involved in this study.

Cytokine measurements

Peripheral blood samples were collected from 50 patients in the control group. All samples were collected in tubes containing a coagulator and immediately centrifuged at 2,000 rpm for 15 min. After centrifugation, the supernatants were stored in sealed polypropylene tubes at −80 °C until further analysis.

We analyzed the hematoma fluid and preoperative and postoperative peripheral blood samples using the 20-plex human panel A system (R&D Systems, Minneapolis, MN, USA), Luminex system (Luminex, Austin, TX, USA), and Bioplex software (BioRad, Hercules, CA, USA). We evaluated IL-1α, IL-6, IL-8, IL-10, Angiopoietin-2, platelet-derived growth factor-BB (PDGF-BB), MMP-1, MMP-2, MMP-3, MMP-8, MMP-9, D-dimer, epidermal growth factor (EGF), C-C motif chemokine ligand 2 (CCL2), tumor necrosis factor (TNF-α), hepatocyte growth factor (HGF), VEGF, insulin-like growth factor binding protein-3 (IGFBP-3), prolactin, and VEGF receptor-2 (VEGFR2) levels.

Differentially expressed gene screening

We searched the genes corresponding to cytokines through PubMed. The overall differential gene expression was evaluated by using the ggplot2 package in the R statistical software. Furthermore, the LIMMA package was used to select DEGs.

TABLE 1 Age and sex in preoperative chronic subdural hematoma (CSDH), postoperative CSDH, and normal groups.

Group	Age (years)	Gender	
		Male	Female
Preoperative CSDH group	66.73 ± 15.14	76	7
Postoperative CSDH group	62.63 ± 15.17	17	0
Normal group	67.16 ± 4.13	34	16

We used the empirical Bayes moderated *t*-test to calculate the *p*-values for each cytokine. The adjusted *p*-values were calculated based on the false discovery rate. Only genes with a $\log_2$ fold change > 2 and false discovery rate < 0.01 were considered DEGs.

Immunohistochemistry

CSDH membrane tissues were placed in 4% paraformaldehyde for 20 h at 4 °C. The tissue was embedded in paraffin, and 4 μm serial sections were cut. The sections were deparaffinized in xylene and dehydrated using descending dilutions of ethanol (100% and 95%). The primary antibodies (Goat monoclonal, Anti-MMP-8, No: AF908-SP, 1:50, R&D Systems; Rabbit monoclonal, Anti-MMP-9, No: ab76003, 1:50, Abcam, Cambridge, UK) were incubated for 30 min at 25 °C and overnight at 4 °C and stained using the avidin-biotin peroxidase method and 3, 3'-diaminobenzidine as a chromogen. Finally, the sections were counterstained with Mayer's hematoxylin and mounted using an aqueous mounting medium.

Statistical analysis

Statistical analyses were performed using the Mann–Whitney *U*-test. Data are presented as mean ± standard deviation. All analyses were performed using the SPSS software. Statistical significance was set at $p < 0.05$.

Results

Patient characteristics

The mean age in the preoperative CSDH group was 67.16 ± 4.13 years. The general characteristics of each group are presented in Table 1.

TABLE 2 Differential expression of all cytokines in peripheral blood samples between the preoperative CSDH and normal groups.

Gene	logFC	AveExpr	*t*	*p*-value	adj.p.Val	*B*
MMP-2	921,853.2	647,819.4	32.36068	2.82×10^{-63}	5.65×10^{-62}	−3.4005
PDGF-BB	12,105.66	8,795.523	22.97331	4.09×10^{-47}	4.09×10^{-46}	−3.51766
IL-10	56.93396	46.3614	17.42905	1.61×10^{-35}	1.07×10^{-34}	−3.65504
EGF	572.5483	504.8891	15.49331	4.42×10^{-31}	2.21×10^{-30}	−3.72463
IL-1α	101.4245	62.9607	13.51954	2.25×10^{-26}	8.99×10^{-26}	−3.81145
CCL2	833.6593	744.0045	13.47686	2.85×10^{-26}	9.51×10^{-26}	−3.81352
Angiopoietin-2	3,864.163	3,543.209	12.12706	5.68×10^{-23}	1.62×10^{-22}	−3.88385
IL-6	59.11894	49.43651	10.86112	7.52×10^{-20}	1.88×10^{-19}	−3.95836
MMP-8	16,494.91	15,772.37	10.41476	9.49×10^{-19}	2.11×10^{-18}	−3.98664
VEGF	267.819	275.1433	9.980343	1.11×10^{-17}	2.22×10^{-17}	−4.01513
VEGFR2	10,538.92	15,761.35	9.8638	2.15×10^{-17}	3.90×10^{-17}	−4.02294
HGF	602.7063	669.2817	9.530186	1.41×10^{-16}	2.34×10^{-16}	−4.04566
MMP-9	−204,543	143,571	−9.10685	1.51×10^{-15}	2.32×10^{-15}	−4.07523
IGFBP-3	256,976.4	730,131.4	8.702437	1.42×10^{-14}	2.03×10^{-14}	−4.10423
TNF-α	70.08539	67.17581	7.703415	3.26×10^{-12}	4.35×10^{-12}	−4.17849
IL-8	76.15073	76.41651	5.749083	6.29×10^{-08}	7.87×10^{-08}	−4.32906
Prolactin	25,706.85	32,042.06	4.318917	3.13×10^{-05}	3.68×10^{-05}	−4.4343

MMP, Matrix metallopeptidases; PDGF-BB, platelet-derived growth factor-BB; IL, interleukin; EGF, endothelial growth factor; CCL2, C–C motif chemokine ligand 2; VEGF, vascular endothelial growth factor; VEGFR2, VEGF receptor 2; HGF, hepat2ocyte growth factor; IGFBP-3, insulin-like growth factor binding protein-3; TNF-α, tumor necrosis factor-alpha; logFC, differential expression multiple; AveExpr, mean expression level; t, T value (paired-samples t-test); adj.p.Val, adjusted p-value; B, logarithm of the standard deviation after Bayes analysis.

Identification of DEGs

All peripheral blood samples obtained from the preoperative CSDH and normal groups were analyzed. An overview of the differential gene expression is presented in Table 2. MMP-2, PDGF-BB, IL-10, EGF, IL-1α, CCL2, Angiopoietin-2, IL-6, MMP-8, VEGF, VEGFR2, HGF, MMP-9, IGFBP-3, TNF-α, IL-8, and Prolactin were DEGs between the preoperative and normal groups. MMP-1, MMP-3, and D-dimer were not significantly different between the preoperative and normal groups. All peripheral blood samples obtained from the postoperative and normal groups were analyzed. An overview of the differential gene expression is presented in Table 3. CCL2, EGF, IL-10, IL-1α, Angiopoietin-2, IL-6, MMP-8, HGF, TNF-α, MMP-9, IL-8, VEGFR2, VEGF, prolactin, D-dimer, IGFBP-3, MMP-1, and PDGF-BB were identified as DEGs between postoperative and normal groups. MMP-2 and MMP-3 were not significantly different between the postoperative and normal groups.

Data analysis

The concentrations of MMP-8 and MMP-9 in the control (normal) group are shown in Table 4 ($p < 0.01$). Based on our previous study (11), the concentration of MMP-8 was significantly higher in the normal group compared to that in both preoperative and postoperative CSDH groups, while that of MMP-9 was significantly lower. All CSDH membranes were immunostained for MMP-8 and MMP-9 in all samples. These proteins were positively immunostained in vascular endothelial cells. The results for the immunostained membranes are shown in Figures 1, 2.

Discussion

Based on our previous study, MMP-8 and MMP-9 may contribute to CSDH pathogenesis in different ways (11). We found that the MMP-8 concentration was significantly higher in the normal group compared to that in preoperative and postoperative groups, whereas the MMP-9 concentration was significantly lower. Simultaneously, we observed that both MMP-8 and MMP-9 were expressed in vascular endothelial cells. Nowadays, an increasing number of studies consider that CSDH formation may be related to the growth of new vessels and inflammation (1, 13). In addition, MMPs significantly contribute to blood vessel formation, remodeling, and angiogenesis by regulating the functions or behaviors of stem/progenitor and vascular cells (14).

Although CSDH is the most common neurosurgical disease, a few questions remain to be answered. Tamura et al. (15) indicated that the split dural border cell layer produced a dural hematoma by forming the inner and outer membranes in CSDH. The outer membranes drive inflammation and angiogenesis. After studying the role of MMPs in the development of CSDH, Nakagawa et al. (16) found that MMPs degrade the integrity

TABLE 3 Differential expression of all cytokines in peripheral blood samples between the postoperative CSDH and normal groups.

Gene	logFC	AveExpr	*t*	*p*-value	adj.p.Val	*B*
CCL2	988.5303	1,032.101	21.16245	7.22×10^{-30}	1.44×10^{-28}	−4.03779
EGF	762.2283	682.9133	20.75541	2.06×10^{-29}	2.06×10^{-28}	−4.04051
IL-10	79.30262	63.22905	16.70569	1.71×10^{-24}	1.14×10^{-23}	−4.07664
IL-1α	118.1598	98.51254	15.5764	5.56×10^{-23}	2.78×10^{-22}	−4.09068
Angiopoietin-2	5,129.373	4,748.264	15.33773	1.19×10^{-22}	4.74×10^{-22}	−4.09395
IL-6	80.18971	67.46492	14.74762	7.92×10^{-22}	2.64×10^{-21}	−4.1025
MMP-8	23,775.32	20,468.85	14.63503	1.14×10^{-21}	3.10×10^{-21}	−4.10422
HGF	902.3919	832.87	14.61023	1.24×10^{-21}	3.10×10^{-21}	−4.1046
TNF-α	98.88158	87.63968	14.45219	2.08×10^{-21}	4.63×10^{-21}	−4.10706
MMP-9	−306,457	88,102.92	−14.0502	7.92×10^{-21}	1.58×10^{-20}	−4.11359
IL-8	113.0108	97.32476	10.75424	9.67×10^{-16}	1.76×10^{-15}	−4.18463
VEGFR2	13,529.04	19,157.61	10.10128	1.15×10^{-14}	1.92×10^{-14}	−4.20335
VEGF	355.4574	358.676	10.06004	1.35×10^{-14}	2.07×10^{-14}	−4.20459
Prolactin	40,781.43	38,473.71	3.968871	0.000192	0.000274	−4.47445
D-dimer	1,788,130	3,265,902	3.009334	0.003797	0.005062	−4.52305
IGFBP-3	135,979.4	859,112.6	2.618526	0.011113	0.013891	−4.54107
MMP-1	2,094.374	8,114.673	2.457844	0.01682	0.019789	−4.54806
PDGF-BB	2,048.92	15,908.91	2.352573	0.021871	0.024301	−4.55248

MMP, Matrix metallopeptidases; PDGF-BB, platelet-derived growth factor-BB; IL, interleukin; EGF, endothelial growth factor; CCL2, C–C motif chemokine ligand 2; VEGF, vascular endothelial growth factor; VEGFR2, VEGF receptor 2; HGF, hepat2ocyte growth factor; IGFBP-3, insulin-like growth factor binding protein-3; TNF-α, tumor necrosis factor-alpha; logFC, differential expression multiple; AveExpr, mean expression level; t, T value (paired-samples t-test); adj.p.Val, adjusted p-value; B, logarithm of the standard deviation after Bayes analysis.

TABLE 4 Concentration of MMP-8 and MMP-9 in the normal, preoperative, and postoperative groups ($p < 0.01$).

Factor	MMP-8 (ng/mL)	MMP-9 (ng/mL)
Preoperative serum	9.18 ± 9.78	217.19 ± 155.02
Normal serum	25.89 ± 6.09	15.178 ± 2.47
Postoperative serum	2.97 ± 3.80	354.13 ± 231.55

MMP, Matrix metallopeptidases.

of the extracellular matrix in the outer membranes of CSDH, which can cause the exudation of interstitial edematous fluid from membrane vessels into the hematoma cavity. This seemed to be the reason for CSDH enlargement. Some studies have shown that MMP-8 plays an important role in endothelial cell angiogenesis (12, 14). In our study, the change in the MMP-8 concentration indicated that MMP-8 might be inhibited when neovascularization proceeds and increases after the formation of new vessels are suspended. In future studies, we will focus on MMP-8 in CSDH formation.

The role of MMP-9 in the pathophysiological pathways of CSDH has been reported in many studies (1, 10, 11, 13). MMP-9 expression in vascular endothelial cells confirmed that CSDH formation was related to MMP-9 expression. MMP-9 is regarded as one of the factors contributing to the formation of fragile, leaky capillaries (5). Hua et al. (10) considered that the MMP/VEGF system may be involved in angiogenesis associated with CSDH, because of the relation of the concentrations of MMP-2 and MMP-9 and the VEGF concentration in the hematoma fluid. Xu et al. (6) found that the formation of neovessels might be correlated with the increased production of pro-angiogenic factors, including MMP-9 and VEGF, in rats. Furthermore, studies have indicated that MMP-9 can reduce CSDH absorption by increasing vascular permeability, enhancing inflammation, and reducing vascular maturation (13). Huang et al. (3) found that atorvastatin plays a similar role to MMP-9 and can promote hematoma absorption, reduce tissue inflammation, and improve neurological function. We propose that when the trigger began, the MMP-9 concentration increased rapidly, while that of MMP-8 decreased. These biomolecules interact with and may influence each other. With the development and treatment of CSDH, the concentration of MMP-9 also increased, indicating that it could promote the formation of new normal vessels to repair normal physiological function.

Our understanding of CSDH pathogenesis is constantly being updated, and researchers are currently focusing on developing appropriate treatments. It has been found that atorvastatin inhibits inflammation and angiogenesis (17, 18). Based on a study of SDH in rats, it may eliminate SDH and improve neural function by using atorvastatin (19). In addition, Soleman et al. (20) concluded that atorvastatin is valid and safe for treating asymptomatic or mildly symptomatic patients

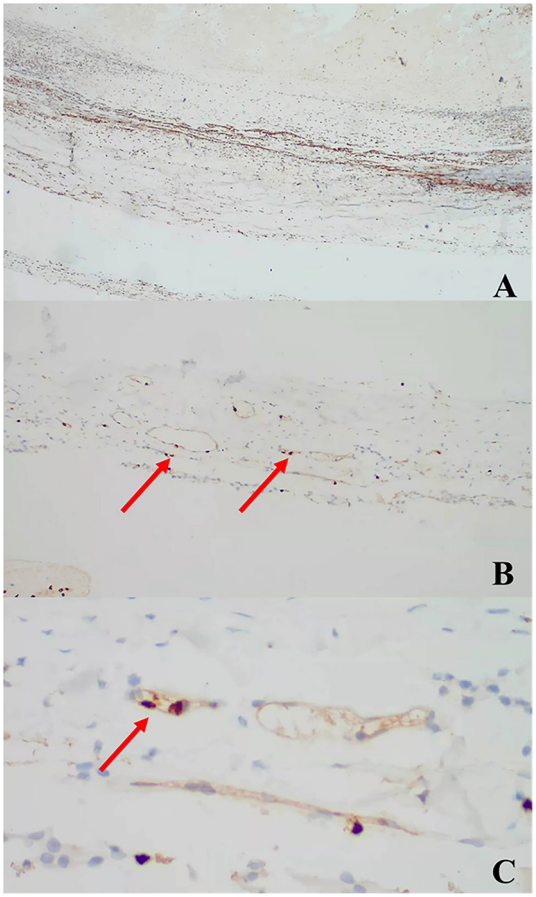

FIGURE 1
Anti-MMP-8 antibody immunostaining: **(A)** ×40, **(B)** ×100, **(C)** ×400 (arrows).

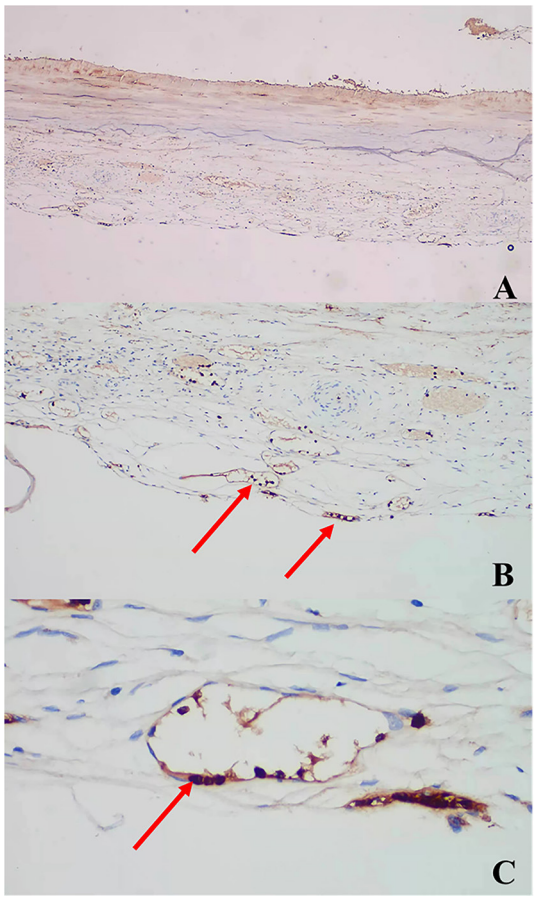

FIGURE 2
Anti-MMP-9 antibody immunostaining: **(A)** ×40, **(B)** ×100, **(C)** ×400 (arrows).

with CSDH. Atorvastatin may enhance angiogenesis to reduce CSDH-related inflammation (21). Fan et al. (22) found that Krüppel-like factor 2 (KLF-2) plays a key role in drug therapy for CSDH. It was found that combination therapy with atorvastatin and low-dose dexamethasone can inhibit the expression of KLF-2 to attenuate robust endothelial inflammation and permeability (22). In a randomized placebo-controlled trial, effective function was confirmed in patients treated with atorvastatin and low-dose dexamethasone (23). Our findings indicate that MMP-8 and MMP-9 may serve as accessible markers of CSDH formation. Future studies should focus on the relationship between MMP-8 and MMP-9 in CSDH fluid and their membrane activity. Moreover, we wish to determine the relationship between these two cytokines and CSDH prognosis and identify a way to prevent recurrence in patients with CSDH. More important in the clinic, understanding CSDH mechanisms would help physicians restore neurological deficits in patients with CSDH and improve their quality of life (24).

There were some limitations in this study. Firstly, from our limited number of cases, it is difficult to represent the wide spectrum of patients with CSDH. Further studies including a larger sample of patients will be needed to clarify this point. Secondly, the experimental analysis of the CSDH membrane was relatively limited, and so the results may not be completely convincing. More approaches are needed to verify the expression and role of MMP-8 and MMP-9 on the membrane.

Conclusions

Our study provides evidence of MMP-8 and MMP-9 expression in CSDH. In addition, the expression of MMP-8 and MMP-9 is indicative of angiogenesis in CSDH formation. Identification of the biomolecules involved in CSDH formation may be helpful in the development of new clinical therapies. However, further studies are necessary to clarify the association between MMP-8 and MMP-9 expression during the transformation and progression of CSDH.

Data availability statement

The original contributions presented in the study are included in the article/supplementary material, further inquiries can be directed to the corresponding author.

Ethics statement

The studies involving human participants were reviewed and approved by Institutional Ethics Committee of Shenzhen Second People's Hospital. Written informed consent to participate in this study was provided by the participants' legal guardian/next of kin.

Author contributions

Conceptualization, methodology, and project administration: G-JS, DZ, and X-JH. Validation, resources, and investigation: G-JS and DZ. Software: J-NW, C-WW, and X-JZ. Formal analysis: Y-HD, C-WW, and X-JZ. Data curation, visualization, and writing—original draft preparation: G-JS. Writing—review and editing and supervision: X-JH. Funding acquisition: X-JH and X-JZ. All authors contributed to the article and approved the submitted version.

Funding

This research was funded by the Natural Science Foundation of China, Grant Number 81301062, Shenzhen Double Chain Grant, Grant Number (2018) 256, Discipline Construction Capacity Improvement Project of the Shenzhen Municipal Health Commission, Grant Number SZXJ2018057, and Basic Research Fund of the Shenzhen Science and Technology Program, Grant Numbers JCYJ20180228163034627 and JCYJ20190806162210754.

Acknowledgments

The authors would like to thank the physicians and nurses of Shenzhen Second People's Hospital Department of Neurosurgery.

Conflict of interest

The authors declare that the research was conducted in the absence of any commercial or financial relationships that could be construed as a potential conflict of interest.

Publisher's note

References

1. Feghali J, Yang W, Huang J. Updates in chronic subdural hematoma: epidemiology, etiology, pathogenesis, treatment, and outcome. *World Neurosurg.* (2020) 141:339–45. doi: 10.1016/j.wneu.2020.06.140

2. Kolias AG, Chari A, Santarius T, Hutchinson PJ. Chronic subdural haematoma: Modern management and emerging therapies. *Nat Rev Neurol.* (2014) 10:570–8. doi: 10.1038/nrneurol.2014.163

3. Huang J, Gao C, Dong J, Zhang J, Jiang R. Drug treatment of chronic subdural hematoma. *Expert Opin Pharmacother.* (2020) 21:435–44. doi: 10.1080/14656566.2020.1713095

4. Iliescu IA, Constantinescu AI. Clinical evolutional aspects of chronic subdural haematomas–Literature review. *J Med Life.* (2015) 8:26–33.

5. Edlmann E, Giorgi-Coll S, Whitfield PC, Carpenter KLH, Hutchinson PJ. Pathophysiology of chronic subdural haematoma: inflammation, angiogenesis and implications for pharmacotherapy. *J Neuroinflammation.* (2017) 14:108. doi: 10.1186/s12974-017-0881-y

6. Xu X, Wang D, Han Z, Wang B, Gao W, Fan Y, et al. A novel rat model of chronic subdural hematoma: Induction of inflammation and angiogenesis in the subdural space mimicking human-like features of progressively expanding hematoma. *Brain Res Bull.* (2021) 172:108–19. doi: 10.1016/j.brainresbull.2021.04.024

7. Quan W, Zhang Z, Tian Q, Wen X, Yu P, Wang D, et al. A rat model of chronic subdural hematoma: Insight into mechanisms of revascularization and inflammation. *Brain Res.* (2015) 1625:84–96. doi: 10.1016/j.brainres.2015.08.017

8. Wada T, Kuroda K, Yoshida Y, Ogasawara K, Ogawa A, Endo S. Local elevation of the anti-inflammatory interleukin-10 in the pathogenesis of chronic subdural hematoma. *Neurosurg Rev.* (2006) 29:242–5. doi: 10.1007/s10143-006-0019-7

9. Pripp AH, Stanišić M. Association between biomarkers and clinical characteristics in chronic subdural hematoma patients assessed with Lasso regression. *PLoS One.* (2017) 12:e0186838. doi: 10.1371/journal.pone.0186838

10. Hua C, Zhao G, Feng Y, Yuan H, Song H, Bie L. Role of matrix metalloproteinase-2, matrix metalloproteinase-9, and vascular endothelial growth factor in the development of chronic subdural hematoma. *J Neurotrauma.* (2016) 33:65–70. doi: 10.1089/neu.2014.3724

11. Su GJ, Gao J, Wu CW, Zou JF, Zhang D, Zhu DL, et al. Serum levels of MMP-8 and MMP-9 as markers in chronic subdural hematoma. *J Clin Med.* (2022) 11:902. doi: 10.3390/jcm11040902

12. Bassiouni W, Ali MAM, Schulz R. Multifunctional intracellular matrix metalloproteinases: Implications in disease. *FEBS J.* (2021) 288:7162–82. doi: 10.1111/febs.15701

13. Holl DC, Volovici V, Dirven CMF, Peul WC, van Kooten F, Jellema K, et al. Pathophysiology and nonsurgical treatment of chronic subdural hematoma: From past to present to future. *World Neurosurg.* (2018) 116:402–11.e2. doi: 10.1016/j.wneu.2018.05.037

14. Chen Q, Jin M, Yang F, Zhu J, Xiao Q, Zhang L. Matrix metalloproteinases: Inflammatory regulators of cell behaviors in vascular formation and remodeling. *Mediators Inflamm.* (2013) 2013:928315. doi: 10.1155/2013/928315

15. Tamura R, Sato M, Yoshida K, Toda M. History and current progress of chronic subdural hematoma. *J Neurol Sci.* (2021) 429:118066. doi: 10.1016/j.jns.2021.118066

16. Nakagawa T, Kodera T, Kubota T. Expression of matrix metalloproteinases in the chronic subdural haematoma membrane. *Acta Neurochir.* (2000) 142:61–6. doi: 10.1007/s007010050008

17. Wang B, Sun L, Tian Y, Li Z, Wei H, Wang D, et al. Effects of atorvastatin in the regulation of circulating EPCs and angiogenesis in traumatic brain injury in rats. *J Neurol Sci.* (2012) 319:117–23. doi: 10.1016/j.jns.2012.04.015

18. Araújo FA, Rocha MA, Mendes JB, Andrade SP. Atorvastatin inhibits inflammatory angiogenesis in mice through down regulation of VEGF, TNF-alpha and TGF-beta1. *Biomed Pharmacother.* (2010) 64:29–34. doi: 10.1016/j.biopha.2009.03.003

19. Li T, Wang D, Tian Y, Yu H, Wang Y, Quan W, et al. Effects of atorvastatin on the inflammation regulation and elimination of subdural hematoma in rats. *J Neurol Sci.* (2014) 341:88–96. doi: 10.1016/j.jns.2014.04.009

20. Soleman J, Nocera F, Mariani L. The conservative and pharmacological management of chronic subdural haematoma. *Swiss Med Wkly.* (2017) 147:w14398. doi: 10.4414/smw.2017.14398

21. Fu S, Li F, Bie L. Drug therapy for chronic subdural hematoma: Bench to bedside. *J Clin Neurosci.* (2018) 56:16–20. doi: 10.1016/j.jocn.2017.07.034

22. Fan Y, Wang D, Rao C, Li Y, Rong H, Wang Z, et al. Atorvastatin combined with low-dose dexamethasone treatment protects endothelial function impaired by chronic subdural hematoma via the transcription factor KLF-2. *Drug Des Dev Ther.* (2020) 14:3291–9. doi: 10.2147/DDDT.S256050

23. Wang D, Gao C, Xu X, Chen T, Tian Y, Wei H, et al. Treatment of chronic subdural hematoma with atorvastatin combined with low-dose dexamethasone: Phase II randomized proof-of-concept clinical trial. *J Neurosurg.* (2020) 134:235–243. doi: 10.3171/2019.11.JNS192020

24. Guo X, Xue Q, Zhao J, Yang Y, Yu Y, Liu D, et al. Clinical diagnostic and therapeutic guidelines of stroke neurorestoration (2020 China version). *J Neurorestoratology.* (2020) 8:241–51. doi: 10.26599/JNR.2020.9040026

frontiers | Frontiers in Neurology

TYPE Original Research
PUBLISHED 19 October 2022
DOI 10.3389/fneur.2022.1008717

OPEN ACCESS

EDITED BY
Lutz Schomburg,
Charité Universitätsmedizin
Berlin, Germany

REVIEWED BY
Patrick Haubruck,
University of Sydney, Australia
Raban Heller,
Heidelberg University, Germany

*CORRESPONDENCE
Young Sun Ro
Ro.youngsun@gmail.com

SPECIALTY SECTION
This article was submitted to Neurotrauma, a section of the journal Frontiers in Neurology

RECEIVED 01 August 2022
ACCEPTED 23 September 2022
PUBLISHED 19 October 2022

CITATION
Park GJ, Ro YS, Yoon H, Lee SGW, Jung E, Moon SB, Kim SC, Shin SD and Pan-Asia Trauma Outcomes Study for Traumatic Brain Injury (PATOS-TBI) research network (2022) Serum vitamin E level and functional prognosis after traumatic brain injury with intracranial injury: A multicenter prospective study.
Front. Neurol. 13:1008717.
doi: 10.3389/fneur.2022.1008717

Serum vitamin E level and functional prognosis after traumatic brain injury with intracranial injury: A multicenter prospective study

Gwan Jin Park[1,2], Young Sun Ro[2,3,4]*, Hanna Yoon[2,3], Stephen Gyung Won Lee[2,5], Eujene Jung[2,6], Sung Bae Moon[2,7], Sang Chul Kim[1,2], Sang Do Shin[2,3,4] and Pan-Asia Trauma Outcomes Study for Traumatic Brain Injury (PATOS-TBI) research network

[1]Department of Emergency Medicine, Chungbuk National University Hospital, Cheongju, Republic of Korea, [2]Laboratory of Emergency Medical Services, Seoul National University Hospital Biomedical Research Institute, Seoul, Republic of Korea, [3]Department of Emergency Medicine, Seoul National University Hospital, Seoul, Republic of Korea, [4]Department of Emergency Medicine, Seoul National University College of Medicine, Seoul, Republic of Korea, [5]Department of Emergency Medicine, Seoul National University Boramae Medical Center, Seoul, Republic of Korea, [6]Department of Emergency Medicine, Chonnam National University Hospital, Gwangju, Republic of Korea, [7]Department of Emergency Medicine, School of Medicine Kyungpook National University and Kyungpook National University Hospital, Daegu, Republic of Korea

Background: Traumatic brain injury (TBI) is a major public health problem with high mortality and disability. Vitamin E, one of the antioxidants for treatment of TBI, has not been sufficiently evaluated for predicting prognosis of TBI. This study aimed to evaluate the prognostic value of vitamin E on functional outcomes of TBI patients with intracranial injury.

Methods: A multi-center prospective cohort study was conducted in five university hospitals between 2018 and 2020. Adult TBI patients who visited the emergency department (ED) with intracranial hemorrhage or diffuse axonal injury confirmed by radiological examination were eligible. Serum vitamin E levels (mg/dL) were categorized into 4 groups: low (0.0–5.4), low-normal (5.5–10.9), high-normal (11.0–16.9), and high (17.0–). Study outcomes were set as 1- and 6-month disability (Glasgow outcome scale (GOS) 1–4). Multilevel logistic regression analysis was conducted to calculate the adjusted odds ratios (AORs) of vitamin E for related outcomes.

Results: Among 550 eligible TBI patients with intracranial injury, the median (IQR) of serum vitamin E was 10.0 (8.0–12.3) mg/dL; 204/550 (37.1%) had 1-month disability and 197/544 (36.1%) had 6-month disability of GOS 1–4. Compared with the high-normal group, the odds of 1-month disability and 6-month disability increased in the low and low-normal group (AORs (95% CIs): 3.66 (1.62–8.27) and 2.60 (1.15–5.85) for the low group and 1.63 (1.08–2.48) and 1.60 (1.04–2.43) for the low-normal group, respectively).

Conclusion: Low serum vitamin E level was associated with poor prognosis at 1 and 6 months after TBI with intracranial injury.

KEYWORDS

vitamin E, prognosis, biomarker, traumatic brain injury, trauma

Introduction

Traumatic brain injury (TBI) is a serious public health burden worldwide, with more than 10 million people worldwide hospitalized or dead annually from TBI (1). TBI occurs frequently in younger age, which results in high mortality or leaving a permanent impairment (2). In addition, the disease burden of TBI is expected to increase further due to aging of the population as well as improvement in immediate life-saving treatment (3, 4).

Vitamin E is a lipid-soluble antioxidant that reduces reactive oxygen species. Vitamin E deficiency causes degeneration of neurons, particularly peripheral axons and posterior column neurons, which results in peripheral neuropathy, ataxia, and skeletal myopathy (5, 6). In the pathophysiology of TBI, increased production of free radicals and reactive oxygen species after injury leads to oxidative stress and secondary neurotoxicity (7). In cases where there is a deficiency of various antioxidants, involved in recovery of brain tissue post injury, treatment with antioxidants may be theoretically effective in preventing propagation of tissue damage as well as in improving short- and long-term survival/functional outcomes (8–12). Several animal studies have evaluated that vitamin E supplementation before TBI reduced oxidative stress and improved learning and memory (13, 14). Vitamin E administration after TBI also reduced microscopic brain damage, promoted nerve regeneration, and improved cognitive function in animal models (15–17). In clinical settings, early antioxidant supplementation including vitamin E in critically ill patients, including TBI patients, was associated with decrease in organ failure and hospital stay (18, 19). Vitamin E supplementation showed a significant reduction in mortality and improvement of long-term functional outcomes of TBI patients (20).

Given the evidence of the beneficial effects of vitamin E, it was hypothesized that vitamin E deficiency would be associated with poor survival outcomes and functional recovery after TBI with intracranial injury, and that serum vitamin E levels could be utilized as a nutritional biomarker for clinical outcomes after TBI. This study aimed to determine the association between serum vitamin E levels and functional/survival outcomes among TBI patients with intracranial injury.

Methods

Study design, setting, data source

This was a multi-center prospective cohort study conducted in five participating university hospitals in Korea based on the Pan-Asian Trauma Outcome Study (PATOS) registry (21). The PATOS-TBI study is a collaborative research network that started in 2018 throughout Korea for in-depth research on TBI (ClinicalTrials.gov, ID: NCT04718935). The objectives of PATOS-TBI study are to identify nutritional and metabolic biomarkers related to prognosis of TBI with intracranial injury, and to develop a prognostic predictive model of long-term prognosis that applies them to select high-risk populations funded by the National Research Foundation of Korea (22).

The inclusion criteria were TBI patients with intracranial injury confirmed by a brain radiological examination. Intracranial injury was defined as intracranial hemorrhage or diffuse axial injury (ICD-10 S06.1–06.9). Patients with TBI over 18 years of age who visited participating hospitals' ED using emergency medical services (EMS) within 72 h of injury were enrolled. Patients with penetrating brain injury, history of psychiatric or neurological disorders, terminal cancer, pregnant women, and those transferred after surgery from other hospitals were excluded from the study.

The PATOS-TBI study registry comprises of several variables including the patient's demographics, injury-related information, emergency medical service (EMS) records, clinical findings, laboratory test results, brain imaging findings, diagnoses and medical treatment in hospitals, and patient outcomes at time of hospital discharge and follow-up.

Upon confirmation of intracranial injury on brain computer tomography (CT) and magnetic resonance imaging (MRI), an emergency physician obtained informed consent for enrollment and registered the patients to the PATOS-TBI study during the ED treatment process and blood samples were obtained for biomarker analysis. Based on the informed consent from the patient or guardians, primary surveillance data were collected by an emergency physician. A trained research coordinator from each participating hospital collected and entered the registry through interviews and electronic medical records review. Serum biomarker levels were not reported to physicians, and patient management was not altered by the study. Follow-up

data at 1- and 6-months after the injury were captured *via* telephone surveys. All research coordinators were required to receive education and training prior to participation in the study and periodically during the study period. Data were collected using a standardized data collection protocol, a case report form, and a web-based data collection system. The Quality Management Committee (QMC) reviewed the data monthly and provided regular feedback for quality assurance (22, 23).

Study population

The study population included all adult TBI patients who visited the participating EDs between 2018 and 2020 with intracranial injury (intracranial hemorrhage or diffuse axonal injury, ICD-10 S06.1–06.9) confirmed by brain CT or MRI. Patients with unknown information regarding vitamin E levels and 1-month GOS score were excluded.

Main outcomes

The primary outcome was 1-month disability after injury, which was defined as Glasgow Outcome Scale (GOS) score of 1 to 4. GOS was scored from 0 to 5 as follows: 1 (dead), 2 (vegetative state), 3 (severe disability), 4 (moderate disability), and 5 (good recovery) (24). The secondary outcome was 1-month mortality and the tertiary outcomes were 6-month disability and 6-month mortality.

Analysis of serum biomarkers

Upon confirmation of intracranial injury on brain CT or MRI and patients' consent for study enrollment, 24 mL of blood was drawn *via* venipuncture in the ED. Centrifugation was performed at 3,000 rpm for 10 min at room temperature within an h of blood sampling. Levels of serum α-tocopherol, the most biologically active form of vitamin E, were analyzed. Vitamin E is a collective term that refers to eight fat-soluble forms with antioxidant activities. The liver preferentially re-secretes only α-tocopherol *via* the α-tocopherol transport protein and degrades all other forms of vitamin E. Therefore, α-tocopherol is the most recognized form of vitamin E in human body, and most research on vitamin E is performed using α-tocopherol level (25).

Serum samples were kept frozen at −20°C and were analyzed within 7 days for serum biomarkers. After dispensing 500 μL of calibrator and dispensing the sample into a 15 mL conical tube, six calibration standard solutions were prepared for each standard concentration. The solutions were adjusted to the total volume of 500 μL, with addition of 1 mL of ethanol for deproteinization. Next, 3 mL of N-Hexane was added, then centrifuging at 3,000 rpm for 5 min. After transferring 2 mL of the supernatant to the test tube and evaporating with nitrogen gas, 150 μL of methanol was added to the residue and transferred to a vial. These pretreated samples were analyzed after standard testing with High-performance liquid chromatography (HPLC).

Variables and measurements

Considering the normal range of vitamin E level in adults, the plasma vitamin E level was categorized into four groups: low (0.0–5.4 mg/dL), low-normal (5.5–10.9 mg/dL), high-normal (11.0–16.9 mg/dL), and high group (17.0– mg/dL) (26).

Information were collected including the patients' demographics (age, sex, education, comorbidities, body mass index, and pre-injury disability), injury characteristics (mechanism of injury (road traffic injury, fall, blunt trauma, and others), date and time of injury, and alcohol intake at injury, ED (Glasgow coma scale score at arrival to the ED, transfer from other hospitals, time interval from injury to ED, type of intracranial injury on brain CT or MRI, injury severity, and length of stay in ED), and outcomes (ED disposition and hospital outcome, 1-month and 6-month follow up outcomes).

Statistical analysis

Descriptive analysis was conducted to compare the characteristics of study population according to serum vitamin E levels. Categorical variables were reported as counts and proportions and continuous variables were reported as medians and interquartile ranges. Differences between groups were compared using Pearson's chi-square test and Wilcoxon rank sum test.

Adjusted odds ratios (AORs) with 95% confidence intervals (CIs) were calculated using multilevel multivariable logistic regression analysis to examine associations between serum vitamin E levels and study outcomes in TBI patients after adjusting for hospital clustering. Potential confounders were selected based on directed acyclic graph (DAG) models and included age, sex, obesity (body mass index $\geq$25), high education (college and more), comorbidities (hypertension and diabetes mellitus), pre-injury disability (mRS score 3–5), and injury severity (AIS score of TBI $\geq$3). Variables were adjusted in the model as potential confounders if they block all back-door paths from the main exposure to the outcome in DAG models (Supplementary Figure 1); affect the outcome; and are not mediators in a causal pathway (27, 28). Akaike information criterion (AIC) and Bayesian information criterion (BIC) values were calculated to evaluate a goodness-of-fit of the model.

Receiver operating characteristic (ROC) analysis was performed to evaluate the performance of serum vitamin E levels and Youden's Index was used to find the best cut-off point of serum vitamin E levels in predicting study outcomes.

A two-sided $P < 0.05$ was defined as significant. All statistical analyses were performed using SAS software, version 9.4 (SAS Institute Inc., Cary, NC, USA).

Ethics statement

The study was approved by the Institutional Review Board of all participating hospitals (IRB no.: SNUH-1806-078-951; CNUH-2018-297; KNUH-2018-10-014-007; CBNUH-2018-09-018; BMC-30-2018-85). Informed consent was obtained from the patients or family members/legal representatives of unconscious patients. Patient information was anonymized prior to analysis.

Results

A total 550 adult TBI patients out of 606 patients were included in this study, excluding 56 patients for whom information on 1-month GOS was unknown.

Table 1 presents the demographics of TBI patients according to the vitamin E levels. The median (IQR) of serum vitamin E was 10.0 (8.0–12.3) mg/dL and vitamin E deficiency was observed in 35/550 (6.4%) of the study population. The proportion of 1-month disability after injury was 37.1% (204/550) in study population, and 1-month mortality was 18.7% (103/550). Among 544 patients who were followed up to 6-months after injury, 36.1% (197/544) had disability of GOS 1–4 and 20.5% (112/544) had mortality. The proportions of 1-month disability after injury were 65.7% (23/35) for the low group, 40.5% (123/304) for the low-normal group, 27.3% (50/183) for the high-normal group, and 28.6% (8/28) for the high group, respectively ($p < 0.001$).

Table 2 shows the characteristics of TBI patients by 1-month disability. The medians (IQR) of serum vitamin E levels were 9.2 (7.3–11.4) mg/dL for 204 patients who had GOS 1–4 at 1-month after injury and 10.5 (8.6–12.5) mg/dL for 346 patients with GOS 5 ($p < 0.001$).

Table 3 presents the associations between serum vitamin E levels and study outcomes. In the multilevel logistic regression analysis, patients with low vitamin E had higher odds of disability and mortality. The adjusted odds for 1-month disability increased in the low-normal and the low groups when compared with the high-normal group (adjusted ORs (95% CIs): 3.66 (1.62–8.27) for the low group and 1.63 (1.08–2.48) for the low-normal group). Regarding 1-month mortality, 6-month disability, and 6-month mortality, the trends were similar (adjusted ORs (95% CIs): 4.77 (1.96–11.62) and 2.31 (1.28–4.15) for 1-month mortality, 2.60 (1.15–5.85) and 1.60 (1.04–2.43) for 6-month disability, and 4.91 (1.98–12.17) and 2.36 (1.34–4.15) for 6-month mortality, respectively).

In the ROC analysis, the area under the curve (AUC) of serum vitamin E was 0.63 (95% CIs, 0.58–0.68) (Figure 1). The optimal cut-off value of vitamin E was 8.4 mg/dL, corresponding to a sensitivity of 44.0% and a specificity of 76.9%. Serum vitamin E levels <8.4 mg/dL were significantly associated with poorer outcomes (adjusted ORs (95% CIs): 2.69 (1.82–3.97) for 1-month disability, 2.49 (1.53–4.07) for 1-month mortality, 2.37 (1.57–3.57) for 6-month disability, and 2.54 (1.57–4.10) for 6-month mortality, respectively) (Table 4).

Discussion

This multi-center prospective cohort study evaluated the prognostic value of serum vitamin E levels on functional/survival outcomes for TBI patients with intracranial injury. There was an association between serum vitamin E levels and 1-month disability (adjusted ORs (95% CIs): 3.66 (1.62–8.27) for the low group and 1.63 (1.08–2.48) for the low-normal group, when compared with the high-normal group). Regarding survival outcomes, there was an association between serum vitamin E levels and 1-month mortality (adjusted ORs (95% CIs): 4.77 (1.96–11.62) for the low group and 2.31 (1.28–4.15) for the low-normal group). These results suggest serum vitamin E as a potential biomarker related to functional and survival outcomes of TBI with intracranial injury.

Reactive oxygen species-induced oxidative damage has been identified as a major contributor to secondary injury from TBI, which has resulted in further damage to neuronal tissue and vasculature. Therefore, various antioxidants such as vitamin B, C, D, zinc, and magnesium have been used before and after TBI to prevent further brain damage (8, 10). Among them, vitamin E has been highlighted because it can easily be implemented in emergency care. It is an inexpensive, safe, and ubiquitous dietary supplement. It is also well tolerated and easily administered *via* enteral feeding (12, 29). Some animal studies have shown the efficacy of vitamin E in exerting a neuroprotective effect by decreasing reactive oxygen species. Vitamin E supplements before and after TBI reduced oxidative stress and showed significant beneficial effects on cognition and mortality (13, 16, 17). Vitamin E is also known as one of the factors inhibiting genetically programmed cell death, and has been used in studies to treat degenerative brain diseases (30). Vitamin E depletion is one of the major factors that increase vulnerability to TBI (8, 9).

The preclinical data supporting vitamin E in TBI are strong. However, only a select few studies have been conducted *in vivo*. Some studies reported that plasma vitamin E levels were rapidly decreased following TBI, which showed early vitamin E depletion and the subsequent need for further supplementation (31, 32). The results of this study also showed similar results, that lower serum levels of vitamin E were associated with poorer outcomes after TBI with intracranial injury. The low and low-normal vitamin E level groups showed significantly

TABLE 1 Demographics of study patients according to the serum vitamin E levels.

	Total		Serum vitamin E level (mg/dL)								
			Low (0.0–5.4)		Low-normal (5.5–10.9)		High-normal (11.0–16.9)		High (17.0–)		
	N	%	N	%	N	%	N	%	N	%	*P*–value
Total	550		35		304		183		28		
Sex, female	173	31.5	6	17.1	89	29.3	68	37.2	10	35.7	0.072
Age, year											0.673
18–60	173	31.5	9	25.7	101	33.2	57	31.1	6	21.4	
60–80	285	51.8	19	54.3	152	50.0	95	51.9	19	67.9	
80–120	92	16.7	7	20.0	51	16.8	31	16.9	3	10.7	
Median (IQR)	68 (56–77)		72 (59–79)		68 (55–77)		65 (56–77)		72 (62–76)		0.353
Education											0.087
High school or less	398	72.4	27	77.1	220	72.4	129	70.5	22	78.6	
College or more	100	18.2	1	2.9	58	19.1	38	20.8	3	10.7	
Others	52	9.5	7	20.0	26	8.6	16	8.7	3	10.7	
Pre-injury disability, mRS 3–5	43	8.0	5	14.3	27	8.9	7	4.4	4	14.3	0.165
Underlying disease											
Hypertension	216	39.3	10	28.6	125	41.1	69	37.7	12	42.9	0.484
Diabetes mellitus	141	25.6	8	22.9	85	28.0	40	21.9	8	28.6	0.475
Chronic liver disease	25	4.5	5	14.3	11	3.6	7	3.8	2	7.1	0.325
Chronic kidney disease	34	6.2	1	2.9	23	7.6	10	5.5	0	0.0	0.348
Body mass index, $\geq$ 25 kg/m^2	117	21.3	5	14.3	70	23.0	31	16.9	11	39.3	0.029
Day of injury, weekend	162	29.5	10	28.6	89	29.3	57	31.1	6	21.4	0.768
ED visit time, nighttime	215	39.1	15	42.9	115	37.8	77	42.1	8	28.6	0.494
Alcohol intake at injury	50	9.1	2	5.7	32	10.5	15	8.2	1	3.6	0.484
Mechanism											0.057
Road traffic injury	223	40.5	17	48.6	128	42.1	69	37.7	9	32.1	
Fall	239	43.5	14	40.0	136	44.7	78	42.6	11	39.3	
Blunt trauma	69	12.5	1	2.9	30	9.9	30	16.4	8	28.6	
Others	19	3.5	3	8.6	10	3.3	6	3.3	0	0.0	
Transfer from other hospitals	242	44.0	18	51.4	128	42.1	82	44.8	14	50.0	0.640
Glasgow coma scale score											<0.001
3–8	126	22.9	17	48.6	68	22.4	37	20.2	4	14.3	
9–12	52	9.5	4	11.4	32	10.5	14	7.7	2	7.1	
13–15	372	67.6	14	40.0	204	67.1	132	72.1	22	78.6	

(Continued)

10.3389/fneur.2022.1008717

TABLE 1 (Continued)

	Total		Serum vitamin E level (mg/dL)								
			Low (0.0–5.4)		Low-normal (5.5–10.9)		High-normal (11.0–16.9)		High (17.0–)		
	N	%	N	%	N	%	N	%	N	%	*P*–value
Time interval from injury to ED, hour, median (IQR)	1.7 (0.7–3.3)		1.6 (0.8–3.1)		2.0 (0.7–3.7)		1.3 (0.6–3.0)		1.7 (0.6–3.1)		0.307
Time interval from injury to blood sampling, hour, median (IQR)	0.6 (0.5–0.7)		0.6 (0.5–0.7)		0.6 (0.5–0.8)		0.6 (0.5–0.6)		0.6 (0.5–0.8)		0.785
Type of intracranial injury											
Diffuse axonal injury	36	6.5	2	5.7	20	6.6	14	7.7	0	0.0	0.732
Intracerebral hemorrhage	121	22.0	3	8.6	70	23.0	43	23.5	5	17.9	0.223
Subarachnoid hemorrhage	216	39.3	11	31.4	123	40.5	70	38.3	12	42.9	0.726
Subdural hemorrhage	411	74.7	28	80.0	225	74.0	139	76.0	19	67.9	0.695
Epidural hemorrhage	80	14.5	2	5.7	47	15.5	27	14.8	4	14.3	0.492
Intraventricular hemorrhage	47	8.5	5	14.3	28	9.2	12	6.6	2	7.1	0.149
Injury severity											
AIS score of TBI, 3–6	462	84.0	32	91.4	258	84.9	151	82.5	21	75.0	0.309
ISS, median (IQR)	17 (10–25)		20 (10–27)		17 (10–25)		16 (9–22)		13 (9–22)		<0.001
ED length of stay, hour, median (IQR)	3.1 (2.0–5.4)		3.9 (2.4–5.5)		2.9 (1.9–5.3)		3.1 (1.9–5.4)		3.5 (2.1–7.1)		0.665
Outcomes											
1-month disability, GOS 1–4	204	37.1	23	65.7	123	40.5	50	27.3	8	28.6	<0.001
GOS 1	103	18.7	16	45.7	66	21.7	18	9.8	3	10.7	<0.001
GOS 2	8	1.5	3	8.6	2	0.7	2	1.1	1	3.6	
GOS 3	50	9.1	2	5.7	27	8.9	20	10.9	1	3.6	
GOS 4	43	7.8	2	5.7	28	9.2	10	5.5	3	10.7	
GOS 5	346	62.9	12	34.3	181	59.5	133	72.7	20	71.4	
1-month mortality	103	18.7	16	45.7	66	21.7	18	9.8	3	10.7	<0.001
6-month disability, GOS 1–4 (n=544)	197	36.1	20	58.8	120	39.5	49	27.1	8	29.6	<0.001
6-month mortality (n=544)	112	20.5	16	47.1	72	23.7	21	11.6	3	11.1	<0.001

IQR, interquartile range; ED, emergency department; mRS, modified Rankin Scale; TBI, traumatic brain injury; AIS, abbreviated injury scale; ISS, injury severity score; GOS, Glasgow outcome scale.

10.3389/fneur.2022.1008717

TABLE 2 Characteristics of study population according to 1-month Glasgow outcome scale score.

	Total		GOS 1–4		GOS 5		p-value
	N	%	N	%	N	%	
Total	550		204	37.1	346	62.9	
Vitamin E, mg/dL, median (IQR)	10.0 (8.0–12.3)		9.2 (7.3–11.4)		10.5 (8.6–12.5)		<0.001
Sex, female	173	31.5	55	27.0	118	34.1	0.081
Age, year, median (IQR)	68 (56–77)		72 (57–79)		65 (55–75)		0.004
Education							0.007
High school or less	398	72.4	145	71.1	253	73.1	
College or more	100	18.2	30	14.7	70	20.2	
Others	52	9.5	29	14.2	23	6.6	
Pre-injury disability, mRS 3–5	43	7.8	31	15.2	12	3.5	<0.001
Underlying disease							
Hypertension	216	39.3	80	39.2	136	39.3	0.983
Diabetes mellitus	141	25.6	53	26.0	88	25.4	0.887
Chronic liver disease	25	4.5	8	3.9	17	4.9	0.590
Chronic kidney disease	34	6.2	11	5.4	23	6.6	0.555
Body mass index, ≥25 kg/m^2	117	21.3	50	24.5	67	19.4	0.154
Day of injury, weekend	162	29.5	61	29.9	101	29.2	0.860
ED visit time, nighttime	215	39.1	76	37.3	139	40.2	0.498
Alcohol intake at injury	50	9.1	13	6.4	37	10.7	0.089
Mechanism							0.748
Road traffic injury	223	40.5	85	41.7	138	39.9	
Fall	239	43.5	85	41.7	154	44.5	
Blunt trauma	69	12.5	25	12.3	44	12.7	
Others	19	3.5	9	4.4	10	2.9	
Transfer from other hospitals	242	44.0	98	48.0	144	41.6	0.143
Glasgow coma scale score							<0.001
3–8	126	22.9	112	54.9	14	4.0	
9–12	52	9.5	34	16.7	18	5.2	
13–15	372	67.6	58	28.4	314	90.8	
Type of intracranial injury							
Diffuse axonal injury	36	6.5	18	8.8	18	5.2	0.097
Intracerebral hemorrhage	121	22.0	52	25.5	69	19.9	0.129
Subarachnoid hemorrhage	216	39.3	82	40.2	134	38.7	0.734
Subdural hemorrhage	411	74.7	162	79.4	249	72.0	0.052
Epidural hemorrhage	80	14.5	22	10.8	58	16.8	0.055
Intraventricular hemorrhage	47	8.5	20	9.8	27	7.8	0.418
AIS score of TBI, ≥3	462	84.0	181	88.7	281	81.2	0.020
Injury severity score, median (IQR)	17 (10–25)		22 (14–25)		16 (9–22)		<0.001

GOS, Glasgow outcome scale; IQR, interquartile range; ED, emergency department; mRS, modified Rankin Scale; TBI, traumatic brain injury; AIS, abbreviated injury scale.

poorer survival and functional outcomes. The relative decrease in antioxidant capacity may correlate with the severity of brain injury and suggests a dose-response relationship between vitamin E deficiency and poor neurological outcomes.

Two randomized trials for vitamin E administration in critically ill patients showed only short-term benefits such as reduction of rates of organ failure, inflammatory responses, and a shorter length of stay in the intensive care unit (18, 19). Since the above studies were conducted for critically ill patients, including TBI patients, the interpretation of the results may be limited. The only randomized clinical trial conducted in TBI patients reported that vitamin E administration has showed a beneficial effect in significantly reducing mortality rates and improving functional outcomes at discharge and follow-up (20).

TABLE 3 Multilevel logistic regression analysis between serum vitamin E levels and study outcomes.

	Total	Outcomes		Model 1	Model 2	Model 3
	N	*N*	%	OR (95% CI)	aOR (95% CI)	aOR (95% CI)
1-month disability, GOS 1–4						
Vitamin E level	550	204	37.1			
Low (0.0–5.4 mg/dL)	35	23	65.7	5.10 (2.36–11.03)	3.76 (1.67–8.47)	3.66 (1.62–8.27)
Low-normal (5.5–10.9 mg/dL)	304	123	40.5	1.81 (1.21–2.69)	1.65 (1.09–2.50)	1.63 (1.08–2.48)
High-normal (11.0–16.9 mg/dL)	183	50	27.3	Ref	Ref	Ref
High (17.0– mg/dL)	28	8	28.6	1.06 (0.44–2.58)	0.73 (0.28–1.91)	0.75 (0.29–1.99)
AIC / BIC				711.4 / 728.7	692.0 / 756.7	690.1 / 759.1
1-month mortality						
Vitamin E level	550	103	18.7			
Low (0.0–5.4 mg/dL)	35	16	45.7	8.71 (3.71–20.45)	5.44 (2.19–13.53)	4.77 (1.96–11.62)
Low-normal (5.5–10.9 mg/dL)	304	66	21.7	2.71 (1.54–4.77)	2.47 (1.36–4.47)	2.31 (1.28–4.15)
High-normal (11.0–16.9 mg/dL)	183	18	9.8	Ref	Ref	Ref
High (17.0– mg/dL)	28	3	10.7	1.16 (0.31–4.28)	0.68 (0.16–2.92)	0.66 (0.16–2.81)
AIC / BIC				501.4 / 499.5	479.9 / 473.6	483.6 / 552.5
6-month disability, GOS 1–4						
Vitamin E level	544	197	36.2			
Low (0.0–5.4 mg/dL)	34	20	58.8	3.82 (1.79–8.16)	2.67 (1.19–6.00)	2.60 (1.15–5.85)
Low-normal (5.5–10.9 mg/dL)	303	120	39.6	1.75 (1.17–2.62)	1.61 (1.06–2.45)	1.60 (1.04–2.43)
High-normal (11.0–16.9 mg/dL)	180	49	27.2	Ref	Ref	Ref
High (17.0– mg/dL)	27	8	29.6	1.13 (0.46–2.74)	0.77 (0.29–2.04)	0.80 (0.30–2.12)
AIC / BIC				704.5 / 721.7	682.7 / 747.2	681.7 / 750.5
6-month mortality						
Vitamin E level	544	112	20.6			
Low (0.0–5.4 mg/dL)	34	16	47.1	7.75 (3.32–18.07)	5.08 (2.05–12.59)	4.91 (1.98–12.17)
Low-normal (5.5–10.9 mg/dL)	303	72	23.8	2.56 (1.50–4.38)	2.39 (1.36–4.20)	2.36 (1.34–4.15)
High-normal (11.0–16.9 mg/dL)	180	21	11.7	Ref	Ref	Ref
High (17.0– mg/dL)	27	3	11.1	0.98 (0.27–3.61)	0.57 (0.14–2.37)	0.56 (0.13–2.38)
AIC / BIC	27	3	11.1	522.0 / 520.0	503.0 / 496.7	502.3 / 495.6

Model 1: unadjusted.
Model 2: adjusted for age, sex, obesity, education, comorbidities (hypertension and diabetes mellitus), and pre-injury disability.
Model 3: adjusted for variables in the Model 2, and injury severity (AIS score of TBI, ≥3).
GOS, Glasgow outcome scale; aOR, adjusted odds ratio; CI, confidence interval; AIC, Akaike information criterion; BIC, Bayesian information criterion; AIS, abbreviated injury scale; TBI, traumatic brain injury.

This study is worthwhile in that it prospectively constructed a cohort of TBI patients and identified a relationship between serum vitamin E levels and short-/long-term clinical outcomes after TBI. Currently used diagnostic imaging techniques for TBI are well known to have high initial diagnostic accuracy for intracranial injury, but the clinical role of these on predicting long-term cognitive and physical impairment is limited (33, 34). Based on the results of this study, it can be expected that high-risk groups with poor prognosis will be screened, and the disability and burden of TBI will be reduced through early vitamin E correction and treatment.

This study has several limitations. First, blood samples in this study were collected only at the ED. Serial measurements of vitamin E during hospitalization and understanding the kinetics of vitamin E over time after TBI would be needed to better interpret the findings of this study. Second, potential confounders were selected based on the DAG model. Using the rules of DAG models, the variables in Model 3 were chosen as a minimally sufficient conditioning set to estimate the unbiased effect of serum vitamin E levels. However, there is a possibility that there is some back-door path which can bias the vitamin E levels effects on study outcomes. There may also be unmeasured potential effect modifiers which may violate the assumption of independent effect of vitamin E levels on the study outcome, such as brain volume and anatomical location affected by intracranial injury, and patients' other nutritional status. Third, there were no available data on the history of vitamin E levels before injury, diet diary, and nutritional status, which would

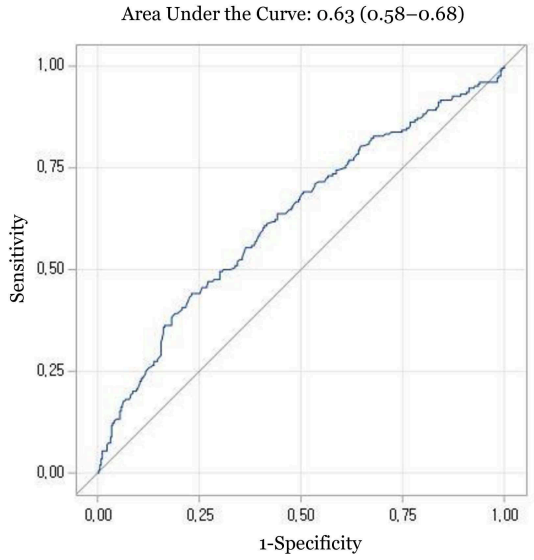

FIGURE 1
Receiver operating characteristic curve for prediction of 1-month disability with serum vitamin E levels.

have been related to serum vitamin E levels at the ED. Moreover, there were no information about whether vitamin E was supplemented before/after TBI. Fourth, selection bias may arise because the TBI patients with unknown 1-month disability were excluded. Finally, there would be unmeasured and uncontrolled bias when considering the complex pathophysiological processes after TBI. Caution should be taken when interpreting the study results of this study given the significant limitations.

In conclusion, serum vitamin E level is associated with long- and short-term disability and mortality for TBI patients with intracranial hemorrhage and diffuse axonal injury. This study suggests that serum vitamin E may be a potential biomarker in predicting the long- and short-term prognoses of TBI patients with intracranial injury. Further research is needed to evaluate the benefit of vitamin E supplementation in improving the long-term outcomes of TBI patients.

Data availability statement

The raw data supporting the conclusions of this article will be made available by the authors, without undue reservation.

TABLE 4 Association between serum vitamin E levels (binary) and study outcomes.

	Total	Outcomes		Model 1	Model 2	Model 3
	N	*N*	%	OR (95% CI)	aOR (95% CI)	aOR (95% CI)
1-month disability, GOS 1–4						
Serum vitamin E level	550	204	37.1			
0.0–8.3 mg/dL	166	88	53.0	2.61 (1.79–3.79)	2.54 (1.71–3.79)	2.69 (1.82–3.97)
8.4– mg/dL	384	116	30.2	Ref	Ref	Ref
AIC / BIC				704.0 / 712.6	681.9 / 737.9	679.9 / 740.2
1-month mortality						
Serum vitamin E level	550	103	18.7			
0.0–8.3 mg/dL	166	50	30.1	2.93 (1.86–4.62)	2.54 (1.56–4.13)	2.49 (1.53–4.07)
8.4– mg/dL	384	53	13.8	Ref	Ref	Ref
AIC / BIC				505.4 / 504.2	481.7 / 476.2	478.0 / 472.2
6-month disability, GOS 1–4						
Serum vitamin E level	544	197	36.2			
0.0–8.3 mg/dL	164	84	51.2	2.53 (1.73–3.70)	2.42 (1.61–3.63)	2.37 (1.57–3.57)
8.4– mg/dL	380	113	29.7	Ref	Ref	Ref
AIC / BIC				695.0 / 693. 8	672.3 / 666.8	671.4 / 665.6
6-month mortality						
Serum vitamin E level	544	112	20.6			
0.0–8.3 mg/dL	164	53	32.3	2.87 (1.84–4.47)	2.58 (1.60–4.15)	2.54 (1.57–4.10)
8.4– mg/dL	380	59	15.5	Ref	Ref	Ref
AIC / BIC				524.5 / 523.4	504.2 / 498.8	503.4 /497.5

Model 1: unadjusted.
Model 2: adjusted for age, sex, obesity, education, comorbidities (hypertension and diabetes mellitus), and pre-injury disability.
Model 3: adjusted for variables in the Model 2, and injury severity (AIS score of TBI, ≥3).
GOS, Glasgow outcome scale; aOR, adjusted odds ratio; CI, confidence interval; AIC, Akaike information criterion; BIC, Bayesian information criterion; AIS, abbreviated injury scale; TBI, traumatic brain injury.

Ethics statement

The studies involving human participants were reviewed and approved by of all participating hospitals (Seoul National Univesity Hospital, Seoul National University Boramae Medical Center, Chungbuk National University Hospital, Kyungpook National University Hospital, and Chonnam National University Hospital). Written informed consent to participate in this study was provided by the participants' legal guardian/next of kin.

Author contributions

Conceptualization, had full access to all of the data in the study, and take responsibility for the integrity of the data as well as the accuracy of the data analysis: GP and YR. Data curation: GP, HY, SL, EJ, and SM. Formal analysis and software, funding acquisition, and writing–original draft: GP. Investigation: YR, HY, SL, EJ, and SM. Methodology: GP, YR, SK, and SS. Supervision: YR, SK, and SS. Validation: HY, SL, EJ, and SM. Visualization: GP and SK. Writing—review and editing: YR and SS. Approval of final manuscript: all authors.

Funding

This work was supported by the National Research Foundation of Korea (NRF) grant funded by the Korean government (MSIT) (Grant no.: NRF-2018R1C1B6007625 and NRF-2021R1A2C4002898). This funding source had no role in the study design, execution, analyses, interpretation of the data, or decision to submit results.

Conflict of interest

The authors declare that the research was conducted in the absence of any commercial or financial relationships that could be construed as a potential conflict of interest.

Publisher's note

All claims expressed in this article are solely those of the authors and do not necessarily represent those of their affiliated organizations, or those of the publisher, the editors and the reviewers. Any product that may be evaluated in this article, or claim that may be made by its manufacturer, is not guaranteed or endorsed by the publisher.

Supplementary material

The Supplementary Material for this article can be found online at: https://www.frontiersin.org/articles/10.3389/fneur.2022.1008717/full#supplementary-material

References

1. Hyder AA, Wunderlich CA, Puvanachandra P, Gururaj G, Kobusingye OC. The impact of traumatic brain injuries: a global perspective. *NeuroRehabilitation.* (2007) 22:341–53. doi: 10.3233/NRE-2007-22502

2. Stocchetti N, Zanier ER. Chronic impact of traumatic brain injury on outcome and quality of life: a narrative review. *Crit Care.* (2016) 20:148. doi: 10.1186/s13054-016-1318-1

3. Maas AIR, Menon DK, Adelson PD, Andelic N, Bell MJ, Belli A, et al. Traumatic brain injury: integrated approaches to improve prevention, clinical care, and research. *Lancet Neurol.* (2017) 16:987–1048. doi: 10.1016/S1474-4422(17)30371-X

4. Gardner RC, Dams-O'Connor K, Morrissey MR, Manley GT. Geriatric traumatic brain injury: epidemiology, outcomes, knowledge gaps, and future directions. *J Neurotrauma.* (2018) 35:889–906. doi: 10.1089/neu.2017.5371

5. Herrera E, Barbas C. Vitamin E: action, metabolism and perspectives. *J Physiol Biochem.* (2001) 57:43–56. doi: 10.1007/BF03179812

6. Medicine Io. *Dietary Reference Intakes for Vitamin C, Vitamin E, Selenium, and Carotenoids*. Washington, DC: The National Academies Press. (2000) p 528.

7. Gilgun-Sherki Y, Rosenbaum Z, Melamed E, Offen D. Antioxidant therapy in acute central nervous system injury: current state. *Pharmacol Rev.* (2002) 54:271–84. doi: 10.1124/pr.54.2.271

8. Vonder Haar C, Peterson TC, Martens KM, Hoane MR. Vitamins and nutrients as primary treatments in experimental brain injury: Clinical implications for nutraceutical therapies. *Brain Res.* (2016) 1640:114–29. doi: 10.1016/j.brainres.2015.12.030

9. Hall ED, Vaishnav RA, Mustafa AG. Antioxidant therapies for traumatic brain injury. *Neurotherapeutics.* (2010) 7:51–61. doi: 10.1016/j.nurt.2009.10.021

10. Shen Q, Hiebert JB, Hartwell J, Thimmesch AR, Pierce JD. Systematic review of traumatic brain injury and the impact of antioxidant therapy on clinical outcomes. *Worldviews Evid Based Nurs.* (2016) 13:380–9. doi: 10.1111/wvn.12167

11. Horn SD, Kinikini M, Moore LW, Hammond FM, Brandstater ME, Smout RJ, et al. Enteral nutrition for patients with traumatic brain injury in the rehabilitation setting: associations with patient preinjury and injury characteristics and outcomes. *Arch Phys Med Rehabil.* (2015) 96:S245–55. doi: 10.1016/j.apmr.2014.06.024

12. Institute of Medicine Committee on Nutrition T, the B. In: Erdman J, Oria M, Pillsbury L, editors. *Nutrition and Traumatic Brain Injury: Improving Acute and Subacute Health Outcomes in Military Personnel.* Washington (DC): National Academies Press (US). (2011).

13. Aiguo W, Zhe Y, Gomez-Pinilla F. Vitamin E protects against oxidative damage and learning disability after mild traumatic brain injury in rats. *Neurorehabil Neural Repair.* (2010) 24:290–8. doi: 10.1177/1545968309348318

14. Inci S, Ozcan OE, Kilinç K. Time-level relationship for lipid peroxidation and the protective effect of alpha-tocopherol in experimental mild and severe brain injury. *Neurosurgery.* (1998) 43:330–5. doi: 10.1097/00006123-199808000-00095

15. Conte V, Uryu K, Fujimoto S, Yao Y, Rokach J, Longhi L, et al. Vitamin E reduces amyloidosis and improves cognitive function in Tg2576 mice following repetitive concussive brain injury. *J Neurochem.* (2004) 90:758–64. doi: 10.1111/j.1471-4159.2004.02560.x

16. Yang J, Han Y, Ye W, Liu F, Zhuang K, Wu G. Alpha tocopherol treatment reduces the expression of Nogo-A and NgR in rat brain after traumatic brain injury. *J Surg Res.* (2013) 182:e69–77. doi: 10.1016/j.jss.2012.11.010

17. Ishaq GM, Saidu Y, Bilbis LS, Muhammad SA, Jinjir N, Shehu BB. Effects of α-tocopherol and ascorbic acid in the severity and management of traumatic brain injury in albino rats. *J Neurosci Rural Pract.* (2013) 4:292–7. doi: 10.4103/0976-3147.118784

18. Nathens AB, Neff MJ, Jurkovich GJ, Klotz P, Farver K, Ruzinski JT, et al. Randomized, prospective trial of antioxidant supplementation in critically ill surgical patients. *Ann Surg.* (2002) 236:814–22. doi: 10.1097/00000658-200212000-00014

19. Berger MM, Soguel L, Shenkin A, Revelly JP, Pinget C, Baines M, et al. Influence of early antioxidant supplements on clinical evolution and organ function in critically ill cardiac surgery, major trauma, and subarachnoid hemorrhage patients. *Crit Care.* (2008) 12:R101. doi: 10.1186/cc6981

20. Razmkon A, Sadidi A, Sherafat-Kazemzadeh E, Mehrafshan A, Jamali M, Malekpour B, et al. Administration of vitamin C and vitamin E in severe head injury: a randomized double-blind controlled trial. *Clin Neurosurg.* (2011) 58:133–7. doi: 10.1227/NEU.0b013e3182279a8f

21. Kong SY, Shin SD, Tanaka H, Kimura A, Song KJ, Shaun GE, et al. Pan-Asian Trauma Outcomes Study (PATOS): rationale and methodology of an international and multicenter trauma registry. *Prehosp Emerg Care.* (2018) 22:58–83. doi: 10.1080/10903127.2017.1347224

22. Jung E, Ro YS, Park JH, Moon SB, Lee SGW, Park GJ, et al. Vitamin D deficiency and prognosis after traumatic brain injury with intracranial injury: a multicenter observational study. *J Neurotrauma.* (2022). doi: 10.1089/neu.2022.0053

23. Lee SGW, Ro YS, Jung E, Moon SB, Park GJ, Yoon H, et al. Serum acylcarnitine and long-term functional prognosis after traumatic brain injury with intracranial injury: a multicenter prospective study. *J Neurotrauma.* (2022). doi: 10.1089/neu.2022.0096

24. Maas AI, Stocchetti N, Bullock R. Moderate and severe traumatic brain injury in adults. *Lancet Neurol.* (2008) 7:728–41. doi: 10.1016/S1474-4422(08)70164-9

25. Blaner WS. Vitamin E: the enigmatic one! *J Lipid Res.* (2013) 54:2293–4. doi: 10.1194/jlr.E042267

26. Traber MG. *Vitamin E: Metabolism and Requirements. In: Caballero B, editor. Encyclopedia of Human Nutrition (Third Edition).* Waltham: Academic Press. (2013) p. 383–9. doi: 10.1016/B978-0-12-375083-9.00278-6

27. Rothman KJ, Greenland S, Lash TL. *Modern Epidemiology. 3rd ed.* Philadelphia, PA: Lippincott, Williams & Wilkins. (2012).

28. Greenland S, Pearl J, Robins JM. Causal diagrams for epidemiologic research. *Epidemiology.* (1999) 10:37–48. doi: 10.1097/00001648-199901000-00008

29. Diplock AT. Safety of antioxidant vitamins and beta-carotene. *Am J Clin Nutr.* (1995) 62:1510s—6s. doi: 10.1093/ajcn/62.6.1510S

30. Xiao R, Wang S, Guo J, Liu S, Ding A, Wang G, et al. Ferroptosis-related gene NOX4, CHAC1 and HIF1A are valid biomarkers for stomach adenocarcinoma. *J Cell Mol Med.* (2022) 26:1183–93. doi: 10.1111/jcmm.17171

31. Paolin A, Nardin L, Gaetani P, Rodriguez YBR, Pansarasa O, Marzatico F. Oxidative damage after severe head injury and its relationship to neurological outcome. *Neurosurgery.* (2002) 51:949–54. doi: 10.1227/00006123-200210000-00018

32. Hans P, Franssen C, Pincemail J, Bertrand Y, Hannique G, Damas P, et al. Plasma myeloperoxidase and vitamin E levels in head injury: preliminary results related to outcome. *J Neurosurg Anesthesiol.* (1992) 4:26–30. doi: 10.1097/00008506-199201000-00005

33. Currie S, Saleem N, Straiton JA, Macmullen-Price J, Warren DJ, Craven IJ. Imaging assessment of traumatic brain injury. *Postgrad Med J.* (2016) 92:41–50. doi: 10.1136/postgradmedj-2014-133211

34. Smith LGF, Milliron E, Ho ML, Hu HH, Rusin J, Leonard J, et al. Advanced neuroimaging in traumatic brain injury: an overview. *Neurosurg Focus.* (2019) 47:E17. doi: 10.3171/2019.9.FOCUS19652

Frontiers in Neurology

Explores neurological illness to improve patient care

The third most-cited clinical neurology journal explores the diagnosis, causes, treatment, and public health aspects of neurological illnesses. Its ultimate aim is to inform improvements in patient care.

Discover the latest Research Topics

See more →

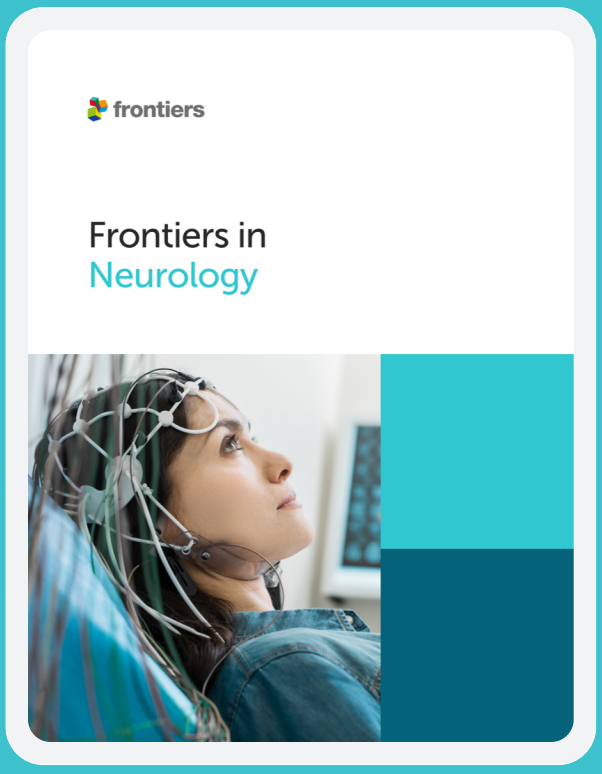

Frontiers

Avenue du Tribunal-Fédéral 34
1005 Lausanne, Switzerland
frontiersin.org

Contact us

+41 (0)21 510 17 00
frontiersin.org/about/contact